

UNIVERSIDADE FEDERAL DE SÃO CARLOS  
CENTRO DE CIÊNCIAS EXATAS E DE TECNOLOGIA  
DEPARTAMENTO DE QUÍMICA  
PROGRAMA DE PÓS-GRADUAÇÃO EM QUÍMICA

**“The implementation of NMR techniques for measuring  
interactions between small organic molecules/inhibitors and  
enzyme Acetylcholinesterase: a step towards Alzheimer’s control”**

**Nazish Urooj\***

A thesis submitted to the Federal  
University of São Carlos for the  
degree of Doctor in Philosophy, in  
organic chemistry

**Orientador: Prof. Dr. Antonio Gilberto Ferreira**

**\* bolsista (CAPES)**

**São Carlos - SP  
2015**

**Ficha catalográfica elaborada pelo DePT da  
Biblioteca Comunitária/UFSCar**

U78in

Urooj, Nazish.

The implementation of NMR techniques for measuring interactions between small organic molecules/inhibitors and enzyme Acetylcholinesterase : a step towards Alzheimer's control / Nazish Urooj. -- São Carlos : UFSCar, 2015.  
187 f.

Tese (Doutorado) -- Universidade Federal de São Carlos, 2015.

1. Ressonância magnética nuclear. 2. Alzheimer, Doença de. I. Título.

CDD: 547 (20<sup>a</sup>)



**UNIVERSIDADE FEDERAL DE SÃO CARLOS**


Centro de Ciências Exatas e de Tecnologia  
Programa de Pós-Graduação em Química

---

**Folha de Aprovação**

---

Assinaturas dos membros da comissão examinadora que avaliou e aprovou a Defesa de Tese de Doutorado da candidata Nazish Urooj, realizada em 21/05/2015:



---

Prof. Dr. Antonio Gilberto Ferreira

UFSCar



---

Prof. Dr. Luciano Morais Lião

UEG



---

Prof. Dr. Andersson Barison

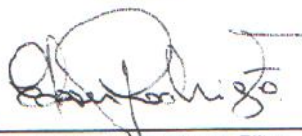
UFPR



---

Prof. Dr. João Batista Fernandes

UFSCar



---

Prof. Dr. Edson Rodrigues Filho

UFSCar

***In the name of Allah, the Compassionate, and the most Merciful.  
Recite! (Or read!) In the name of your Lord who created (1) Created  
man from clots of blood (2) Recite!, your Lord is the most Gracious  
(3) Who taught by the pen (4) Taught the man what he knew not (5).  
(The first verses of the holy Quran that revealed to Prophet  
Muhammad (P. B. U. H) from the sky)***

# *Dedications*

*To my parents.*

*For their love, prayers, caring and sacrifices for educating and preparing me for my future.*

*To my dear husband*

*The reason of what I become today.*

*Thanks for your prayers, great support and continues care.*

*To my adorable daughter*

*God's most precious gift in my life.*

*Thanks for bringing happiness in my life.*

## **Memorandum**

The work published in this thesis has been carried out at the Department of Chemistry Federal University of São Carlos, São Carlos SP Brazil, between March 2011 and May 2015. This thesis presents the original work of the author unless stated elsewhere and otherwise. Additionally, none of this work has been submitted for any other degree prior to this.

The copyright of this thesis rest with the author and the Federal University of São Carlos. No single quotation from this thesis can be published or presented without the prior written consent of the author, and more importantly, information derived from it should be acknowledged properly.

# SUMMARY

## Contents

SUMMARY .....	vii
List of Abbreviations used in this thesis .....	xii
List of tables .....	xvi
List of figures .....	xvii
<i>Acknowledgement</i> .....	xxii
List of Publications.....	xxiv
Abstract.....	<b>Error! Bookmark not defined.</b>
Resumo .....	<b>Error! Bookmark not defined.</b>
1. Introduction .....	2
1.1 Alzheimer’s Disease (AD) .....	2
1.1.1 Historical Background of AD .....	2
1.1.3 Characterization and different stages of AD .....	3
1.1.4 Alzheimer’s Pathology .....	4
1.1.4.1 Amyloidal Plaques .....	4
1.1.4.2 Tau Protein Misfolding .....	5
1.1.5 Alzheimer’s Disease mechanism .....	6
1.1.5.1 Cholinergic Hypothesis .....	7
1.1.5.2 Amyloid Hypothesis.....	8
1.1.5.3 Tau Hypothesis.....	10
1.2 Acetylcholinesterase (AChE).....	10
1.2.1 AChE Structure .....	11

1.2.2 AChE Functions .....	13
1.2.2.1 Hydrolysis Mechanism.....	14
1.3 Inhibition of AChE.....	16
1.3.1 Reversible Inhibitors (competitive or non-competitive).....	17
1.3.2 Irreversible Inhibitors (Organophosphorus Compounds OPs) .....	19
1.4 Nuclear Magnetic Resonance and Drug Discovery .....	23
1.4.1 Nuclear Magnetic Resonance.....	23
1.4.1.1 NMR working principle .....	24
1.4.1.2 Boltzmann distribution/ Energy population.....	28
1.5 NMR as a toll for ligand-receptor interaction studies.....	29
1.5.1 Receptor-based NMR screening methods.....	31
1.5.2 Ligand-based NMR screening methods.....	32
1.5.2.1 NOE-based methods.....	32
1.5.2.2 Principle of Tr-NOESY experiment .....	33
1.5.3 Saturation Transfer Difference (STD) NMR: .....	35
1.5.3.1 Principle of the Experiment: .....	38
1.5.3.2 STD NMR Applications.....	39
1.5.4 WaterLOGSY (Water-Ligand Observed via Gradient SpectroscopY)..	40
1.5.4.1 Principle of the experiment .....	41
1.5.4.2 Experimental Conditions:.....	42
1.5.6 Diffusion-based NMR spectroscopy .....	42
1.5.7 $T_1$ & $T_2$ relaxation methods as a tool to see the interaction.....	44
1.6 Docking Simulations .....	46
2. Scope of the Thesis.....	50



3. Materials and Methods .....	54
3.1 Equipments Used.....	54
3.1.1 NMR spectrometers.....	54
3.1.2 Analytical Balance .....	55
3.1.3 Biomixer.....	55
3.1.4 Sonicator.....	55
3.2 Chemicals and Solvents used .....	55
3.3 Sample preparation.....	56
3.3.1 Buffer Preparation (PBS) .....	56
3.3.2 AChE Stock Solution .....	56
3.3.3 Ligand stock solution for worked demonstrated in chapter 4 and chapter 5 .....	57
3.3.3.1 Sample for the STD build-up experiment (chapter: 4 and chapter 5) .....	57
3.3.3.2 STD-NMR Titration for KD calculation (chapter: 4 and chapter 5) .....	57
3.3.3.3 Sample preparation for NOESY experiment (Chapter: 4, 5 and Chapter 6).....	58
3.3.3.4 Sample preparation for DOSY experiment (Chapter: 5 and Chapter 6).....	58
3.3.3.5 Sample preparation for plant extract (chapter: 6) .....	59
3.4 NMR Acquisition and processing .....	59
3.4.1 <sup>1</sup> H-NMR Spectrum .....	59
3.4.2 90° Pulse Calibration.....	60
3.4.3 Solvent suppression.....	60

3.4.4 Saturation Transfer Difference NMR .....	61
3.4.5 NOESY and Tr-NOESY .....	65
3.4.6 Diffusion Ordered Spectroscopy Studies .....	65
3.4.7 1D DOSY experiment .....	68
3.5 Theoretical Experiments .....	69
3.5.1 Molecular Docking.....	69
4. Coumarin-derivatives AChE Inhibitors Binding Interactions and Dissociation Constant Calculations.....	72
4.1 Abstract .....	72
4.2 Introduction .....	72
4.3 Results and Discussion.....	75
4.4 Conclusions .....	102
5. Binding Competition and Group Epitope Mapping of the AChE inhibitors by STD NMR, Tr-NOESY, DOSY and Molecular Docking studies .....	106
5.1 Abstract .....	106
5.2 Introduction: .....	107
5.3 Result and Discussion: .....	110
5.3.1 <sup>1</sup> H-NMR and STD NMR Studies .....	110
5.3.2 Transferred NOESY Studies .....	114
5.3.3 STD NMR Titration Studies .....	117
5.3.4 Diffusion-Ordered Spectroscopy Studies.....	120
5.3.5 Molecular Docking Studies.....	122
5.3.6 Conclusions: .....	126
6. NMR Binding Recognition Study of <i>Terminalia Chebula</i> extract; New Insights into AChE Binding Behaviour .....	128

6.1 Abstract .....	128
6.2 Introduction .....	129
6.3 Results and discussion.....	132
6.4 Conclusions .....	148
7. Salient Features of the Thesis .....	150
8. Bibliography .....	154

## List of Abbreviations used in this thesis

1D	One-dimensional
2D	Two-dimensional
ACh	Acetylcholine
AChE	Acetylcholinesterase
AD	Alzheimer's Disease
Ala	Alanine
APP	Amyloid precursor protein
Arg	Arginine
Asn	Asparagine
Asp	Aspartate
A $\beta$	Amyloid $\beta$
BuChE	Butyrylcholinesterase
CAS	Catalytic anionic site
CD	Circular Dichroism
CNS	Central Nervous system
CORCEMA	Complete Relaxation and Conformational Exchange Matrix
COSY	COrrrelation SpectroscopY
CP	Cross Polarization
CWA	Chemical Warfare nerve Agents
Cys	Cysteine
d1	Relaxation delay
D <sub>2</sub> O	Deuterium oxide
DMSO	Dimethylsulfoxide
DOSY	Diffusion Ordered SpectroscopY
DQ	Double Quantum
DQF	Double Quantum Filtered

FBDD	Fragment Based Drug Design
FDA	Food & Drugs Administration
FID	Free Induction Decay
GEM	Group Epitope Mapping
Glu	Glutamine
Gly	Glycine
<i>hAChE</i>	Human Acetylcholinesterase
His	Histidine
HMBC	Heteronuclear Multiple Bond Correlation
HSQC	Heteronuclear Single Quantum Coherence
Ile	Isoleucine
IR	Infrared
$K_D$	Dissociation constant
$K_{off}$	Dissociation rate
$K_{on}$	Association rate
lb	Line broadening
ILOE	Inter-Ligand Overhauser Effect
LC	Liquid Chromatography
LC-MS	Liquid Chromatography - Mass Spectrometry
Leu	Leucine
Lys	Lysine
<i>m</i>	Magnetic Quantum
MeOH	Methanol
Met	Methionine
MHz	Megahertz
min	minute
MW	Molecular Weight
NMDAR	<i>N-methyl-D-Aspartic Acid</i> Receptor
NMR	Nuclear Magnetic Resonance

NOE	Nuclear Overhauser Effect
NOESY	Nuclear Overhauser Effect and Exchange Spectroscopy
NS	Number of scans
OPs	Organophosphorus Compounds
PBS	Phosphate Buffer Saline
Phe	Phenylalanine
PKN	Parkinson's disease
PNS	peripheral nervous systems
Pro	Proline
S/N	Signal to noise ratio
SAR	Structure Activity Relationship
Ser	Serine
SPE	Solid Phase Extraction
STD	Saturation Transfer Difference
STDD	Saturation Transfer Double Difference
SW	Spectral Width
T	Tesla
T <sub>1</sub>	Longitudinal relaxation time
T <sub>1ρ</sub>	Relaxation time in rotating coordinates
T <sub>2</sub>	Transverse relaxation time
TcAChE	<i>Torpedo Californica</i> Acetylcholinesterase
TD (F1)	Size of FID in F1 (Increments)
TD (F2)	Size of FID in F2 (Increments)
Thr	Threonine
TINS	Target Immobilized NMR Screening
TMS	Tetramethylsilane
TOCSY	Total Correlation Spectroscopy
TPPI	Time Proportional Phase Increment
Tr-NOE	Transferred Nuclear Overhauser Effect

Trp	Tryptophan
Tyr	Tyrosine
UV	Ultra-Violet
v/v	volume by volume
Val	Valine
WATERGATE	Water suppression by Gradient Tailored Excitation
WaterLOGSY	Water Ligand Observation with Gradient Spectroscopy
$\tau_m$	Mixing time

## List of tables

<b>Table 1:</b>	Chemicals, solvents used in this thesis.....	56
<b>Table 2:</b>	The concentrations of AChE vs. Inhibitor excess, used for the STD titration studies .....	58
<b>Table 3:</b>	Acquisition parameters for the STD NMR experiment.....	64
<b>Table 4:</b>	General acquisition parameters for DOSY NMR..... Experiment.....	67
<b>Table 5:</b>	Comparison of dissociation constant (KD) values and MOE binding energies of inhibitors.....	97
<b>Table 6:</b>	Comparison of dissociation constant (KD) values, Diffusion Coefficient values and MOE binding energies of inhibitors.....	123
<b>Table 7:</b>	Diffusion coefficients values of the compounds as calculated from the linear fit of the series of 1D-DOSY spectra.....	147



## List of figures

<b>Figure 1:</b>	Comparison of normal human brains and Alzheimer's affected brain.....	03
<b>Figure 2:</b>	Comparison of normal human neurons and Alzheimer's affected neurons.....	06
<b>Figure 3:</b>	The schematic representation of the acetylcholinesterase enzyme and acetylcholine within the synaptic cleft of the human brain.....	09
<b>Figure 4:</b>	The schematic representation of the TcAChE highlighting some important active binding and sub-binding sites.....	12
<b>Figure 5:</b>	Schematic representation of Hydrolysis of ACh into Choline and Acetate ion by the action of AChE.....	14
<b>Figure 6:</b>	Steps of Hydrolysis of ACh into Choline and Acetate ion by the action of AChE.....	16
<b>Figure 7:</b>	Structures of some of the important reversible inhibitors that used in the pharmacotherapy of AD.....	18
<b>Figure 8:</b>	General structure and classification of OPs AChE irreversible inhibitors.....	19
<b>Figure 9:</b>	Schematic representation of AChE inhibition through OPs.....	21

<b>Figure 10:</b>	Structures of some of the important irreversible OPs inhibitors that used in Insecticides.....	22
<b>Figure 11:</b>	Energy level diagram for $\frac{1}{2}$ spin state nucleus.....	27
<b>Figure 12:</b>	The schematic representation of Tr-NOESY experiment.....	34
<b>Figure 13:</b>	The schematic representation of STD-NMR experimen.....	37
<b>Figure 14:</b>	Schematic representations of ‘Zgcppr’ pulse sequence.....	60
<b>Figure 15:</b>	Schematic representation of 1D-NOESY pulse sequence.....	61
<b>Figure 16:</b>	WATERGATE coupled STD sequence for solvent suppression.....	62
<b>Figure 17:</b>	Conventional STD pulse sequence coupled with excitation sculpting for solvent suppression.....	62
<b>Figure 18:</b>	The pictorial representation of the selected inhibitors.....	76
<b>Figure 19:</b>	$^1\text{H}$ -NMR spectra of compound 1 with and without protein...	77
<b>Figure 20:</b>	1D-STD NMR spectra of compounds and Tacrine.....	78
<b>Figure 21:</b>	$^1\text{H}$ -NMR spectra of compound 2 with and without protein..	79
<b>Figure 22:</b>	$^1\text{H}$ -NMR spectra of compound 3 with and without protein..	80
<b>Figure 23:</b>	$^1\text{H}$ -NMR spectra of compound 4 with and without protein..	81
<b>Figure 24:</b>	Stacked plot of 1D STD NMR spectra of compound 1 with varying saturation times.....	82
<b>Figure 25:</b>	Stacked plot of 1D STD NMR spectra of compound 2 with	

	varying saturation times.....	83
<b>Figure 26:</b>	Stacked plot of 1D STD NMR spectra of compound 3 with varying saturation times.....	84
<b>Figure 27:</b>	Stacked plot of 1D STD NMR spectra of compound 4 with varying saturation times.....	85
<b>Figure 28:</b>	Stacked plot of 1D STD NMR spectra of Tacrine with varying saturation times.....	86
<b>Figure 29:</b>	Saturation curve Plot and titration curve plot of the compound 1.....	87
<b>Figure 30:</b>	Concentration curve plots for compounds 2, 3, 4 and standard tacrine respectively.....	88
<b>Figure 31:</b>	Two-dimensional standard NOESY spectra of compounds 1, 2, 3 and 4 without AChE.....	90
<b>Figure 32:</b>	Two-dimensional standard NOESY spectra of compounds 1, 2, 3 and 4 with AChE.....	91
<b>Figure 33:</b>	Active site residues surrounding tacrine bound inhibitor.....	93
<b>Figure 34:</b>	Molecular docking model of compound 1.....	94
<b>Figure 35:</b>	Molecular docking model of compound 2.....	96
<b>Figure 36:</b>	Molecular docking model of compound 3.....	98

<b>Figure 37:</b>	Molecular docking model of compound 4.....	100
<b>Figure 38:</b>	Molecular docking model of Tacrine.....	101
<b>Figure 39:</b>	Molecular structures of the targeted compounds.....	110
<b>Figure 40:</b>	<sup>1</sup> H-NMR spectra of targeted compounds (Scopoletin, 4-Methylumbelliferone and gallic acid).....	111
<b>Figure 41:</b>	Stack plot of saturation time-dependent STD NMR spectra..	112
<b>Figure 42:</b>	<sup>1</sup> H-NMR (A), <i>Off</i> -resonance (B) and STD NMR spectrum (C) of targeted compounds.....	114
<b>Figure 43:</b>	2D-NOESY (A) and 2D Tr-NOESY (B) spectra of targeted compounds.....	116
<b>Figure 44:</b>	Stacked spectra of concentration-dependent STD-NMR experiments.....	118
<b>Figure 45:</b>	STD amplification factor curve plot.....	119
<b>Figure 46:</b>	A double display of 2D-DOSY NMR spectrum.....	121
<b>Figure 47:</b>	Molecular Docking model of inhibitor A.....	123
<b>Figure 48:</b>	Molecular Docking model of inhibitor B.....	124
<b>Figure 49:</b>	Molecular Docking model of inhibitor C.....	125
<b>Figure 50:</b>	Isolation scheme of the Terminalia Chebula RETZ fruit.....	133
<b>Figure 51:</b>	The <sup>1</sup> H-NMR spectra and STD NMR spectrum ethyl acetate fraction of the <i>Terminalia Chebula</i> extract.....	134

<b>Figure 52:</b>	The $^1\text{H}$ -NMR spectra with HOD signal suppression and STD NMR spectrum of water suspended fraction from ethyl acetate portion of the <i>Termilania Chebula</i> extract.....	135
<b>Figure 53:</b>	2D HSQC spectrum of the <i>Termilania Chebula</i> extract.....	136
<b>Figure 54:</b>	Mass spectrum of the <i>Termilania Chebula</i> extract.....	137
<b>Figure 55:</b>	Structures of the recognized compounds.....	140
<b>Figure 56:</b>	A side by side view of the 2D NOESY and Tr-NOESY spectrum.....	142
<b>Figure 57:</b>	The intensity attenuations of the three selected peaks.....	144
<b>Figure 58:</b>	Scattered plot for the signal intensity attenuations vs. square of gradients strength.....	146

## **Acknowledgement**

*All praises for Almighty **ALLAH**, Who is the most Omnificent, Omniscient, Omnipotent, and Omnipresent, heartily thanks for giving me the strength to fulfil this task,*

*I am showing my humble obedience to the heart and soul of the world and the world hereafter; The Holy Prophet **Mohammad** (Peace be upon him), whose life is an ideal pattern for us.*

*The work presented in this thesis was impossible without the invaluable guidance, keen interest and valuable suggestions of my ingenious and determined research supervisor **Prof. Dr Antonio Gilberto Ferreira** to whom, wish to acknowledge my indebtedness and sincere thanks. I also pay my thanks to **Asst. Prof. Dr. Tiago Venancio**, faculty here in the laboratory of NMR UFSCar; the work embodied here could never be accomplished without the encouragement and precious attention.*

*I wish to express my thanks to who have extended their co-operation in providence of research assistance to me during the entire course of this work, prominent among them are **Ms. Luciana Vizotto** our lab mechanical technician, **Mr. Paulo R. Lambertuci** the electrical technician and my lab members for their cooperation and nice hospitality during the stay of Sao Carlos.*

*Here I would like to specially thank to the **Prof. Dr. Arlene G Correa**, from natural product synthesis research group for the providence of newly synthesized Samples to me.*

*I owe my deepest gratitude, to referees; **Prof. Dr. Edinho R. Filho**, **Prof. Dr. João Batista Fernandês**, **Prof. Dr. Luciano Lião** and **Prof. Dr. Aderson Barrisson** for their generosity to accept my request and sparing time for review my thesis. I offer my utmost gratitude to my funding Agencies (CAPES) who supported me from beginning of the research to the end of this thesis.*

*The whole work was carried out, completed, and made accessible with the excellent facilities at Laboratory of NMR, department of chemistry Federal University of São Carlos SP, Brazil. I owe my deepest gratitude to all faculty members for their cooperation, valuable*

*suggestions, and the deepest thanks for the technical and nontechnical staff of Federal university of São Carlos.*

*Especial thanks to my husband, who help me at every step of my life. I want you to know that being your wife has been the greatest gift God has ever given me. Not just because of how happy you make me, but because of WHO YOU ARE. You are defined by loyalty, trust, and commitment. Thank you for telling me that what I want is possible and thank you for all the sacrifices you have made to see me reach to my goals. Thank you for teaching me about the things you love and being enthusiastic about my interests too. I cannot find words to utter, but I just want to say I love you, and I want to thank you for all you have done for me. A million of thanks to my sweet husband.*

*Thanks to my daughter, the most precious gift of God, who was born before this dissertation was completed. In the hard time when I look at my daughter, her smiles give me the strength. I adore her smile; I cherish her hugs, I admire her heart but most of all... I love that she is MY DAUGHTER.*

*At last but not least, how can I forget to thank my parents, sisters and brothers, whose continues support and eternal prays keep me safe thousands mile long from my home.*

*Nazish Urooj Tanoli*

## List of Publications

1. **Tanoli, N. U.;** Tanoli, S. A. K.; Ferreira, A. G. An NMR dissection of *Terminalia Chebula* extract for the potential Acetylcholinesterase blocker by effective recognition methods like STD NMR, Tr-NOESY and diffusion edited studies: New Insights into AChE binding inhibitions. *Submitted—Journal Medicinal Chemistry*
2. **Tanoli, N. U.;** Tanoli, S. A. K.; Ferreira, A. G.; Gul, S.; Ul-Haq, Z. Evaluation of binding Competition and group epitopes of Acetylcholinesterase inhibitors by STD NMR, Tr-NOESY, DOSY and Molecular Docking: An old approach but new findings. *Submitted—New Journal of Chemistry*
3. **Tanoli, N. U.;** Tanoli, S. A. K.; Gul, S.; Vieira, L. C. C.; Monteiro, J. L.; Venâncio, T.; Correa, A. G.; Ul-Haq, Z.; Ferreira, A. G. Coumarin-derivatives as AChE inhibitors with three simultaneous interacting locus; an important Alzheimer scaffold as afforded by STD NMR, Tr-NOESY and Docking Simulations. *Submitted—Future Journal of Medicinal Chemistry.*
4. Tanoli, S. A. K.; **Tanoli, N. U.;** Bondancia, T. M.; Usmani, S.; Ul-Haq, Z.; Fernandes, J. B.; Thomasi, S. S.; Ferreira, A. G. Human serum albumin-specific recognition of the natural herbal extract of *Stryphnodendron polyphyllum* through STD NMR, hyphenations and docking simulation studies. *RSC Advances* **2015**, 5, 23431.
5. Tanoli, S. A. K.; **Tanoli, N. U.;** Usmani, S.; Ul-Haq, Z.; Ferreira, A. G. The exploration of interaction studies of smaller size, mostly ignored yet intrinsically inestimable molecules towards BSA; An example of STD and DOSY NMR. *Central European Journal of Chemistry* **2014**, 12 (3), 332-340.



6. Tanoli, S. A. K.; **Tanoli, N. U.**; Bondancia, T. M.; Usmani, S.; Kerssebaum, R.; Ferreira, A. G.; Fernandes, J. B.; Ul-Haq, Z. Crude to leads: a triple-pronged direct NMR approach in coordination with docking simulation. *Analyst* **2013**, *138* (17), 5137-5145.
7. Zia Ud Din, Sheraz Ahmad Khan Tanoli, **Nazish Urooj Tanoli**, Sajjad Hussain, Saima Gul, Sabir Khan, Pir Muhammad Khan, Shabnum. Nutritional potential and antioxidant activity of solanum nigrum and oenothera speciosa from northern area of Pakistan, *International Journal of Biological & Pharmaceutical Research*. **2012**, *3*(8):974-979.

## ABSTRACT

THE IMPLEMENTATION OF NMR TECHNIQUES FOR MEASURING INTERACTIONS BETWEEN SMALL ORGANIC MOLECULES/INHIBITORS AND ENZYME ACETYLCHOLINESTERASE: A STEP TOWARDS ALZHEIMER'S CONTROL. The inhibition of the acetylcholinesterase (AChE) might be an excellent therapy in controlling Alzheimer's disease as stated by the cholinergic hypothesis. In this context, the inhibitors of AChE, are of medical and commercial paramount interest as therapeutics for Alzheimer's disease and as pesticides. However, the conformational changes in inhibitors with AChE complex facilitate the rational design of some novel inhibitors with increased potency and specificity. Therefore, solution state NMR is a novel approach that seems to fulfil almost all conditions necessary to investigate the AChE-inhibitor complex. In this perspective, a combined strategy of STD, Tr-NOESY, DOSY, and docking simulations were applied to compare the bindings of four synthetic coumarin derivatives to tacrine for their binding potentials. Intriguingly, one of them (compound **1**) was found to have not only the stronger affinity than the control but could bind with three sites. Furthermore, a competition of three inhibitors (gallic acid, 4- methylumbelliferone, and scopoletin) was performed by taking help of the STD NMR experiments. Interestingly, none of them was competing for the some particular binding site. Nevertheless, in titration studies gallic acid was found best based on dissociation constant values. Moreover, an ethyl acetate fraction and its water suspension of the *Terminalia Chebula* RETZ, fruit extract was studied. Three compounds (4-hydroxycinnamic acid, Ethyl-4-hydroxycinnamate and lupeol) were seen to involve in interaction that were later recognized by 2D NMR and ESI mass techniques. Moreover, for the first time in the Federal University of São Carlos, these NMR methods for the determination of the bound conformation of any inhibitors towards AChE using NMR spectroscopy have been applied.

## Resumo

IMPLEMENTAÇÃO DE TÉCNICAS DE RMN PARA MEDIR INTERAÇÕES ENTRE MOLÉCULAS ORGÂNICAS INIBIDORAS DA ENZIMA ACETILCOLINESTERASE: UM PASSO PARA O ESTUDO DO ALZHEIMER. A inibição da acetilcolinesterase (AChE) pode representar um caminho para o controle da doença de Alzheimer se consideramos a hipótese colinérgica. Neste contexto, os inibidores de AChE, representam interesse tanto para a área médica como comercial utilizando-os como agentes terapêuticos para a doença de Alzheimer e como pesticidas. O entendimento das mudanças conformacionais envolvidas no complexo com os inibidores de AChE pode facilitar o planejamento racional de novos compostos, procurando aqueles com maior potencial terapêutico e melhor especificidade. Portanto, a RMN em solução é uma ferramenta muito útil para se investigar possíveis inibidores da AChE. Para tanto, uma estratégia combinando as técnicas de STD, Tr-NOESY, DOSY, e simulações computacionais foram utilizadas para comparar as interações de quatro derivados sintéticos de cumarina com o composto tacrine, utilizado como controle. Curiosamente, para um dos compostos (composto **1**) foi encontrada uma maior afinidade que o próprio controle, além dele interagir em três regiões distintas. Além disso, foi realizado um experimento de competição de três inibidores (ácido gálico, 4- metilumbeliferona e escopoletina) ao mesmo tempo, através dos experimentos de STD, sendo que nenhum deles mostrou competição para uma região específica da AChE. No entanto, estudos de titulação via RMN mostrou que o ácido gálico foi o que apresentou melhor resultado baseado nos valores das constantes de dissociação medidas por RMN. Além disso, também se avaliou uma fração do extrato bruto de acetato de etila e da sua suspensão em água, oriundas dos extratos dos frutos da espécie *Terminalia chebula* RETZ. Três compostos (4-hidroxicinâmico, Etil-4-hidroxicinamato e lupeol) apresentaram interação com a AChE e as suas estruturas foram caracterizadas por RMN 2D e espectrometria de massas. Este

trabalho representou o primeiro estudo, na UFSCar, onde se avaliou interações de possíveis inibidores da AChE utilizando técnicas de RMN.



# **1. Introduction**

## **1.1 Alzheimer's Disease (AD)**

It is the most common form of the progressive chronic neurodegenerative, which starts slowly and ends worse, manifested by cognitive and intellectual deteriorations that results in a collective impairments of day-to-day life activities, behavioural changes, and difficulties in speaking, mood swings, and some other variety of psychiatric symptoms. <sup>1-3</sup> Alzheimer's disease is abbreviated herein as AD throughout this thesis. Being a leading cause of death particularly in the aged population, always remains mysterious to diagnose, and progressively kills a human between the average duration of 8-8.5 years from the first manifestation of a symptom of death. <sup>4</sup> However, to date, there is no possible diagnostic procedure exist to finish this massacre disease prior to autopsy reports, and more importantly, it is supposed to become more aggressive and potential within coming 2 to 3 decades. <sup>4, 5</sup> Prevalence studies have shown that the America, China, and Western Europe are among the most affected countries and by 2040 these regions will be expected to home of around 60% of the total population that affected across the world. <sup>6</sup> In America alone, the death toll per year exceeds than a half million peoples, as recorded in a very recent report, <sup>7</sup> and declared Alzheimer's as the seventh fatal disease in the region.

### **1.1.1 Historical Background of AD**

Alois Alzheimer (1864-1915), a German neurologist was the first, who discovered the AD in 1906 through manifestations the case of a 51 years old woman Auguste D., who were under his treatment since 1901. <sup>8</sup> Initially, she reported on the problems associated with speaking, and anti-modern history of impairing memory. During the course of her treatment, Dr. Alzheimer could get

any conclusion about the nature of disease, however, after her death, in autopsy reports he declared that she was affected by severe dementia. It was the first time that he observed the neurofibrillary tangles and a dramatic shrinkage of the brain cortex, (as shown in Figure 1) which latterly named after his name as Alzheimer disease in 1910. The conclusions that Dr. Alzheimer presented in 1906 are still considered as the basis of today AD. <sup>1-4</sup>

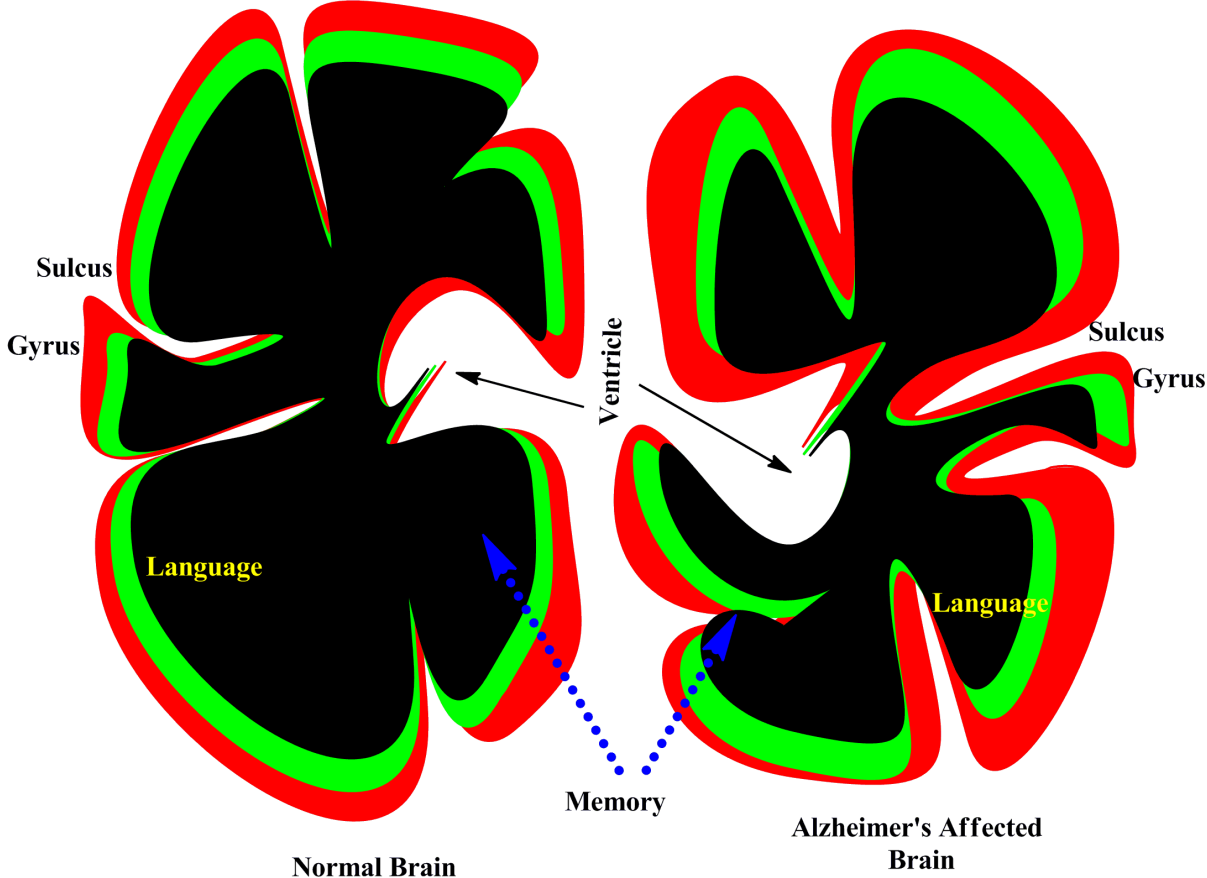


**Figure 1:** Comparison of human brains: normal (left-hand side) and Alzheimer’s affected (right-hand side), picture theme adopted from Bright Focus Foundation USA. <sup>9</sup>

**1.1.3 Characterization and different stages of AD**

Types of AD characterization based totally on the symptoms occurrences in the victim, if population younger than 65 got affected, is called the familial AD, because there might be some family history of this disease because of gene

mutations. Conversely, sporadic AD affects only older population than 65.<sup>10</sup> The characterization of AD against normal aging and other dementias is easy e-g, gradual loss of weight, hairs and bone density is common in aging along some weakness in memories, but cognitive decline in memory is normal process of aging. Likewise, significant cognitive loss owing to different diseases does not mean AD. Each kind of disease has its dementia, e-g brain stroke as results in vascular dementia, when blood flow decreases.

Different stages of AD depend on two factors, A) the severity of disease with respect to the symptoms and B) the length of the period of the disease after the first diagnoses. The long lasting disease consists of three stages, 1) early-stage, 2) moderate stage and 3) severe-stage AD. The length of each step different and longer to the earlier one, e-g early-stage comprises 2-4 years from first diagnostics while moderate-AD represents a longer 2-10 years of the stage. Symptoms become more significant in the initial moderate stage, which becomes more aggressive and increases potential in the later stage, and finally the severe stage ends with the death.

### **1.1.4 Alzheimer's Pathology**

Pathology of AD is dependent on the some hallmark features those associated with neuronal loss, the formation of plaques and neurofibrillary tangles.<sup>11</sup> The cholinergic system starts damaging in the early stages of the AD. However, the overall degenerations AD accounts for, are involving noradrenergic, serotonergic and cholinergic systems.<sup>12, 13</sup>

#### **1.1.4.1 Amyloid Plaques**

Small spherical depositions of amyloid-beta protein (generally represented as A $\beta$ ) as a result of some cleavage enzyme (beta amyloid cleavage enzyme) are referred as amyloid plaques. By nature, the A $\beta$  is a sticky protein that gradually gathers into the clumps and hence, forms the extracellular



plaques.<sup>14</sup> However, the mostly seen aggregations of these proteins are of A $\beta$ -42 type.<sup>14, 15</sup> Plaques formation is not a uniform or stable state it further shows mutations in the amyloid precursor protein (APP), which is more common in familial AD, and more importantly, indicates the progression of the disease. However, amyloid cascade is generally not common in sporadic AD, in addition, it equally found in the non-demented population.<sup>16</sup>

#### **1.1.4.2 Tau Protein Misfolding**

The collections of intracellular helical filaments in the brain, which are mostly insoluble, mark the second hallmark for the AD,<sup>11</sup> known as neurofibrillary tangles. The insolubility characterized by the phosphorylation and dephosphorylation process otherwise in normal condition tau protein is soluble. However, the abnormal process of phosphorylation collapses the neuron that subsequently leads to the death of the neuron cell.<sup>17</sup> A microtubule-associated protein is the major component of these neurofibrillary tangles known as tau protein, which provides structural firmness to the cell after binding with microtubulin. The detachment of tau from microtubulin protein forms the tau aggregations<sup>18</sup>, which subsequently left few grades on the chemistry of microtubules in the form of some disassemblies in its structure.<sup>19</sup> A comparison of a normal neuron with the affected neuron clearly shows the hallmark changes that are responsible for the AD, as shown in Figure 2.

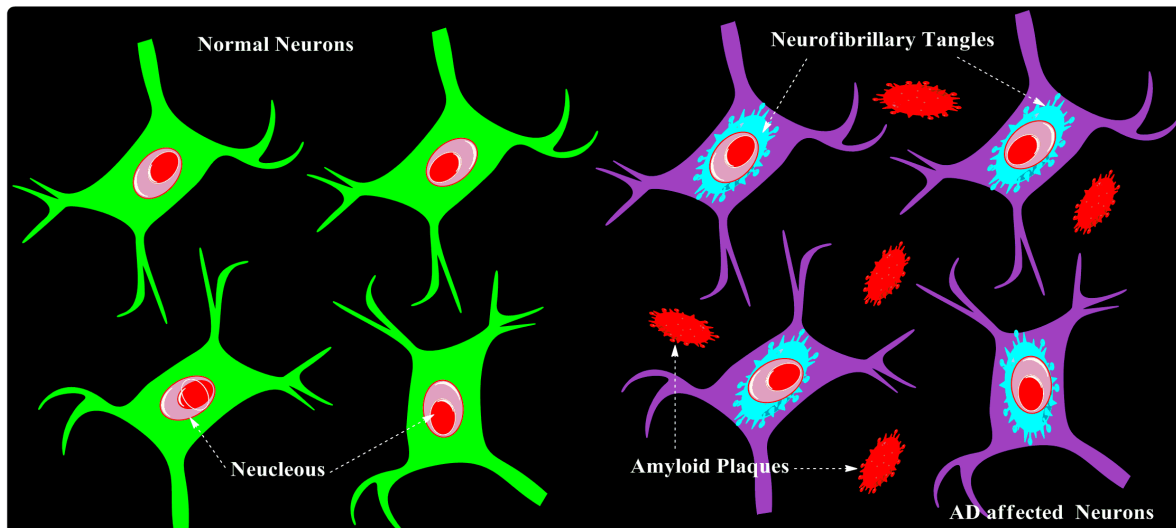


**Figure 2:** Comparison of human neurons: normal (left-hand-side with green colors) and Alzheimer’s affected (right hand-side with purple color), picture theme adopted from Bright Focus Foundation USA. <sup>9</sup>

A parallel research showed that for the proper functioning of the neuron it is necessary for microtubule to work perfectly, otherwise the neuron might have itself some dysfunction responsible for AD <sup>20</sup>, and more importantly, if the tau aggregates are in excess they can also mutate other proteins binding to microtubules. <sup>20</sup>

Apart from aforementioned characteristically factors, a number of other aetiological interconnected features that may have some important role in AD are inflammation, <sup>21, 22</sup> oxidative stresses, <sup>23</sup> cholinergic effects, <sup>24, 25</sup> etc.

### 1.1.5 Alzheimer’s Disease mechanism

Despite hard works from scientist across the world over the decades, AD is yet to be discovered about to the real facts that happen during the course, instead of symptomatic treatments. In addition, the difference in rates of succession in different individual and more importantly intensification with the passage of time and proper treatment, etc., still needs to work. Three major hypothesis are advanced that explain the causes that might involve in the

intensification of dementia, progression with high rates, targeting mostly the elderly population, etc., and are supposed to be the primary cause of AD. The first and oldest one is a cholinergic hypothesis,<sup>1</sup> which states the cholinergic signaling are directly responsible for this initiative in the progression of AD. Conversely, the other two hypotheses suggest that either misfolding of A $\beta$  protein or neurofibrillary tangles from tau protein are the root causes that provide a healthy start to AD. However, the scientists are not yet to solve that which of the earlier hypotheses is responsible for the advanced anatomical changes resulting from AD. Therefore, a number of studies have been published up to date, where scientific community believe in misfolding of A $\beta$  (amyloid hypothesis) to be a more dominant among others,<sup>14, 15, 26-28</sup> but is not clear yet.

#### **1.1.5.1 Cholinergic Hypothesis**

Being the oldest hypothesis, it could get hype, as did the later two counterparts. The main reason for this discrepancy is the medication for the treatment of cognitive dysfunctions resulting from this theme, provided undesirables side effects.<sup>16, 29</sup> According to the cholinergic hypothesis, the annihilation of cholinergic pathway due to the activity of AChE, results in deficiency of a neurotransmitter (ACh)—responsible for cholinergic response.<sup>16, 30</sup> Most of the early research focused this concept of the hypothesis and tried to find the new results, however, outfits were not beneficent to cure the AD. Although, these conclusions infer that acetylcholine may not a direct casual to AD but also involve in damaging other brain tissues. Later on, in another report made claim that the cholinergic effects are the main causative agents responsible for later accumulation of the A $\beta$  plaques as well as the Tau protein tangles and hence leading to neuroinflammation in the body.<sup>31</sup> The success of these results makes this hypothesis stronger, and the basic concept of improving the cholinergic effect need to be explored. More importantly, in an indirect way it also involves in the later two hypotheses. Therefore, the level of AChE

reduction as a result of some inhibitors can suppress the hydrolysis of ACh in the synaptic cleft and hence regenerate the cholinergic effect. By taking advantages of the review, <sup>1</sup> published in 2004, the relation between the cholinergic effect and acetylcholinesterase enzyme is explained in figure 3 that how and where this process of hydrolysis take place.

### **1.1.5.2 Amyloid Hypothesis**

The amyloid hypothesis based on the accumulation of small spherical depositions of Amyloid-beta  $A\beta$  as result of some cleavage enzyme or due to overproduction or failure of clearance mechanisms is referred as Amyloid plaques, which are responsible for the cholinergic impairments. This hypothesis was supported by some observations carried upon mouse model and human beings, which show the  $A\beta$  and their variant proteins, are responsible for the formation of some cascade—enhance the cholinergic impairments. <sup>32, 33</sup> The actual linked mechanism of memory impairment and  $A\beta$  protein is needed to be elucidated but the importance of the  $A\beta$  is undeniable. The formation of the  $A\beta$  plaques takes place from amyloid precursor protein (APP) as has been explained in the previous section (1.1.4.1). APP also involving some synaptic regulation self-functions, when examine this point of view in mice, the mice lacking APP and their variant showed deficiencies in synaptic functioning and structure. <sup>34, 35</sup> In conclusion, the broad community of the “Baptist” who believe the amyloid precursors production, degradation and deposition are responsible for AD, on the basis of some recently reported studies. <sup>35-37</sup>

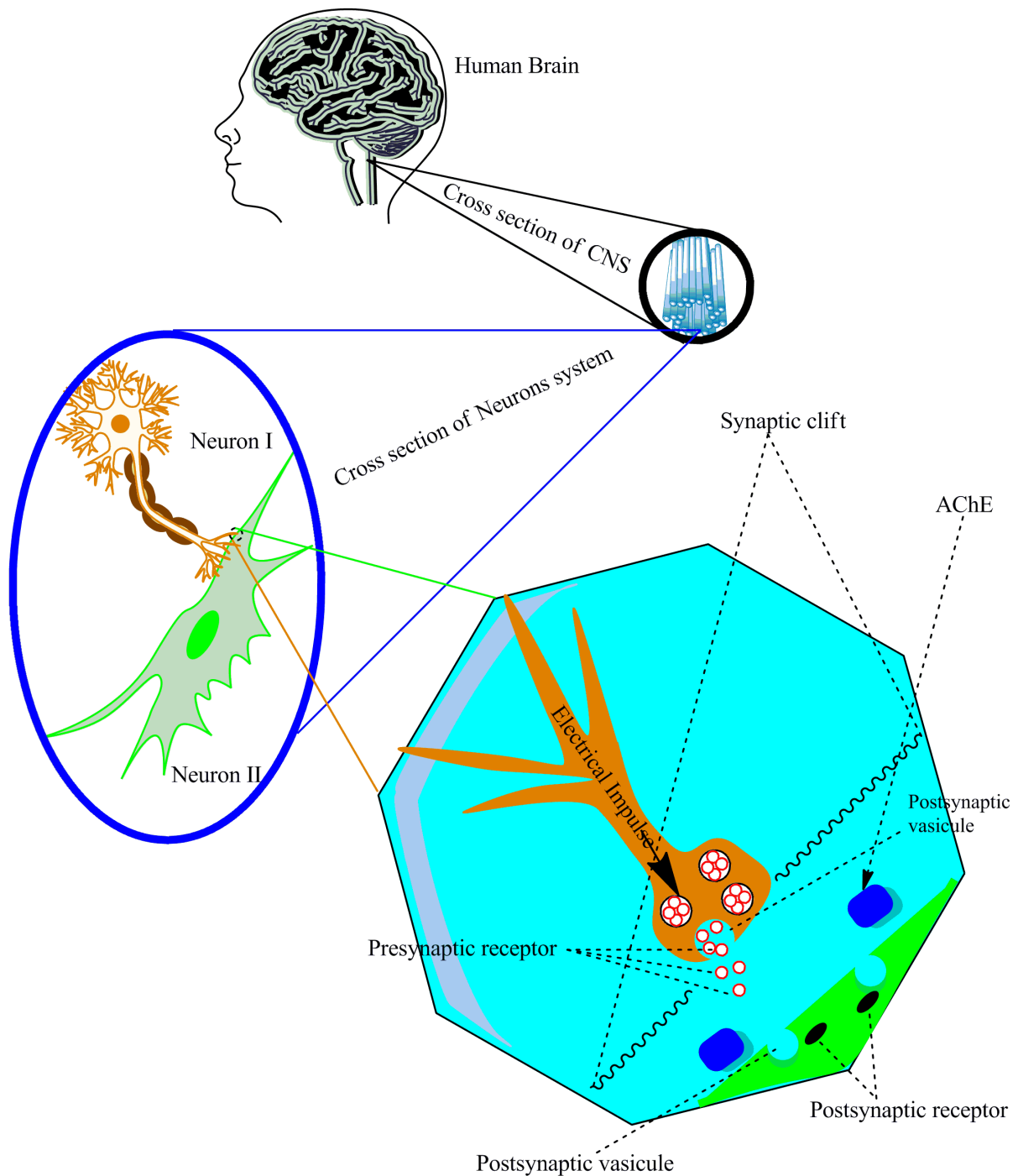


**Figure 3:** The schematic representation of the acetylcholinesterase enzyme and acetylcholine within the synaptic cleft of the human brain, where different cross sections are made to explain the actual presence of the neurons in CNS system. The idea for this figure was taken from the reference 1.

### **1.1.5.3 Tau Hypothesis**

The collections of intracellular helical filaments in the brain, which are mostly insoluble, mark the second hallmark for the AD,<sup>11</sup> known as neurofibrillary tangles. A $\beta$  protein shows some sort of interaction with the signaling pathways associated with the phosphorylation of tau protein, which in turn disrupts the hyperphosphorylation of tau from its normal functioning that leads to neurofibrillary tangles.<sup>38</sup> However, in a normal situation, the phosphorylation regulated by the balance coordination of kinases and phosphatases.<sup>39</sup> There are number of supportive materials published regarding the tau hypothesis. However, the conclusion about the final cause are yet not decided. Tau hypothesis is advanced because of some diseases, collectively known as tauopathies, where the misfolding of this protein was found.<sup>40</sup> Although the mystery of the AD is yet not clear but, the Tau-ists who believe, the abnormalities within this protein are responsible for pathogenic disease cascades.

## **1.2 Acetylcholinesterase (AChE)**

AChE is a hydrolase enzyme, which hydrolysis ACh and perishes the activity, ACh renown for that is carrying electrical impulses to one neuron to other. This enzyme belongs to the subfamily of cholinesterase enzymes, which comprises AChE and BuChE (Butyrylcholinesterase). The distinguishing features of these subfamilies depend upon their specificities towards the substrate as well as their nature of inhibitor.<sup>41</sup> In recent years, it is well noted that, besides the nervous transmission, the AChE also involve in a number of different functions, including worked as an adhesion protein, in neurite growth, as a bone matrix and specifically, the amyloid fibrils production in AD patients.<sup>42</sup> Therefore, I would say, it is the one of the most vital and catalytically well-organized enzyme ever known to human.

### 1.2.1 AChE Structure

Much of the structural information and kinetic behavior available now related to AChE are, as results of the X-ray crystallography of amino acids residues studies mostly based on Electric eel, *Torpedo Californica*. However, the human AChE (*hAChE*) crystal structure and amino acid residues are much similar to *TcAChE*. This enzyme possesses a complex structure comprising hydrolase type folds of  $\alpha/\beta$  protein,<sup>43</sup> whereof 12-stranded central  $\beta$ -sheet bounded by 14  $\alpha$  helices.<sup>44</sup> In a gross manner, AChE possess some ellipsoidal type of structure, having two prominent regions, a deep groove commonly known as gorge groove located about 20 Å deep and a peripheral anionic site (PAS) which located about 14 Å above the gorge.<sup>43, 44</sup> PAS varies among different sources of AChEs, in electric eel *Torpedo californica* (*TcAChE*) five amino acids residues (Phe 290, Tyr 70, Tyr 121, Trp 279, Asp 72) are very important as in shown in figure 4.

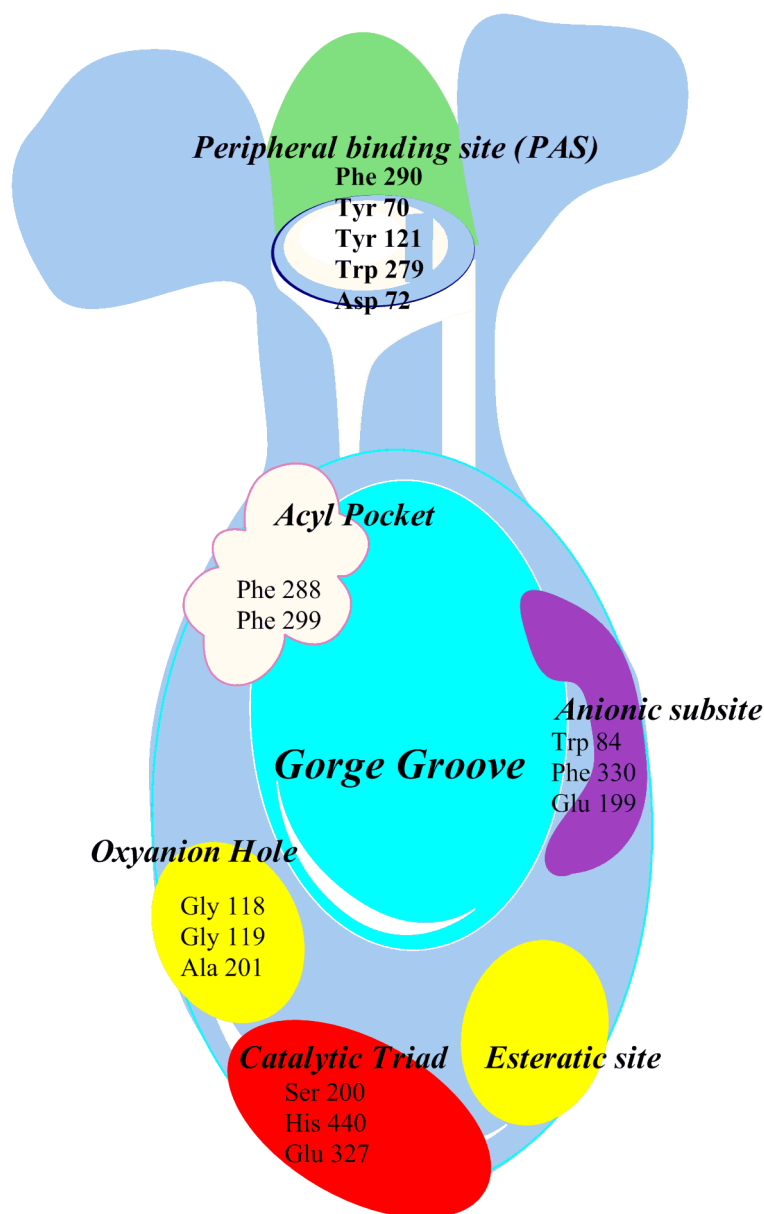


**Figure 4:** The schematic representation of the *TcAChE* highlighting some important active binding and sub-binding sites, as defined elsewhere.<sup>43, 44</sup>

It is obvious that the reversible inhibitors mostly use binding site of PAS and this implication cause a direct passage of substrate to catalytic gorge cavity through some steric blockade and electrostatic functions. Hence, play an important role in hydrolysis of ACh and aid in other substrates to access the active site through some allosteric variations.<sup>43, 44</sup> The catalytic site of AChE consists of triad (glutamate 327, histidine 440, and serine 200) amino acids residues, which play an important role in ACh hydrolysis in either acidic or



basic fashion. On either side of catalytic site, an esteratic and oxyanion, sub-sites exist—mostly catalytic machinery of these sub-sites depends upon the catalytic sites. The oxyanion and esteratic sub-binding sites are believed to help in positioning the ACh or other substrate through hydrogen bonding during the hydrolysis process of catalytic site.<sup>43</sup> Another important site is, ‘anionic subsite’ comprising aromatic residues including Trp84, Glu199 and Phe330, which has a greater affinity towards the quaternary ammonium ligands or other hydrophobic ligands through *p-p* interactions. The positive charge of the quaternary ammonium type ligands and choline forms a stable complex with the aromatic  $\pi$  bonding system that provide a support the ligand to positioning itself down into gorge. The Acyl binding pocket is another important site comprising two amino acid residues (Phe290 and Phe288), is supposed to be involved in size reduction of the substrate during the hydrolysis process and hence, making more efficient the process of hydrolysis.<sup>45</sup>

### 1.2.2 AChE Functions

In accordance with the rapid hydrolysis activity of the AChE that results in a loss of cholinergic response by the termination of ACh within the synaptic cleft, it is most important enzyme yet known to man. More specifically, AChE regulates different functions besides nerve transmissions including worked as an adhesion protein, in neurite growth, as a bone matrix.<sup>43</sup> Above all the implications of AChE in loss of cholinergic response and the amyloid fibrils production in AD patients,<sup>42</sup> makes it more high-flying to be explored. Annihilation of nerve transmission from AChE regulates in both central nervous systems (CNS) as well as the peripheral nervous systems (PNS). However, the reaction locus is different but involving the same mode of hydrolysis. Once the nerves impulses are triggered by the ACh, the hydrolysis process terminates them at the post-synaptic neuronal ACh receptor in CNS, whereas, the nicotinic receptors at the neuromuscular junction in PNS.<sup>46</sup>

### 1.2.2.1 Hydrolysis Mechanism

In response to a potential action, ACh is released in presynaptic nerves that diffuses through the neuron fluid and had to carry the electric impulse to postsynaptic nerves by ACh receptors. At the same moment AChE, which is readily available between the synaptic cleft rapidly hydrolysis this ACh and terminates the ACh receptor gated ion channel and hence, the annihilation of the nerve transmission (Figure 5). The primary function of the PAS is to increase the concentration of ACh in the mouth of the narrow and deep gorge groove; therefore, it ensures the sufficient amount of neurotransmitter (ACh) that readily going to be hydrolyzed.

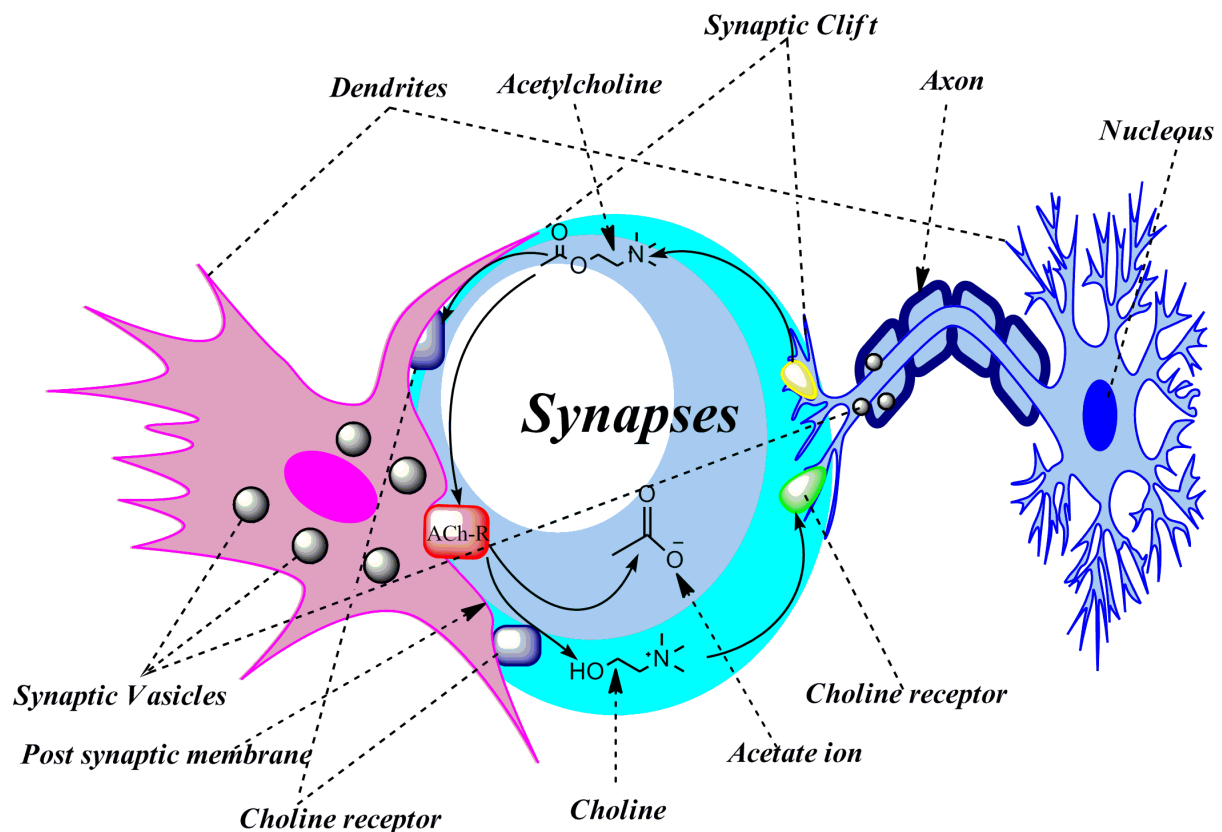


**Figure 5:** Schematic representation of hydrolysis of ACh (acetylcholine) into choline and acetate ion by the action of AChE (acetylcholinesterase) in the synapses.

The mechanism of hydrolysis operates in two steps, the acylation of the active binding site takes place in the first step, and the deacylation follows in the second step, on the same moiety. During the process of hydrolysis, a tetrahedral intermediate state continuously prevails before and after the release of acetate and choline. In the catalytic site, serine residue involve itself covalently with the substrate (ACh), however, other two residues (glutamic acid and histadine) most of the time act as proton acceptor/donor and provide the support to the tetrahedral type of intermediate.<sup>43, 44, 47</sup> After the acylenzyme generation further mechanistic phase completes by using a conserved water molecule within the system—leading all the way back to the unbound state of the enzyme by deacylation process. In addition, there are some researchers who claimed that the ACh exists in larger concentration and gets implicate with the PAS site as well, with all kind of AChEs and specifically, forms the Michaelis complex as result of acylation. This kind of ACh implication is common where; the existence of either steric blockade or some charge repulsion exists, might lead to the enzyme inhibition.<sup>48, 49</sup> The detailed mechanism of the acylation and deacylation that predominantly involves in this process is shown schematically in Figure 6. There are also crystal structures evidential proofs that suppose in the presence of a steric hindrance because of aromatic residues, which make CAS too narrow that is enough to accommodate the ACh, for instance.<sup>50, 51</sup> On the other hands, the molecular dynamics believes in the formation of some gate that opens and close rapidly and allowing entering and exiting the substrate easily.<sup>52,</sup><sup>53</sup> AChE possess remarkably catalytic activity that can approach up to the degradation of approximately 25000 molecules per AChE unit, and hence, almost near to diffusion-controlled reactions.<sup>54, 55</sup>

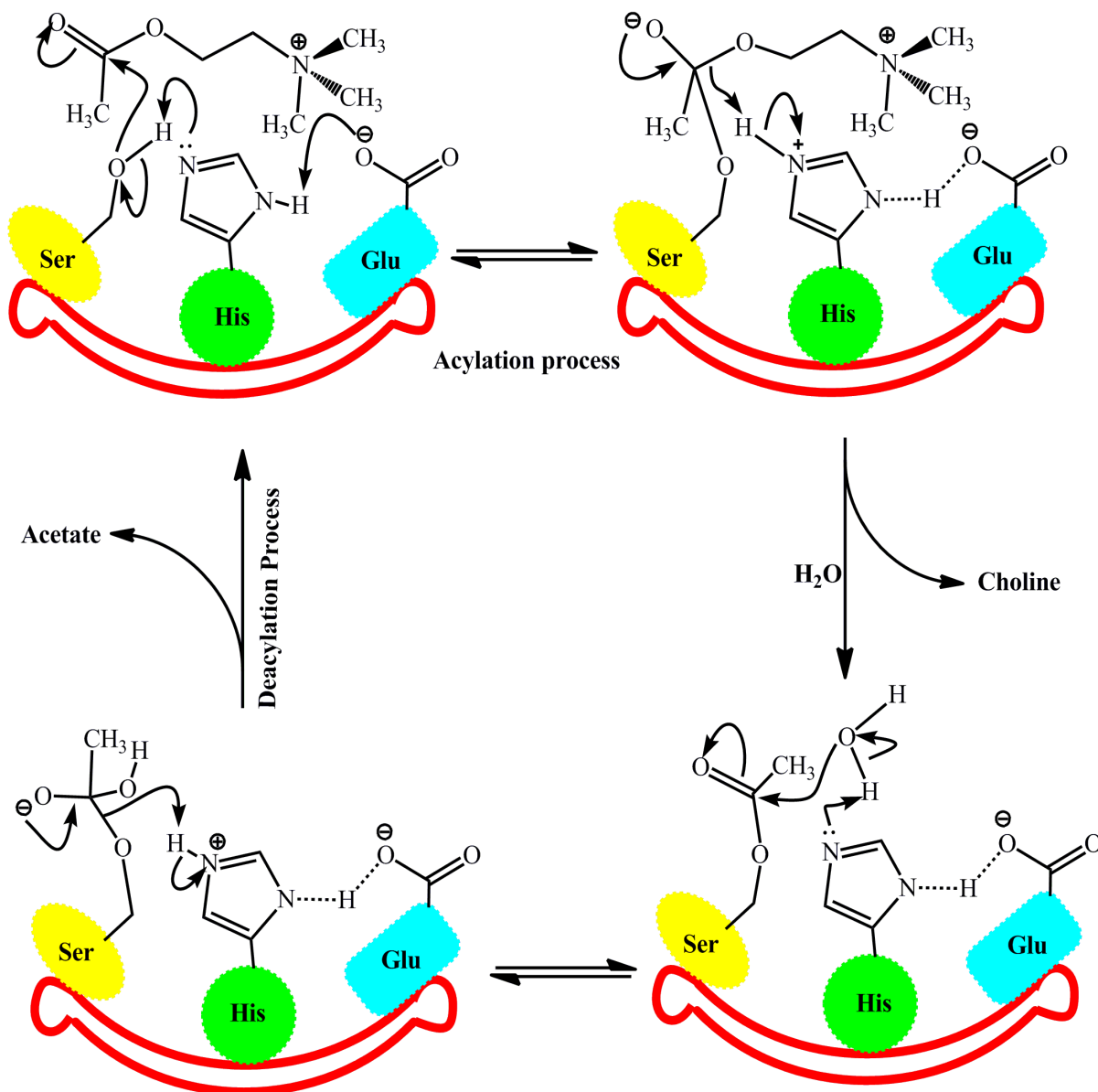


**Figure 6:** Schematic representation of Hydrolysis of ACh into Choline and Acetate ion by the action of AChE in the synapses, which operates in two steps: 1) acylation and 2) deacylation as characterized elsewhere.<sup>43</sup>

### 1.3 Inhibition of AChE

The AChE inhibition is quite important in controlling different lethal diseases that associated with the activity of AChE. Therefore, the type of compounds, which stops/terminates the activity of AChE, is called the inhibitor/anti-cholinesterases. The AChE inhibitors mainly work, not all the

time, safely in termination the AChE activity and increasing the duration and level of ACh in the synaptic cleft, for an instant.<sup>47</sup> However, in some cases, the inhibition becomes challenging especially while dealing with irreversible inhibitors without having an idea of detaching the inhibitors after their function. Therefore, based on the function the inhibitors they can be divided into two groups: irreversible and reversible. Pharmacologically reversible inhibitors are further sub-divided into competitive or non-competitive that are mostly used for therapeutic purposes. However, irreversible are deemed to be toxic and used, mostly, as an AChE activity modulators.<sup>47</sup>

### **1.3.1 Reversible Inhibitors (competitive or non-competitive)**

Reversible inhibitors have a significant role in pharmacological manipulations related to AChE activity. While treating different types of dementia, AChE inhibition is a special area of interest from various aspects. For instance, inhibition of AChE remains a core issue whether targeting neurological disorders or some muscular activities or chemical warfare nerve agents (CWA).<sup>43</sup> Therefore, among inhibitors, the reversible inhibitors that have nowadays been applied for various diagnostic or treatments purposes such as AD, myasthenia gravis, bladder distension, postoperative ileus, glaucoma, as well as antidote to anticholinergic overdose.<sup>47</sup> Among reversible inhibitors, Tacrine was the first of the AChE inhibitors approved by the FDA (US. Food & Drugs Administration) for the AD treatment in 1993, however, later on its use has been abandoned because of side effects issues related to hepatotoxicity.<sup>56, 57</sup> However, Donepezil, Rivastigmine, and Galantamine are among others AChE reversible inhibitors who got the approval of FDA and EMA (Europeans Medicine Agency) to be used in the treatment of AD.<sup>47</sup> Most of the time the Donepezil has been used for the treatment of moderate AD symptoms, however, in some researches; it has been used for the patients with severe AD. In addition to these receptors, the Memantine was also considered as NMDAR (*N-methyl-D-*

*Aspartic Acid Receptor*) antagonist.<sup>58, 59</sup> Rivastigmine is powerful carbamate inhibitors that inhibit not only AChE but also the BuChE, as well, an unlike behavior to donepezil. Chemical structures of the few reversible inhibitors are in Fig. 7.

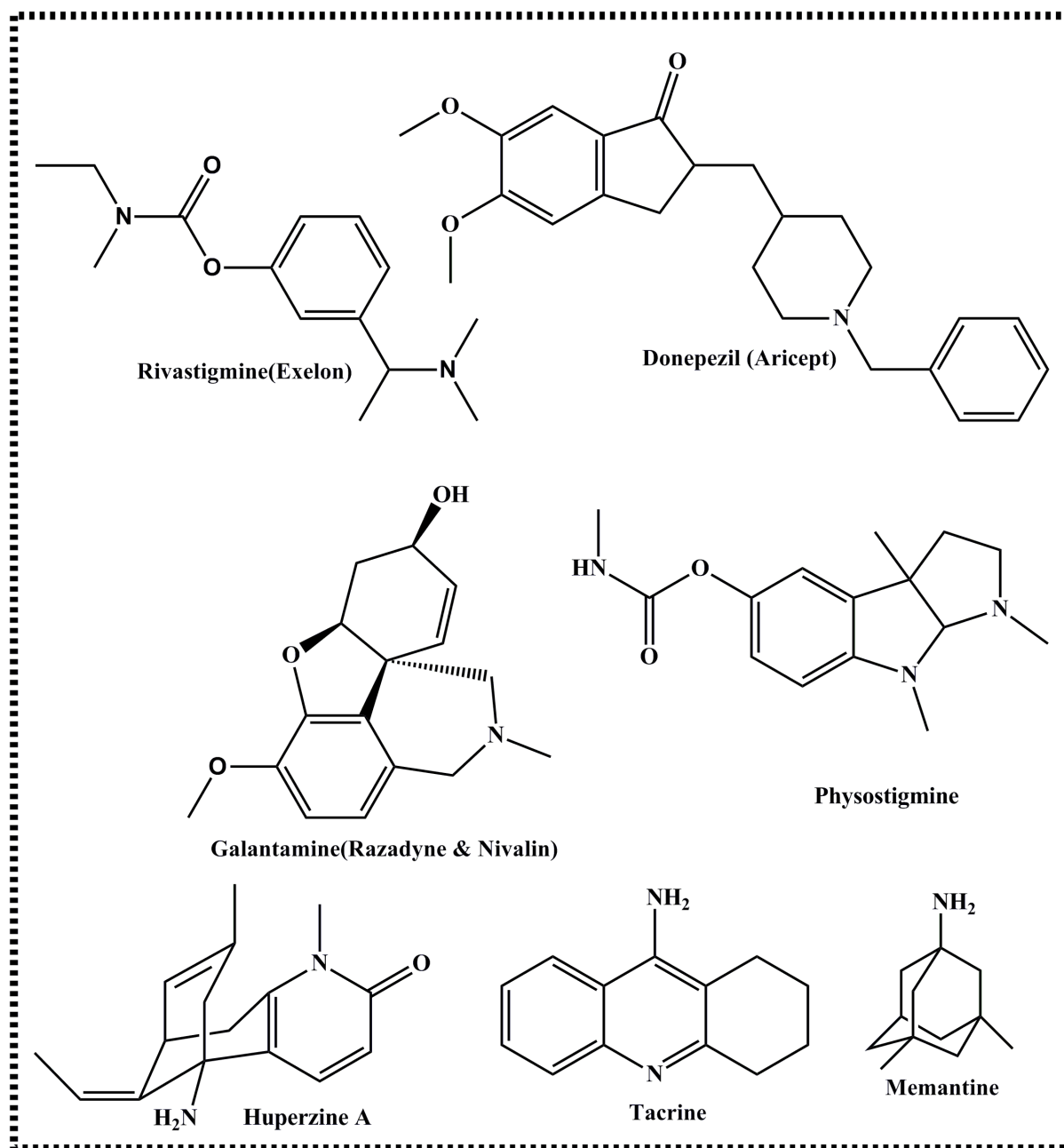


**Figure 7:** Structures of some of the important reversible inhibitors that used in the pharmacotherapy of AD.

### 1.3.2 Irreversible Inhibitors (Organophosphorus Compounds OPs)

The discovery of the OPs compounds as AChE inhibitors lead to a new era in both pesticides development and also in CWA. The organophosphorus compounds are the esters or thiol groups of the compound, which are derived from the Phosphoric, phosphinic, phosphonic, and phosphoramidic acids with the general structure provided in Figure 8.

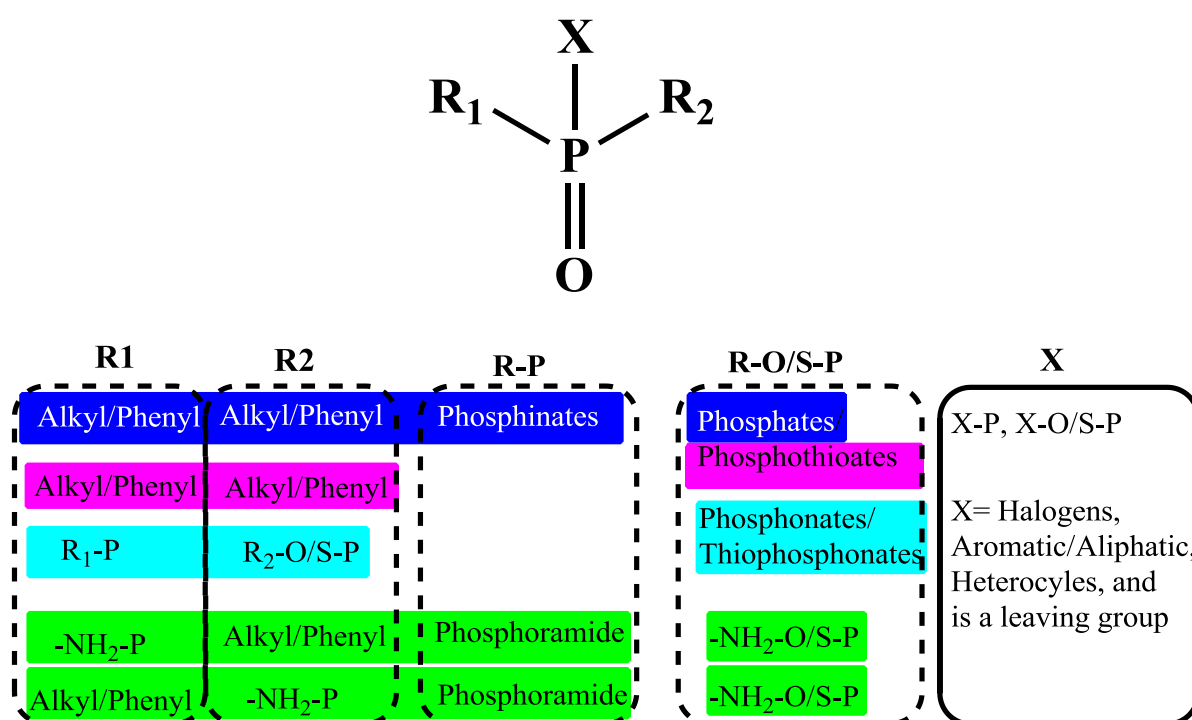


**Figure 8:** General structure and classification of OPs AChE irreversible inhibitors.

In the agriculture and medicine parlance, organophosphates (blue highlighted in Fig.8) are the compounds most often used as insecticides and CWA.<sup>60</sup> In accordance with the scheme presented in Fig. 8, the OPs compounds may have the alkyl or phenyl substituent that can be directly linked to central phosphorus atom or either through indirectly by oxygen or sulphur atom.<sup>47</sup> Moreover, the only **R<sub>2</sub>** substituent can make a bond indirectly through central phosphorus by an

oxygen or sulphur group while  $R_1$  remains directly linked, for an instant, in the case of phosphonates or thiophosphonates. Similarly,  $R_1$  and the  $R_2$  group can be replaced with a primary or secondary amine group that in turn can also make direct or indirect bond to central phosphorus. The symbol  $X$  represents the leaving group that may be any kind heterocyclic, aromatic or aliphatic group, and more, importantly, can be bonded directly or indirectly through oxygen or sulfur.<sup>47</sup>

The irreversible inhibitors are analogous to the ACh molecules and enter into the CNS system where they bond themselves covalently with the serine-OH residue of the active site, and thereby phosphorylation occurs in the AChE. This irreversible phosphorylation causes the acute toxicity to the CNS.<sup>47, 61</sup> Moreover, this phosphorylated AChE remains unable to hydrolyse the ACh which, causes an accumulation of this neurotransmitter in the synaptic cleft and hence, an over stimulation occurs in both muscarinic and nicotinic ACh receptors. As these ACh receptors are involved in pulse transmissions, therefore, create problems. Some of the examples that are associated acute poisoning are muscles weakness, agitation, sweating, etc., and the severe case may lead to confusion, unconsciousness, and even death.<sup>62, 63</sup>

The reaction of OPs with the AChE is similar to that of hydrolysis process of ACh in its initial stages. However, once the adduct of the OPs and AChE is formed, the reactivation of the enzyme is taken place either through water or in the presence of oxime re-activator. To rejoice the enzyme activity depends upon the structure of OPs, the spontaneous hydrolysis with water or oxime treatments. Another important process, which carried out while this OPs-AChE adduct formed and is known as aging. During this OP-AChE adduct intermediate the dealkylation takes place that forms a phosphyl anion in the active cavity of AChE, this is known as aged-AChE. The stability of this aged-AChE mostly depends upon the hydrogen bonding between the histadine residue and the



phosphyl anion (Figure 9). In this situation, the nucleophilic attack of the oxime to the adduct remained fruitless and prevented by hydrogen bonding.<sup>64</sup>

Examples of the some of the OPs compounds, which are most commonly used as an insecticides, CWA, and some pharmacological purposes, are shown in Figure 10.

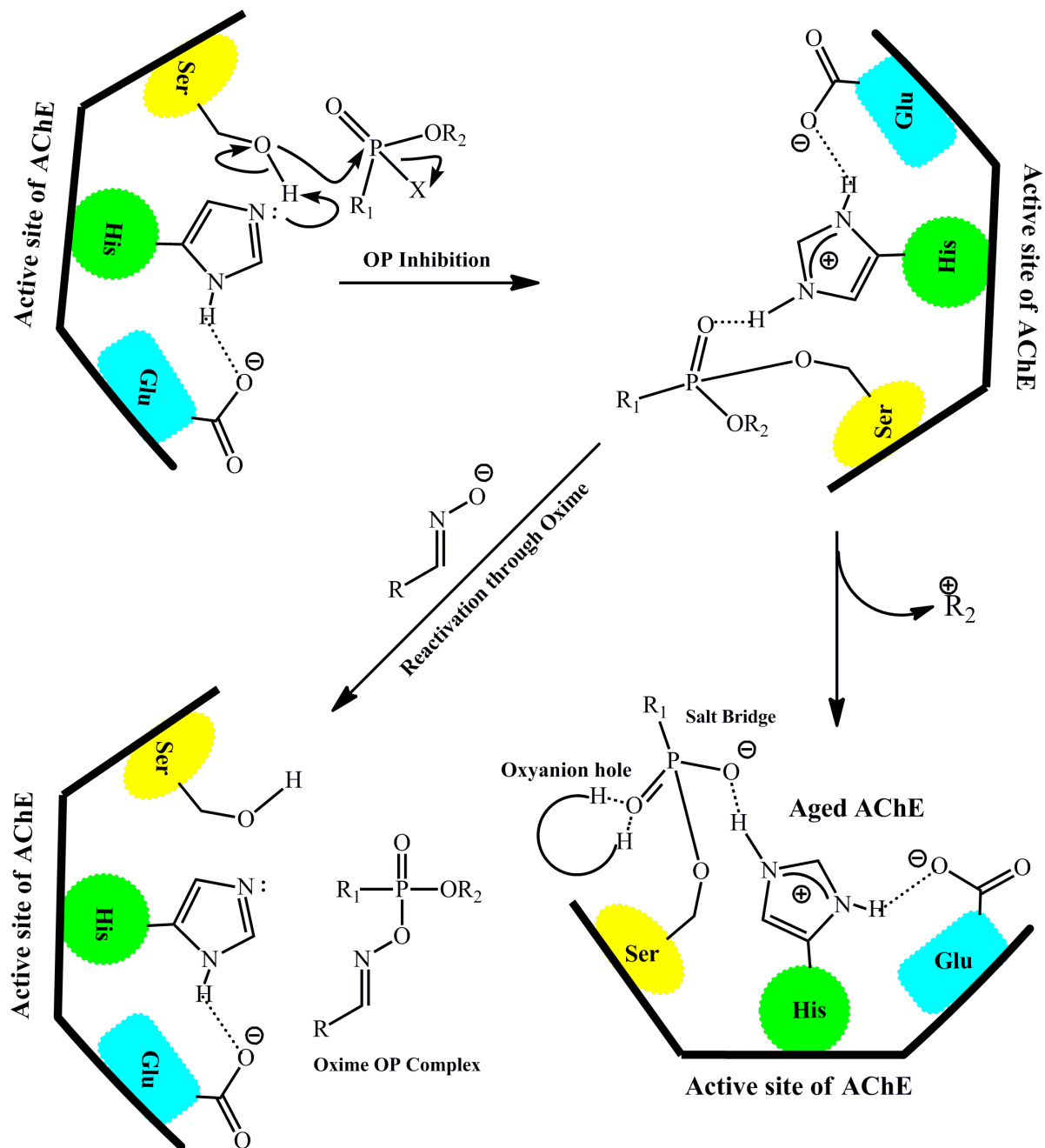


**Figure 9:** Schematic representation of AChE inhibition through OPs, the formation of aged AChE, and reactivation by oxime as explained elsewhere.<sup>47</sup>

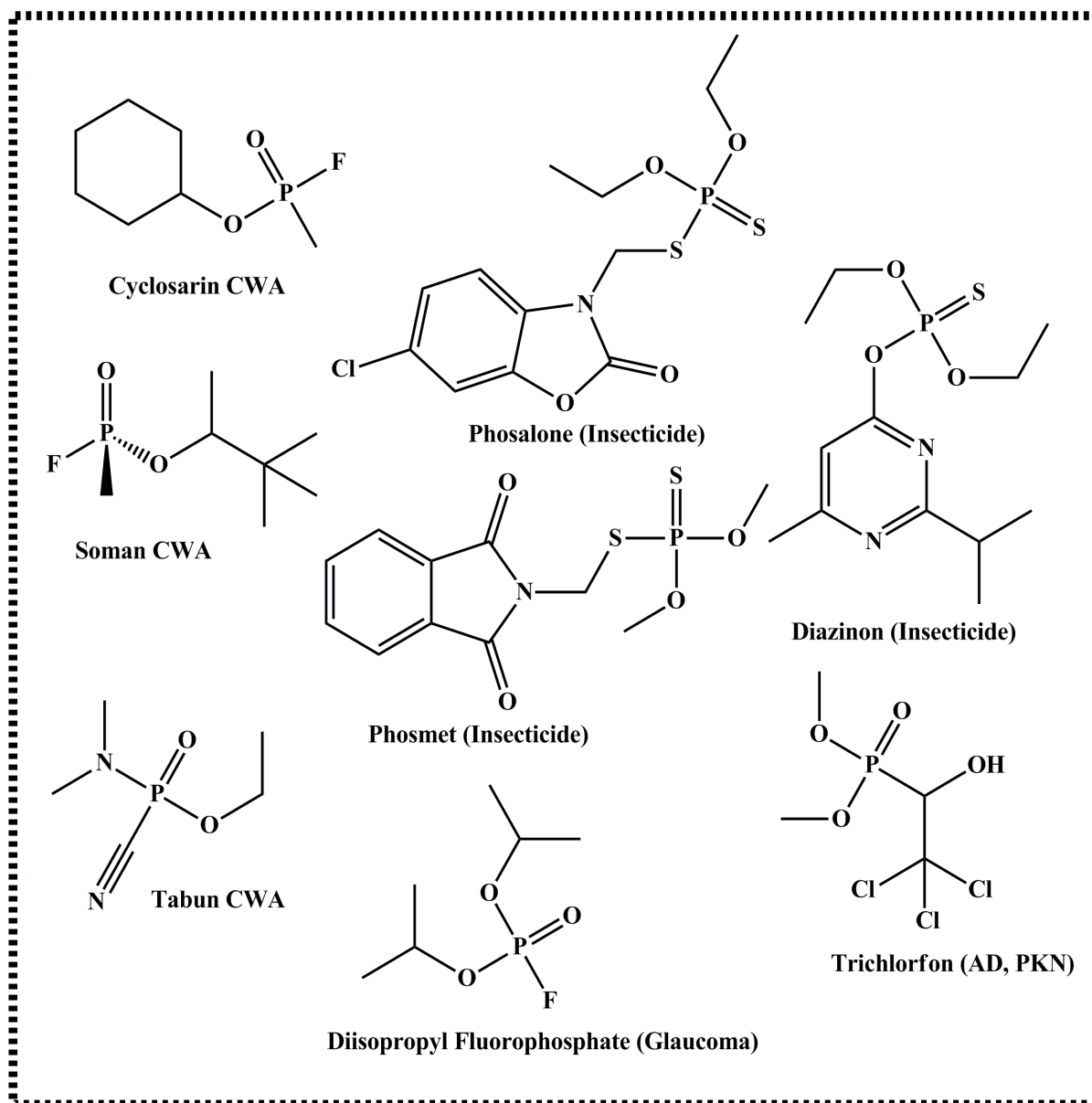


**Figure 10:** Structures of some of the important irreversible OPs inhibitors that used in Insecticides, Chemical War nerve Agents (CWA), AD and Parkinson's disease (PKN).<sup>47</sup>

## 1.4 Nuclear Magnetic Resonance and Drug Discovery

### 1.4.1 Nuclear Magnetic Resonance

The phenomenon of the NMR has been established, about 70 years ago, first by the two independent groups in 1946,<sup>65, 66</sup> and just six years later, for this new and progress achievements they awarded in common a noble price. Since then, it has been successfully applied in different areas of the science as an analytical tool in industry as well as in academics, including: medicine, chemistry, biology, biochemistry, materials science and geology etcetera. However, before the last two decades, NMR has gained widespread acceptance as a pervasive tool for the structural characterization of the small compounds (natural or synthetic compounds, and metabolites) to macromolecular assemblies.<sup>67</sup> Besides this structural characterization, this emerging field of science also got valued in the analysis of macromolecular and supramolecular dynamics and, as a tool to see the static and transient state in the proteomics.

From last two decades or more, nuclear magnetic resonance spectroscopy prejudiced much more the recognition studies because the molecular recognition lies at the center of all life process. Since, most of our body processes based on the complex interaction mechanism, therefore, these interactions existing amongst the protein-protein or ligand-protein or inhibitor-enzyme are very important, for instance. NMR has an upper edge over the other spectroscopic techniques, involving binding interactions, in being detecting the binding at sub-atomic level with greater sensitivity and without the requisite knowledge of any prior function of the protein.<sup>68</sup> This is not enough here, NMR also helps in the optimization process of the hits into leads through providing the structural information of both ligands and receptors as well, those linked to one another through a loosely binding. Furthermore, group epitope mapping aids in the information related to the binding conformations within the complex; which part

of the small molecule is attached to which part of the target. Therefore, on the basis of the information that can provide the nuclear magnetic resonance, there are two types of the binding approaches available up to date.<sup>69</sup> 1) ligands-based 2) receptor-based studies. The scope of the binding interactions is so broad, in sense of NMR applications, that to cover both types of screening is impossible within this thesis; therefore, the basic concern of this project would focus only the ligand-based screening.

#### 1.4.1.1 NMR working principle

An atom consists of two parts, the electrons, and nucleus, which further comprises nucleons. However, the basic principle of the NMR related to the nucleus that exhibits magnetic moments ( $\mu$ ) and nuclear spin ( $I$ ). All nucleus holds nuclear charge and rotation around its own axis. According to the classical physics, all particles having charge and continues motion (angular momentum) can generate a small magnetic moment, which interacts with an external applied magnetic field ( $B_o$ ). Therefore, this magnetic moment  $\mu$  for a particular nucleus can be expressed as

$$\mu \propto I \cdot \rho \quad (1)$$

$$\mu = \gamma I \cdot \rho \quad (2)$$

Where,  $\gamma$  is gyromagnetic ratio, is a constant depends upon the characteristic of a particular nucleus and,  $\rho$  is the angular momentum of the nucleus. The relationship between the magnetic moment and angular momentum is given by the equation 3, where,  $m$  represents the magnetic quantum number. Since spin quantum numbers depend upon the magnetic quantum as  $m = (2I + 1)$ , it means if anyone knows the spin quantum number can easily calculate the magnetic quantum number, therefore,

$$\rho = \frac{h}{2\pi} m \quad (3)$$

Hence, the equation 2 can further be modified accordingly as under,

$$\mu = \gamma \cdot \frac{h}{2\pi} m \quad (4)$$

However, the magnetic resonance arises from the only nucleus with  $I \neq 0$ , so when such a nucleus is placed under the influence of the external magnetic field. Here,  $\mu$  is a quantize value and can have certain specific values, which can be calculated from  $m$  values. Most routinely used nucleus for the NMR are having  $I = 1/2$ , means nucleus having two spin quantum numbers;  $+1/2$  and  $-1/2$  and, including the  $^1\text{H}$ ,  $^{13}\text{C}$ ,  $^{15}\text{N}$ ,  $^{19}\text{F}$  and  $^{31}\text{P}$  etc. The energy distribution (difference) between the two spin states depends upon the magnetic strength applied, larger the magnetic field greater will be the difference and, vice versa. The energy of the magnetic dipole of the nucleus under the static magnetic field ( $B_0$ ), can be written as

$$E = \mu \cdot B_0 \quad (5)$$

By putting the values of the magnetic moments  $\mu$ , from equation 4, the relation between the energy and magnetic field become clear as

$$E = \gamma \cdot \frac{h B_0}{2\pi} m \quad (6)$$

The static magnetic field along the z-axis turns this equation as

$$E = \gamma \cdot \frac{h B_z}{2\pi} m \quad (7)$$

Therefore, from the equation 6 and 7 the nucleus having +1/2 system can be calculated as,

$$m = (2I + 1)$$

Hence, by adding the value of  $I = 1/2$ ,

$$m = (2 \left( +\frac{1}{2} \right) + 1)$$

$$m = (1 + 1) \gg = 2 \quad (8)$$

There are two possible spin states exist for the nucleus with 1/2 spin as shown in figure 11, the energy can be calculated as

$$\Delta E = (E_2 + E_1) \quad (9)$$

$$m_1 = \left( +\frac{1}{2} \right)$$

$$m_2 = \left( -\frac{1}{2} \right)$$

$$E = \gamma \cdot \frac{h B_0}{2\pi} \cdot \left( +\frac{1}{2} \right) \quad \text{for } m_1 \text{ state} \quad (10)$$

$$E = \gamma \cdot \frac{h B_0}{2\pi} \cdot \left( -\frac{1}{2} \right) \quad \text{for } m_2 \text{ state} \quad (11)$$

Similarly, for the spin state  $I = 1$  for instance deuterium, there will be 3 energy states or the magnetic number and so on. So, by putting the values of  $m_2$  and  $m_1$  in equation 9 the energy difference of the half spin system can be calculated as

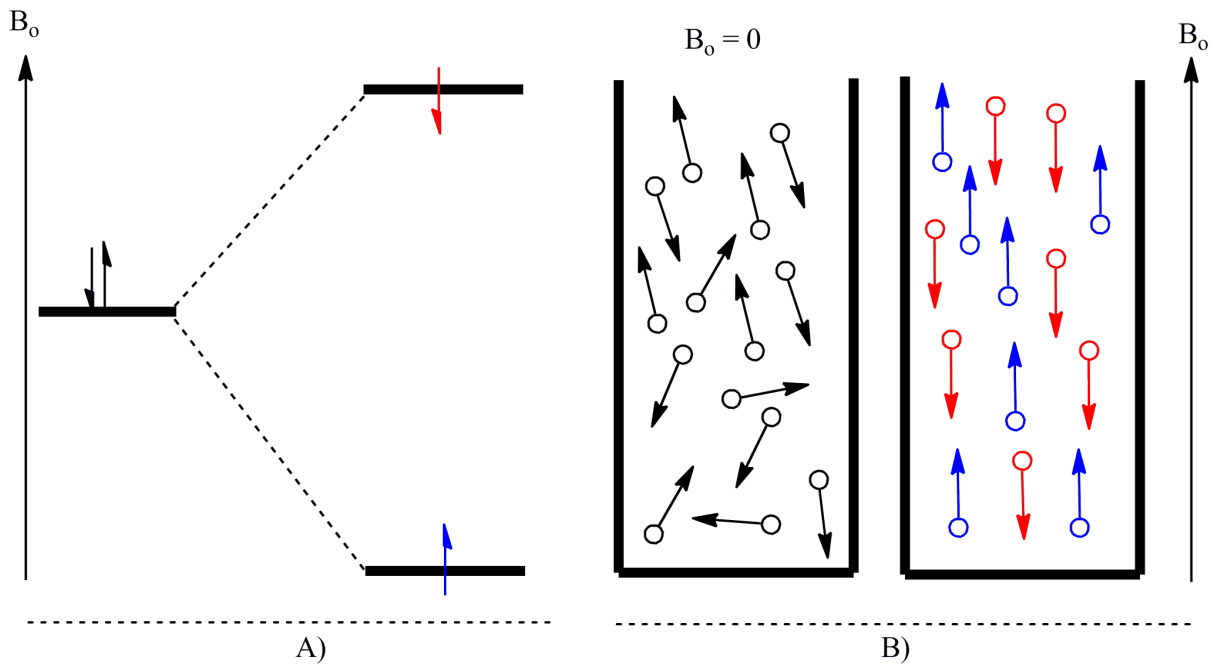


**Figure 11:** A) Energy level diagram for  $\frac{1}{2}$  spin state nucleus, B) Orientation of protons in the absence ( $B_0 = 0$ ) and in the presence of magnetic field  $B_0$ .

$$\Delta E = \gamma \cdot \frac{h B_0}{2\pi} \cdot \left(+\frac{1}{2}\right) - \gamma \cdot \frac{h B_0}{2\pi} \cdot \left(-\frac{1}{2}\right) \quad (12)$$

$$\hookrightarrow \Delta E = \frac{\gamma h B_0}{2\pi} \quad (13)$$

The direct relationship between the energy difference between the spin states to the applied magnetic field represents the larger the magnetic field greater will be the difference in energies of the nucleus, moreover, when there will be no magnetic field there is no energy differences between the spins, both will be equal and  $\Delta E = 0$ .

Once the nucleus is placed under the static homogeneous magnetic field, the establishment of the two would take place, the transition between these two spins energy states can be set up by the use of proper energy in the form of radiofrequency ( $\nu$ ).

According to the Max-Planck equation of energy,

$$E = h\nu \quad (14)$$

By combining the equation 13 and 14 frequency responsible for the absorption can be calculated,

$$\hookrightarrow E = h\nu = \frac{\gamma h B_0}{2\pi} \quad (15)$$

Therefore, by canceling Planks constant from the both sides of the equation 15, provides the actual NMR equation that explains the resonance phenomenon.

$$\Rightarrow \nu = \frac{\gamma B_0}{2\pi} \quad (16)$$

In the above equation 16 there are two variables, 1) frequency and 2) magnetic field, which affect the resonance. Resonance is possible by manipulating either of them (variables) and keeping other ones constant, which is known as *Continuous Wave Spectrometry* (CWS)—no more available, especially in structure elucidation.<sup>70</sup> If the frequency was varied while keeping the magnetic field constant, is called *Frequency-Sweep* method, and, on the other hand, if the frequency is kept constant and magnetic field was altered then this would call *Field-Sweep* method. Nowadays, FT (Fourier Transform) instruments have superseded CWS.

#### 1.4.1.2 Boltzmann distribution/ Energy population

Now consider the energy levels  $E_2$  and  $E_1$  to  $N_\beta$  and  $N_\alpha$ , respectively and, in another way, the  $N_\alpha$  is the excited state or the number of protons that align the external field and  $N_\beta$  are the protons in the ground state or that are antiparallel to the applied magnetic field. The distribution of the energy levels can be represented by Boltzmann equation as



$$\frac{N_{\alpha}}{N_{\beta}} = e^{-\frac{\Delta E}{KT}} \quad (17)$$

The combination of equation 13 and 17 gave the idea about how the NMR signals come into being

$$\frac{N_{\alpha}}{N_{\beta}} = e^{-\frac{\gamma h B_0}{2\pi KT}} \quad (18)$$

Where,  $\gamma$  is the gyromagnetic ratio;  $K$  is the Boltzmann constant, and  $T$  is the temperature. By adding the values of the strength of the magnetic field, applied along with the others constant gave the minute difference of energy populations between the two (excited and ground) spin states—makes NMR relatively insensitive technique. Conversely, when both the excited and the ground states equal in their energy populations then, there will be no signal at all and, the condition is called the saturation.

Apart from the aforementioned factors, some other features may have some significant implication in a better NMR signals, including; proper and right providence of the radiofrequency pulse, proper relaxation of the excited nucleus after the pulse applied, and the effect of the shielding and deshielding etcetera. The focus of the dissertation is to observe the interaction between enzyme and inhibitors through NMR, which will be discussed in detail in the later sections.

## **1.5 NMR as a toll for ligand-receptor interaction studies**

The Human body is a unique gift of God, complex in its structure and having diversity in its functions. However, intermolecular recognition processes mainly control all functional diversities. In fact, these molecular recognitions are responsible for the maintenance, regulations as well as the progression of the body. Therefore, these recognitions could be involved the ligand-receptor or receptor-receptor type of molecular interactions that implicate in the

physiological events.<sup>68</sup> In this viewpoint, the events involving the ligand-receptor interaction are focused, highlighted and explored by using the nuclear magnetic resonance will be remained the core of this thesis. More importantly, it would not be so easy to see the physio-chemical changes, involve in this ligand-receptor interaction without the in-depth observations up to an atomic level. Thus, high-resolution NMR is the most promising solution to see these changes, which rely on the comparison of the free and bound states of the molecule.<sup>71</sup>

In this context, the use of the high-resolution NMR has extensively been applied in the past few years to monitor the molecular recognitions in drug discovery, chemistry, biochemistry, cell biology and chemical biology as well.<sup>67, 72</sup> Nowadays, a number of NMR methods that are being used in the academics as well as in industries for this purpose. However, there is still an open challenge available for the scientist working in this domain for the further development of new NMR methods to unravel the problems associated with this interesting recognition process.

NMR is a most powerful tool used for the characterization of ligand-receptor interactions under physiological conditions especially; where many physical techniques might be unable to give any answer because of the inherently weak and transient binding and even, where ligand-receptor complex does not exist as a single crystal form.<sup>72</sup> The affinity constant values of NMR methods, which spanning between the nM to mM ranges have contributed well in the molecular recognition process.<sup>68, 72, 73</sup> Nuclear Magnetic Resonance has therefore become an ideal choice for both screening purposes and to see the Structure Activity Relationship (SAR) towards the efficacy of drug discovery.<sup>72</sup>

In NMR, the binding events can be monitor through the changes observed in both ligands and macromolecular parameters. Therefore, on the basis of the method observed, this screening and characterization can be either ligand-observed and/or receptor-observed methods.<sup>68, 69</sup> The parameters that are

affected by this process are the rate of relaxation, the chemical shifts, the diffusion coefficient values, and intermolecular NOEs. Thus, there are a number of NMR methods available to-date, which are responsible for detecting changes within the ligand-receptor complex system including, STD NMR, ILOEs, INPHARMA, DOSY NMR,  $T_1$  and  $T_2$  Relaxation methods, WATERLOGSY, Line Broadening methods, heteronuclear experiments ( $^{13}\text{C}$ ,  $^{15}\text{N}$ ) etc. So, based on the perturbations a ligand/macromolecule receives, the NMR detection principle can be utilized either ligand-observed or macromolecule-observed methods.

### 1.5.1 Receptor-based NMR screening methods

To identify the specific binding from the non-specific ones, receptor-based NMR methods are used, however, among those, the chemical shift changes is easiest to follow the perturbations as result of the ligands addition into the macromolecular solution.<sup>72-74</sup> More importantly, even a three-dimensional structures of the macromolecules can be resolved with the help of receptor-based methods like  $^{13}\text{C}$  and  $^{15}\text{N}$ -HSQC.<sup>74</sup> The dissociation constant ( $K_D$ ) calculation is also possible, usually by using an equimolar concentration of protein and ligands.<sup>75</sup> In this way, the binding locus of the small molecule can be tracked within the binding cavity of the protein through observing the chemical shift changes in the macromolecule.<sup>69</sup> Nevertheless, there are few constraints present in using these methods e-g., need of isotopically enriched protein; the size should not exceed than the 50 KDa e-g., for SAR through NMR,<sup>76</sup> apart from highly soluble protein and the long run time of experiments. A high affinity ligand could be sort out through the process known as SAR (Structure-activity-relationship) by NMR through the landmarks available from an already available weak ligand for a specific target.<sup>72</sup> This approach provides a way to produce a high-rank lead by combining the results from all chemical

linkers. In addition to the augmentation of lead affinity, these SAR by NMR methods also help in finding the bidentate ligands as well.<sup>77, 78</sup>

On the other hand, ligand-based NMR methods are widely used to see the interactions, although observing both specific and non-specific bindings. Nevertheless, none of the ligand-observed method demanding a labeled protein, a high solubility or size limits of protein important for receptor-based NMR screening. By considering a broad applicability of these methods, rely the changes in ligands will be focused, highlighted and explained in this thesis.

## **1.5.2 Ligand-based NMR screening methods**

In NMR parlance, ligand-observed methods can further be characterized based on the nature of observance they offer, for example, relaxation-based NMR methods, NOE-based methods, Magnetization-transferred NMR methods and diffusion-dependent methods. Following sections of this thesis will discuss each method thoroughly with appropriate examples.

### **1.5.2.1 NOE-based methods**

Nuclear Overhauser Effect Spectroscopy (NOESY) is well established for its characterization of macromolecules,<sup>73</sup> in mixture screening<sup>79</sup> and also for observing the interaction studies.<sup>68, 69, 71</sup> As a tool to see the interaction within a complex system, including ligands and macromolecule depends upon the changes in parameters of the free state ligand as compared to bound state ligands. Therefore, upon binding, a ligand shows various behavioral changes that can easily be detected through nuclear magnetic resonance spectra. These changes include relaxation parameters, change in correlation times as well as the tumbling rates.<sup>71, 80</sup>

### 1.5.2.2 Principle of Tr-NOESY experiment

A small molecule of size (1-2 KDa) in the presence of a substoichiometric amount of protein has been taken into a uniform solution and then the spectrum is recorded under chemical equilibrium. Since this experiment based on the transfer of spin relaxation of smaller ligand while inbound state to the free state, therefore, another spectrum comprising only the ligand molecule is also necessary for comparison. Smaller molecule moves fast possess fast tumbling rates, large relaxation rates and short correlation time, which is responsible for the weak positive NOEs at slow rates (Figure 12).<sup>68, 69, 71</sup> Whereas, larger molecules possess small tumbling rates, large correlation time and short relaxation that leads to strong negative NOEs with fast development rates.<sup>81</sup> Therefore, when a small molecule binds into a macromolecule cavity it adopts the small tumbling rate of that macromolecule during this transient bound-time and hence, provided a negative NOEs in Tr-NOESY spectrum—a characteristic of macromolecule.<sup>82</sup>

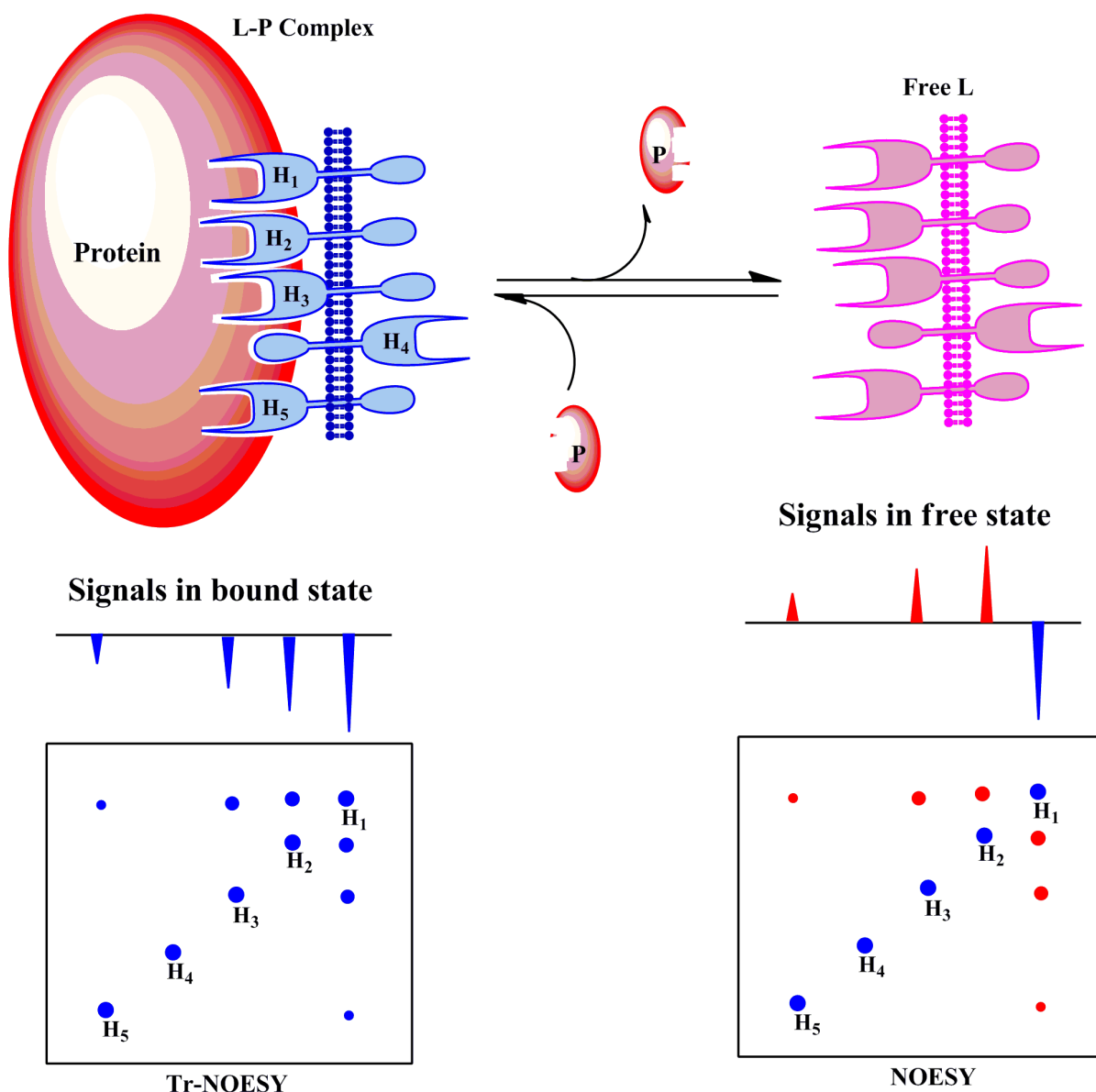


**Figure 12:** The schematic representation of Tr-NOESY experiment, showing the sign of NOE through the ligand-receptor exchange system, as shown elsewhere.

80

However, a major disadvantage associated with Tr-NOE related to the fast  $K_{off}$  rate ( $K_{off} \gg$  relaxation rate), which is necessary for a successful experiment; otherwise, the necessary information will be lost through relaxation process before the dissociation of the small molecule with the receptor.<sup>80</sup> In Tr-NOESY spectrum, the binding molecules can therefore be characterized by cross peaks, which showed change in their sign in the presence of macromolecule, on the

other hand, the cross peaks of the non-binding molecules either vanish or reduce and possess the same sign to the diagonal as shown in figure 12.

The Tr-NOESY experiment can successfully be applied to a complex system of the possible discrimination of the binders from the non-binder ones, where the significant structure similarities exist between the ligands that might lead to overlapped signals otherwise.<sup>83</sup> Moreover, the conformational changes of the ligand at receptor's binding site can be deduced perfectly on the basis of the Tr-NOE experiments. Another advantage that this experiment provided is the requisite of small amount protein/macromolecule/receptor, which usually in the mM amount with the 1:5 to 1:50 ratio of protein versus ligand excess.

In a particular situation when two ligands having similar residence times, bind simultaneously to adjacent sites of the receptor and forming a ternary complex with receptor, providing a strong ligand-ligand NOEs called as ILOEs (Inter-ligand NOEs).<sup>84-86</sup> However, NOEs cross peaks are detected for all involving ligand pairs with such effects; therefore, it could lead insufficient information related to ternary complex, alternatively this represents the relative orientation of the two ligands.<sup>87</sup> Parallel to ILOEs another variant of NOE effect also exists, known as ILOE for pharmacophore mapping (INPHARMA).<sup>88</sup> However, the mixing time is the only parameter that might discriminate between the INPHARMA, ILOEs and other NOESY-based experiments. Usually, 70 ms of the mixing time found to be paramount for the INPHARMA, whereas, for Tr-NOESY this can be varying between the 150-600 ms depending upon the nature of the small molecule. On the other hand, in ILOEs this mixing time can be even longer than Tr-NOESY experiments.<sup>81</sup>

### **1.5.3 Saturation Transfer Difference (STD) NMR:**

From the past sixteen years or so, saturation transfer difference has successfully been applied in academic as well as in industries. STD NMR

method permits in deducing a clear discrimination between the interacting and non-interacting ligands towards the protein. It a fast and robust NMR method to observe binding of ligands to protein, which in favorable conditions, can also provide information related to epitopes as well as the binding conformations.<sup>68,</sup>  
<sup>69</sup> More importantly, the calculation of the dissociation constant values ( $K_D$ ) of the weakly binding ligands are also feasible within the range of  $10^{-8}$  to  $10^{-3}$  molar.<sup>68, 69, 81</sup> Like Tr-NOESY, STD NMR also rely on the magnetization transfer from the bound hydrogen to the free ones.<sup>68, 69, 85</sup> Therefore, in term of amount of target used, normally in micromole concentration, STD NMR is even smarter technique than Tr-NOE experiments.<sup>81</sup>



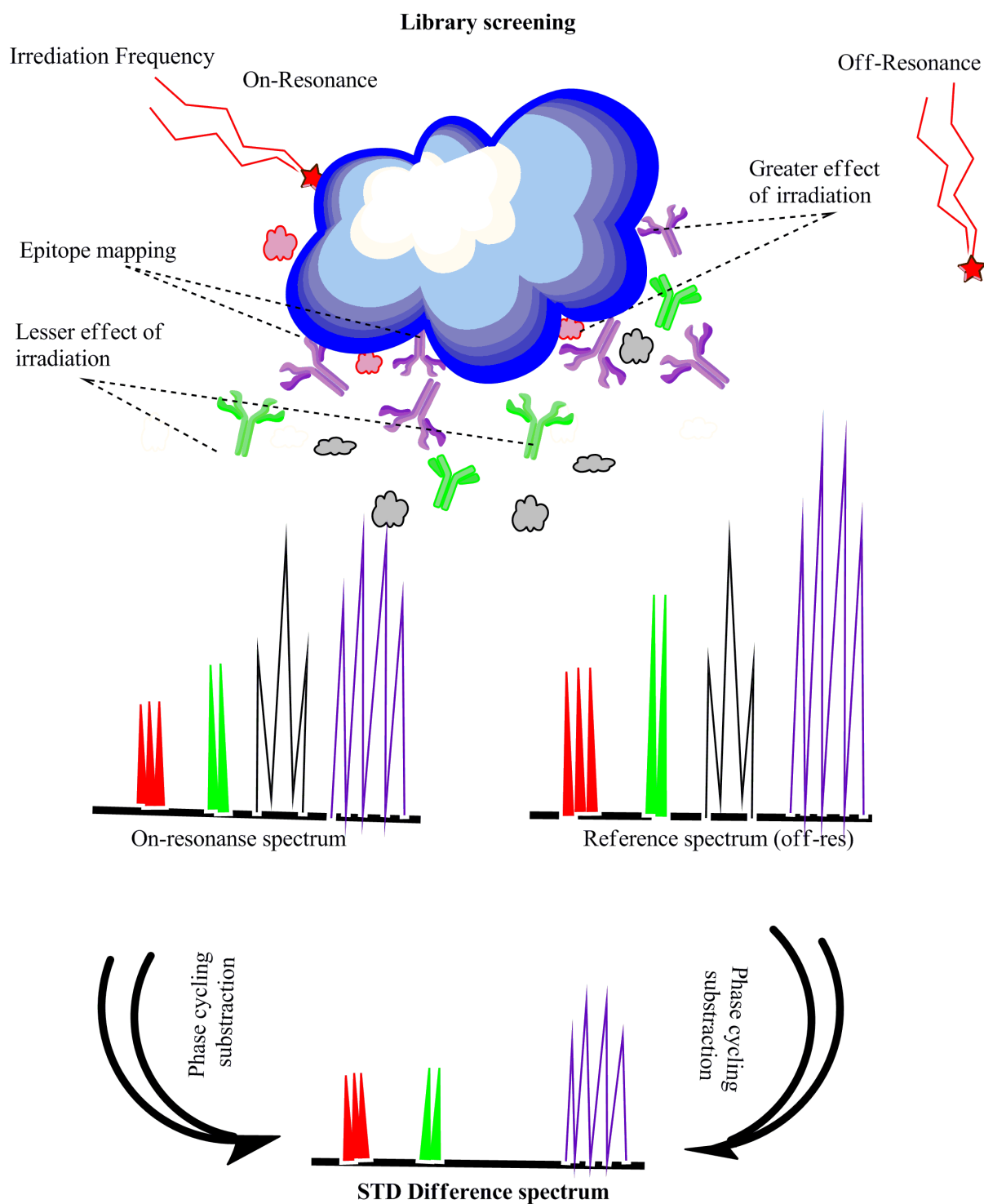


**Figure 13:** The schematic representation of STD-NMR experiment, two FIDs are obtained as a result of selective irradiation of the protein region (*on-resonance*) and non-protein region (*off-resonance*). In the processing, subtraction of the *on-resonance* spectrum from the *off-resonance* by phase cycling is done

that provides the STD difference spectrum, having signals from molecules that bind to the protein only.

### 1.5.3.1 Principle of the Experiment:

Usually, ligands concentrations are kept higher compared to protein concentration (1:100 to 1:1000 (L: P)) because of the large binding pockets of the proteins,<sup>68, 69, 71</sup> to acquire a STD spectrum. Mostly, micromolar concentrations of the protein are utilized in and depend upon the size of the protein. A pseudo two-dimensional experiment is run by selectively irradiating the protein signals, generally not showing interference with any ligand's signal, by the use of a train of soft Gaussian pulses through FR. This FR is referred to the *on-resonance* frequency that was used to saturate the protein molecule. Similarly, an *off-resonance* frequency is also placed away from any signals of protein as well as from ligands signal to ensure the irradiation of the ligands that have not entered within the protein vicinity.<sup>68</sup> The saturation of protein depends upon the saturation times, and the propagation of this affect through entire protein molecule takes place through effective spin diffusion. Then through cross-relaxation effect, ligands molecule entering into the protein vicinity get this irradiation and in turn transfer this saturation to other molecules. At the end of this pseudo two-dimension experiments two types of spectra can be obtained as an outcome, however, a higher number of spectra can also be acquired.<sup>89</sup> In the processing, the only signals that provide interaction are appeared as a result of subtraction of on-resonance spectrum from the off-resonance spectrum through phase cycling as shown in figure 13.

A single experiment with one saturation time is more than enough to the binding of small molecules, however, the use of different saturation times is recommended, especially for quantitative purposes.<sup>68, 90, 91</sup> In addition, it well-understood that the relaxation effect plays an important role in the STD NMR. Therefore, it is better to run relaxation experiment before performing a STD

experiment.<sup>80, 81, 92</sup> Another paramount parameter, which has a greater influence on the results, is the pulse sequence that runs experiments should be a perfect match in term of the requirements of the experiment. A number of pulse sequences are present as provided by different NMR vendors, however, in order to get better and even best spectra, especially, where the problem of overlap exists or need to suppress some unwanted solvent signals, STD sequence is coupled with other pulse sequences. For example selective TOCSY,<sup>93</sup> STD-TOCSY,<sup>94</sup> STD-HMQC/HSQC,<sup>95</sup> STD-WATERGATE,<sup>96</sup> etc.

### 1.5.3.2 STD NMR Applications

Over the last decade, STD NMR has become an emerging tool to identify the ligand-receptor interactions, for screening the natural extracts of unknown compositions,<sup>94, 97</sup> screening carbohydrates towards various receptors,<sup>98</sup> for the calculation of inhibitions constants,<sup>99</sup> to determine the dissociation constants for the weekly binding ligands,<sup>96, 100, 101</sup> for the quantitative purpose,<sup>102</sup> etc. The wide spread of this NMR technique can be attributed to its simple sample preparations, use of small protein amount, no protein size constraint as in the case of FBDD methods, and more importantly, it provides all necessary information underlying binding, conformational and quantitative purposes. A number of reviews are available up-to-date those describing utility of this robust techniques in various area including: fragment-based drug design,<sup>103</sup> recent developments in STD,<sup>104</sup> in carbohydrate recognition towards different receptors,<sup>80</sup> comparisons with different screening methods.<sup>68, 69, 81</sup>

Originally, CORCEMA (Complete Relaxation and Conformational Exchange Matrix ) approach was developed and applied to the NOE experiments, which later on, extended to STD NMR to remove the T1 bias,<sup>105</sup> normally occurs in the calculation of STD effect.<sup>102, 106</sup> This theoretical approach helps in understanding the thermodynamic and kinetics of the binding experiments. CORCEMA-ST approach has been utilized in STD NMR for the

different purposes like quantitative structural interpretation in STD data,<sup>107</sup> for the comparison of building curves with other experimental data available. Additionally, this CORCEMA-ST is best evaluated for the ligands that bind more than one site simultaneously, where the rebinding factors can co-exist.<sup>106, 108, 109</sup>

In order to make the STD NMR more practical in term of solvent signal suppression, another variant was introduced--STDD (saturation transfer double difference).<sup>110</sup> This STDD method was successfully applied to an integrin  $\alpha$ IIb $\beta$ 3 and cyclic-peptide system in 2005. In this case, a second experiment was performed without the ligand addition to removing the STD signals resulting from other recognition events. Furthermore, marine natural products were also screened through this method for the specifically targeting the cannabinoid G-protein-couple receptors CB1 and CB2.<sup>111</sup>

STD NMR is the most routinely used experiment to observe the affinity, structural information and dynamic studies of the ligand-receptor complex since right after the first time application. Therefore, with few core examples with a brief experimental detail this topic is closed since it not possible to discuss completely in this introduction. Nevertheless, after reading the provided references to this method, ones may get the theme of this amazing technique.

#### **1.5.4 WaterLOGSY (Water-Ligand Observed via Gradient Spectroscopy)**

It is a one-dimension experiment, another variant of STD experiment, which provides information related to bound ligand through the bulk water on the surface of the protein. As opposed to STD experiments, here the irradiation frequency is place at the centre of water signal rather than protein signal and secondly, only one frequency is used instead of two as in the case of STD NMR. However, both experiments are same in the transfer of magnetization through

NOE and spin diffusion and hence both experiments based on NOESY effect.<sup>81</sup> The transfer of magnetization takes place either through water surrounding the ligands or through the water in between the ligands and protein.<sup>112-114</sup>

#### **1.5.4.1 Principle of the experiment**

It is a 1D technique based on NOESY experiment, where the gradient was preferred in order to reduce the radiation damping effect, suppression of solvent signals and to enhance the sensitivity of the experiment. During the NOE mixing time, the excited magnetization is transfer to the bound ligand via two mechanisms, e-g., 1) indirectly through water to protein and then from protein to ligands or 2) directly from water to ligands. However, the propagation of this inverted magnetization as a result of WaterLOGSY can be through excited water molecules to proteins mobile protons (amide, hydroxyl etc.) via chemical exchange and then cross-relaxation/ dipole-dipole as well as spin diffusion takes place that affects the bound ligands.<sup>81</sup> In other words, there are two ways how the ligand interacts with bulk water and consequently to protein, first, water-ligand-protein and protein-ligand complex. In the final spectrum, the distinction between the bound and nonbound ligand is very easy and can only be done by observing the signals. The change in correlation time made this possible to be distinguished the bound against the non-bound ligands. The smaller molecules, those get a transfer of magnetization directly from the water generate small NOE changes because both (water and ligands) have short correlation rates and hence, show positive NOE. On the other hand, the ligands that receive magnetization through protein indirectly, due to binding to macromolecule they show negative NOE. Therefore, normal versus opposite signals can be observed in the WaterLOGSY spectrum for the protein-bound and free ligands, respectively.<sup>112-</sup>

114

#### 1.5.4.2 Experimental Conditions:

Ligand concentration is the paramount important thing while selecting the WaterLOGSY experiment because for this experiment ligand to protein ratio should not exceed than the 100: 1 ratio, since it only reflects the bound and free ligand state.<sup>69, 81</sup> Second important parameter is the NOE mixing time, it should be longer enough to get the proper spin diffusion. Therefore, it recommended that mixing time should be between 1-3 s. A number of best pulse sequences are present however; recently two new pulse sequences come forward with increase sensitivity by the factor of 2.<sup>115</sup> The relaxation delay and mixing time can also be shortened up to 0.7 s or 1 s by working with the water flip-back approach.<sup>116</sup>

Primarily, it is the best experiment for the screening purpose, especially where there is no need of GEM (group epitope mapping). It is the method of choice in the FBDD (Fragment Based Drug Design) approach for the screening of weakly binding ligands,<sup>113</sup> however, normally for the ligands that bound too tightly, for example the ligand beyond the  $K_D$  range in  $10^{-9}$  M it is not good to choose this technique like STD NMR.<sup>117</sup>

Later on, in 2007 SALMON (Solvent accessibility and protein-ligand bound studied by NMR spectroscopy) was introduced to remove the shortcomings associated with WaterLOGSY like lack of information regarding the GEM. The only changes, which are countable, are the gradient used. In WaterLOGSY, the gradient was used for the phase cycling while in the SALMON these were applied for the purpose of transfer pathway. In addition to the different gradient function, short NOESY mixing time was also preferred in order to avoid the massive spin diffusion from the solvent (water).<sup>118, 119</sup>

#### 1.5.6 Diffusion-based NMR spectroscopy

The interaction can also be targeted through a comparison of the diffusion coefficient of the ligands that well correlate to the molecular

translational mobility's of the ligands with and without the addition of the macromolecule. Since the diffusion of a molecule related to the various physical parameters of the molecule itself, for instance, shape, size, geometry, temperature, aggregation state and viscosity of the solvent etcetera.<sup>120</sup> Based on this idea, a supplementary dimension along vertical axis was added in the typical NMR spectrum that accounts for diffusion coefficient values besides the chemical shift values along the abscissa.<sup>121, 122</sup> The diffusion-based NMR methods underlying the same primary function as does the relaxation study, however, the former targets the translational mobility and later rotational ones.<sup>71</sup> Since from its starts, the diffusion coefficient edited experiments become an important tool in the host-guest chemistry, ligand-receptor studies and for the experiments rely on the physiological separations. However, the first-time application as a tool to observe the affinities of ligands against protein was put forwarded by the Shapiro and co-workers in 1997.<sup>123</sup> Mostly used diffusion filters are based on one of the two pulse programs; 1) stimulated echo (STE) and 2) pulsed field gradient spin echo (PFG-SPE).<sup>124, 125</sup>

In a practical way, for the system with a ligand in a fast exchange between the free and protein-bound state, the diffusion coefficient observed ( $D_{obs}$ ) will be equal to its mole fraction of the free ligand and the translational diffusion coefficient of the free and bound state, as shown in the following equation 19,,

$$D_{OBS} = D_{Free} X_{Free} + D_{Bound} (1 - X_{Free}) \quad (19)$$

Where,  $X_{Free}$  represents mole fraction of free ligand,  $D_{Free}$  and  $D_{Bound}$  for the diffusion in free and bound state respectively.

A sample 2D diffusion spectrum accounts for two simultaneously information; the observed diffusion and chemical shifts, therefore, this experiments become a method of choice for two groups of peoples working with NMR. At first place, as it provides the physiological non-invasive separations,

make it the best tool for a few component separation technique; hence sometimes, DOSY owes another name NMR chromatography.<sup>126, 127</sup> On the other hand, based on the difference in the diffusion coefficient of the small molecules before and after the addition of the receptor protein, it works well as an affinity tool. In contrast to the ligands showing affinity towards some specific target, those ligands, which don't show affinity they devoid of alteration in their diffusion coefficient in both conditions (with or without receptor-protein). There are plenty of practical examples in different areas exist, where DOSY NMR used for this purposes. For instance, for the calculation of dissociation constant,<sup>128</sup> for binding of antitumor agents to DNA,<sup>129</sup> for the epitope mapping,<sup>130</sup> for counterfeit drug analysis,<sup>131</sup> for the analysis of polymers and small molecular complex,<sup>132</sup> ligand-receptor affinity,<sup>100, 133, 234</sup> and for the tracking the reaction intermediates.<sup>135</sup>

### **1.5.7 $T_1$ & $T_2$ relaxation methods as a tool to see the interaction**

The relaxation experiments are the one of the oldest and well-established class of binding assay that can be easily performed by using NMR. The basic methodology relies on the comparison of the small molecular relaxation with and without the macromolecular addition. In NMR spectroscopy, the relaxation refers to the phenomenon of restoring the equilibrium magnetization and arbitrary phase of the nucleus after getting perturb by any means. However, there are two kinds of relaxation methods exist;  $T_1$  means longitudinal relaxation while the  $T_2$  represents the transverse relaxation. Both relaxations occur parallel to one another. Therefore, one mostly presents in the transverse plane ( $T_2$ ) and other in the verticle line ( $T_1$ ).<sup>69</sup> Macromolecules present broadened linewidth in NMR spectrum because of the slow tumbling rates and longer correlation rates<sup>68</sup> and hence, possess the large  $T_2$  as opposed to a group of small molecules. In fact, the relaxation methods depend upon the rotational mobilities i-e internal



motion of the molecules. Therefore, the relaxation methods reflect only the rotational tumbling rates and the hydrodynamic radius of the molecule in solution.<sup>134</sup> Based on the correlation factors, smaller molecule provides an increase in  $T_2$  relaxation time during the inbound state with some macromolecule as compared to the free state.

Fesik and co-workers were the first who successfully utilized the relaxation method for the screening the large library of the ligands for FK506 protein and provided an excellent example of this.<sup>136</sup> The effectiveness of the longitudinal relaxation methods can be achieved by providing the protein an equilibrium state while keep disturbing the ligand signals otherwise, it would not be considered as a sensitive biomarker to observe the changes.<sup>69</sup> If the protein resonances are in equilibrium then the rest of the experiments with ligand exhibit the same principle as does the reverse NOE pumping.<sup>137</sup>

A study describes the use of acetylcholinesterase as a target for the relaxation study as well as the line broadening method was evaluated first time in 2007 by Delfini and co-workers, where a comparison was made between the tacrine and its derivatives.<sup>138</sup> A year later, another study has put forwarded by Chinese group, which describes the interactions of salvianolic acid B and rosmarinic acid towards acetylcholinesterase.<sup>139</sup>

In 2007, Segal and co-workers presented another variant of relaxation method (*Target Immobilized NMR Screening (TINS)*), by using the solid support (Sepharose beads or glass) to make protein immobilized in a solution, and observed difference spectra (beads with and without protein) with high sensitivity.<sup>140</sup> In the outcome of the study, the only signals from the ligands those implicated in interaction were existed. Similarly, SLAPSTIC (*Spin Labels Attached to Protein Side chains as a Tool to identify Interacting Compounds*) also based on relaxation method, which determines line broadening of that ligand that present close to the protein.<sup>141</sup> However, this experiment is

applicable to a highly dilute solution ( $< 100 \mu\text{M}$ ) to observe the vicinity of the ligands in protein binding sites.

## 1.6 Docking Simulations

Docking is a computational method designed to examine intermolecular bindings and respective conformations between two or more entities.<sup>142, 143</sup> It contains the procedure for producing a model of a complex given the known three-dimensional structures of its segments, i.e. the receptor (protein, macromolecule) and the ligand (a small molecule, a peptide), free or bound to different species.<sup>144</sup> Based on the energetic information it predicts the binding conformations of the small molecules within a complex. Also, these conformations are further refined with a numbers of time by taking account into different binding poses.<sup>145, 146</sup> However, docking simulation demands the precise and complete receptor and ligand structures before any data input. Quick estimation of the binding poses could be obtained by using the scoring function—a mathematical procedure. Most of the time docking targets only a single receptor because a protein molecule possesses hundreds of amino acid residues offering numerous types of binding to the respective ligands.<sup>147</sup> Hydrogen bonding, pi-pi interactions, hydrophobic-hydrophilic interactions, Vander Waal and dipole interactions are common types of binding that stabilize a ligand-receptor complex. However, besides these interactions, water and solvent effects also provide an enormous degree of freedom and are important, but most of the time excluded from the calculation to make the process fast.<sup>71</sup> Although docking necessitates a specialist hand to proceed and prepare a receptor structure but, is still a method of choice in the drug discovery process<sup>148</sup> and in virtual screening.<sup>149</sup>

To begin this DS process, the 3D protein (apo and holo structure) structure is vital, which demands the proper preparing the structure such as protonation,

structure repair, and so forth, before experiencing calculations.<sup>145, 149</sup> Along these lines, before posing and scoring, ligands are included into the protein structure and subsequently, posing that might be systematic or random can lead the actual dock. Another important factor that can reduce the sampling time is the structure rigidity that typically reduce the conformational complexity. Nevertheless, sometimes this rigid approximations is converted to flexible structures because upon addition of small molecule, both structures (ligand, and protein) show rearrangements. Consequently, the posing can be executed diversely on diverse frameworks, e-g., Glide, FlexX,<sup>150</sup> TrixX,<sup>151</sup> Enovo,<sup>152</sup> and Dock<sup>153</sup> project can approach the systematic posing while, Gold 154 or Autodock can do random posing.<sup>155</sup>

Docking studies help in comprehension the coupling destinations and diverse conformational impacts that make the overwhelming steady.





## 2. Scope of the Thesis

Alzheimer's disease (AD) was considered as a ghost that can have led the infected to death since late nineteenth century. Nevertheless, the cholinergic hypothesis came forward stating that the inhibition of the acetylcholinesterase (AChE) might be an excellent therapy in controlling Alzheimer affect. In this viewpoint, the inhibitors of AChE, therefore, are of great medicinal and commercial paramount interest as therapeutics in the treatment of Alzheimer's disease and as pesticides in agriculture field. Nuclear Magnetic Resonance seems to be an ideal approach for the understanding of the conformation of inhibitors in the binding site and enables the rational design of some novel inhibitors with increased potency and even greater specificity. The non-invasiveness in action and physiologically evergreen in operation nature of NMR makes it perfect to be utilized for observing weak bindings where, ordinary spectroscopic methods are unable to provide any answer.

The overall goal of the thesis is mainly devoted to the application of liquid state NMR spectroscopy as a tool for drug discovery. Conversely, automated docking procedures are a rich source of information on the binding process of potential medical agents towards any receptors. In this perspective, nuclear magnetic resonance-based binding studies were accomplished out to probe the binding competitions and the inhibitions potentials by the selected targets. Therefore, we have employed STD-NMR, Tr-NOESY, DOSY-NMR and docking simulations combined strategy as a powerful tool to provide substantial information regarding the molecular recognition of the compounds towards the protein. The intensity of a signal under consideration in a STD NMR spectrum is proportional to the proximity of the corresponding ligand proton to receptor's protons at the binding site. This strategy could help in understanding the rational drug design based on inhibitors structural features.

A comparison between the STD concentration-dependent studies with the docking results with reference to a control (Tacrine) provided excellent results that can be utilized for future development of better coumarin-based AChE inhibitors. Particularly, for the study that would target the influence of the different extensions on the parent coumarin structure. The new synthesized coumarin derivatives with different positions of the substitutions having potent to moderate inhibition of AChE activity were compared to Tacrine. The worth noting results are presented in chapter four where the compound 1 possess a similar inhibition and stronger binding to Tacrine. The data mentioned here can further be utilized for clinical trial might help to replace and even remove the sides affect associated with Tacrine.

A similar study was employed for the chapter five, where the three inhibitors were titrated against each other for their binding site selectivity. Interestingly, the STD NMR concentration-dependent experiments afforded that none of these was competing for the same binding site. Moreover, the dissociation constant values suggested that the gallic acid has the stronger affinity to AChE than the 4-methylumbelliferon and scopoletin. Furthermore, in extract screening studies provided the way that how AChE selectively recognized its inhibitor from the library of compound available. This testing method provided an exact agreement between an early experimental approach performed in 2013 where AChE selectively identified rosmarinic acid—a known AChE inhibitor to its binding. Therefore, this experimental approach provided a fast method to screen a large library for the potent inhibitors of AChE that might help in controlling AD. Therefore, a significant progress has been made towards the investigations of the binding of the different class of inhibitors towards AChE of *Electrophorus Electricus*. And, for the first time in the Federal University of São Carlos, Brazil, this determination of the bound conformation of any inhibitors to AChE by means of NMR spectroscopy was successfully performed.







## 3. Materials and Methods

### 3.1 Equipments Used

#### 3.1.1 NMR spectrometers

All the practical experiments were performed in the laboratory of Nuclear Magnetic Resonance, Department of Chemistry, Federal University of São Carlos, SP Brazil whereas, the theoretical part (Docking simulation) was performed by the Dr. Zaheer Ul-Haq's lab and co-workers (Dr. Panjwani Center for Molecular Medicine and Drug Research, International Center for Chemicals and Biological Sciences, University of Karachi, Karachi Pakistan).

All NMR spectra were performed and recorded on a Bruker Avance III 600.23 MHz—14.1 T, (Hydrogen nucleus) spectrometer at 296-302K° temperature, equipped with a 5mm cryo-probe TCI (triple resonance  $^{13}\text{C}/^{15}\text{N}/^1\text{H}$ ) having pulse field gradients along z direction, with the gradient strength of 53.5 G/cm and with automatic tuning and matching unit (ATMA). Data acquisition and processing were performed with the Bruker software Topspin 3.0 version installed on the machine (especially for 2D experiments) and also took help of Mestrenova (8.1.2) for processing 1D analysis.

However, sometimes Bruker AVANCE III-9.14 T with 400.13 and 100.62 MHz for hydrogen and carbon nucleus respectively, have also been used for recording two-dimensional NOESY spectra. The spectrometer is equipped with multinuclear broadband inverse detection probe (BBI) with 5mm of diameter, and gradients are along the z direction having the maximum strength of 50 G/cm and ATMA unit as well.

### **3.1.2 Analytical Balance**

For NMR experiments, chemical compounds were measured by the help of electronic balance Biopercisa Model (FA 2104N) with a weighing limit to 0.01 mg.

### **3.1.3 Biomixer**

Moderately soluble extract and slightly soluble ligands were shaken through QL-901 Biomixer (Brazil), for complete solubility and to achieve homogeneity.

### **3.1.4 Sonicator**

All the samples that were not completely soluble in the normal conditions, after adding the NMR solvent were well solubilised and degassed through the Symphony Model sonicator with 35 KHz operating frequency, for 1-30 minutes, and up to 50 °C heating temperature.

## **3.2 Chemicals and Solvents used**

The solvents and commercially available chemicals are given in the Table 1. Furthermore, for the natural extract study, *Terminalia Chebula* RETZ fruit was purchased from the local market of Karachi, Pakistan. Nevertheless, the extraction was performed at the Federal University of Sao Carlos, UFSCar.

**Table 1.** Chemicals, solvents used in this thesis with a complete description of their sources. CIL= Cambridge isotope laboratories.

Chemical or solvent	Description	Supplier
<b>AChE protein</b>	Acetylcholinesterase	Sigma (C2888)
<b>Scopoletin</b>	7-Hydroxy-6-methoxycoumarin	Sigma (S2500)
<b>4-Methylumbelliferone</b>	7-Hydroxy-4-methylcoumarin	Sigma (M1381)
<b>Gallic acid</b>	3,4,5-Trihydroxybenzoic acid	Sigma (G7384)
<b>Tacrine</b>	1,2,3,4-tetrahydroacridin-9-amine	Sigma
<b>CD<sub>3</sub>OD</b>	Deuterated Methanol, 99%	CIL
<b>D<sub>2</sub>O</b>	Deuterated water or deuterium oxide, 99%	CIL
<b>NaCl</b>	Sodium salt	Baker
<b>TFA</b>	Trifluoroacetic acid	Fluka
<b>Na<sub>2</sub>HPO<sub>4</sub></b>	Sodium monophosphate	Fluka
<b>NaH<sub>2</sub>PO<sub>4</sub></b>	Sodium diphosphate	Fluke

### 3.3 Sample preparation

#### 3.3.1 Buffer Preparation (PBS)

5ml of phosphate buffer solution was prepared by using Na<sub>2</sub>HPO<sub>4</sub>=146.25 mg, NaH<sub>2</sub>PO<sub>4</sub> = 26.25 mg and NaCl = 2.63 mg in D<sub>2</sub>O with pH = 7.2 at room temperature, afterwards, degassed by sonicating the mixture up to 2-3 mints.

#### 3.3.2 AChE Stock Solution

10μM solution of AChE Electric eel (*Electrophorus Electricus*) sample was prepared by dissolving in deuterated saline PBS. After this preparation, the stock solution was stored at -28°C.

### **3.3.3 Ligand stock solution for worked demonstrated in chapter 4 and chapter 5**

All selected inhibitors solution was prepared in 5: 95 % v/v methanol-d<sub>4</sub> and deuterated buffer (PBS) respectively. Sonication was applied for complete dissolution.

#### **3.3.3.1 Sample for the STD build-up experiment (chapter: 4 and chapter 5)**

<sup>1</sup>H-NMR spectra of all inhibitors, and saturation time-dependent STD NMR were obtained by using 1:100 AChE: inhibitor concentrations by making a final volume of 100-120 µl in a 3mm NMR tube (Norrel, Inc. USA). Where, the final concentration of each inhibitor was almost 1mM for the epitope mapping experiments.

#### **3.3.3.2 STD-NMR Titration for KD calculation (chapter: 4 and chapter 5)**

For concentration-dependent STD NMR experiments, the inhibitor concentrations were kept between 0.10 mM to 2.0 mM solution. In term of ligand to protein ratio, the concentration-dependent experiments were performed in between the 20-400 times ligands excess over protein (AChE) can be seen in Table 2.

**Table 2.** The concentrations and AChE vs. Inhibitor excess, used for the STD titration studies are shown where 15 $\mu$ L solution of AChE was utilized.

Excess of ligand	Volume of Coumarin $\mu$ L	Volume of AChE $\mu$ L	Volume of Buffer $\mu$ L	Concentration of ligand in mM
20	5	50	65	0.12
32	8	50	62	0.2
40	16	80	24	0.4
72	32	88	--	0.8
120	45	75	-	1.12
133	48	72	-	1.4
200	60	60	-	1.5
333	72	42	8	1.75
400	80	40	-	2.0

### 3.3.3.3 Sample preparation for NOESY experiment (Chapter: 4, 5 and Chapter 6)

The samples for NOESY and tr-NOESY experiments were prepared with a final make-up volume of 100 $\mu$ l with 2mM of each inhibitor in 50 $\mu$ M AChE concentrations. Where, the inhibitor-enzyme concentration was almost 40: 1 for each experiment. However, for the extract screening the only known concentration of AChE was used that was kept to 50 $\mu$ M whereas; 1-2 mg of the extract amount was utilized, in chapter 6.

### 3.3.3.4 Sample preparation for DOSY experiment (Chapter: 5 and Chapter 6)

5 mM concentrations of inhibitors were used to obtain the DOSY spectra. However, the protein concentration was maintained to 50  $\mu$ M. On the other

hand, for the extract screening 1-2 mg of crude extract was utilized for the diffusion-edited experiment performed in chapter 6.

### **3.3.3.5 Sample preparation for plant extract (chapter: 6)**

For the NMR experiments, a 2 mg of ethyl acetate fraction from the *Terminalia Chebula* fruit extract was dissolved in deuterated PBS buffer and CD<sub>3</sub>OD, (95: 5 % v/v) while the AChE protein solution was prepared in sodium phosphate buffer (pH 7.2) in D<sub>2</sub>O.

STD NMR studies were performed with the 50μM solution of AChE protein in the phosphate buffer pH 7.2 in D<sub>2</sub>O and 2mg of crude extract (*Terminalia Chebula*) in deuterated buffer and CD<sub>3</sub>OD (95:5% v/v) respectively.

## **3.4 NMR Acquisition and processing**

### **3.4.1 1H-NMR Spectrum**

After injecting the sample inside the NMR spectrometer, locked the spectrometer on the respective solvent and then to achieve the homogeneity of the magnetic field, shimming was performed around all axis to ensure the homogeneity. Adjusted the pulse program to ZG and then first tried to get solvent-probe parameters by typing (getprosol). Following this, adjusted some other important parameters such as data points, spectral width, relaxation delay, number of scans, etc., and so on. Finally, acquired the receiver gain and then gave the first acquisition to see the spectrum.

### 3.4.2 90° Pulse Calibration

Beginning from the small duration of the hard pulse, a series of experiments were carried out to achieve the null point means no signal in the spectrum—towards the Pulse calibration. The null point represents the 180°. In order to obtain 90° pulse, the calculated time duration was then divided by digit 2 that provided the signal with maximum intensity after the acquisition. For authentication, the same procedure was performed twice or thrice with multiplying the null point pulse duration by digit 2 and then dividing by four and so on. The acquisition after the 90° pulse calibration provided the  $^1\text{H}$ -NMR with maximum intensity. However, for some time to save the time just used the automatic calibration command ‘paropt’ or ‘pulsecal sn’.

### 3.4.3 Solvent suppression

For the solvent suppression, a new file was created from the formerly pulse calibrated and perfectly shimmed  $^1\text{H}$ -NMR—to get rid of adjusting all parameters, particularly the offset. Various pulse sequences have been tested and developed during the course of this thesis. Among other pulse sequence used, the most significant were zgcppr (Figure 14) and lc1pnf2 (Figure 15).

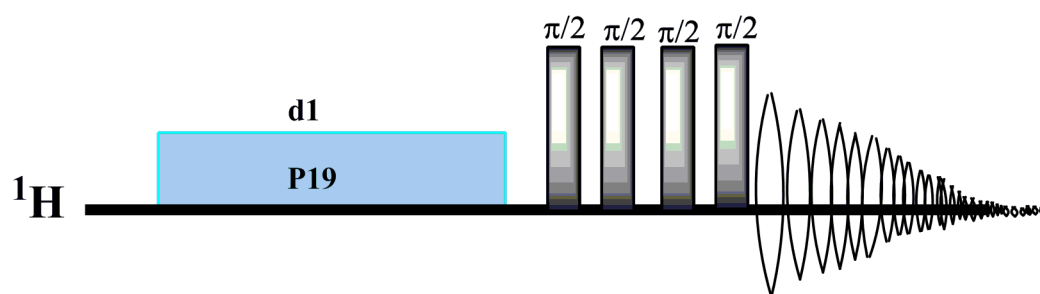


**Figure 14.** Schematic representations of ‘zgcppr’ pulse sequence, given that solvent suppression was performed by using composite pulses.<sup>156</sup>



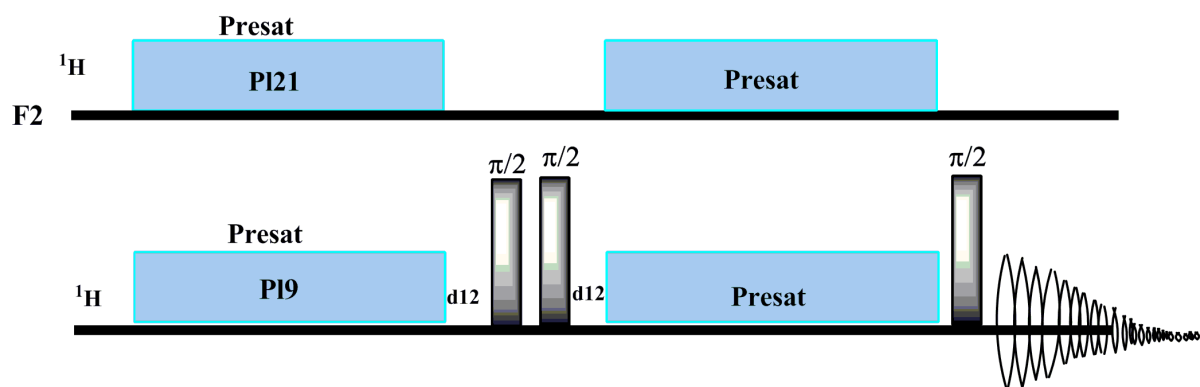


**Figure 15.** Schematic representation of 1D-NOESY based double pre-suppression by using two channels and two-pulse power for presaturation.<sup>157</sup>

The perfect solvent suppression can be achieved by increasing the power of the composite pulses or mixing time in case of 1D NOESY sequence. The power for ‘p19’ and ‘p121’ was adjusted between the 43-50db and usually, the mixing time was pre-defined to 8 ms (d8). Both pulse sequences were widely used for solvent suppression in this thesis.

### 3.4.4 Saturation Transfer Difference NMR

Saturation transfer difference NMR studies were carried out by using a variety of pulse sequence and according to the necessity of the experiment; little modification of pulses had been applied. Usually, at least two solvents were involved in all experiments. Therefore, to eliminate the solvents peaks Bruker standard STD pulse sequence with water suppressions was applied. However, two STD pulse sequences with water suppression were applied extensively; STD coupled with WATERGATE sequence (Figure 16) and STD coupled with excitation sculpting (Figure 17).

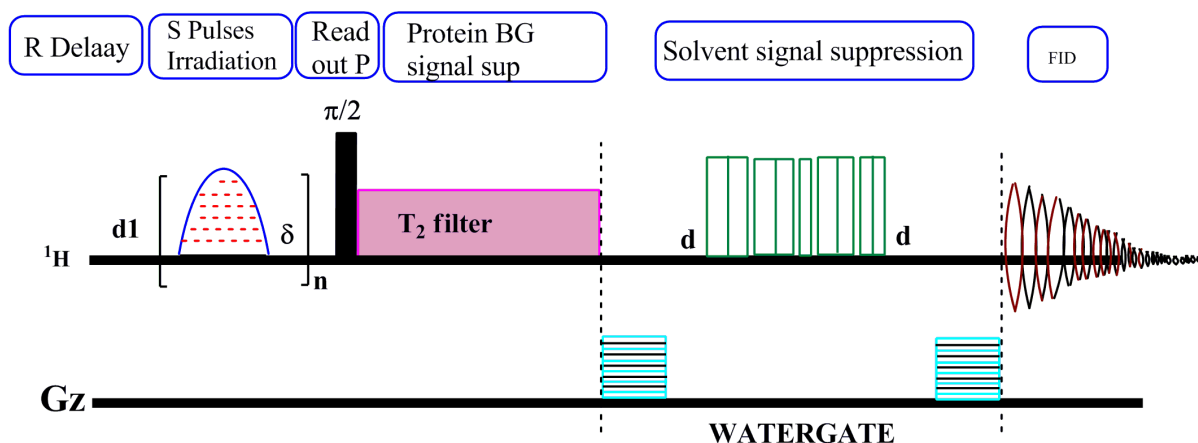


**Figure 16.** WATERGATE coupled STD sequence for solvent suppression.<sup>96</sup>

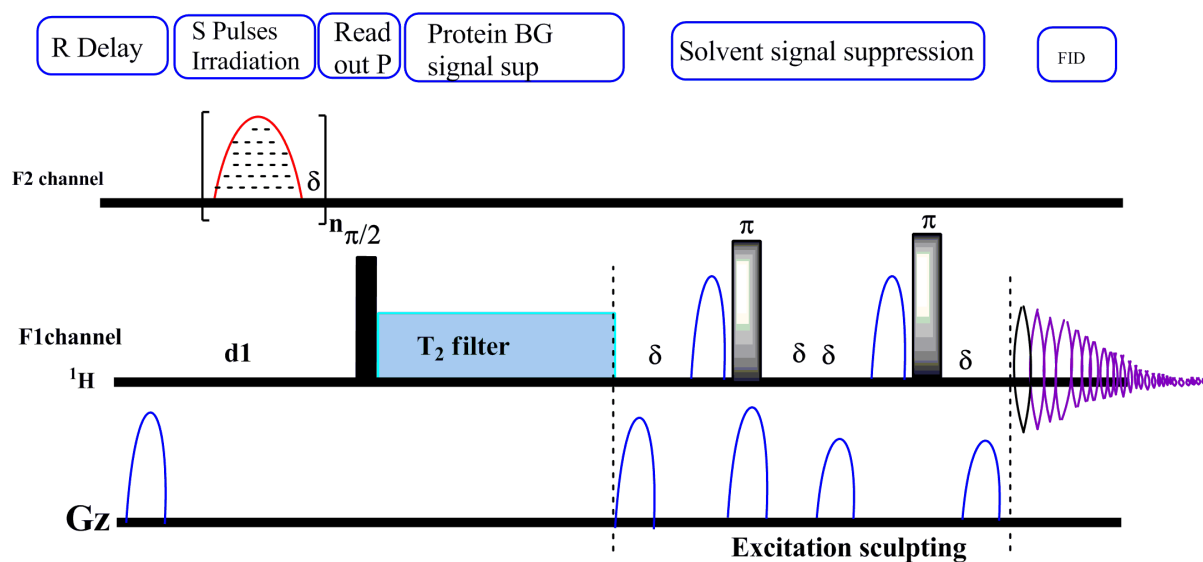


**Figure 17.** Conventional STD pulse sequence coupled with excitation sculpting for solvent suppression.<sup>96</sup>

All STD experiments were recorded on a Bruker 600 MHz (for Hydrogen nucleus) AVANCE III NMR spectrometer at a temperature of 296-298 K. For all saturation time-dependent experiments, the inhibitor concentration of 1mM in 10  $\mu$ M AChE solution was maintained at the final volume of 100  $\mu$ l in a 3mm NMR tube. While, in all concentration dependent STD NMR experiments, the

inhibitors concentration were varied between 0.10mM to 2.0mM. Furthermore, STD NMR experiments were recorded by using a Bruker stander pulse sequence with water suppression, with a pseudo-2D setup through an interleaved acquisition of on-resonance and off-resonance. Selective irradiation (saturation) of AChE was achieved by using a train of soft Gaussian shaped pulses with truncation of 1% and between 45-55 dB attenuation levels, having a 50ms of length where, each pulse was separated with 2ms. Frequency, chosen for selective irradiation of AChE was at -0.5ppm for On-resonance and 30ppm for off-resonance. STD saturation curves were acquired by using the saturation time range between 0.5 and 5 s, and with 5 to 10 numbers of experiments. STD amplification factor (AF) was calculated by calculating the signal intensity of the STD difference spectrum, relative to the reference (off-resonance) according to the following equation 20.<sup>100</sup>

$$A_{STD} = \frac{I_o - I_{STD}}{I_o} \times \frac{[L]}{[P]} \quad (20)$$

Where,  $A_{STD}$  is the amplification factor of the hydrogen under observation,  $I_o$  and  $I_{STD}$  are the intensities of the given hydrogen in the reference and STD spectra correspondingly, and [L] and [P] are the concentrations of ligand and protein respectively. For the percent AF, the hydrogen signal with greater integral intensity was given 100% values whereas; all other signals were normalized with respect to this larger signal. Similarly, for the calculation of dissociation constant  $K_D$  through the concentration-dependent STD experiment by acquiring 5 to 10 experiments for each sample with the help of the following equation 21.<sup>100</sup>

$$A_{STD} = \frac{\alpha_{STD}[L]}{K_D + [L]} \quad (21)$$

Where,  $A_{STD}$  is the STD signal intensity, and  $\alpha_{STD}$  is the maximum STD intensity assuming infinite concentration, and [L] is ligands concentration. After

calculating the  $A_{STD}$  and  $\alpha_{STD}$  values, line fitting of concentration curves was performed through Ms excels (2007) and plotted by using the origin (8.0).

In all experiments, the number of scans for every analysis were kept different from one another, therefore, for complete experimental details see the reference <sup>97, 100</sup> and in Table 3.

**Table 3.** Acquisition parameters for the STD coupled with solvent suppression techniques.

<b>Experimental conditions</b>	
<b>Parameter for STD with water suppression</b>	<b>Values</b>
Instrument	600.23 MHz ( <sup>1</sup> H Nucleus)
Solvents	CD <sub>3</sub> OD/D <sub>2</sub> O
Spectral width	Variable (15-60) ppm
On- resonance frequency	-0.5ppm
Off- resonance frequency	30ppm
saturation time	Variable (0.5-5 s)
shaped pulse for saturation	50ms
spinlock time	20-40ms
Gradient pulse	3ms
relaxation delay	1-3sec
delay for homospoil/gradient recovery	200μsec
Power of shaped pulse for saturation	45-55 dB (31.22-316.22 W)
td2	32-64K
LB	0-1Hz
NS	16-256
Temperature	296-302K
td1	2
O1	At solvent frequency

### 3.4.5 NOESY and Tr-NOESY

Standard NOESY pulse sequence with Gradient Phase-sensitive spectra were acquired in deuterated PBS buffer and CD<sub>3</sub>OD (95:5% v/v respectively) solution for each inhibitor at 295-298K temperature, whereas, Tr-NOESY spectra in AChE (50 $\mu$ M, in the deuterated PBS buffer, pH 7.2). All experiments were performed on two different magnets; Bruker AVANCE III 600 MHz with triple resonance inverse probe TCI (gradient along the z direction) and Bruker 400 MHz spectrometer (for NOESY spectra). For the transfer NOESY, Bruker standard phase sensitive pulse sequence was modified by putting the spinlock of 3500Hz after the first 90° pulse to remove the spurious peaks of protein signals.<sup>97,101</sup> The mixing time ranged between 250 ms to 400 ms (Chapter 4 and Chapter 5) and 300 ms (Chapter 6) for both NOESY and Tr-NOESY experiments with a spectral width of 6000Hz in both dimensions (F<sub>1</sub> and F<sub>2</sub>) on 600MHz, and 4000Hz for 400 MHz spectrometer. The observed build-up rate for the Tr-NOESY experiments was very fast as compared to the standard NOESY without AChE.<sup>139</sup> Furthermore, 16 and 32 transients were recorded in t<sub>1</sub> with 4K data points and 256 increments in t<sub>2</sub> for Tr-NOESY and NOESY experiments respectively. A relaxation delay of 2 s was enough to allow full relaxation between the scans with 10  $\mu$ s of pre-scan time. The processing performed with Bruker Topspin 3.0, consists of apodization with a squared cosine window function, followed by zero-filling and Fourier transformation 4K (t<sub>2</sub>) x 1K (t<sub>1</sub>) data matrices.

### 3.4.6 Diffusion Ordered Spectroscopy Studies

To obtain the DOSY spectra, Bruker LED pulse sequence has been used for both with and without the addition of AChE. Where, the gradient length of 1000-1400  $\mu$ s, 5 ms of longitudinal eddy current delay and 200  $\mu$ s of recovery

times between the gradient was applied to the experiments that performed in chapter 5 and 6. A total diffusion time of 60 ms by optimizing 64 different gradient amplitudes were applied for both spectra, therefore, strength of the gradients was kept between 1.07G/cm to 53.5 G/cm for 256 numbers of scans. In each case (with and without AChE addition), the relaxation delay kept to 3 s with the pre-scan delay of 16 $\mu$ s, and with automatically baseline correction. Topspin 3.0 (default set on the computer) was applied to the spectral processing with the line broadening function of 1 and 0.30 Hz along F<sub>2</sub> and F<sub>1</sub> dimensions respectively. DOSY macros with 64 data points, with the addition of the threshold factor for the noise sensitivity to 24 and 0.01 Hz of Gaussians function, were run. Comparison of diffusion coefficients in the presence or absence of protein was measured by taking the water signal as standard; all acquisition parameters are given in Table 4.

**Table 4.** General acquisition parameters that were used to obtain 2D-DOSY spectrum, shown in chapter 5.

Acquisition Parameters	Values
Instrument	600.23MHz for $^1\text{H}$
Solvents	$\text{CD}_3\text{OD}/\text{D}_2\text{O}$
Pulse sequence	ledbpgp2s (chapter 5)
Gradient pulse (little DELTA)	1000-1400 $\mu\text{s}$
Diffusion time (big DELTA) D20	60msec
gpz6 variable in 1D	100%
gpz7	-17.13
gpz8	-13.17
gpnam6	SMSQ10.100
gpnam7	SMSQ10.100
gpnam8	SMSQ10.100
Relaxation delay	3 s
Noise sensitivity factor	24
Delay for gradient recovery (d16)	200 $\mu\text{sec}$
DS	04
td2	64k
LB	0.30
NS	256
Temperature	298K
td1	8

### 3.4.7 1D DOSY experiment

For the calculation of the diffusion coefficients, BPPLIED pulse sequence was utilized on the Bruker 600 MHz spectrometer. The diffusion coefficients were extracted from nonlinear least squares fits of the integrated resonance intensities of the selected peaks that were measured after a series of eight 1D BPPLIED spectra. Two series of 1D-type experiments were acquired, one with AChE and other without this enzyme addition. All experiments were run as a function of gradient amplitude, for instance, each sample with or without protein was run from beginning of gradient at 2.675 G/cm to successive incremented for 8 steps up to 52.43 G/cm with the 80 ms duration of each gradient. Three selected signals without AChE and with addition were monitored for diffusion coefficient calculations. The diffusion coefficient and intensity as a function of the gradients are related to each other according to the equation given bellow.

$$\ln I = -\gamma^2 g^2 \delta^2 \left( \Delta - \frac{\delta}{3} \right) D \quad (22)$$

Where,  $I$  is the intensity of the peak of interest,  $\gamma$  is the gyromagnetic ratio (26750 rad  $g^{-1} s^{-1}$  for  $^1H$ ),  $g$  is the gradient strength in gauss/cm  $\delta$  is the duration (1 ms) of gradient and  $\Delta$  is interval between gradients. The slope of the linear plot of natural log of the intensities of the given signal with AChE ( $I$ ) over without ( $I_0$ ) versus  $-\gamma^2 g^2 \delta^2 \left( \Delta - \frac{\delta}{3} \right) D$  provided the diffusion coefficient of the signal. The change in the diffusion coefficient values of the inhibitor alone and AChE-plus provided the evidence of the interaction.



## 3.5 Theoretical Experiments

### 3.5.1 Molecular Docking

To explore the binding mechanism of selected inhibitors against acetylcholinesterase (AChE), docking simulation was carried out, for Chapter 4 and 5. In order to prepare the structure of these inhibitors, Molecular Operating Environment (MOE) 2011.10 software was used. Each structure was sketched followed by minimization with MMFF94x force field integrated with MOE, and subsequently saved into mol2 format. Similarly, the standard (tacrine) structure was extracted from Tacrine bound protein (PDB codes: 2WG2 and 1ACJ for chapter 4 and 5 respectively) retrieved from Protein Data Bank (PDB). To prepare the structure, ligand bound Tacrine is extracted followed by hydrogen addition and minimization by the MMFF94x force field where all other parameters were set to default value (gradient of 0.05 kcal/mol Å).<sup>158</sup> Since a number of water molecules can be seen within the aromatic gorge of AChE (ref), therefore we keep all the water molecules within 5.0 Å during our docking simulation. In the both PDB files (2WG2 and 1ACJ) with Tacrine bound complex, a number of waters can be seen within the gorge, especially two water molecules were found to be conserved. For software validation purpose, re-docking was carried out into the aromatic gorge of the binding site. After the assurance of MOE performance, all these inhibitors were docked by using default setting into the active site of AChE. Chimera software was utilized to explore the active site residues in the binding pocket of AChE. The selected binding residues includes Asp 72, Phe 75, Phe 78, Ser 79, Gly 80, Ser 81, Glu 82, Met 83, Trp 84, Asn 85, Trp 114, Tyr 116, Gly 117, Gly 118, Gly 119, Phe 120, Tyr 121, Ser 122, Gly 123, Ser 124, Leu 127, Val 129, Tyr 130, Glu 199, Ser 200, Ala 201, Gly 202, Ser 226 Glu 327, Ser 329, Phe 330, Phe 331, Leu 333, Tyr 334, Leu 430, Trp 432, Met 436, Ile 439, His 440, Gly 441, Tyr 442,

Glu 443 and Ile 444 as could be seen from by using Chimera software around 8Å.



## 4. Coumarin-derivatives AChE Inhibitors Binding Interactions and Dissociation Constant Calculations

### 4.1 Abstract

Based on cholinergic hypothesis, the acetylcholinesterase (AChE) inhibition is the most vital therapy among currently available treatments of Alzheimer disease effect. In this context, we have designed structurally simple coumarin-based ligands to study ligand-AChE interactions. By using NMR spectroscopy, we have evaluated the binding epitope, dissociation constant ( $K_D$ ) and bound conformations within the inhibitor-AChE complex of these four new AChE inhibitors. It is worth noting that compound **1** possesses similar inhibition activity to Tacrine (a current drug, used for the treatment of Alzheimer) and also has stronger binding ( $K_D = 30\mu\text{M}$ ) to AChE (*cf*  $K_D = 140\mu\text{M}$  for Tacrine). Moreover, the binding site investigation, as calculated by docking software also provided evidence of simultaneously binding with three sites; (peripheral anionic site (PAS), bottom of the gorge, and quaternary binding site) at the right deep bottom of the gorge. According to early reports,<sup>159, 160</sup> inhibitors which bind with two sites (PAS and a catalytic sub-site), both stop the acetylcholine (ACh) hydrolysis and also help to muffle amyloid aggregation. Thus, in the light of these reports and after the realistic NMR and docking evaluations, here we suggest our potent inhibitor (compound **1**) as a possible alternate to Tacrine and drug candidate for Alzheimer's disease in the future.

### 4.2 Introduction

Alzheimer's disease (AD) a highly pathogenic and is a major threat to the elderly population, especially in the Western world. One of the major undisputed factors that are responsible for the AD is linked to the acetylcholine

(ACh) deficiency in the brain.<sup>161</sup> Since ACh is one of the most significant neurotransmitters that transfers the electrical impulses carried by the nerve cells, from one cell to other. Therefore, the loss of the cholinergic responses and related behavioural abnormalities are the ultimate cause of the decline in the ACh level at the synaptic cleft that act as port for the transfer of messages between the nerve cells (neurons). Acetylcholinesterase exists mainly in the synaptic clefts (between nerves and skeletal muscle) and central nervous system (CNS) of living organisms—responsible mostly for the muscle proper functioning as well as signal transmissions.<sup>138, 162</sup> However, about ten years ago, it had also been found that AChE is be implicated in the production of amyloid fibrils as well as the neurite outgrowth.<sup>163</sup>

Soon after the release of acetylcholine from the nerve endings into the synaptic cleft, it tries to bind to its respective receptors; however, the released ACh enjoys very short half-life because it rapidly hydrolysed into choline and acetate by acetylcholinesterase results in the loss of stimulatory activity.<sup>43, 164-166</sup> Acetylcholine is not only a major neurotransmitter in the human body, but it has also been reported to exist in other vertebrates as well as in arthropods.<sup>167</sup> From last two decades or more so, it is well comprehended now that acetylcholinesterase hydrolysis the ester bond of the released neurotransmitter acetylcholine at synapses, and hence a discontinuation in the nerve impulse transmission takes place, which turn into the loss of cholinergic activities that lead the base to AD.<sup>43, 164-166</sup> Therefore, it is not a surprise that the inhibition of AChE will re-establish the cholinergic response that resulting from the prolongation of acetylcholine activity and hence, can reduce the impact of Alzheimer disease.<sup>167</sup> Thus, in order to re-establish/enhance the cholinergic response, as focused on an earlier cholinergic hypothesis, by the use of AChE inhibitor can be a worth exploring in the new AD drugs. A variety of different approaches resulting in a numbers of studies has therefore been applied, in this perspective so far.<sup>1, 168</sup> To date, the drugs acting as inhibitors of AChE, which

mostly based on the cholinergic approach are galantamine,<sup>169</sup> tacrine,<sup>170</sup> rivastigmine,<sup>171</sup> and donepezil<sup>168</sup> (See figure 7 for the structures of these inhibitors)

Since after the appearance of the first AChE inhibitors as a drug, several techniques have been applied in order to find new inhibitors and to observe their interaction with AChE, for example ultraviolet (UV),<sup>172, 173</sup> circular dichroism (CD),<sup>174</sup> mass spectrometry (MS), fluorescence,<sup>175</sup> LC-mass tandem method,<sup>176, 177</sup> etc. Unfortunately, NMR-based techniques for the interaction-mediated studies have not been explored for long time, mainly due to the problems associated with the solubility of compounds in water. Nevertheless, the first ligand-receptor reported<sup>139, 163</sup> binding NMR studies with an acetylcholinesterase-inhibitor complex were based on NMR line broadening and changes in the longitudinal relaxation time  $T_1$ . However, the data produced by these methods were not conclusive and could only provide some idea about non-specific interactions. Other NMR methods such as the saturation transfer difference (STD-NMR), and transferred Nuclear Overhauser Effect Spectroscopy (Tr-NOESY) provide more robust and precise information about these types of interactions. To date, to the best of our knowledge, there is no single study reported on STD NMR mediated AChE-inhibitors interactions, although, STD NMR provides physiological conditions similar to the human body. Moreover, it is the most routinely used technique for ligands/inhibitors recognition of the larger known<sup>178, 179</sup> and unknown<sup>94, 97</sup> molecular libraries, binding epitopes mapping<sup>94, 97, 178, 179</sup> as well as for calculating dissociation constant<sup>100, 101</sup> of weakly binding molecules.

By taking advantage of the most extensively used techniques (STD NMR and Tr-NOESY), the binding ability of the four new coumarin derivatives has been studied with reference to acetylcholinesterase from *Electrophorus Electricus* (electric eel). However, the selection of electric eel AChE was based

on two factors; 1) a number of earlier reports based on X-ray studies have claimed that, the oligomeric forms from eel organs is structurally similar to AChE from human or other vertebrates,<sup>180, 181</sup> and 2) the easy availability of this electric eel AChE.

### 4.3 Results and Discussion

Hundreds of natural and synthetic AChE inhibitors have been reported, today. Nevertheless, the ability, as ligands to acetylcholinesterase has rarely been identified. In this work, we have selected a set of four recently synthesized coumarin derivatives (Figure 18) with potent to moderate inhibition of AChE activity.<sup>176, 177</sup> The effects were studied by STD NMR and Tr-NOESY experiments, and compared to Tacrine as a control. STD NMR was performed by using the AChE: inhibitor mixture at 1:100 ratios for all non-concentration dependent experiments. The inhibitors were dissolved in a solvent mixture (methanol-d<sub>4</sub> and D<sub>2</sub>O in 5%: 95% v/v, respectively), while the AChE was dissolved in phosphate buffer saline (PBS), pH 7.2 in D<sub>2</sub>O in all experiments. To avoid extensive signals overlapping, separate STD NMR titration studies were performed for each compound instead of the mixture of compounds. For the epitope mapping, we exploited non-competitive studies by varying incremented saturation time (0-5 s) of protein, and STD amplification factors (%) were calculated based on integral values. The largest signal in each experiment was given a 100% STD amplification factor (AF) and all others were normalized with reference to this.

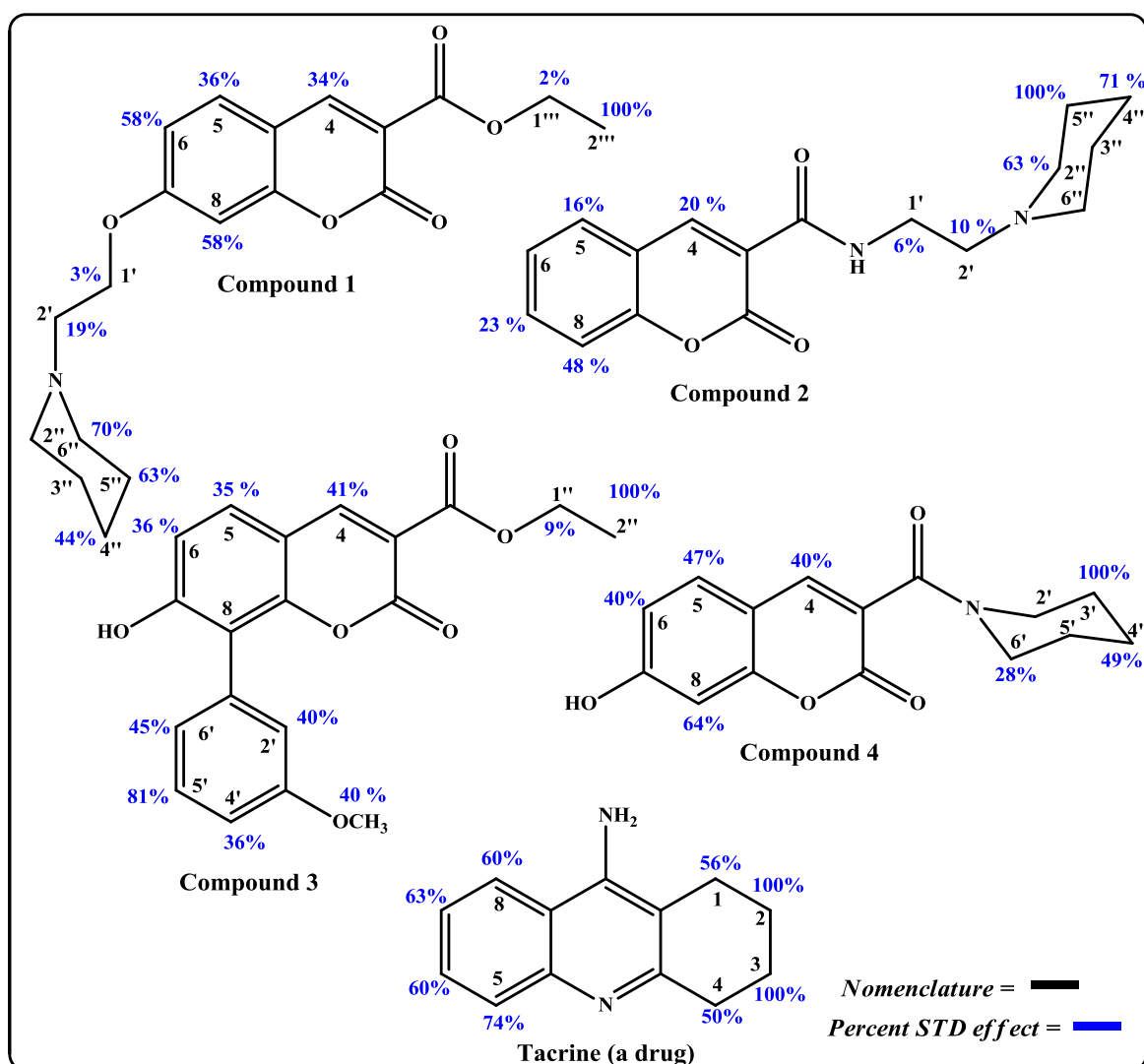


**Figure 18:** The pictorial representation of the selected inhibitors (1-4) including the control (tacrine) structures, nomenclature numbering, and relevant percent STD amplification factor (AF), are shown. The black and blue colors representing the nomenclature numbering and the relevant percent STD AF, respectively, for more clarity.

The signal intensities in STD spectrum are related to binding affinities and proportional to the number of hydrogens and saturation received by the given molecule.<sup>94, 97, 178, 1179</sup> Therefore, the presence of the signals in the STD spectrum clues the existence plausible interaction. In the present study, our focus was to establish the structure-affinity relationship behavior as a result of



the change in STD signal intensities response by varying extensions on parent coumarin.

In the first experiment, we performed STD NMR with compound **1** and on the basis of integral values an amplification factor for each signal was determined according to the experimental section. Chemical shift changes, though are small, observed with the addition of AChE can be seen in Figure 19.

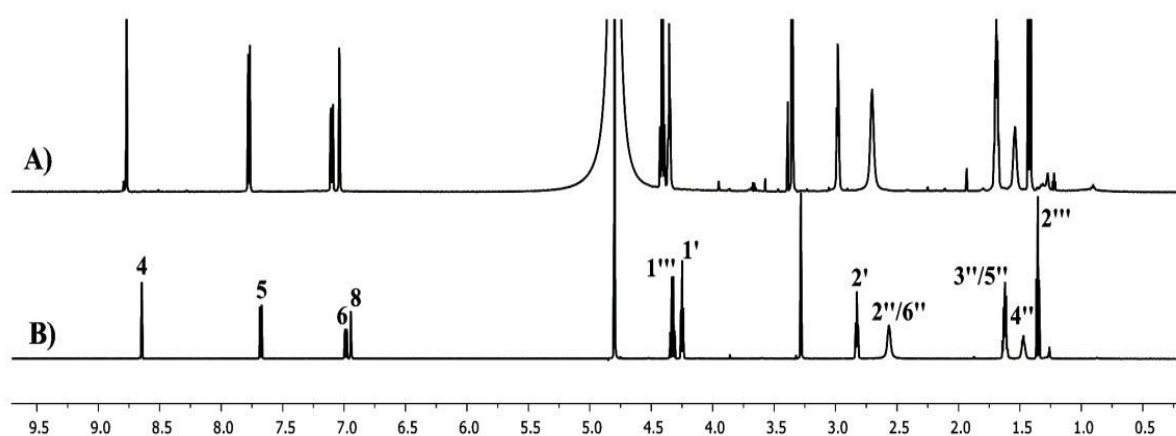


**Figure 19:**  $^1\text{H}$ -NMR spectra of compound **1** with protein (A) and without protein (B).

The signal intensity in STD spectrum reflects the relative vicinity as well as the relative amount of saturation received by the particular hydrogen from the protein via cross-relaxation.<sup>94, 97, 178, 179</sup> The relative STD effect for the compound **1**, clearly showed the methyl group (3H-2'') afforded 100% STD effect. Nevertheless, the piperidinyl group remained predominant with a strong response (Figure 20) of hydrogens 2''/6'' (70%), 3''/5'' (67%), and 4'' (44%). Based on these STD effects, it can be assumed that, the piperidinyl group exhibits the most intimate contact with binding cavities of protein. Similarly, the methylene hydrogens 1' and 1''' showed only negligible STD effects (3% and 2% respectively), suggesting almost no affinity towards protein. Among the aromatic hydrogens from the parent coumarin, hydrogens H-8/H-6 showed the

strongest STD effect (58%) while, H-4, and H-5 were well-nigh similar (34 % and 36%, respectively).

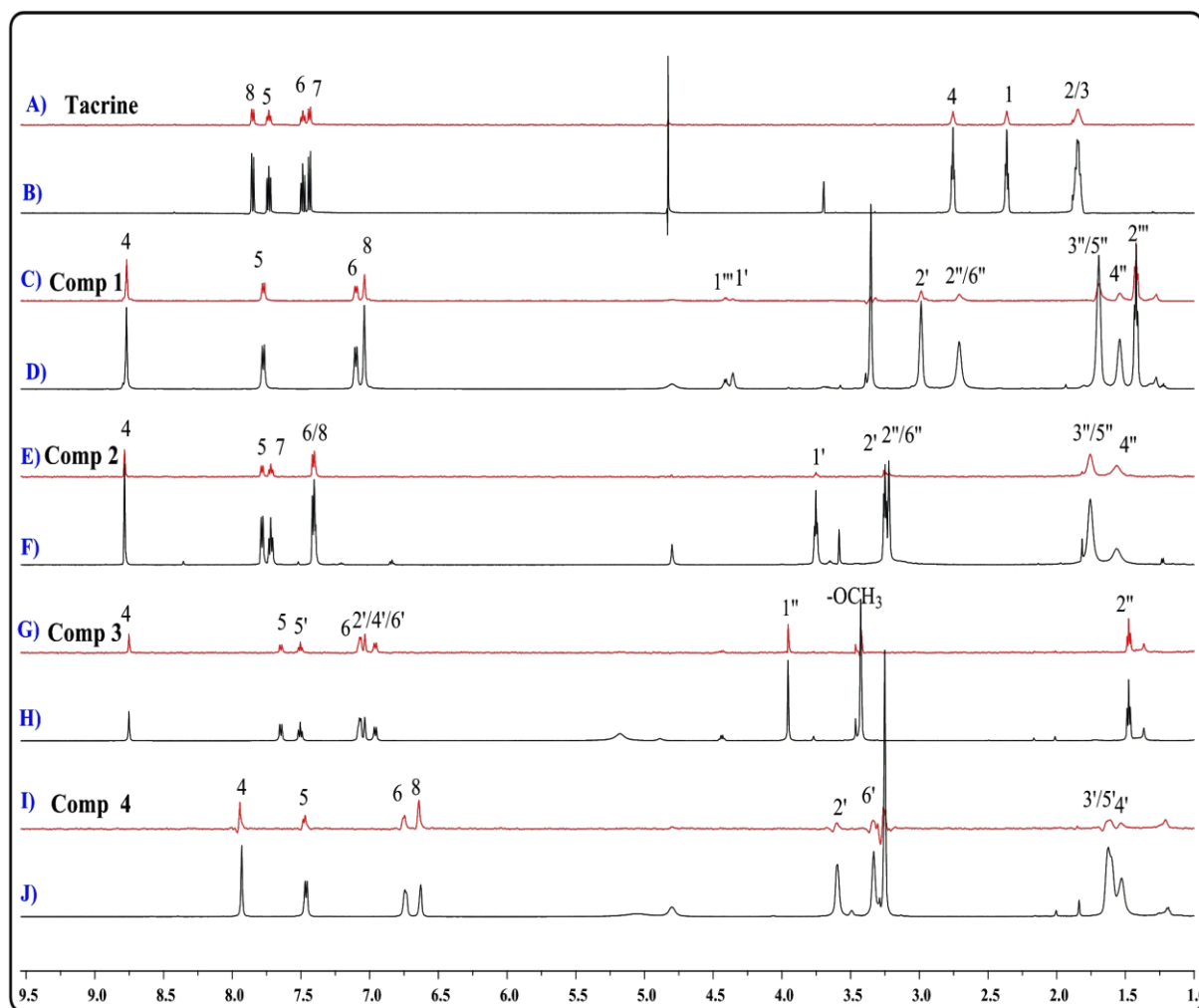


**Figure 20:** 1D STD NMR spectra of compounds (**1-4**) including tacrine, where, all *off-resonance* spectra are represented by (B, D, F, H and J in black color) and respective STD difference NMR spectra with (A, C, E, G and I in red color). The top pair of the spectrum corresponds to tacrine, following that spectrum of compounds **1-4** is given in descending order.

The STD studies of compound **2**, where the ethoxyl side chain was replaced by the piperidinyl group showed almost the same results as that of compound **1** ( Figure 19 and 20E ). The chemical shift changes which observed by the addition of AChE are shown in figure 21.

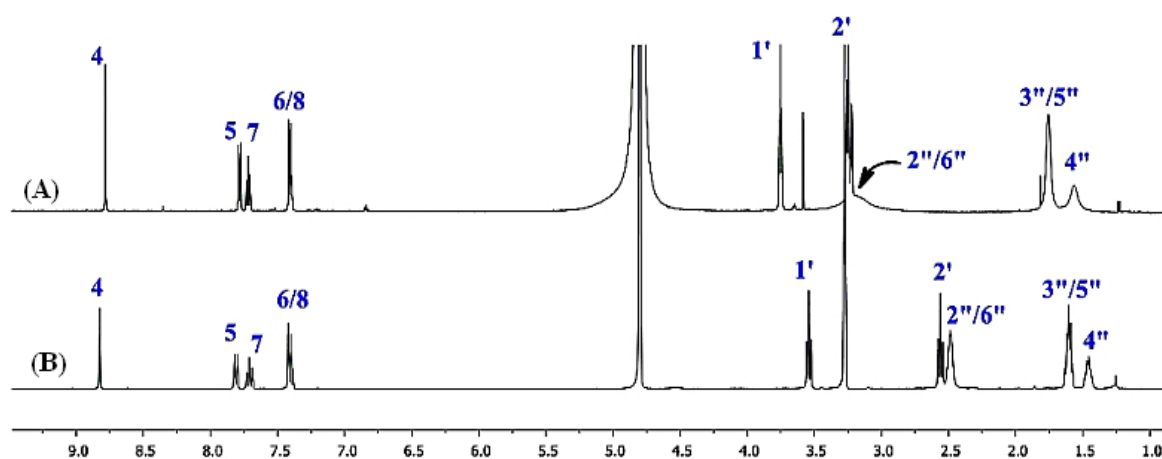


**Figure 21:**  $^1\text{H}$ -NMR spectra of compound **2** with protein (A) and without protein (B) .

The epitopes from compound **2** showed that, the hydrogens  $3''$  from piperidinyll group gave the strongest (100%) STD response, while the hydrogens  $4''$  (71%) and H-8 (48 %) were next most prominent. Some weak interactions were also seen for H-7 and H-4 hydrogens (23% and 29% respectively) (Figure 20E).

STD results from compound **3** suggest the ethoxyl group was responsible for the affinity towards AChE in the absence of the piperidinyll group. From the chemical shift behavior (Figure 22) and the STD spectrum (Figure 20G), the unambiguous representation was achieved which established its binding. Where the epitopes outcome showed the three hydrogens from H- $2''$  provided 100% response towards AChE while, the H- $2'$  and H- $3'$  from phenyl substituent provided 40 % and 81%, respectively.

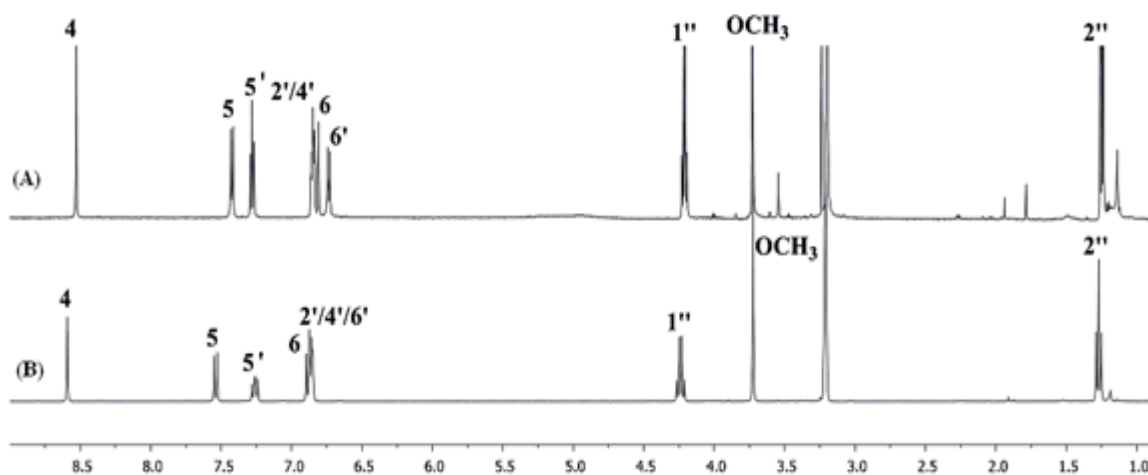


**Figure 22:**  $^1\text{H-NMR}$  spectra of compound **3** with protein (A) and without protein (B) .

From the parent coumarin ring scaffold H-4 was prominent with 43% STD effect and hence, affinity with AChE, while, H-5 and H-6 were well-nighed similar with 35% and 36% affinity (Figure 19). Similarly, compound **4** also showed some level of affinity (Figure 20 I) and chemical shift changes (see Figure 23), as is obvious from the relative STD effect as shown in Figure 19. In compound **4**, the ethoxyl side-branch is replaced with piperidinyl group which provides a major contribution to affinity. Here, the hydrogens H-3' and H-4' from the piperidinyl group were provided 100% and 49 % STD AF respectively, and thereby, interaction towards AChE.

Interestingly, unlike other selected compounds, the aromatic hydrogens (parent ring scaffold) of compound **4** showed strong bindings when compared to some of its piperidinyl hydrogens. The relative STD effect showed that the hydrogen H-8 of the aromatic moiety gave 64% even greater than some of its major hydrogens (2'/6' and 4') of the piperidinyl side-chain. Following this, other aromatic hydrogens like H-6, H-5 and H-4 of compound **4** also provided a good STD outcome between the 45-50 % and in that way, affinity towards AChE. Based on these realistic results, we supposed that this anomalous behavior of compound **4** is because of its smaller size, availability of fewer

rational conformers and lack of large substituent off the parent coumarin ring. Since this molecule is more rigid opposed to the other three structures and most of the entrance into the binding cavity of AChE was as a result of edge contact with a planar shape rather than more crowded or twisted conformation. On the other hand, structures (1-3) with larger extensions off the coumarin ring might help to interact within or across the deeper binding grooves of the AChE.

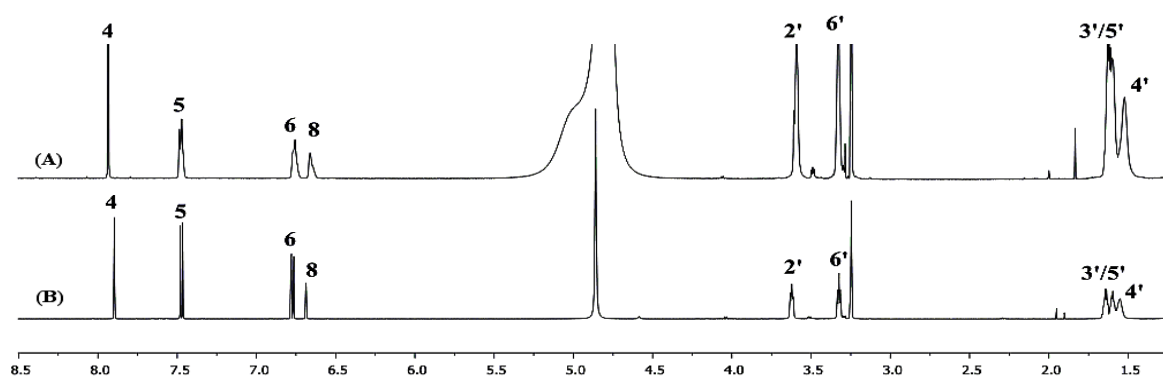


**Figure 23:**  $^1\text{H}$ -NMR spectra of compound **4** with protein (A) and without protein (B) .

From these epitope mapping outcomes, it can be concluded that, the compound **1** interacts at the binding site by both ends via its larger extensions, hence, providing the larger signal intensity in STD NMR spectrum. Indeed, this compound tries to enter into binding cavity from either end; therefore, both ends of compound **1** are getting more saturation transferred from the AChE, which resulted into strong binding as opposed to the central aromatic part. A similar behavior was observed when the ethoxyl scaffold was replaced by piperidinyl scaffold in compound **2** then this end became prominent in the STD AF, in its spectrum. Moreover, a similar fashion of epitope results was also observed for the compounds **3** and **4**, where the side chains (ethoxyl and piperidinyl) provided the 100 % STD AF effect. From these experimental observations, it

could, therefore, be concluded that the only the ends of all selected targets were involved in strong bindings.

It is well understood that the STD signal intensity depends on the length of the saturation time for the irradiation of protein as well as the number of molecules (concentration of the sample).<sup>100, 101</sup> Therefore, these findings are the witnesses to this statement when epitope footprints were evaluated by varying incremented saturation time for the irradiation of AChE. To accomplish this purpose, we performed 6-10 experiments for each single sample by varying saturation time to observe signal intensities and the growth of the stacked plots (see Figure 24-28 for **2**, **3**, **4** and the Tacrine, respectively). The dependence of the STD signals on saturation time a graphical representation of stacked plot for compound **1** can be seen in Figure 29A.

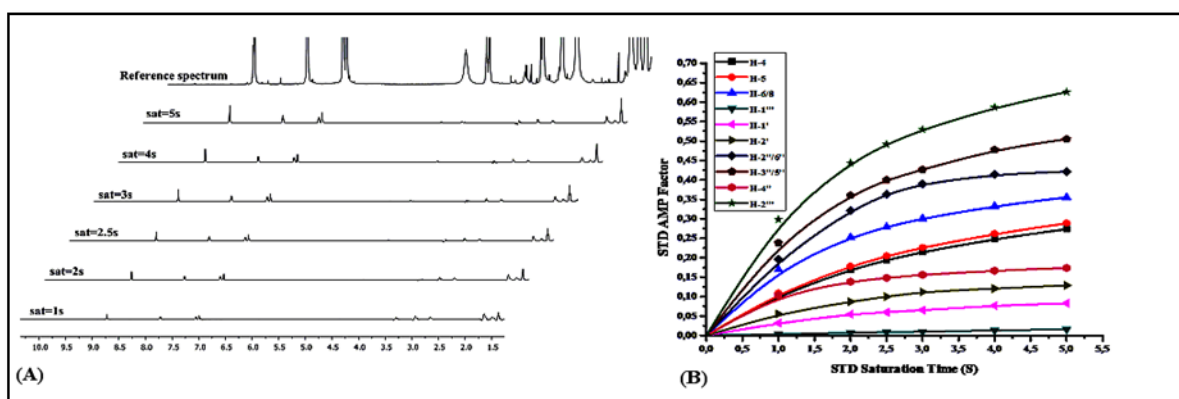


**Figure 24:** Stacked plot of 1D STD NMR spectra of compound **1** with varying saturation times between 1-5 s (A) and respective saturation curve plot (B).

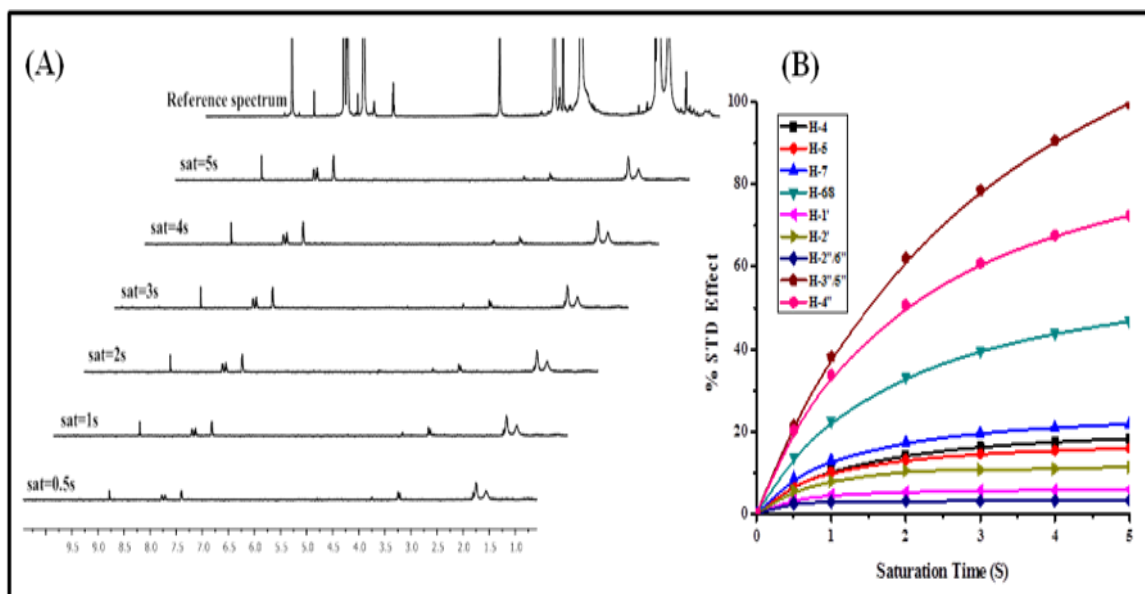


**Figure 25:** Stacked plot of 1D STD NMR spectra of compound **2** with varying saturation times between 1-5 s (A) and respective saturation curve plot (B).

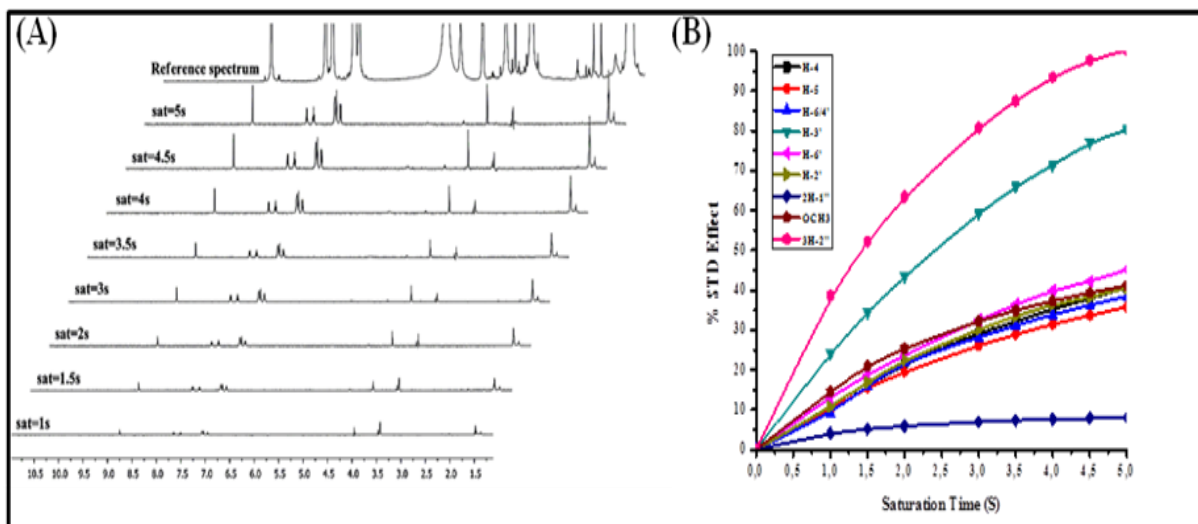


**Figure 26:** Stacked plot of 1D STD NMR spectra of compound **3** with varying saturation times between 1-5 s (A) and respective saturation curve plot (B).



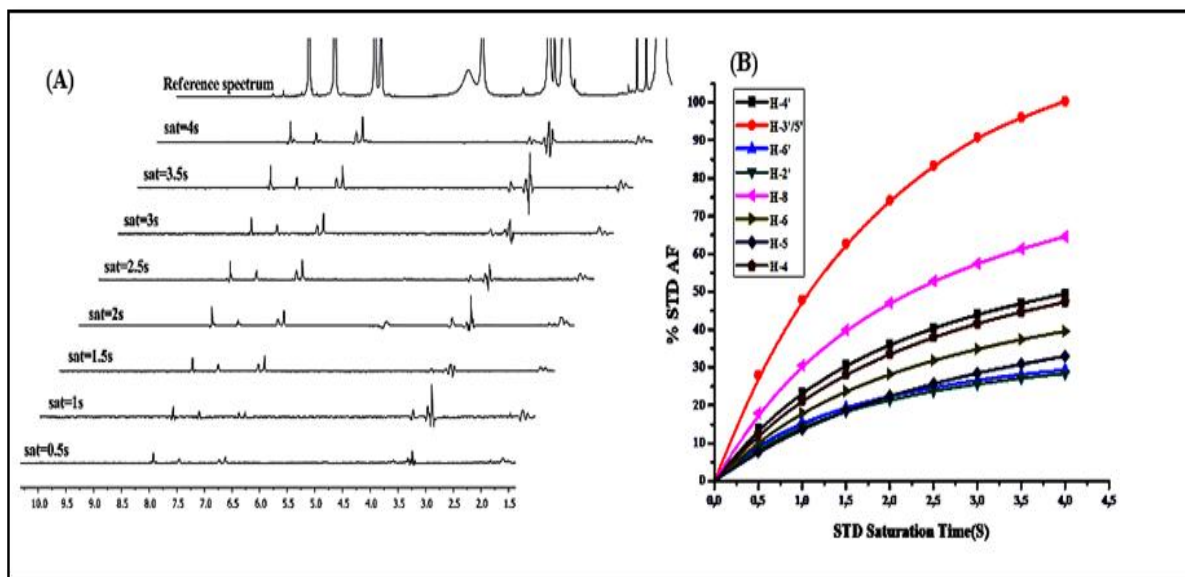


**Figure 27:** Stacked plot of 1D STD NMR spectra of compound **4** with varying saturation times between 0.5-4 s (A) and respective saturation curve plot (B).

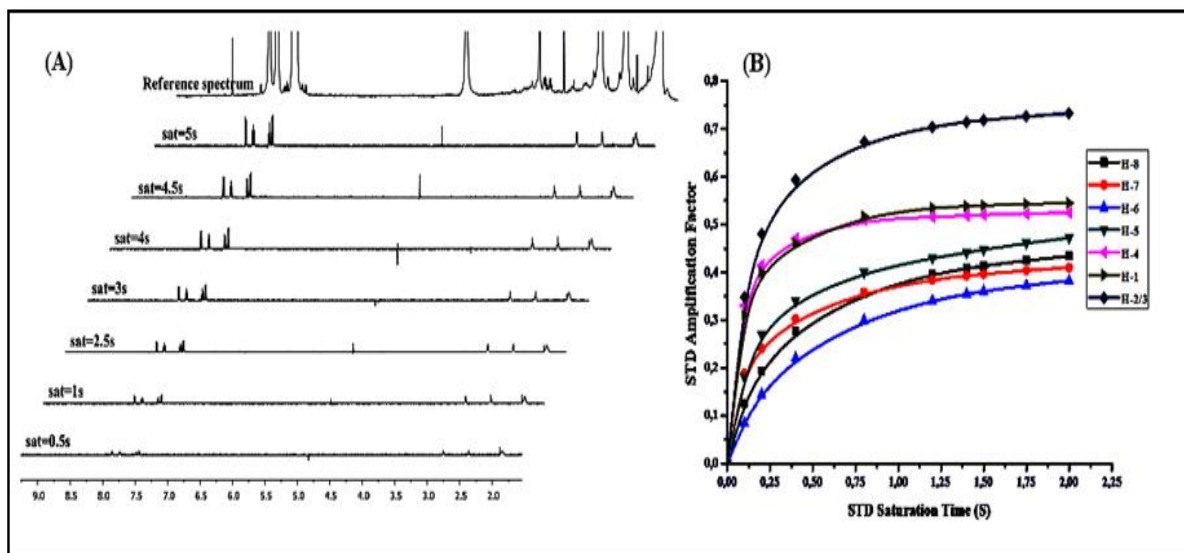


**Figure 28:** Stacked plot of 1D STD NMR spectra of standard Tacrine with varying saturation times between 0.5-5 s (A) and respective saturation curve plot (B).

Moreover, the affinity ranking of these four inhibitors and the control (Tacrine) was defined by making comparisons of the dissociation constant ( $K_D$ ) values. It is well understood that the dissociation constant values justifies the strength of binding of a ligand/inhibitor to protein.<sup>173</sup> For this purpose, the direct measurements of the complex (inhibitor-AChE) dissociation constant for each inhibitor have been performed by using different inhibitor concentration between 0.10-2.0 mM while maintaining fixed protein concentration. These  $K_D$  values were calculated with the help of the method reported elsewhere.<sup>100, 101, 182</sup>

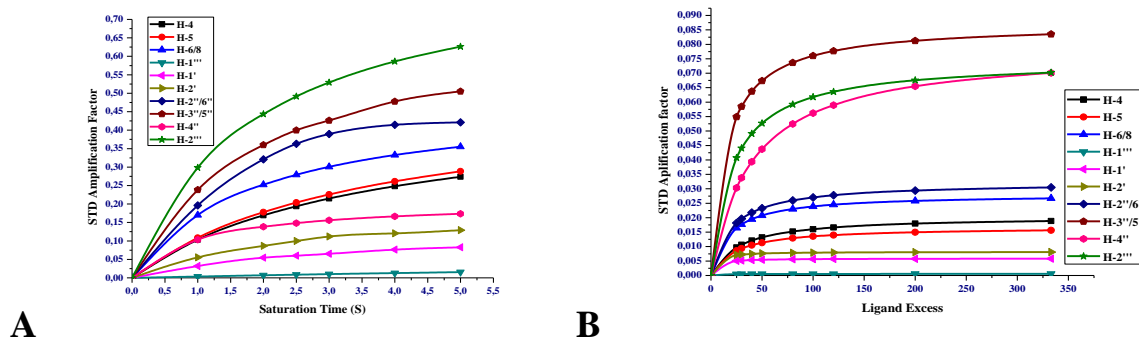


**Figure 29 A-B:** Saturation curve Plot (A) and titration curve plot (B) of the compound **1**, obtained by calculating relative STD-AF by varying incremented irradiation time of protein and inhibitor concentration respectively.

Here in this study, with reference to nine experiments (data not shown here), we could find the dissociation constant value of compound **1**, was  $30\mu\text{M}$ —a graphical representation of the stacked plot growth for this compound has shown in Figure 29 B. Similarly,  $194\mu\text{M}$  value was found in a similar way to the compound **2**. An observed huge difference between the  $K_D$  values of these two compounds (**1** and **2**) could be explained by considering their STD amplification factors as a result of increasing inhibitor concentration. It is worth noting that, in the compound **1**, where both extensions (ethoxyl and piperidinyl) enhanced the affinity towards the AChE whereas, alone piperidinyl group is responsible for major affinity in compound **2**. Thus, it was no wonder to get better dissociation results for compound **1**. On the other hand,  $K_D$  values for compounds **3** and **4** also showed a similar (substitution dependent) behavior and could secure the values  $252\mu\text{M}$  and  $210\mu\text{M}$ , respectively. Intriguingly, a clear decrease in  $K_D$  of compound **3** could be seen as a result of replacing the piperidinyl group by a phenyl group at position-8. Again, provided a same inference that piperidinyl group is the major stakeholder in this affinity. Moreover, a change of the ethoxyl moiety by piperidinyl group, lead the compound **4** to even higher than **3** in this STD-affinity ranking. All these concentration dependent experiments were carried out by keeping the saturation

time 2s fixed for protein irradiation. The resultant curve plots obtained can be seen in figure 30, for the compound 2, 3 and 4 and Tacrine respectively.

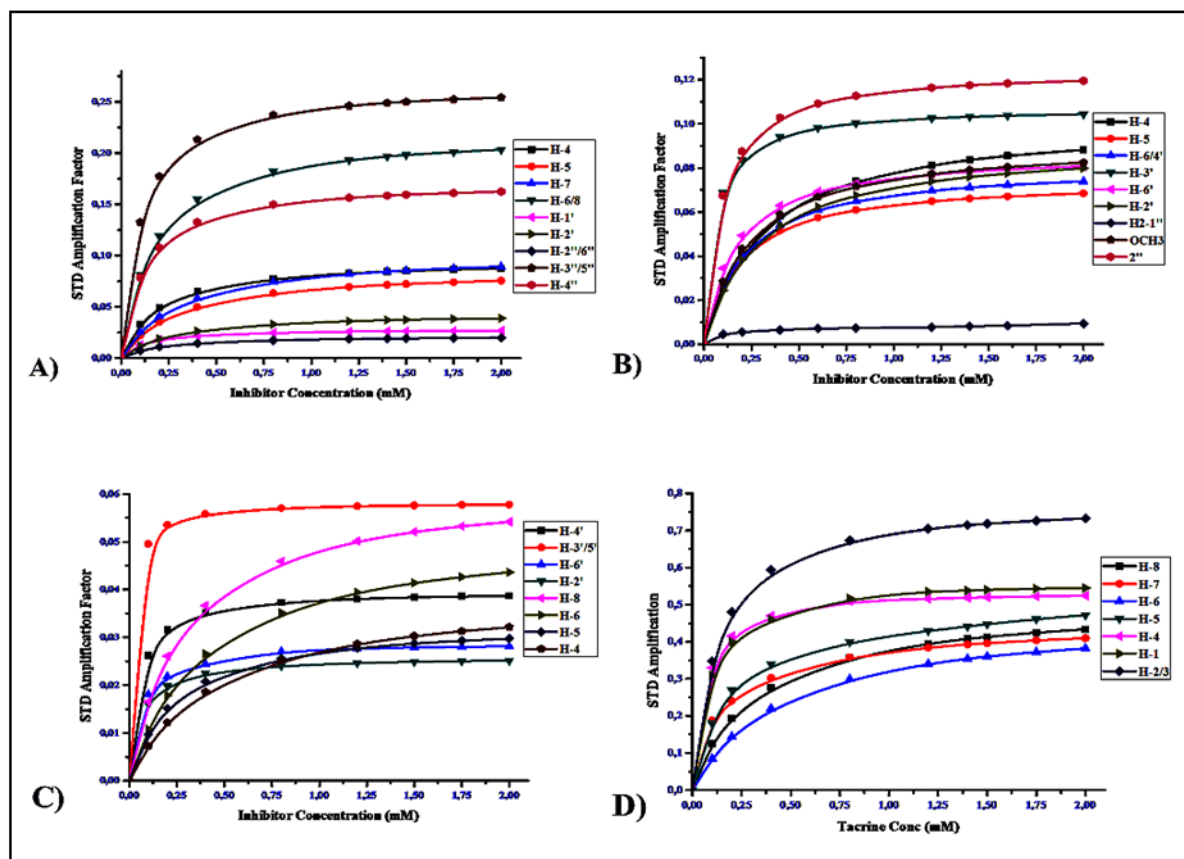


**Figure 30A-D:** Concentration curve plots A, B, C and D for compounds 2, 3, 4 and standard tacrine respectively, obtained as a result of stacked plots (data not shown here) of 1D STD NMR experiment for each compound .

In a similar manner, the Tacrine (the control) was also treated with the same type of concentration studies towards AChE. The determined dissociation constant value was 140 $\mu$ M via STD titration experiment. A curve plot of STD-AF growth as a result of 10 titration experiments was shown in, Figure 30D,. Nevertheless, the value obtained for Tacrine is quite large when compared with earlier Ellman method results.<sup>172-174</sup> The discrepancies occurred between these values might be due to instrumental sensitivity differences that exist between NMR and other spectroscopic techniques, for instance, MS, Fluorescence, etc.

For further consolidation of our STD results, we also investigated the binding affinities of these inhibitors (compounds **1-4**) through 2D Tr-NOESY experiments. These experiments were performed by using the AChE in D<sub>2</sub>O and PBS buffer at pH 7.2 while inhibitors in 5: 95 v/v CD<sub>3</sub>OD and D<sub>2</sub>O respectively. The control experiments (2D NOESY phase sensitive) were performed with inhibitors (**1-4**) 20mM each, while the counterpart 2D Tr-NOESY experiments with inhibitors (**1-4**) 20mM concentration in AChE 50μM solution (Figure 31 and 32).

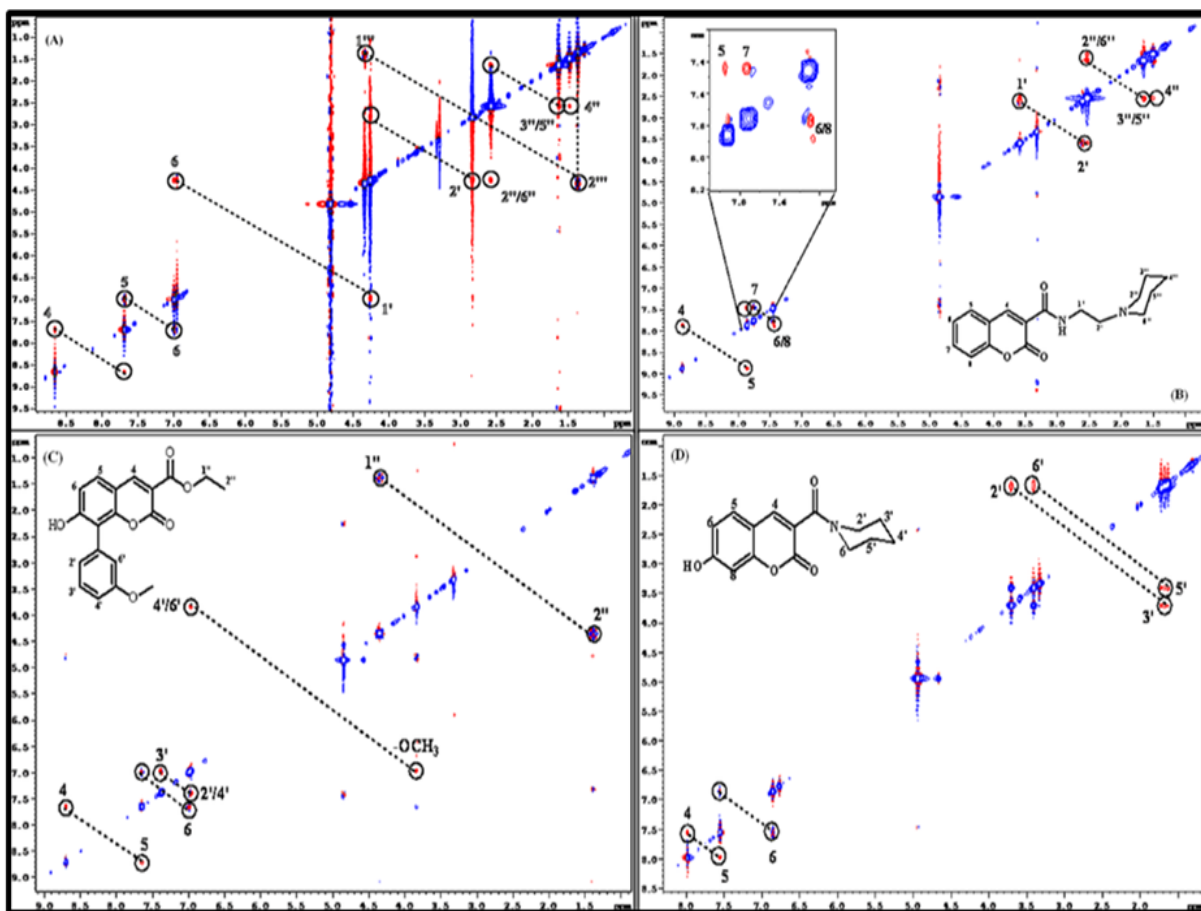


**Figure 31:** Two-dimensional standard NOESY spectra without AChE represented by A, B, C and D for the selected inhibitors **1**, **2**, **3** and **4**, respectively. All cross peaks were of the opposite signs to the diagonal (positive NOE) represented by red color.

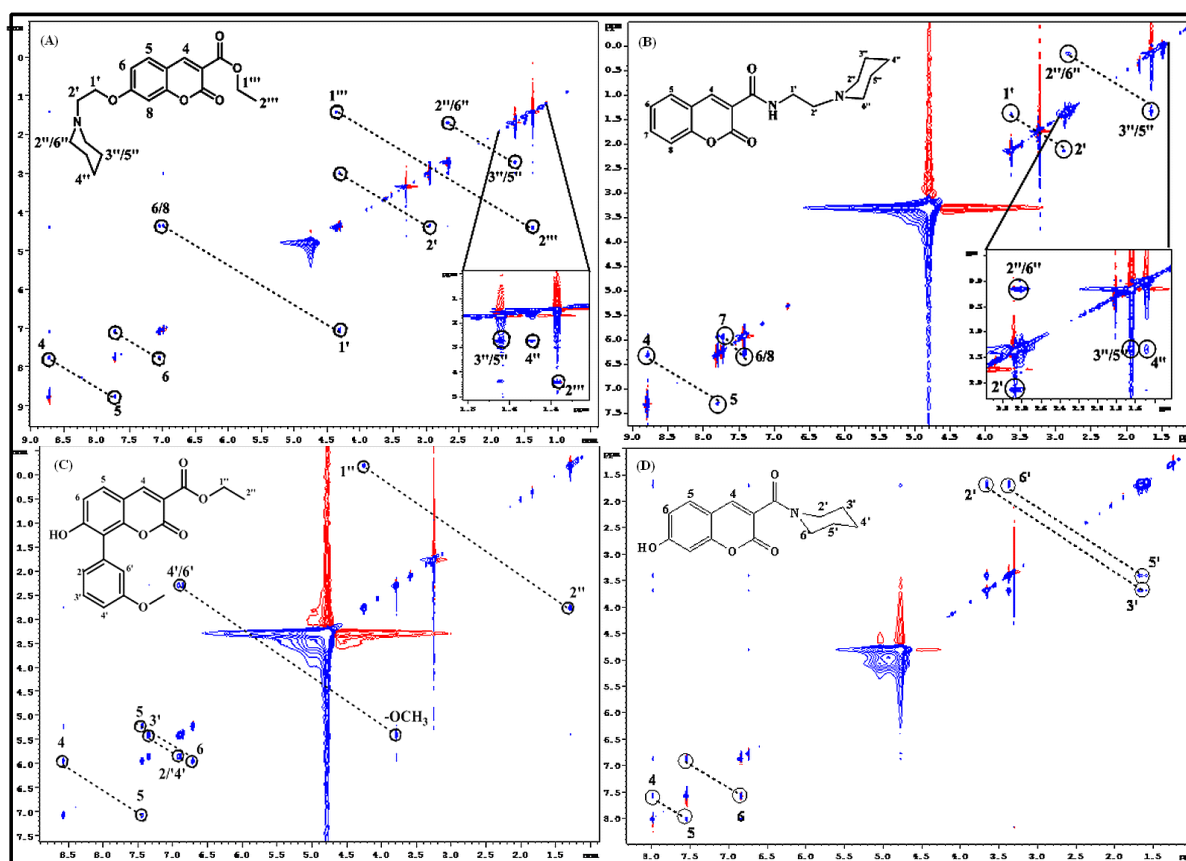


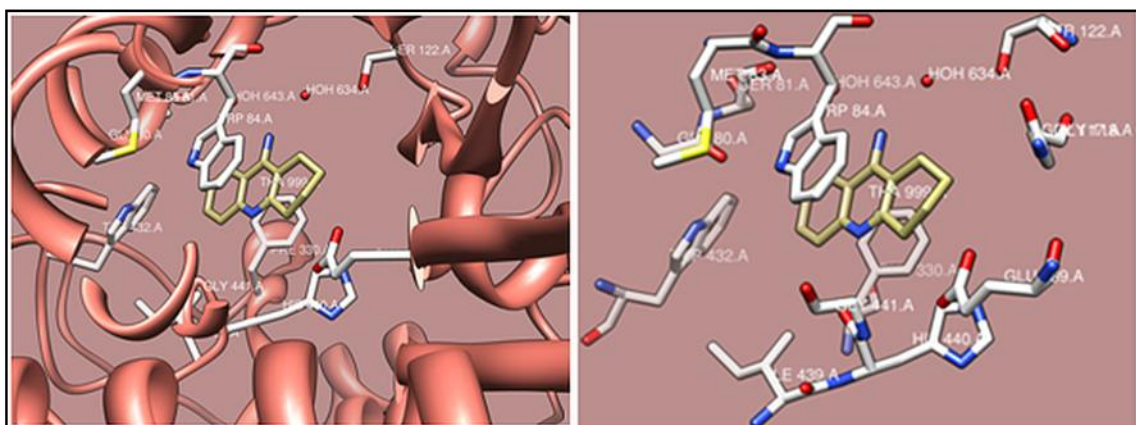
**Figure 32:** Two-dimensional transfer NOESY spectra with AChE represented by **A**, **B**, **C** and **D** for the selected inhibitors **1**, **2**, **3** and **4**, respectively. All cross peaks were of the same signs to the diagonal (negative NOE) represented by blue color.

For the transfer NOESY, Bruker standard phase sensitive pulse sequence was modified by putting the spinlock of 3500Hz after the first  $90^\circ$  pulse to remove the spurious peaks of protein signals.<sup>94, 97</sup> As it was expected for the small molecular size molecules, spectra of free inhibitors showed small positive NOEs (Figure 31,) due to the fast tumbling rate, however, few signals also showed negative NOEs that might be due to uncorrected phase. In contrast, inhibitors within AChE solution showed negative NOEs—a characteristic of macromolecules due to slowly tumbling and fast relaxation rates.<sup>183</sup> The build-up rate of Tr-NOESY was much faster compared to NOESY spectra, despite having short acquisition time. It is worth noting that, NOEs derived from all signals of the piperidinyll group of compounds (**1**, **2** and **4**) showed strong cross

peaks; an excellent agreement to already performed STD NMR spectra (Figure 19 and Figure 20). Interestingly, the aromatic hydrogens of phenyl moiety belonging to compound **3** showed also strong negative cross peaks (Figure 32 C); an unambiguously strong intimate contact to AChE as confirmed by STD NMR between 70 to 80 % STD effect (Figure 19). The generation of negative NOEs in Tr-NOESY experiments of all inhibitors (**1-4**) confirmed the true affinity towards macromolecule. The negative NOEs are might be due to the slow tumbling rates of inhibitors hydrogens in the binding cavity of AChE than the free inhibitors alone. Strong NOEs signals related to piperidinyl ring belonging to compound **1**, **2**, and **4** and aromatic signals of compound **3** gave the same conclusion as we could get before with STD epitope mapping analysis. The strong correlation between the STD epitope results and Tr-NOESY permitted us to the conclusion that the edges of these small molecules are in more intimate contact with the AChE and hence, binding.

STD NMR and Tr-NOESY experimental results provided the evidence of binding regardless of the position of binding sites in the enzyme cavities; which were validated through molecular docking simulation. Again, all inhibitors (**1-4**) were compared well with Tacrine (the control) binding site residues and for free energies. For this purpose, an already published protocol for the selection of binding site residues has been applied.<sup>158</sup> Docking simulations were performed by using Molecular Operating Environment (MOE) 2011.10, where structures were sketched followed by minimization with MMFF94x and protonation. For the reference, Tacrine bound protein (PDB code: 2WG2) was retrieved from Protein Data Bank, see more detail in the experimental section. Active site information was received by using Chimera software (Figure 33) by selecting the only available chain A of AChE. The molecular docking analysis revealed that all inhibitors (**1-4**) showed interactions with the central pocket, in a deep gorge and a peripheral pocket of AChE.

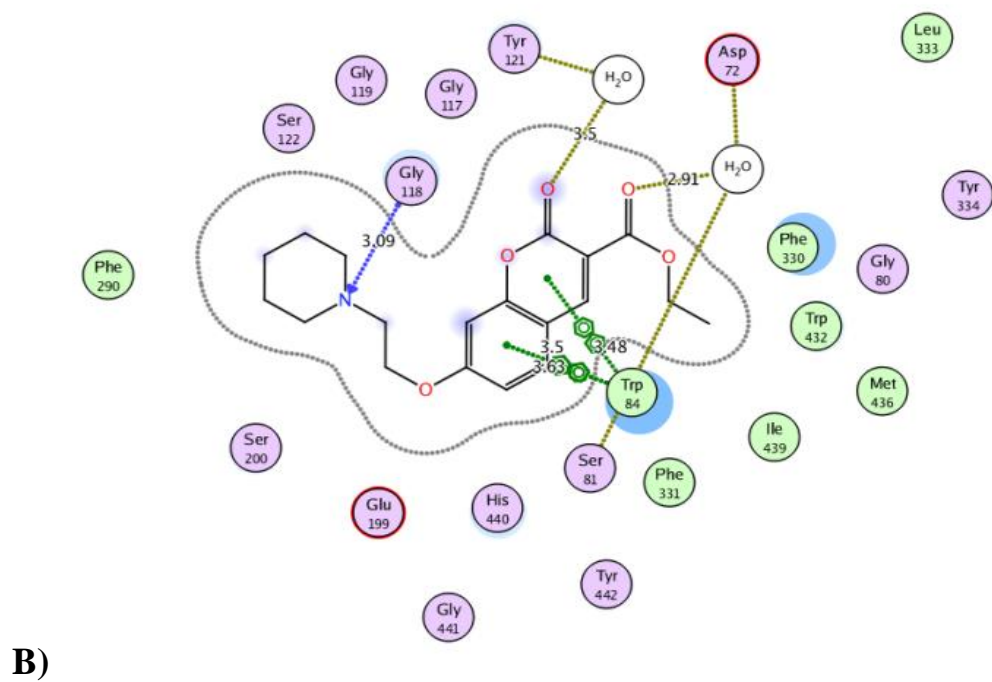
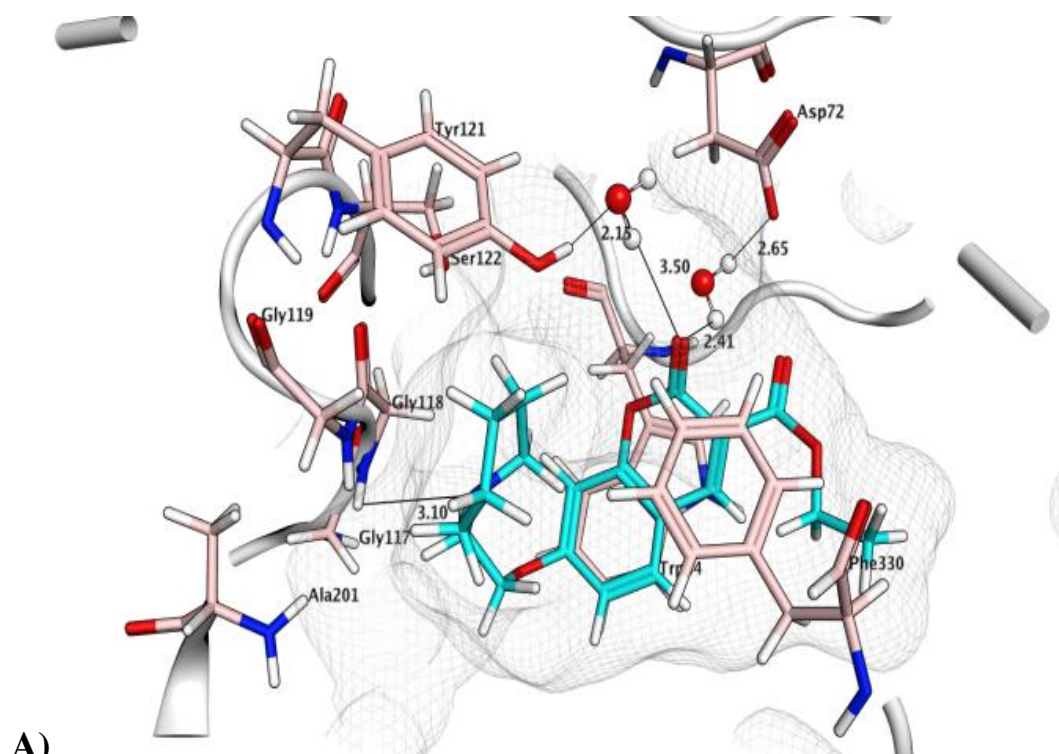


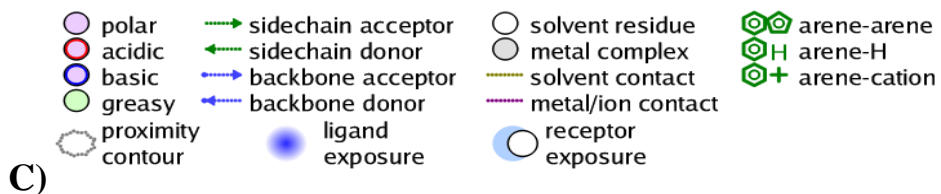


**Figure 33:** Active site residues surrounding tacrine bound inhibitor as obtained through chimera software.

These compounds showed almost all types of interactions, important for the stability of AChE-inhibitor complex, including, hydrophobic contacts, hydrogen bonding,  $\pi$ - $\pi$  interaction and hydrophilic-hydrophobic interactions. Compound **1** showed the water bridging property as well as hydrogen bonding (Figure 34A). It is worth noting that, that MOE (Molecular Operating Environment) ranked this compound **1** to the top position with free energy -7.46 Kcal/mol on the basis of interaction. In this way, docking simulation mimics the STD titration results by nominating compound **1** at the top. Compound **1** showed interaction with multiple binding sites, including Gly118 of anionic sub-sites through hydrogen bonding involving between its N-atom and Gly118 at 3.09 Å (Figure 34B), this might be the presence of two extensions off the coumarin rings helping it to cover large area. In addition, both aromatic rings provided cation- $\pi$  interaction with Trp84 at 3.63 Å and 3.84 Å (quaternary ammonium binding locus). Similarly, Asp72 binds through hydrogen bonding with water that in turn forms another hydrogen bonding with the carbonyl oxygen of ester group at 2.91 Å, and also interacting with Trp84 at the bottom of the gorge<sup>158</sup> (Figure 34B). However, Tyr 121 of the peripheral anionic site

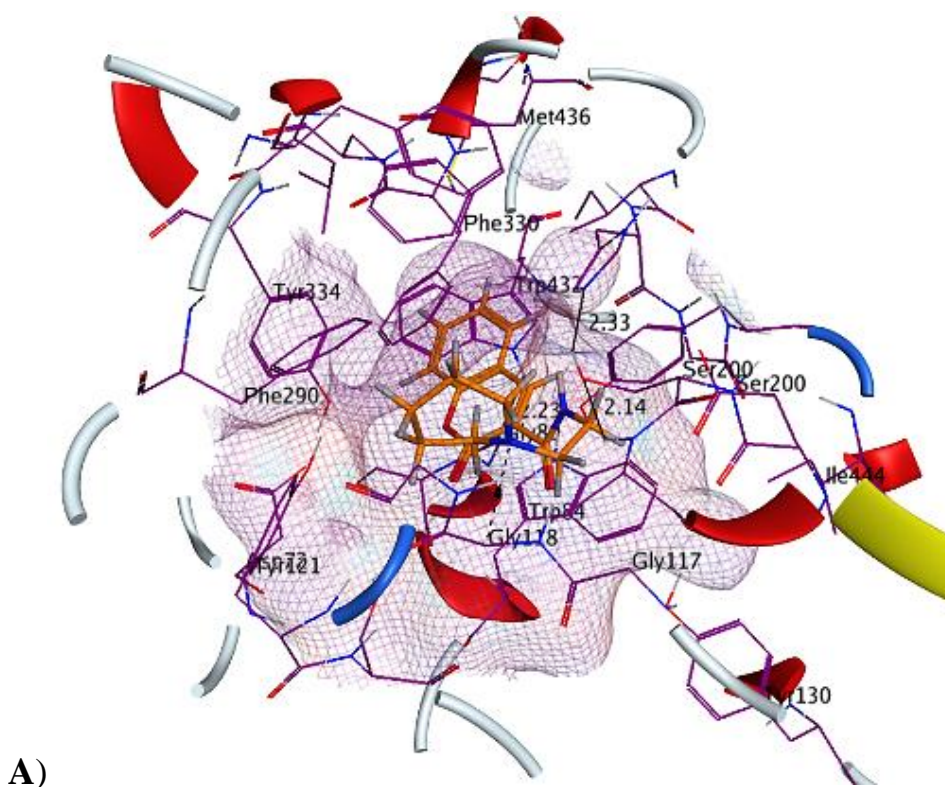
(PAS)<sup>158</sup> gets involved in hydrogen bonding through a water and the carbonyl oxygen in the lactone ring at 3.5 Å.

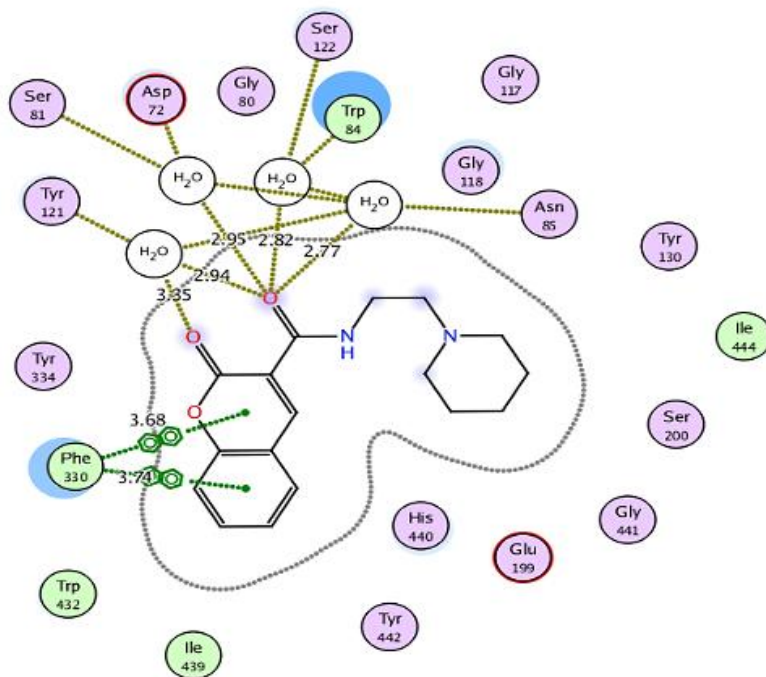




**Figure 34A-B:** A 3D (A) and 2D (B) Molecular docking model of interactions at lowest energy conformations between the acetylcholinesterase and compound 1. For clear understanding, a key (C) with different colors representing different interaction are also provided. See more details in the experimental section.

Similarly, compound 2 approaches second position after compound 1 with the complex binding energy of -7.39 Kcal/mol (Table 5) as it can be seen from pictorial interactions (Figure 35).





**B)**

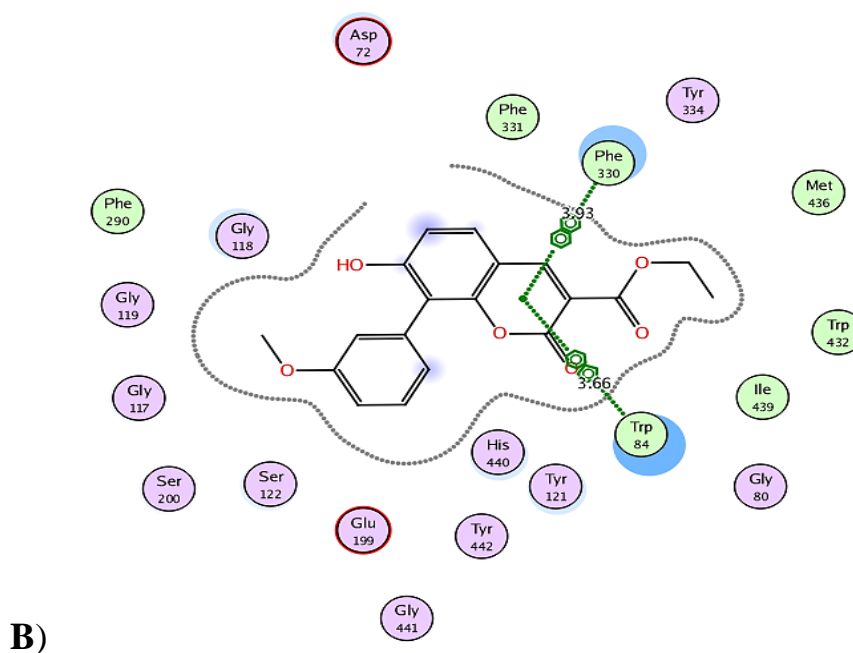
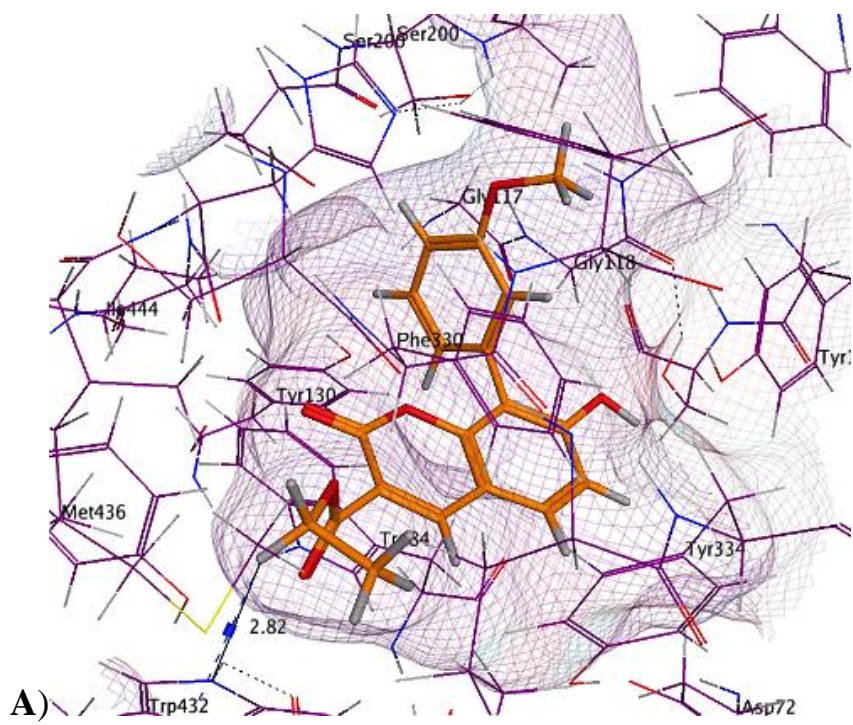
**Figure 354A-B:** Molecular docking models 3D (**A**) and 2D (**B**) of interactions at lowest energy conformations between the acetylcholinesterase (AChE) and selected Inhibitor **2**.

**Table 5:** Comparison of dissociation constant ( $K_D$ ) values of inhibitors (**1-4**) and the control (Tacrine) obtained as a result of concentration-dependent STD NMR results to M.O.E., software. However, the  $K_D$  values are mean,  $\pm$  standard deviations, where standard errors were all within the 5% of the mean.

<b>Compounds</b>	<b>STD Dissociation</b>	<b>MOE Binding</b>
	<b>Constant <math>\mu\text{M}</math></b>	<b>Energies Kcal/mol</b>
<b>Tacrine</b>	140	-5.13
<b>1</b>	30	-7.46
<b>2</b>	194	-7.39
<b>3</b>	252	-4.25
<b>4</b>	210	-6.50

This best-fit accommodation with second highest free energy again supported the fact that single piperidinyll substituent is responsible for major interaction. It provided a water-mediated interaction cage between the electronegative oxygen of carboxyl group that makes interaction with Tyr121, Asp72, Trp84 and Asn85 at a distance of 3.35 Å, 2.95 Å, 2.82 Å, and 2.77 Å, respectively. These interactions and thereby free energies within inhibitor-AChE complex could effectively provide an evidence of the same confirmation of interaction results as we could obtain by STD and Tr-NOESY. Moreover, the binding energies (-4.25 Kcal/mol) of compound **3** further provided an accuracy of NMR results, and therefore led to the conclusion that, the moiety responsible for the excessive interaction is the piperidinyll group (Figure 19 and Figure 20). The interaction residues for compound **3** are provided in detail Figure 36A-B.

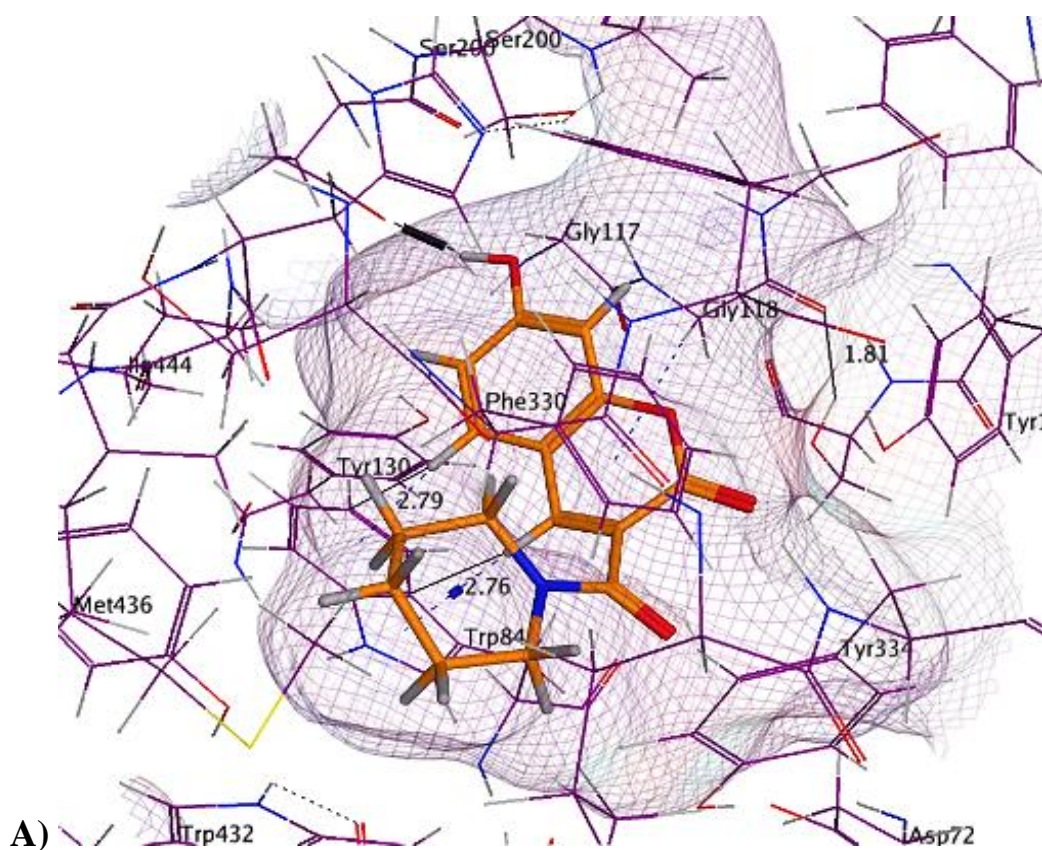


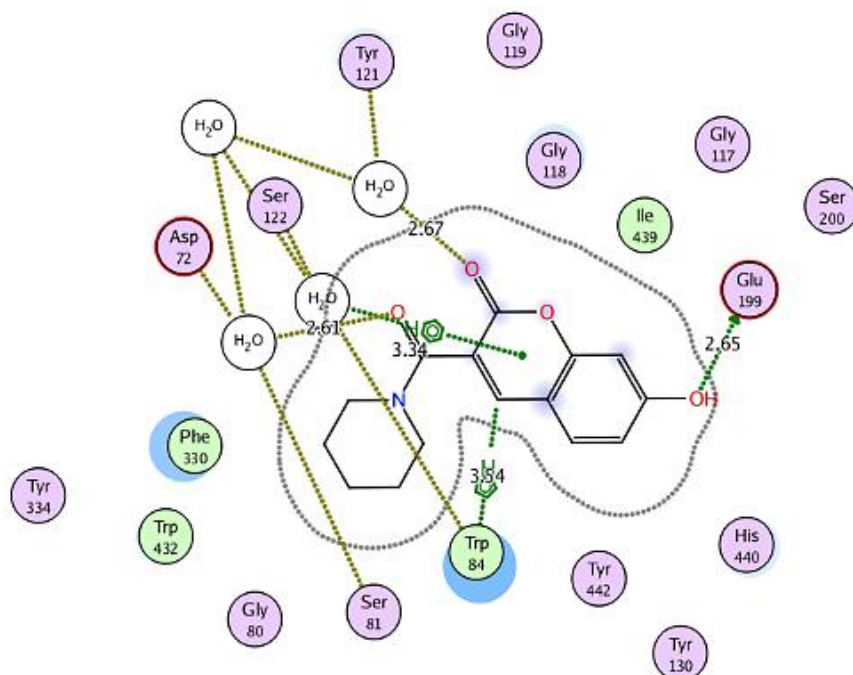


**Figure 36A-B:** Molecular Docking models (3D (A) and 2D (B) of interactions at lowest energy conformations between the acetylcholinesterase (AChE) and selected Inhibitor 3.

Once again, compound 4 ( Figure 19) provided less complex binding energy (-6.50 Kcal/mol) and hence greater stability or adaptability within the complex, even less than compound 3. Even though, it possesses a smaller

structure, however, it remains involved in binding with Phe330 hydrophobic residues through cation- $\pi$  interaction at 3.93 Å as well as with Trp84 by making a cation- $\pi$  interaction at 3.66 Å. The other aromatic amino acid also surrounds the active site including Phe331, Tyr121, and His440 (Figure 37A-B)





**B)**

**Figure 37A-B:** A 3D (A) and 2D (B) molecular docking models of interactions at lowest energy conformations between the acetylcholinesterase (AChE) and selected Inhibitor **4**.

MOE ranked Tacrine (the control) molecule on the fourth position with binding free energy of the complex with  $-5.13$  Kcal/mol that might be due to its rigid structure and lack of the extensions, which aid in adaptability within/ across the binding grooves of AChE, see complete detail of interaction in Figure 38A-B. To find out the best-fit conformation having least inhibitor-AChE complex binding energies, the docking protocol was applied several times with a number of different conformations for each compound and the best fit docked pose with minimum binding energy was determined.



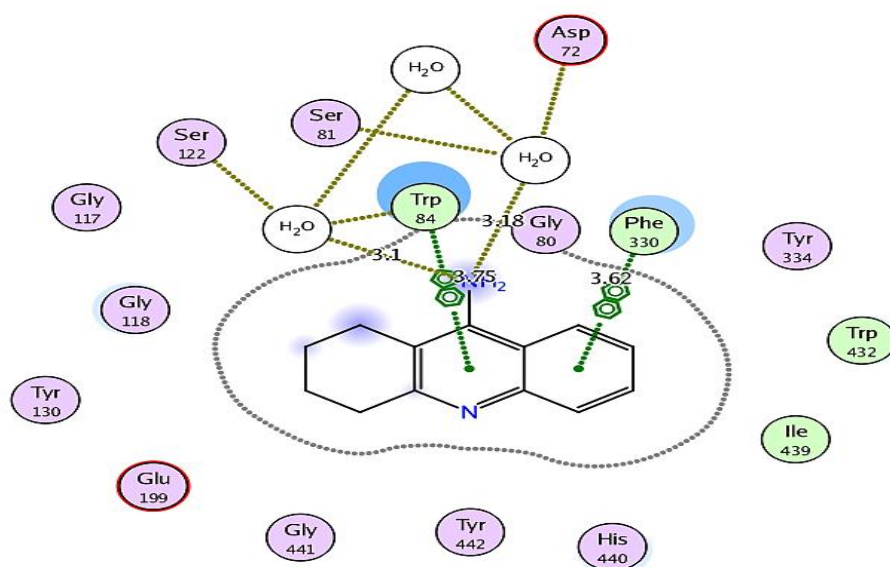
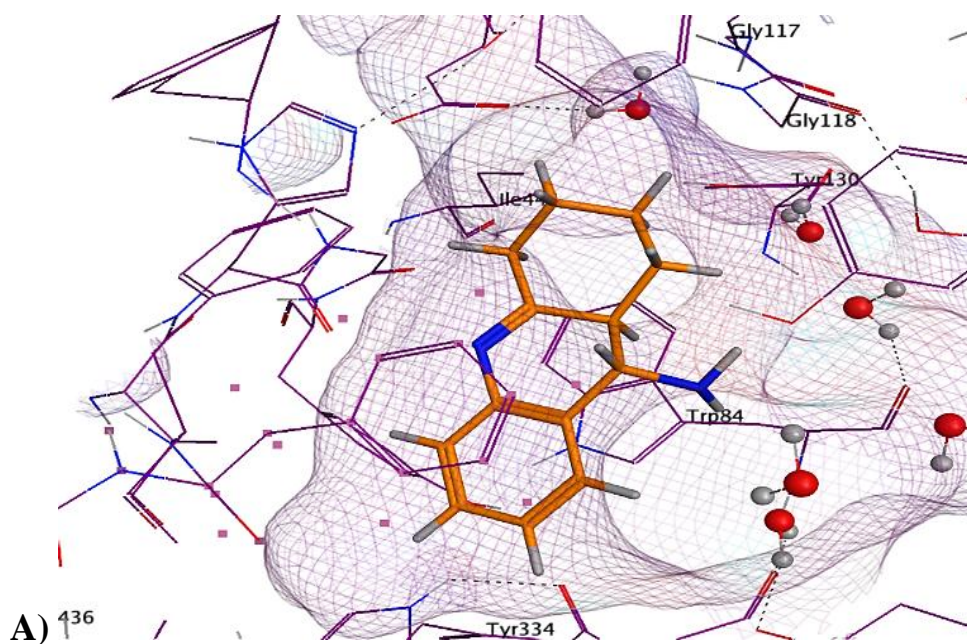


**Figure 38A-B:** A 3D (A) and 2D (B) molecular docking models of interactions at lowest energy conformations between the acetylcholinesterase (AChE) and Tacrine.

## 4.4 Conclusions

Interestingly, from the concentration-dependent and saturation time-dependent experiments, we obtained a direct evidence of piperidinyl involvement as a major stakeholder in this interaction. The inhibitors (**1**, **2** and **4**) with piperidinyl group gave a comparatively a lesser  $K_D$  value and hence, stronger binding than the compound **3**, lacking piperidinyl group. Conversely, the ethoxyl group provided 100% STD effect in both structures deliberately inferred most affinity towards the AChE binding cavities. Therefore, compound **1** with both major binding extensions (piperidinyl and ethoxyl) off the coumarin rings stands tall in affinity towards AChE as provided evidence of STD NMR with  $K_D$  value of 30  $\mu\text{M}$  and Tr-NOESY experiment with clear negative signs cross peaks i-e absolute correlation. Intriguingly, NMR results proved that compound **1** has a better affinity for AChE in all selected compounds (**2-4**), and even better than Tacrine ( $K_D = 140 \mu\text{M}$ ). Intriguingly, docking simulation mimics exactly the STD titration outcomes and nominated compound **1** on the top with its free energy of  $-7.46 \text{ Kcal/mol}$ , this might due to its larger extensions coming off the coumarin ring and cover large surface of the proteins binding grooves. All inhibitors (**1-4**) ideally spaced in the binding cavities of AChE as a result of the cumulative effect of hydrophobic contacts, hydrogen bonding,  $\pi$ - $\pi$  interactions, and hydrophilic-hydrophobic interactions. Indeed, the exclusive involvement of these important substituents with simultaneously three binding sites like Gly118 (anionic subsite) Asp72, Phe330, Tyr334 and Tyr121 (PAS), His440 and Trp84 (quaternary anionic site, bottom of the gorge) made them even more worth full. According to an earlier report,<sup>1</sup> the ligands that can bind two sites can help to prevent the deposition and thereby aggregation of beta-amyloid. Therefore, we supposed that, our library of inhibitors might not be helpful only in stopping the acetylcholine hydrolysis but also can muffle the amyloidal aggregation. More importantly, this study provided a way to

synthesize and generate better AChE inhibitors by piperidine influenced extensions. In addition, though experimental data based on eel AChE, however, structural similarities of this enzyme to vertebrates AChE<sup>180,181</sup> further help in the transfer of these results to the human AChE system. Therefore, based on these realistic results from STD NMR, Tr-NOESY and docking simulations, we suggest our compound **1** as a possible drug candidate for Alzheimer's disease and perhaps can be a possible alternate to tacrine.





## **5. Binding Competition and Group Epitope Mapping of the AChE inhibitors by STD NMR, Tr-NOESY, DOSY and Molecular Docking studies**

### **5.1 Abstract**

Acetylcholinesterase is the most significant enzyme ever known to man and a currently available therapy for controlling the Alzheimer's affect. In this perspective, NMR-based binding studies were performed to probe the inter-ligand binding competitions and the inhibitions potentials towards a selected target. In the ligands recognition assay, AChE-inhibitor complex was also validated through site-specific inhibitor, gallic acid—a known competitive inhibitor. The STD-competition experiments demonstrated that both inhibitors did not compete with gallic acid for the same binding site, and possibly, showing binding with some other site. However, in competition STD experiments the order of binding potential has also been calculated, which declares gallic acid at the top with 157  $\mu\text{M}$  and 4-methylumbelliferone as the least with 165  $\mu\text{M}$   $K_D$  value. Moreover, binding conformations, and diffusion coefficients were calculated by taking advantages of the Tr-NOESY and the DOSY experiments, respectively. Following the NMR results, docking simulations were applied that declared gallic acid, as a second potent inhibitor with a -5.0195 Kcal/mol after 4-methylumbelliferone with a -5.4894 Kcal/mol binding energies. Thus, in conclusions, by combining the realistic NMR and theoretical docking results permitted us to say that these molecular structures and/or their extensions with basic scaffold of coumarin and gallic acid can further be utilized in controlling Alzheimer's disease in near future.

## 5.2 Introduction:

Alzheimer's disease (AD) the lead cause of almost all dementias that can be characterized by severe behavioral abnormalities, memory loss and lessening in intellectual abilities. AD is a progressive neurodegenerative disorder, which in more general, a major threat to the elderly population.<sup>184</sup> As per the cholinergic speculation, the main reason for AD is the decomposition of acetylcholine in the brain, and up-to-date reports counsel that by increasing the level of acetylcholine in the brain through inhibiting the AChE (acetylcholinesterase) activity might be an auspicious direction for AD treatment.<sup>185</sup> AChE exists mainly in the synaptic clefts (in nerves and skeletal muscles) and in central nervous system (CNS) of living organisms<sup>164</sup> that belongs to the family of serine hydrolase enzyme. It catalyzes the hydrolysis of the neurotransmitter acetylcholine (ACh) to choline (Ch) and acetate ions, which plays a critical role in memory and cognition events.<sup>186-188</sup> Typically, inhibitors those bind themselves to catalytic sub-site (CAS) in the deep gorge groove are deemed to possess an essential role in the inhibition of AChE. In addition, as stated in few earlier reports, the AChE inhibitors those bind simultaneously to two sites like peripheral anionic site (PAS) and catalytic anionic subsite (CAS), besides stopping ACh hydrolysis might help in muffle the amyloidal aggregation.<sup>159, 160</sup> Therefore, the use of such a selective inhibitors might be a better option for controlling the acetylcholinesterase activity, and hence, for the treatment of the AD.<sup>189</sup> Novel AChE inhibitors like Physostigmine, Donepezil, Galantamine, and Tacrine are being used for the AD treatments, however, these drugs also suffer from a number of limitations. For instance, Tacrine, the oldest approved drug for the treatment of Alzheimer has few limitations like short half-life and other side effects related to hepatotoxicity.<sup>190</sup> Soon after the day when first AChE inhibitor was introduced as a drug for the treatment of Alzheimer

disease at the market level, small molecules obtained from natural origin retrieve a prominent position.<sup>191</sup>

In this viewpoint, we have selected three (Scopoletin, Gallic acid and 4-Methylumbelliferone) AChE inhibitors and employed the saturation transfer difference (STD) NMR, Transferred NOESY and Diffusion-ordered spectroscopy (DOSY) in order to find the binding affinities and group epitopes towards the AChE. Scopoletin is a coumarin that possesses a large number of pharmacological activities such as spasmolytic,<sup>192</sup> antifungal,<sup>193</sup> antioxidative, antihyperglycemic, antithyroid,<sup>194</sup> antitumor<sup>195</sup> and AChE inhibitory activity.<sup>196, 197</sup> On the other hand, 4-Methylumbelliferone is also a coumarin, which is well known for its AChE inhibitory effect<sup>197</sup> and hyaluronan synthase suppressor activities.<sup>198</sup> Similarly, gallic acid is a type of phenol acid having anticarcinogenic,<sup>199-202</sup> antioxidant,<sup>203, 204</sup> anti-allergic<sup>205</sup> and anti-inflammatory<sup>192</sup> biological activities. Moreover, gallic acid is a competitive inhibitor of AChE and has a similar inhibition pattern as that of Galantamine.<sup>146, 193</sup> Furthermore, gallic acid possess a strong antioxidant property which became the reason for its selection in this binding study. It is well comprehended, that the antioxidant compounds possessing AChE activity may have a better role in controlling the AD. Even though, gallic acid possesses less AChE inhibitory activity, unlike the other AChE inhibitors that are being used for the treatment of AD. However, the additional advantages, in selecting and using these targeted compounds, are associated with low molecular weight and smaller size that might help them to reach the location of action (brain) after the oral or percutaneous administration, and hence, can therefore helpful in the transport of material across the brain barrier. Therefore, these active compounds might help in preventing the further spread of adverse psychological and memory related features operating in some patients with moderate or severe AD, more easily.



Soon after the appearance of first acetylcholinesterase inhibitor, numerous techniques started operating frontward to search out new inhibitors and their interaction studies towards AChE in order to moderate the AD influence. Unfortunately, NMR-based techniques for the ligand-protein interactions have not been investigated extensively because of the problems related to solubility of compounds in water, as it would be in normal conditions. Nevertheless, a few NMR studies, based on line broadening and changes in the longitudinal relaxation time  $T_1$  are accounted for acetylcholinesterase-inhibitor complex, are reported.<sup>138, 139</sup> In fact, information fingered by those NMR methods were remained blur as opposed to the newly NMR methods in term of epitope mapping and conformational information. In contrast, other new NMR techniques, for instance, the saturation transfer difference (STD-NMR) and transferred Nuclear Overhauser Effect Spectroscopy (Tr-NOESY) offer additional conformational and epitope mapping details resulting from these interactions. Additionally, STD NMR is most robust technique that could distinguish the bound ligand from the free ones up to an atomic level precisely. Therefore, nowadays STD NMR is a well-established and linchpin method for NMR-based screening. It requires a very low concentration of protein without isotopic labeling and, with no prior knowledge of its structure and function. More so, there is no restriction on the protein size. Based on the aforementioned facts, it is the foremost routinely used technique for ligands/inhibitors recognition process; of the larger known and unknown molecular libraries,<sup>94, 97</sup> for binding epitope mapping,<sup>94, 97</sup> and for calculating dissociation constant<sup>100</sup> of weakly binding molecules where most of the other analytical methods are unable to provide satisfactory answers.

## 5.3 Result and Discussion:

### 5.3.1 $^1\text{H-NMR}$ and STD NMR Studies

In this work, we have selected a set of two coumarin derivatives—known inhibitors of AChE (Scopoletin and 4-Methylumbelliferone) together with one phenolic acid derivative (Gallic acid) to explore their interactions (Figure 39). Since Gallic acid is a competitive inhibitor, and it shows competition with other substrates for the same binding site as does the Galantamine.<sup>160, 207</sup> Therefore, we intend to report herein a nuclear magnetic resonance spectroscopic binding studies of these three inhibitors against AChE from the electric eel *Electrophorus Electricus*. Specifically, STD-NMR, Tr-NOESY, and DOSY NMR spectroscopic binding investigations have been utilized to portray the comprehensive detail of this inhibitor-AChE complex system. Following this, a docking simulation study has been applied which also provided the same results as we could have through NMR data. By the combination of different approaches, our results have confirmed that all compounds showed strong interactions towards AChE, although showing binding with different locus.

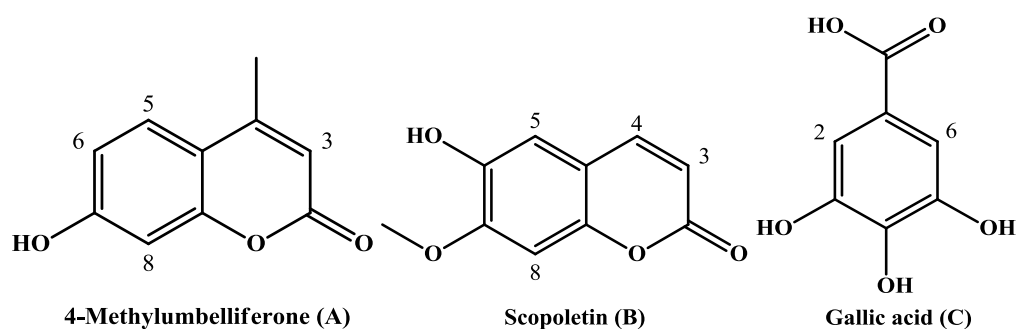


**Figure 39:** Molecular structures of the targeted compounds (AChE inhibitors) for binding interactions.

In the first experiment,  $^1\text{H-NMR}$  spectra without and with protein were performed with the aim to obtain a clear picture of all signal assignments (Figure 40). Interestingly, the merged peaks of gallic acid and H-8 belonging to

the compound (A) turn out to be separate by adding AChE (Figure 40A). Following these hydrogen spectra, the STD NMR experiments were performed by using the AChE: inhibitor mixture at a 1:100 ratio for all non-concentration dependent studies. The inhibitors were dissolved in a mixture of solvents (methanol- $d_4$  and deuterated phosphate buffer saline (PBS) in 5%: 95% v/v, respectively), while the AChE in deuterated PBS, pH 7.2 in all experiments.

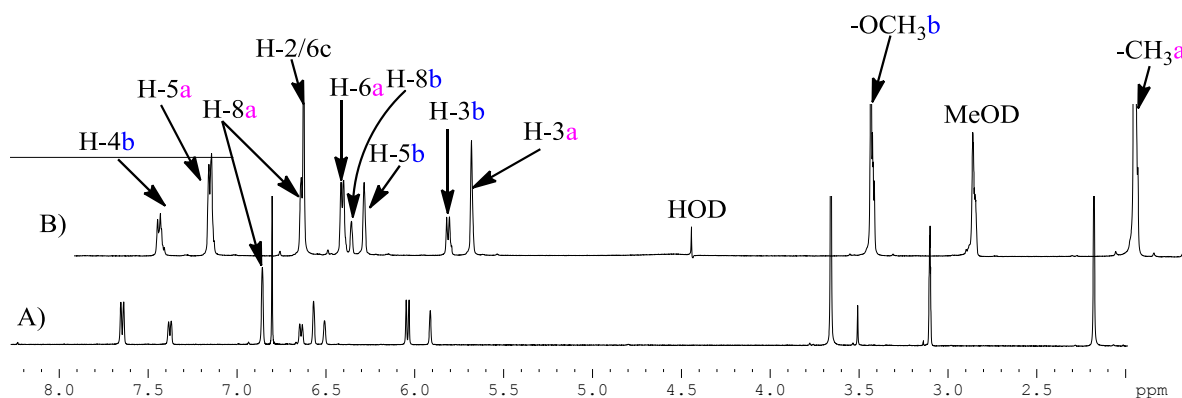


**Figure 40:**  $^1\text{H}$ -NMR spectra of targeted compounds (Scopoletin, 4-Methylumbelliferone and gallic acid) with (A) and without (B) addition of AChE. Where, the signals were made different by giving numbers (a, b and c) with pink, blue and black colors for the compounds 4-methylumbelliferone, scopoletin, and gallic acid respectively.

Primarily, we performed the STD NMR experiment and slight changes in chemical shift values were detected by adding AChE that can be seen in Figure 40. For the epitope mapping, we have done STD NMR experiments with different saturation times (0.5-5 s) and percent STD amplification factors were calculated on the basis of integral values from the stacked plot in Figure 41.

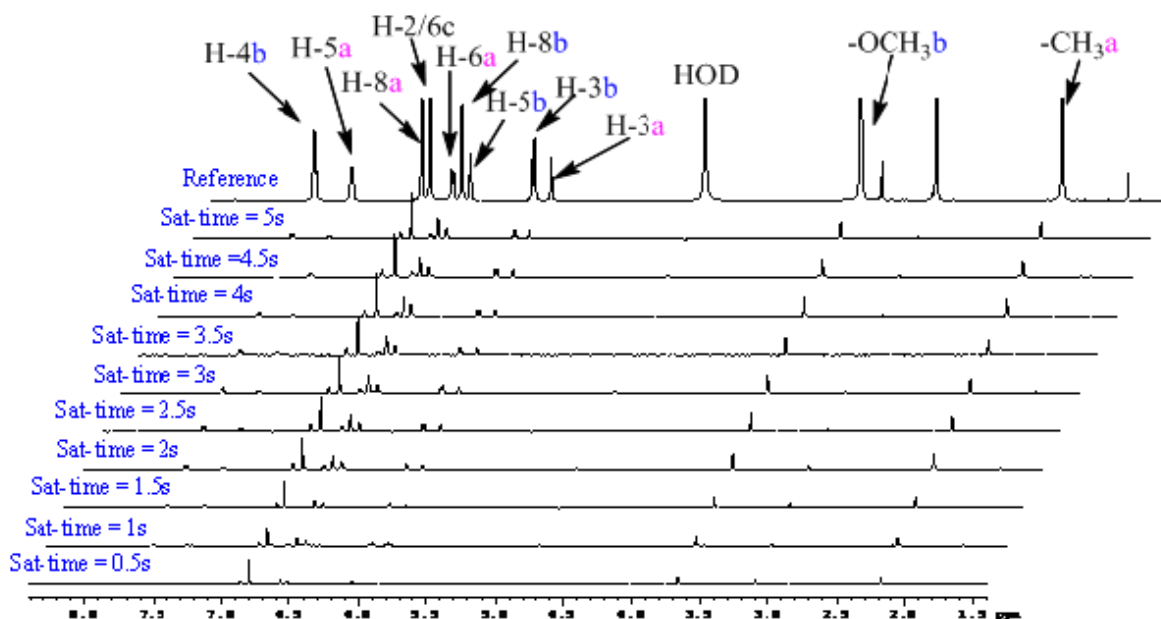


**Figure: 41:** Stack plot of saturation time-dependent STD NMR spectra, for more information, see the experimental details chapter 3.

In all STD NMR experiments, larger signal was given the 100% STD amplification factor (AF), and all other signals were normalized with reference to this. In the STD NMR experiment, the signal intensity not only reflects the relative amount of saturation that received by the particular hydrogen from the protein via cross-relaxation, but also the relative proximity to the protein. In particular, signal intensities in STD NMR spectrum depend on two factors, one is the concentration of ligands and the second is, the saturation that received by the given molecule. As the ligand concentrations and saturation of protein are increased, in response, intensities of STD signals will, therefore, be increased.<sup>94, 97, 100</sup> The relative STD effect as we measured for the gallic acid clearly showed that it had a major affinity towards AChE as shown in Figure 42, which revealed 100% STD effect and remains tall. The second STD effect was obtained for hydrogen H-8 of compound **A** (4-methylumbelliferone) with 75%, while the third largest effect for  $-\text{CH}_3$  group of compound **B** (scopoletin) which remained noticeable with 61% effect. Similarly, the  $-\text{OCH}_3$  group of compound **B**, and hydrogen H-6 of the compound **A** remained prominent with 59% and 51%, STD AF. On the other hand, the hydrogens H-3 and H-4 of compound **B** showed 49%

and 41% and hence, were little more solvent exposed. In contrast to the aforementioned hydrogens, H-8 of compound **A**, H-5 belonging to compound **A** were well-nigh similar to 33 and 32 % STD AF, which supposed that these hydrogens were further far from binding cavity and among other signals which were more solvent exposed. However, H-5 of compound **A** could provide the least STD AF with almost 25%, which clearly infers that this hydrogen was absolutely far or in such a position that it could not receive an irradiation transfer from the AChE. From these STD convincing results, it can be assumed that gallic acid shows more interaction towards the binding cavities of protein. While, the compound **A** (4-methylumbelliferone) and compound **B** (scopoletin) showed lesser bindings towards the AChE or adopted themselves within a shallow or large cavities where they were unable to get proper saturation transfer from protein.

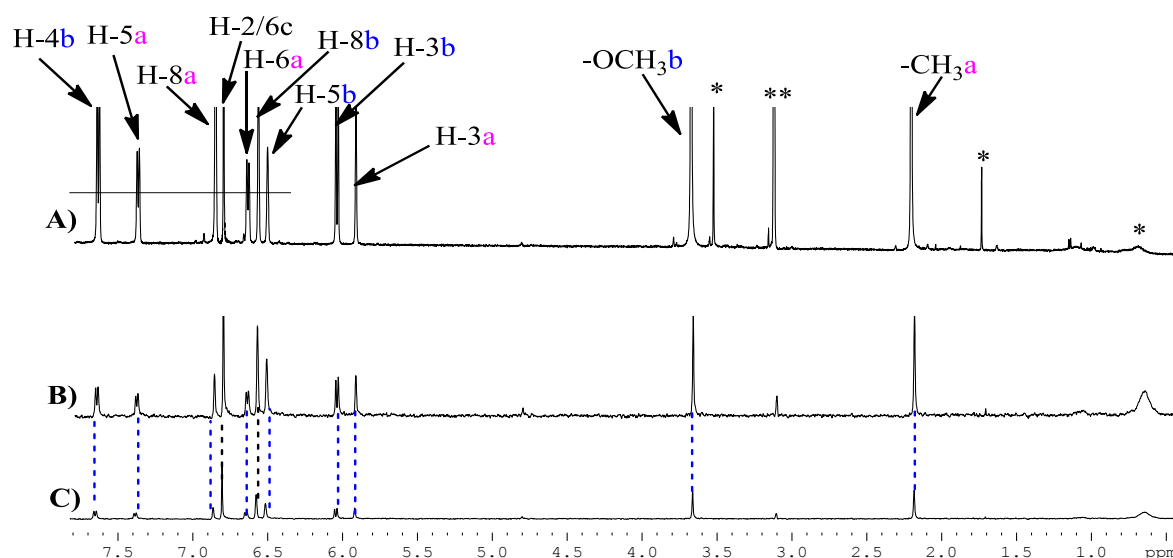


**Figure 42:** <sup>1</sup>H-NMR (A), *Off-resonance* (B) and STD NMR spectrum (C) of targeted compounds (Scopoletin and 4-Methylumbelliferone and gallic acid) in AChE. Where, signals were made distinct by giving numbers (a, b and c) with pink, blue and black colors for the compounds 4-methylumbelliferone, scopoletin and gallic acid respectively.

### 5.3.2 Transferred NOESY Studies

For further support to our STD results, we also probe the binding affinities of the compound (A) (B) and (C) through 2D Tr-NOESY experiment. A solution containing AChE dissolved in D<sub>2</sub>O and PBS buffer (pH 7.2) while inhibitors (compound A, B and C) in 5:95 v/v methanol-*d*<sub>4</sub> and deuterated buffer respectively, was prepared. The 2D NOESY experiment was performed by keeping a fixed concentration of 20 mM for each inhibitor (A, B and C) while, 2D Tr-NOESY experiment was performed with the same concentrations of the inhibitors in a 50 μM concentration of AChE. Importantly, for the Tr-NOESY experiment, a Bruker standard phase sensitive pulse sequence was modified by putting the spinlock of 3500Hz after the first 90° pulse to remove the background signals of protein.<sup>94, 97</sup> Since it is well comprehended that, free small molecular size compounds show positive NOEs due to the fast tumbling and slow relaxation rates. On the other hand, compounds within the

macromolecular solution show negative NOEs because of slowly tumbling and fast relaxation rates.<sup>183</sup> The smaller molecules those show affinities towards some macromolecule they owe the characteristics of the larger molecule and behave like an as a part of the larger molecule, therefore, they show negative NOEs—a characteristic of macromolecule. It is worth mentioning that, as opposed to 2D NOESY, the buildup rate of Tr-NOESY was much faster with short acquisition time, even though, both experiments were performed with equal mixing time (400 ms). In the Tr-NOESY experiment, all inhibitors showed negative NOE because of the slow tumbling rates of hydrogens while in the binding cavity of AChE, unlike the free inhibitors (Figure 43) with positive NOEs. The strong cross peak of the targeted inhibitors showed an excellent agreement to the previously performed STD experiments. These unambiguous results of Tr-NOESY and STD NMR findings allow us to deduce that these small inhibitors showed clear affinity towards AChE.

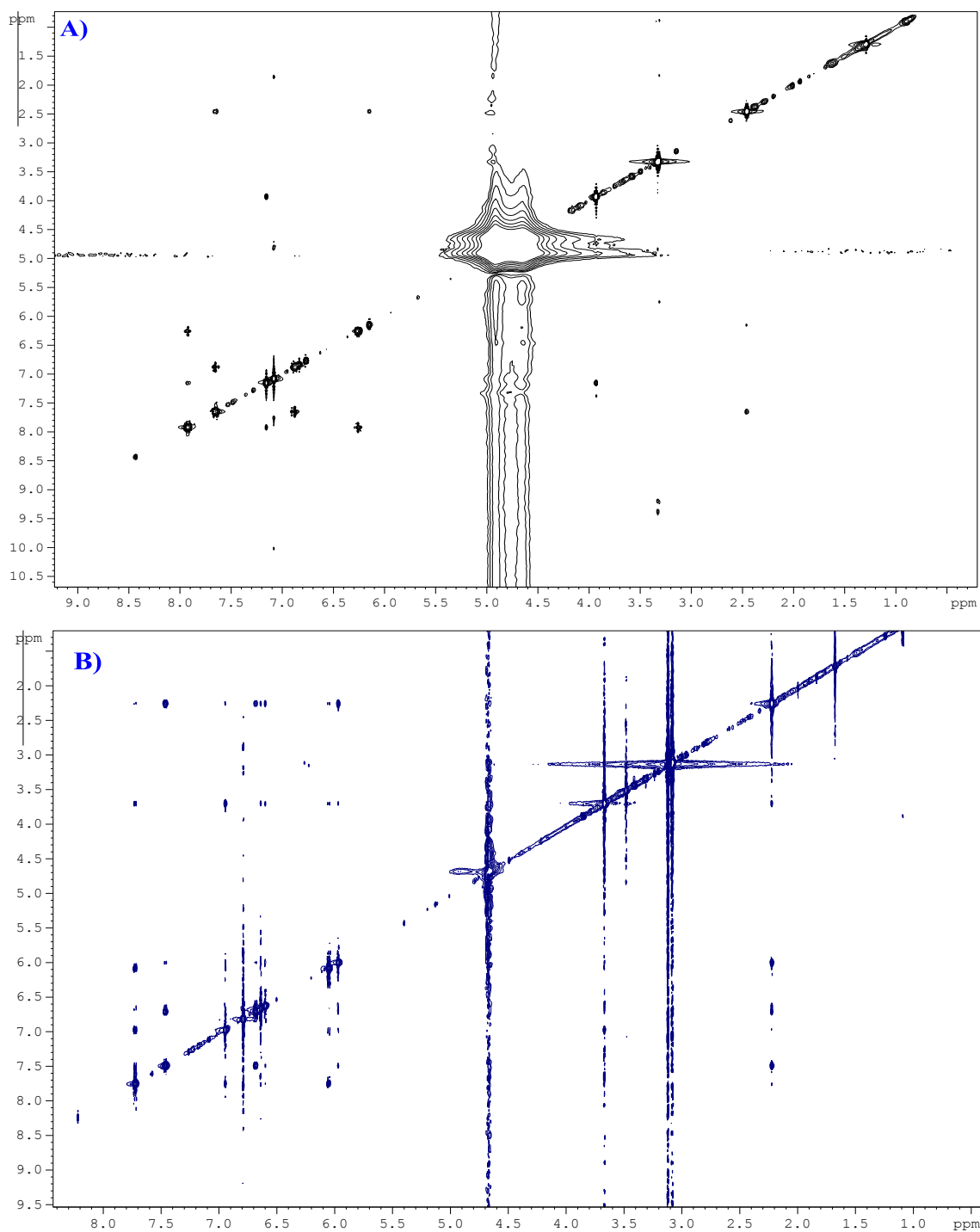


**Figure 43:** 2D-NOESY (A) and 2D Tr-NOESY (B) spectra of targeted compounds (scopoletin and 4-methylumbelliferone and gallic acid) without (A) and with (B) addition of AChE.



### 5.3.3 STD NMR Titration Studies

After obtaining the knowledge associated with the bound conformations of these interacting ligands, through STD NMR and Tr-NOESY towards the AChE, the subsequent step was to seek out the specific binding site for each ligand. To accomplish this goal, a competitive ligand with well-known and delineate binding site (reporter or spy molecule) was evidently necessary to form a comparison with the unknown molecule for the corresponding site hunt. Therefore, in order to achieve this goal, we have applied STD NMR competition studies—a well-known NMR experiment that can confirm that whether the reporter molecule and ligand compete for the same site of protein or not. Since, gallic acid is a well-known and selective binder towards AChE<sup>160, 207</sup> however, it is the first time it has been used for this type of titration studies.

It has been proven earlier that if a reporter molecule will show more affinity towards the specific site of the given protein than to the other unknown ligand, by increasing its concentration the respective STD signal intensity of the other ligand will decrease. On the other hand, if the unknown ligand binds itself more tightly than the reporter molecule does, by an increase in concentration of the reporter molecule does not affect the signal intensity of the respective STD signal. In other words, if the spy molecule is relatively less tight binder for the same site as the unknown ligand then the increase in concentration of unknown ligand will decrease or even wipe out the signal intensity of spy molecule at a specific concentration, in the STD titration studies. However, despite these possibilities, if both compounds (spy and unknown) are binding with different sites, none of the signals is going to be affected.<sup>97</sup>

To make a lucid judgment upon competition, and to find that particular concentration where one of these inhibitors (**A** and **B**) could replace gallic acid, we prepared a solution of these three inhibitors (**A**, **B** and **C**) by using varying concentrations ranging between 0.10-2.0 mM. The first experiment was

performed with a concentration of 0.10 mM of inhibitors by using a constant saturation time of 2 s. At this concentration, inhibitors (**A**, **B**) could not replace gallic acid perhaps gallic acid showed more interaction towards AChE. In the similar way, by gradually increasing concentration of inhibitors while keeping AChE constant, different STD competition experiments were recorded (Figure 44).

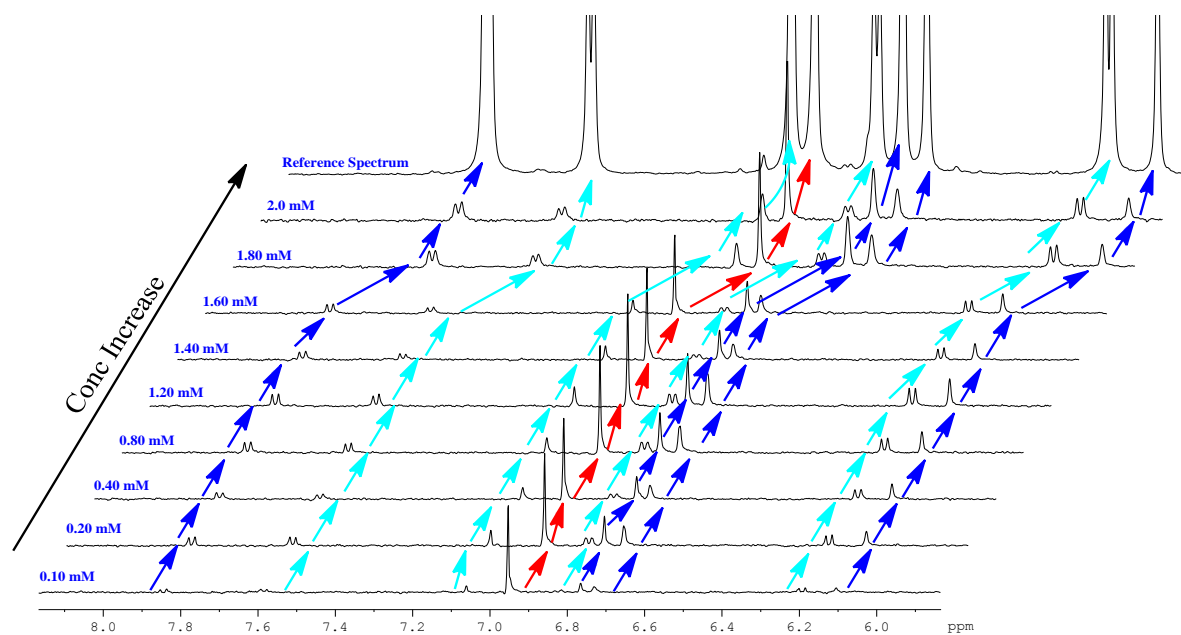


**Figure 44:** Stacked spectra of concentration-dependent STD-NMR experiments of (**A**, **B** and **C**), by varying concentrations (0.1, 0.2, 0.4, 0.8, 1.20, 1.40, 1.60, 1.80 and 2.0 mM) of inhibitors with respect to AChE.

Different experiments by varying the concentration of ligands to 0.20mM, 0.40mM, 0.80mM, 1.20mM, 1.40mM, 1.60mM, 1.80mM and 2.0mM, provided a similar behaviour in the spectra with the same results explaining that, gallic acid was not replaced by any inhibitors (**A**, **B**). From these competition studies a conclusion can be suggested that none of inhibitors (**A**, **B**) compete with gallic acid (see Figure 44) for the same binding site although they showed interaction towards AChE with some other binding locus, therefore, showing binding with different binding sites or behaving as a non-competitive inhibitors. However, a little change in chemical shift values were observed at 1.80 and 2.0 mM

concentration of the inhibitors, as shown in figure 44, although the signal intensity of the gallic acid was not affected. The change in chemical shift values at higher concentrations might due to the overload of inhibitors that turns the bindings with some other site as well. Finally, the dissociation constant ( $K_D$ ) values for each inhibitor was calculated from these concentration-dependent STD experiments by taking help of the method reported elsewhere.<sup>100</sup> The plot of the inhibitor concentrations versus STD signal intensity is shown in figure 45, from where the dissociation value were evaluated. Interestingly, the calculated  $K_D$  values declared gallic acid as a potential inhibitor of AChE as presented in Table 6.

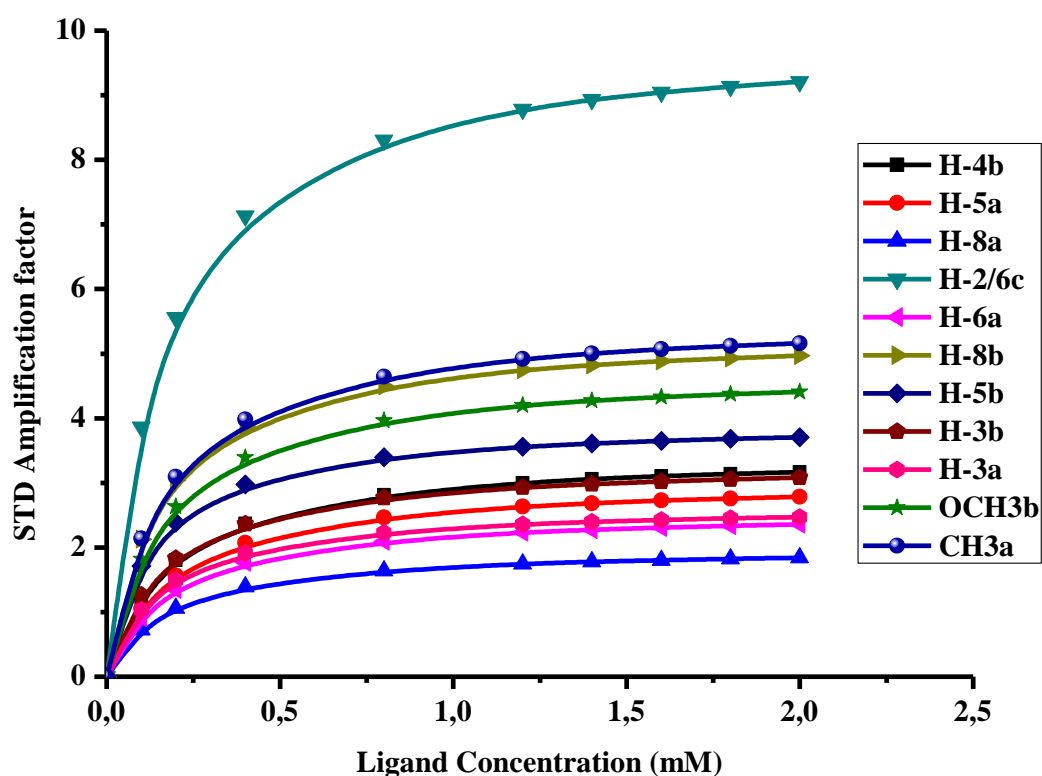


**Figure 45:** STD amplification factor curve plot of **A**, **B** and **C** as a function of varying concentrations for each single parabolic line that determined from the STD concentration-dependent spectra as shown in Figure 44.

### 5.3.4 Diffusion-Ordered Spectroscopy Studies

In addition to STD, Tr-NOESY, we have performed the 2D diffusion-ordered spectroscopy for these targeted inhibitors with and without (Figure 46) the addition of AChE. From years, this technique grows up as a method of choice for the multicomponent systems separation, as well as binding interaction analysis.<sup>208</sup> Moreover, diffusion calculation and spectral understanding is very easy because chemical shift occupies the abscissa (horizontal axis) and while, the vertical axis (ordinate) with diffusions values in  $1 \times 10^{-9} \text{ m}^2/\text{s}$ . First sights look at comparative display of 2D DOSY (Figure 46) demonstrated that all signals of the inhibitors, except the solvents, from both spectra (with protein and without protein), are present between diffusion coefficient  $0.7 \times 10^{-10} \text{ m}^2/\text{s}$  to  $0.3 \times 10^{-10} \text{ m}^2/\text{s}$  along the  $F_1$  dimension (ordinate axis). From two different color signals (Figure 46), the change in diffusion coefficients of these small molecules became quite clear upon addition of AChE. Therefore, based on the results, we conclude that, targeted compounds are showing interaction, as it is well-correlated with the fact that, the particle possessing affinity towards the receptor molecule, exhibits the change in the values of diffusion coefficient by the addition of the receptor.<sup>100, 208</sup>

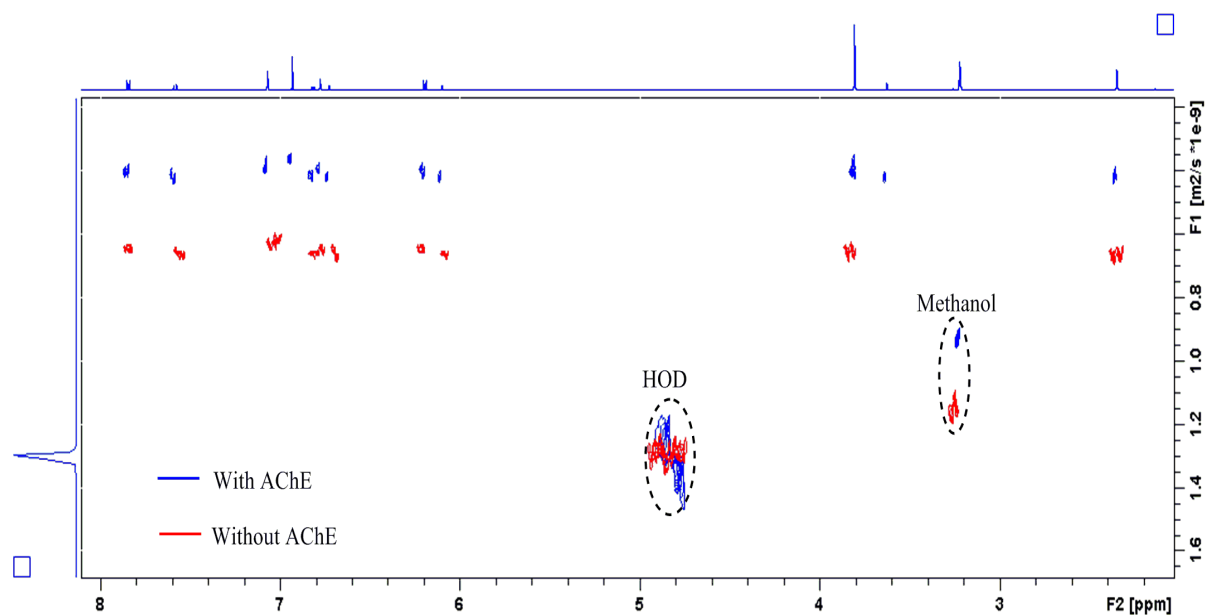


**Figure 46:** A double display of 2D-DOSY NMR spectrum of **A**, **B**, and **C** with Acetylcholinesterase enzyme, where the X-axis contains the standard  $^1\text{H-NMR}$  chemical shifts values, while the y-axis contains the diffusion coefficient values in  $1 \times 10^{-9} \text{ m}^2/\text{s}$ .

By placing two spectra together in double display mode and by adding the HOD signals one upon other in order to get absolute diffusion, the diffusion changes in the spectrum with and without AChE were quite clear. Where, the diffusion coefficient of inhibitor **A** as showed in the spectrum figure 46, is  $4.29 \times 10^{-10} \text{ m}^2/\text{s}$  and  $6.72 \times 10^{-10} \text{ m}^2/\text{s}$  with and without AChE addition respectively, and with a total difference of  $2.43 \times 10^{-10} \text{ m}^2/\text{s}$ . Likewise, the first one, other two inhibitors also afforded changes in their diffusion coefficients. For inhibitor **B**, the values  $6.47 \times 10^{-10} \text{ m}^2/\text{s}$  and  $4.1 \times 10^{-10} \text{ m}^2/\text{s}$  was noted with a difference of  $2.37 \times 10^{-10} \text{ m}^2/\text{s}$  while, the compound **C** was lying between  $6.22 \times 10^{-10} \text{ m}^2/\text{s}$  and  $3.59 \times 10^{-10} \text{ m}^2/\text{s}$  with a total difference of  $2.63 \times 10^{-10} \text{ m}^2/\text{s}$ . This change in the diffusion coefficient by the addition of AChE (Table 6) inferred a clear indication of interactions of these targeted molecules.

### 5.3.5 Molecular Docking Studies

After getting the results from STD, Tr-NOESY, and DOSY NMR, we analyzed the binding mechanism of given inhibitors against Acetylcholinesterase (AChE) through molecular docking simulations. For this purpose, an already published protocol for the selection of binding site residues has been applied.<sup>144</sup> Using Molecular Operating Environment (MOE) 2011.10, docking simulations were performed where structures were sketched followed by minimization with MMFF94x and protonation. Active site information was received through Chimera software by selecting the only available chain A of AChE. The molecular and kinetics analysis revealed that all inhibitors (**A**, **B** and **C**) show interactions towards the central pocket, in the deep gorge and the peripheral site of AChE. All inhibitors displayed almost all types of interaction important for stability of AChE-inhibitor complexes, like hydrogen bonding, hydrophobic contacts, hydrophilic-hydrophobic interactions and  $\pi$ - $\pi$  interaction. gallic acid containing 3 hydroxyl groups at 3, 4 and 5 position of benzoic acid, where, one of the hydroxyl groups is engaged in bridging water molecule at 3.1 Å distance, which in turn links with Asp72 and Ser81 (Figure 47A, B) amino acid residues. The calculated binding energy for gallic acid-AChE complex was -5.0195 Kcal/mol (Table 6).

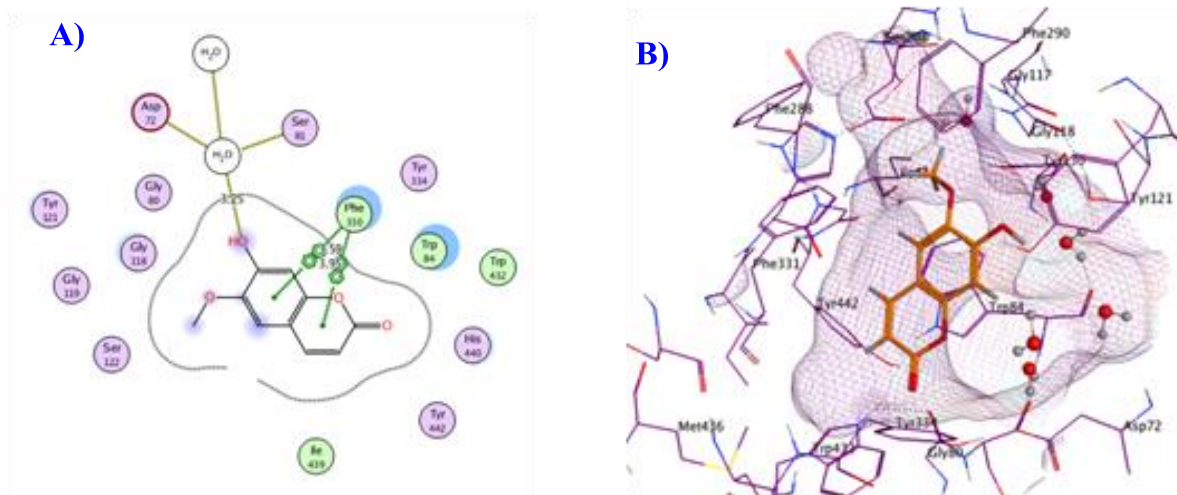


**Figure 47:** A 2D (A) and 3D (B) molecular docking model of inhibitor **A**, showing interactions between the Acetylcholinesterase (AChE) and 4-methylumbelliferone.

**Table 6:** Comparison of dissociation constant ( $K_D$ ) values of inhibitors (**A**, **B** and **C**) obtained a result of concentration-dependent STD NMR and DOSY experimental results to M.O.E. software binding energies, and total change in diffusion values. For more detail, in chapter 3.

Comp	STD Dissociation	MOE Binding	Diffusion Coefficient
	constant $\mu\text{M}$	Energies Kcal/mole	Changes $1 \times 10^{-10}$ ( $\text{m}^2/\text{s}$ )
<b>A</b>	165	-5.4894	2.43
<b>B</b>	162	-4.9313	2.37
<b>C</b>	157	-5.0195	2.63

On the other hands, 4-Methylumbelliferone is involved in hydrogen bonding with Gly441 at 2.84 Å, as well as Trp84, involved in making a cation- $\pi$  interaction at 3.97 Å. Similarly, for water mediating interactions, as other compounds do with the water molecule, the water molecule forms a bridge

between Asn 85 and the hydroxyl group of the ligand at 3.07 Å. In due course, this water molecule forms bridge with another water molecule and Asp72 simultaneously, providing a binding energy of -5.4894 Kcal/mol as the outcome of this overall interaction (Figure 48).

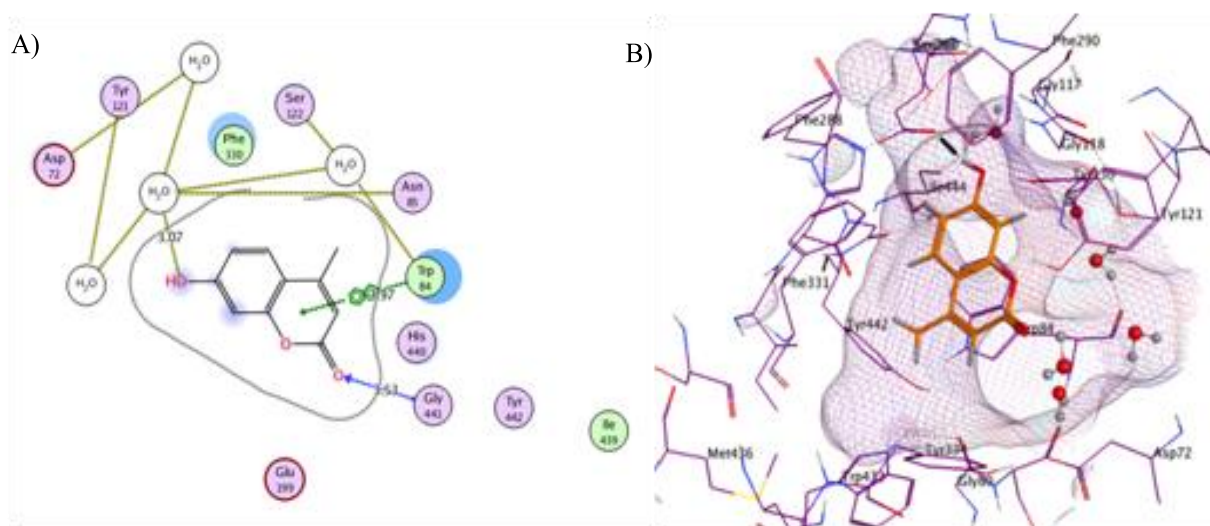
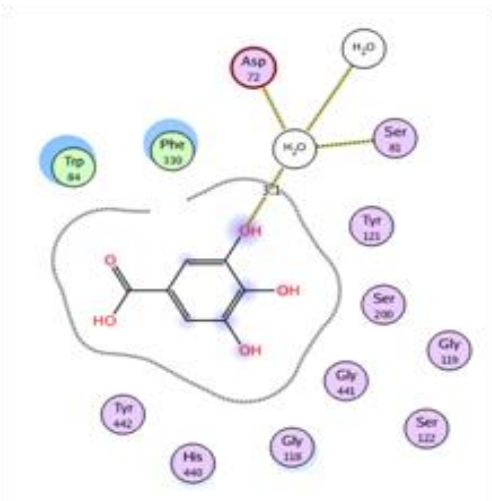


**Figure 48:** A 2D (A) and 3D (B) molecular docking model of inhibitor **B**, showing interactions between the Acetylcholinesterase (AChE) and Scopoletin, generated by using Molecular Operating Environment (MOE) 2011.10.

In the same way, in the Scopoletin a key interacting Phe330 hydrophobic residue is involved in cation- $\pi$  interaction at 3.59 Å and 3.95 Å with two aromatic rings. A water molecule forms bridge between ligand, Asp72 at one end and between ligand Ser81 at a distance of 3.25 Å, on the other hand (Figure 49). The resulting binding energy of this scopoletin-AChE complex was -4.9313 Kcal/mol as provided by MOE software. Comparisons of binding energies of MOE with dissociation values resultant from the STD and DOSY experiments are shown in Table 6. MOE ranked 4-methylumbelliferone (**A**) at the top with binding energy of -5.4894 Kcal/mol, gallic acid (**C**) made it space at second position with binding energy of -5.0195 Kcal/mol, and scopoletin stands third with the binding energy of -4.9313 Kcal/mol (Table 6).



A)



B)

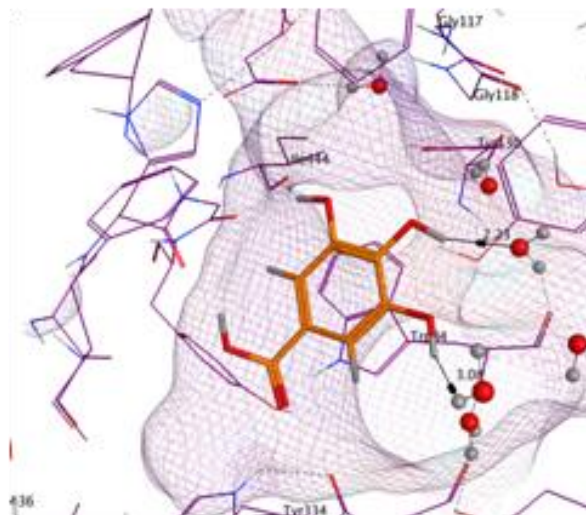


**Figure 49:** A 2D (A) and 3D (B) molecular docking model of inhibitor C, showing interactions between the Acetylcholinesterase (AChE) and gallic acid, generated by using Molecular Operating Environment (MOE) 2011.10.

### 5.3.6 Conclusions:

Based on the cholinergic hypothesis, the inhibition of acetylcholinesterase activity might assist in to control Alzheimer's disease by enhancing the level of cholinesterase in the synaptic cleft between the two neurons. Therefore, with the aim of lessening Alzheimer's affect has prompted us to study ligand recognition assays and the competition studies by using gallic acid through the most extensively and regularly using technique, saturation transfer difference NMR. Saturation-transfer difference and nuclear overhauser effect results clearly showed the evidences of the existence of bindings between these selectively targeted inhibitors and acetylcholinesterase. Moreover, in competition experiments, the dissociation constant value (157  $\mu\text{M}$ ) of gallic acid showed that, it is binding more tightly than the others do. Furthermore, change in the diffusion coefficient by the addition of the AChE in the system also validated the saturation transfer difference results, a further evidence of binding. Finally, by taking help of a theoretical approach—molecular docking, a 3-dimensional model for each compound has also been evaluated. Free binding energies of the acetylcholinesterase-inhibitors complex were calculated by using Molecular Operating Environment software. Interestingly, docking simulation provided the similar results that placed the gallic acid-AChE complex in the second position with the least binding energy of -5.0195 Kcal/mol, might be because it could provide binding through one kind of interaction towards the enzyme. Therefore, we suggest, these new results might open a new window to other scientists, interested in to do further investigation into the potential of coumarin and gallic acid structure-based scaffold and their extensions in controlling Alzheimer's disease.



## 6. NMR Binding Recognition Study of *Terminalia Chebula* extract; New Insights into AChE Binding Behaviour

### 6.1 Abstract

Since antiquity, screening of the natural extract in everyday drug discovery for selective targets plays a vital role, even when there was no papyrus foundation of these remedies as we have today. However, a plethora of medicinal plant extracts are still being used nowadays that are helping in growing scientific interest towards herbals use in the new drug discovery. In this context, *Terminalia Chebula* extract has been explored against acetylcholinesterase (AChE). *T. Chebula* is famous to possess numerous biological activities, which is why it crowned as the kind of medicine. On the other hand, AChE is the one of the primary therapy available against Alzheimer's disease as stated by cholinergic hypothesis. Therefore, by targeting AChE, we have successfully applied the most robust NMR methods such as STD NMR, Tr-NOESY and the 1D- DOSY to find the lead compounds from an ethylacetate fraction and its water suspension. This application provides a rapid means of ligand recognition, as well as their group epitope mapping. The use of NMR methods has unequivocally analysed the implication of three compounds in this interaction study. However, the structural characterization by means of two-dimensional NMR methods such as HSQC, HMBC, and Mass spectrometry confirmed them as 4-hydroxyxinnamic acid **1**, Ethyl 4-hydroxycinnamate **2**, and lupeol, **3**. Moreover, a change in diffusion values by adding AChE as oppose to alone *T. Chebula* extract spectra provided the evidence of interaction. Therefore, the combination of these NMR data not only assured the explicit recognition for AChE but also explain the behaviour of this enzyme in ligand selections.

## 6.2 Introduction

*Terminalia chebula* RETZ (Combretaceae) is a medicinal plant widely distributed throughout the central Asia and is well-known as “king of medicine” because of exhibiting a bundle of potential activities. The dried ripe fruit of *T. chebula* is known as Black Myrobalan has traditionally been used in the treatment of asthma, sour throat, vomiting, hiccough, diarrhea, bleeding piles, gout, and heart and bladder disease.<sup>209, 210</sup> A herbal formulation containing *T.chebula* under the name “TRIPHALA” is very popular traditional medicine in chronic disorders Black myrobalan is reported to have antioxidant and free radical scavenging activities,<sup>211</sup> it is effective against cancer cells<sup>212</sup> and *Helicobacter pylori*.<sup>213</sup> It is also useful as anti-caries agent,<sup>214</sup> in the dermal wound healing,<sup>215</sup> improving gastrointestinal motility,<sup>216</sup> anaphylactic shock,<sup>217</sup> and diabetes mellitus as well.<sup>218</sup> It has been reported that *T.chebula* contains a constituent, which has a wide antibacterial and antifungal spectrum,<sup>219</sup> and also inhibit the growth of *E. coli*, the most common organism responsible for urinary tract infections.<sup>220</sup> It also exhibits activity against uropathogenic *Escherichia coli*.<sup>221</sup> Besides the aforementioned potential bioactivities, a recent report also suggested that the extract of *T. chebula* possess the acetylcholinesterase (AChE) inhibitory activities,<sup>221</sup> however; there is no scientific data available to date regarding the direct identification of the lead compounds from the extract. Thus, the present systematic and methodological investigation has therefore been designed to find the leads from the *T. chebula* extract that might aid in the future process of drug discovery. Present study deals with *in situ* binding recognitions of *T. chebula* RETZ methanolic extract towards the enzyme, acetylcholinesterase, which will disclose the facts that how these compounds in the extract show inhibition of the target through various types of bindings.

In this context, *in situ* molecular recognition towards a specifically targeted macromolecule (AChE) could be paramount important in term of new

drug discoveries. Especially, for the molecular entities those are even sensitive towards the light and the solvents contact, and can oxidize in air or by some environmental changes etcetera. To track such sensitive molecular entities, there must be some analytical tool, which encounters all difficulties associated with. A number of analytical methods, biological assays, and various tools are being used nowadays for the purpose to cope this problem. Importantly among them, the most commonly used analytical tools for the mixture analysis and for exploring bindings are the Mass spectrometry (MS), NMR, Fluorescence (FS), Ultra-violet (UV) and Circular dichroism (CD), etc. Therefore, NMR seems to be an ideal approach that is non-invasive, environmentally friendly, and non-destructive as well as could provide possible all information related to new structure characterization and binding conformations.<sup>183</sup> Moreover, NMR has an upper edge over other analytical methods in observing the weekly binding process, where most of the analytical methods are unable to provide a satisfactory answer.<sup>72</sup> There is no need of volatility of the compounds, not necessary chromophores or unsaturation for the delocalization of the electrons, and no optical absorbance is mandatory.<sup>94</sup> Unlike other analytical approaches, for instance, MS, FS, UV, and CD respectively, demands to see the interactions. Although in term of sensitivity, these techniques are far sensitive to NMR and are therefore used commonly in drug discovery process. However, the restrictions like difference in polarities of various components in mixture, absence of optical absorbance, lack of resolving signals overlaps, and unable to distinguish between the isomers make them unsuitable for the rapid screening method.

Different NMR methods have been using nowadays to explore the molecular recognition process—an utmost important phenomenon exists in our body. Since most of the human body functions and disease controlling mechanism involving, this molecular recognition process through ligand-receptor or receptor-receptor types of interactions. Therefore, to focus molecular

recognition process based on ligand-receptor or receptor-receptor is a prime important domain in new drug discovery. We have selected to target the ligand-based NMR methods for this study, as these method requisites less macromolecular amount without any isotopically labeling. Amongst different ligand-based NMR method saturation transfer difference (STD) NMR technique<sup>178</sup> and Tr-NOESY,<sup>183</sup> is the more sensitive and reliable method available up-to-date in observing binding interactions. Since STD NMR is well-established in providing the binding interaction of the extracts towards a target,<sup>97</sup> aiding in calculating dissociation constant for the ligands within the complex and in group epitope mapping of the binding ligands.<sup>100</sup> On the other hand, Tr-NOESY experiments are known because of proving; the special distance of two interacting counterparts, and in intimate binding conformations.<sup>222</sup>

In the present work, we have utilized the Tr-NOESY and STD NMR experiments for small molecular recognition towards AChE. Since it is well understood that AChE is implicated in hydrolysis of the most important neurotransmitter acetylcholine (ACh) into choline and acetate ion and thereby, destroying the nerve impulses that it carry.<sup>43</sup> This continuous loss of nerve impulses creates a cholinergic deficiency that turns into a disease commonly known as Alzheimer disease (AD)—a neurodegenerative disease that leads to a variety of psychiatric symptoms including memory loss.<sup>223</sup> The cholinergic response can, therefore, be achieved by restoring the cholinergic deficiency in the synaptic cleft through lessening the hydrolysis activity of AChE by its inhibition.<sup>43, 47</sup> Thus, the AChE inhibitors are the best-known symptomatic treatment that could somehow reduce AD effect by lessening or stopping ACh hydrolysis.

To date, to the best of our knowledge, no one has ever used the *terminalia chebula* RETZ extract for the screening of the lead compounds towards the acetylcholinesterase enzyme. The *terminalia chebula* is best known for the

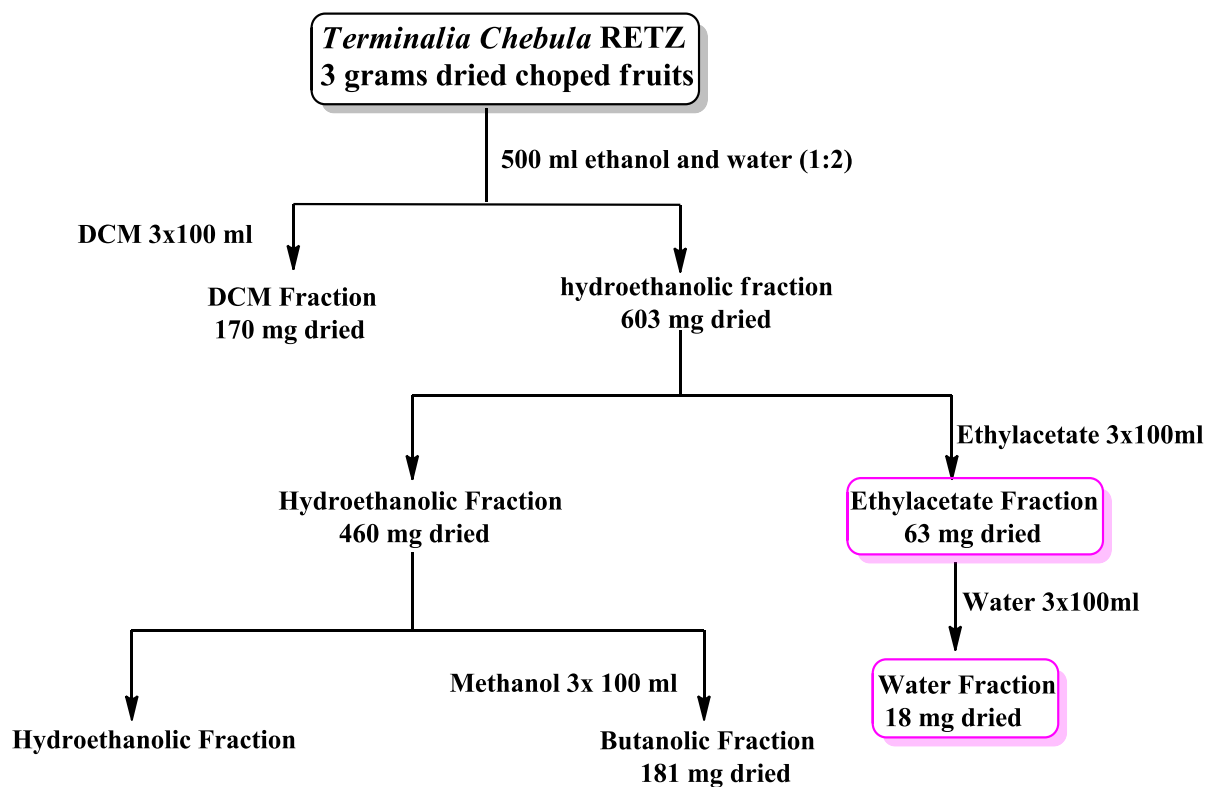
inhibitory activity of the extract and some of its constituents against AChE.<sup>221</sup> Therefore, screening of this extract by using the most robust NMR methods might provide innovative idea in the field of new drug discovery in controlling AD.

### **6.3 Results and discussion**

Based on the controlling AChE activity, the uses of its inhibitor seem to be an excellent treatment for the Alzheimer disease. Since the approval of the first AChE inhibitor as to be a drug, numerous methods get involved to target this enzyme for the new drug discovery. Therefore, among these NMR seems to an ideal choice because of its robustness in operation and non-invasive in nature. In this context, we have been utilizing the advantages of the NMR to evaluate the recognition of *Terminalia* extract towards a specific target (AChE).

In the first step, 2 mg of ethyl acetate fraction (Figure 50) of the extract from this medicinal plant with 1 micromolar solution was triggered into NMR by adding the 5 % methanol-d<sub>4</sub> and 95 % PBS buffer made in ten percent deuterated water solution into NMR spectrometer.

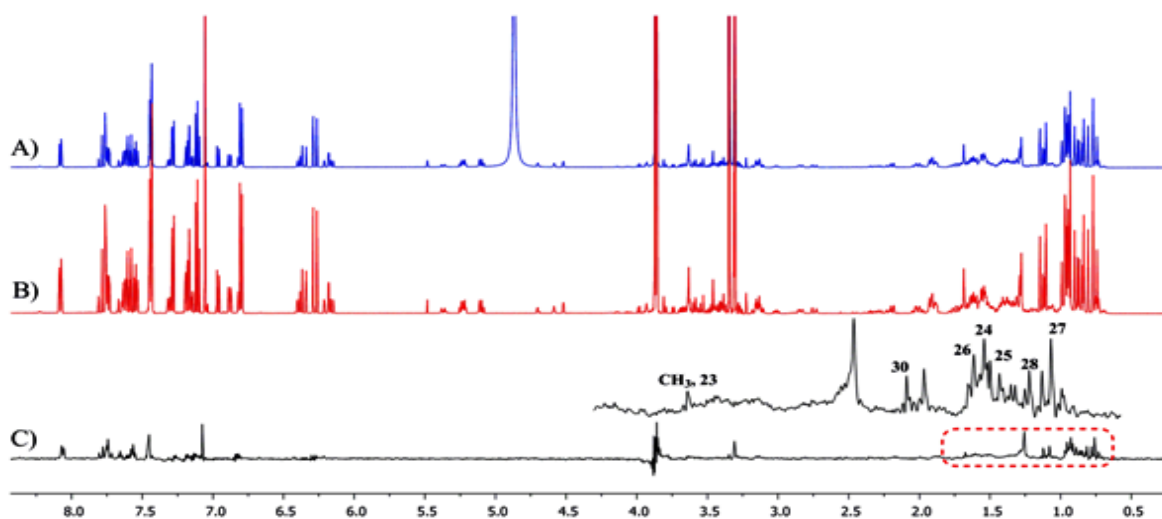




**Figure 50:** Isolation scheme of the *Terminalia Chebula* RETZ fruit, used in this study. The fractions in pink colours were used for this NMR based molecular recognition study.

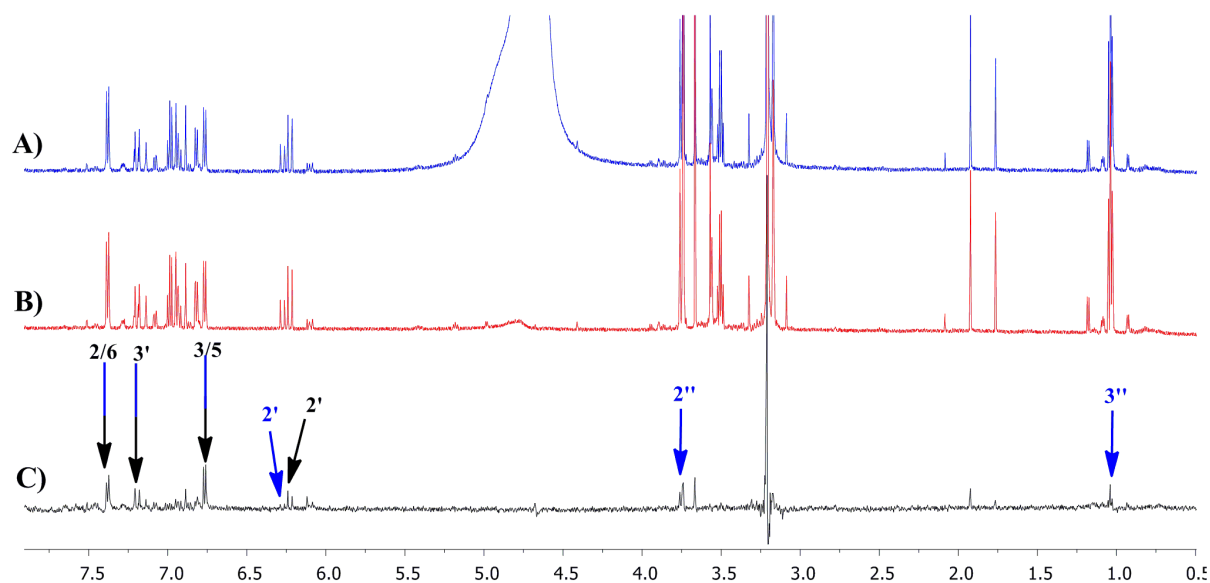
Two 1D  $^1\text{H}$ -NMR spectra (Figure 51) were recorded systematically with normal (zg) and Watergate Bruker pulse sequence in order to see any hidden signals under HOD signal. Following this, saturation transfer difference NMR method was employed to observe binding recognitions. STD NMR results (Figure 51) provided evidences of the involvement of some benzyl hydrogens (6.2-8 ppm) and some  $\text{sp}^3$  hybridized proton region (0.5-2.5 ppm). In the next step, 2D NMR techniques (COSY, HMBC, HSQC, and TOCSY) were acquired in order to characterize the molecular structure of these interacting compounds. The overlapped signals were proven a big hurdle in making a clear distinction between the hydrogens from different AChE blockers. Secondly, in STD spectrum the intensities of interacting signals from different entities were too weak and it was too difficult to characterize all interacting compounds based on these signals. Therefore, this ethyl acetate fraction was further suspended in 100

ml of water, this process was applied thrice, and water was evaporated through rotary vapor apparatus.



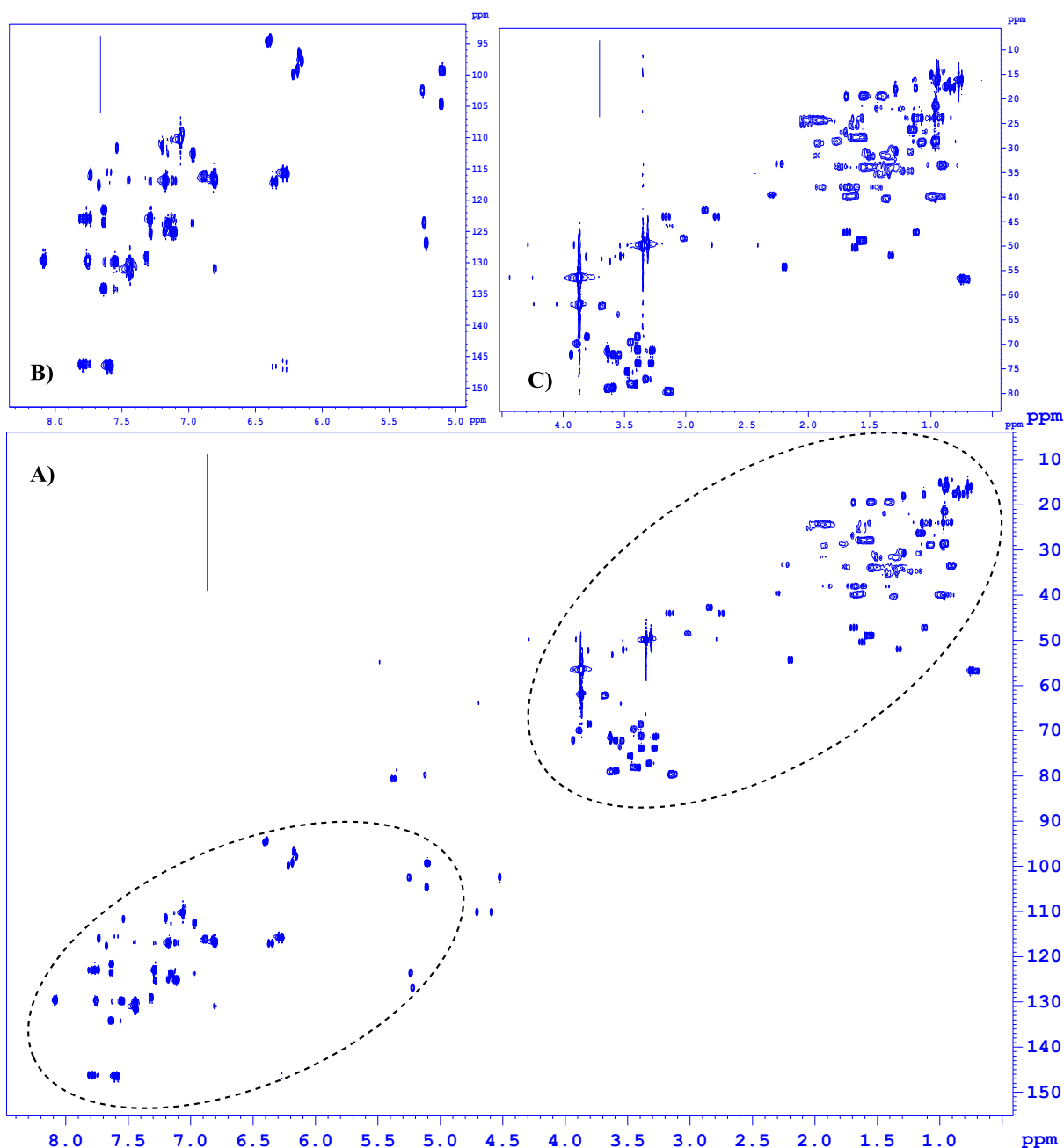
**Figure 51:** The  $^1\text{H}$ -NMR spectra ((A) normal hydrogen and (B) with HOD signal suppression) and STD NMR spectrum (C) of the ethyl acetate fraction of the *Termilania Chebula* extract in a 50 mM solution of AChE.

In a similar fashion, a 2 mg of the sample from the water suspended fraction was dissolved in the same ratio of methanol and deuterated water. Interestingly, the  $^1\text{H}$ -NMR spectra comprised only the benzyl compounds and all other signals that were later on proved as a triterpenoid moiety, disappeared (Figure 52). A few minor benzyl signals that were present in the STD spectrum of the ethyl acetate fraction were also missing that might be due to insolubility in water or less concentration. It is well understood that the STD signals depends on the concentration as well as the irradiation from the macromolecule.<sup>94, 97</sup>



**Figure 52:** The  $^1\text{H}$ -NMR spectra ((A) normal hydrogen and (B) with HOD signal suppression) and STD NMR spectrum (C) of the water suspended fraction from ethyl acetate portion of the *Terminalia Chebula* extract in a 50 mM solution of AChE.

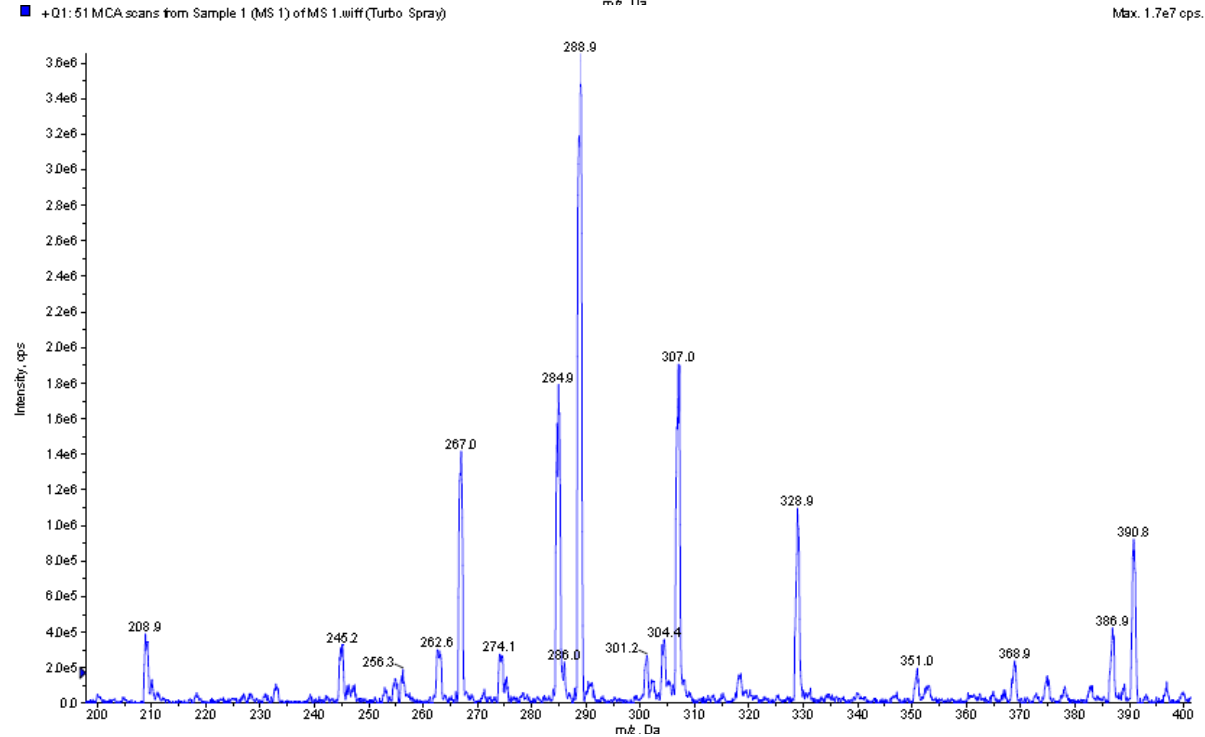
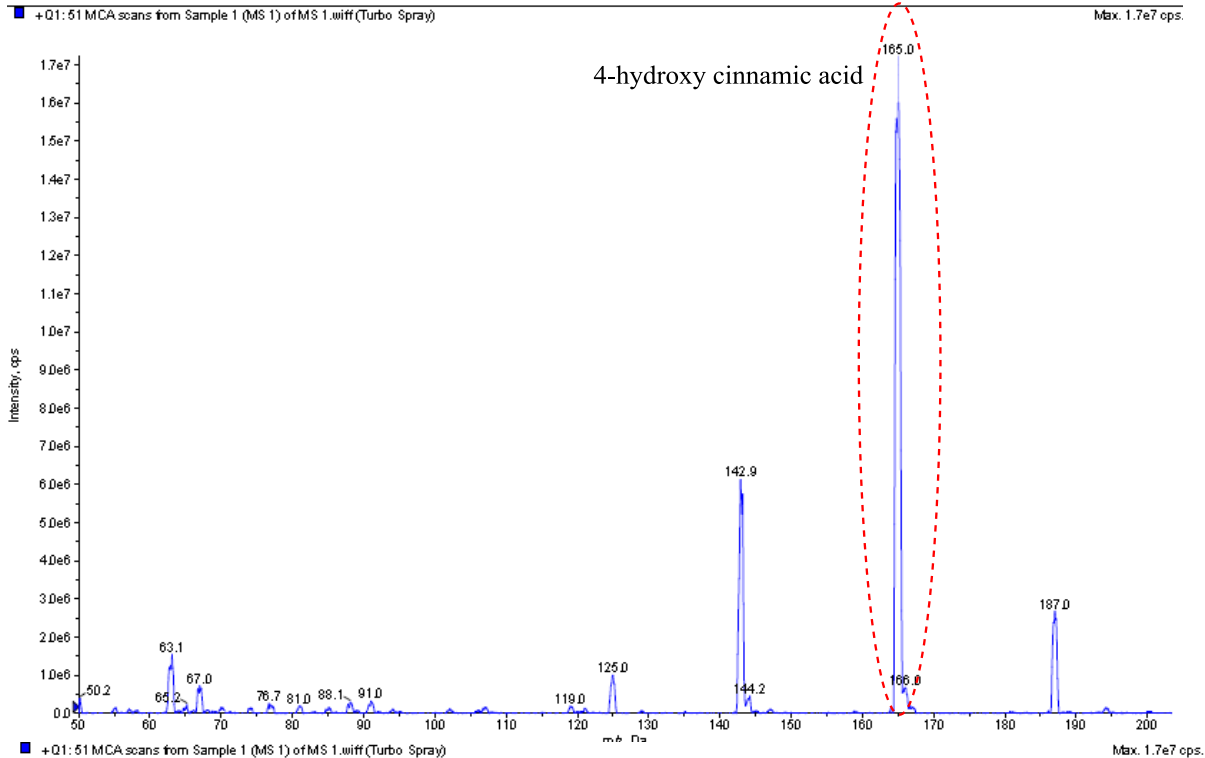
In both extract we were therefore able to characterize three compounds (4-hydroxycinnamic acid (**1**), Ethyl 4-hydroxy cinnamate (**2**) and lupeol (**3**)) by taking help of the two-dimensional NMR spectroscopy (Figure 53) and by making a comparison with an earlier reported data,<sup>209, 224</sup> besides STD spectra. An extra support in identification of these interacting molecules was obtained by mass spectrometry (Figure 54 A-B)—an important identification hallmark. Interestingly, all compounds are reported before from ethyl acetate fraction of *Terminalia Chebula* and also known to have an excellent AChE inhibition activity.<sup>225, 226</sup>



**Figure 53:** A complete 2D- HSQC spectrum (A) of the *Terminalia Chebula* extract, while, the inset B and C representing the major signal regions of compound cinnamic acid derivatives and lupeol, respectively. A 2mg of the extract was dissolved in D<sub>2</sub>O and CD<sub>3</sub>OD in order to obtain the spectrum.

NMR structural characterizations for the compounds **1** and **2** was possible from the peaks 7.42 ppm (*d*, *J* = 8.70 Hz) and 6.66 ppm (*d*, *J* = 8.70 Hz) for the hydrogens 2/6 and 3/5 position as shown in figure 3. However, the HSQC resolved each peak into two hydrogens corresponding to 130 Hz, while the mass

spectrum authenticated this confirmation with the peaks at 165 m/z and 192 m/z (Figure 54).



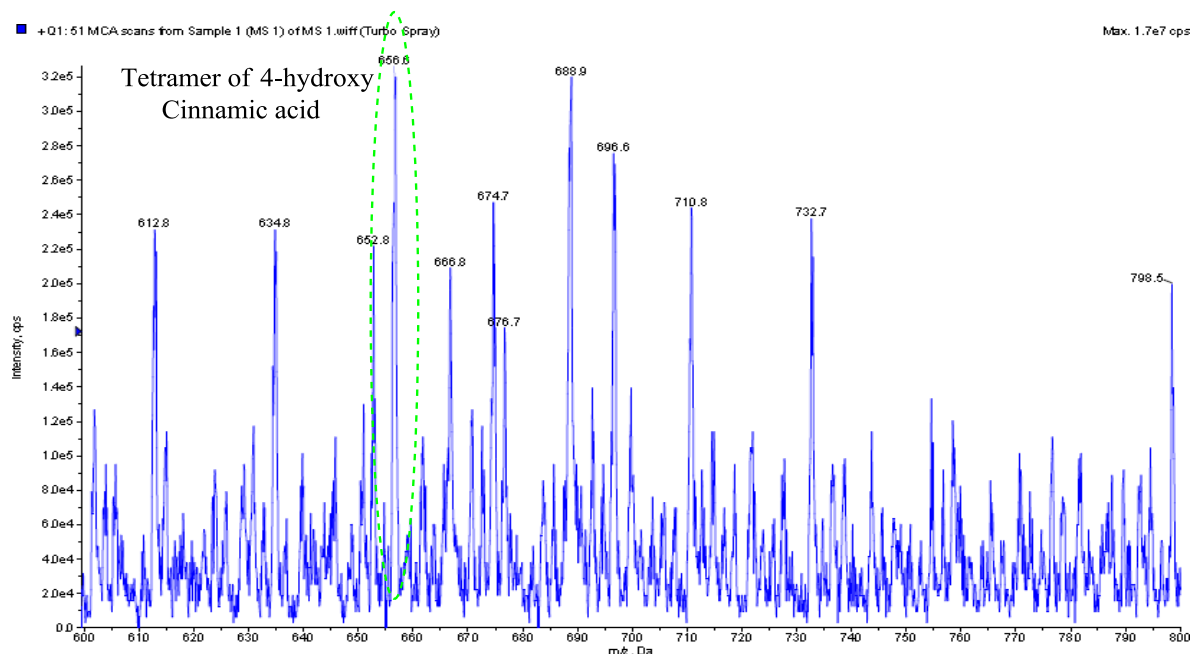
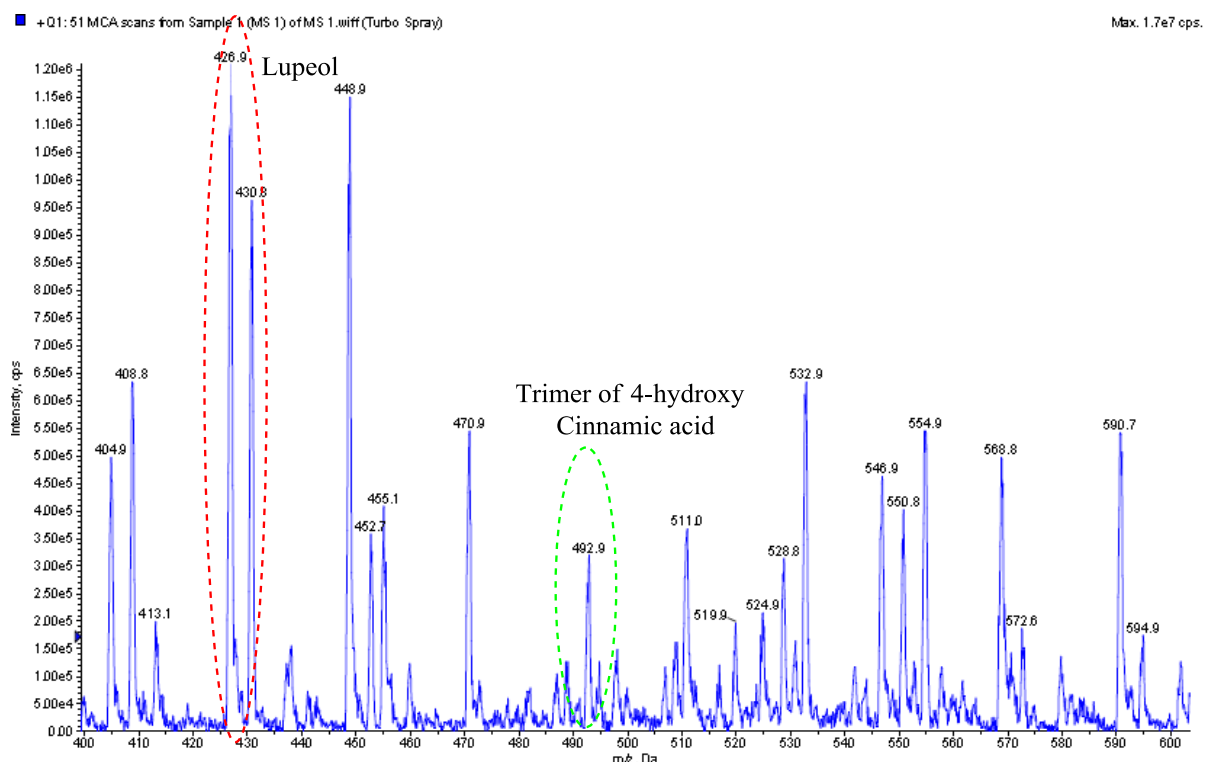


**Figure 54:** ESI spectrum of the ethyl acetate fraction of *Terminalia Chebula* extract, where, for more visibility, this was divided into four sub-spectra with region (5-200, 200-400, 400-600 and 600-800 m/z). The data containing higher molecular mass was not shown here.

On the other hand, the position 3' hydrogen for compound **1** and **2** appeared at 7.24 ppm (*d*,  $J = 15.85$  Hz) and 7.23 ppm (*d*,  $J = 16.12$  Hz)

respectively. Similarly, the counter hydrogen 2' became visible at 6.22 ppm ( $d, J = 16.12$  Hz) and 6.27 ppm ( $d, J = 15.85$  Hz) belonging to compounds **1** and **2** respectively. The methylene hydrogens of **2** were prominent at 3.75 ppm while, the methyl hydrogens at 1.05 ppm in the STD spectrum see in Figure 52C. Likewise, the characteristic peaks of Lupeol were also assigned with the help of 2D NMR spectroscopy and mass spectrometry peaks at 426.7 m/z.

The group epitope mapping (GEM) for the compounds **1**, **2** and **3** was calculated from the two STD NMR spectra (Figure 51C and Figure 52C) from the ethyl acetate fraction and its water suspended portion, respectively. The STD spectrum (Figure 51C) of ethyl acetate fraction indicates the presence of methyl hydrogens from lupeol (**3**) at 1.68, 1.10, 0.96, 0.92, 0.89, 0.82 and 0.76 ppm those representing the nomenclature numbering 23, 30, 26, 24, 25, 28 and 27 respectively as showed in Figure 55. The unequivocal representation of this STD spectrum (Figure 51C) suggests that almost all methyl signals from the Lupeol structure showed some level of enhancement, which establishes that bulky methyl created a cloud around the ethylene hydrogens which remained unable to produce STD effect. The GEM study was made effective by comparing the individual signal integral values and providing the strongest signals as 100 percent effect while the irradiation time for the protein was fixed to 2 s. The rest of the signals were normalized to the signal with the largest effect. Therefore, the given results in the Figure 55 suggest that methyl position 24 provided largest affinity towards AChE, on the other hand, methyls 30 and 23 remained more solvent exposed with the STD effect between the 15-30 percent. It is interesting to note that all the hydrogens oriented above the cyclic ring of the lupeol were remained prominent in the STD spectrum, and hence, stronger interaction.

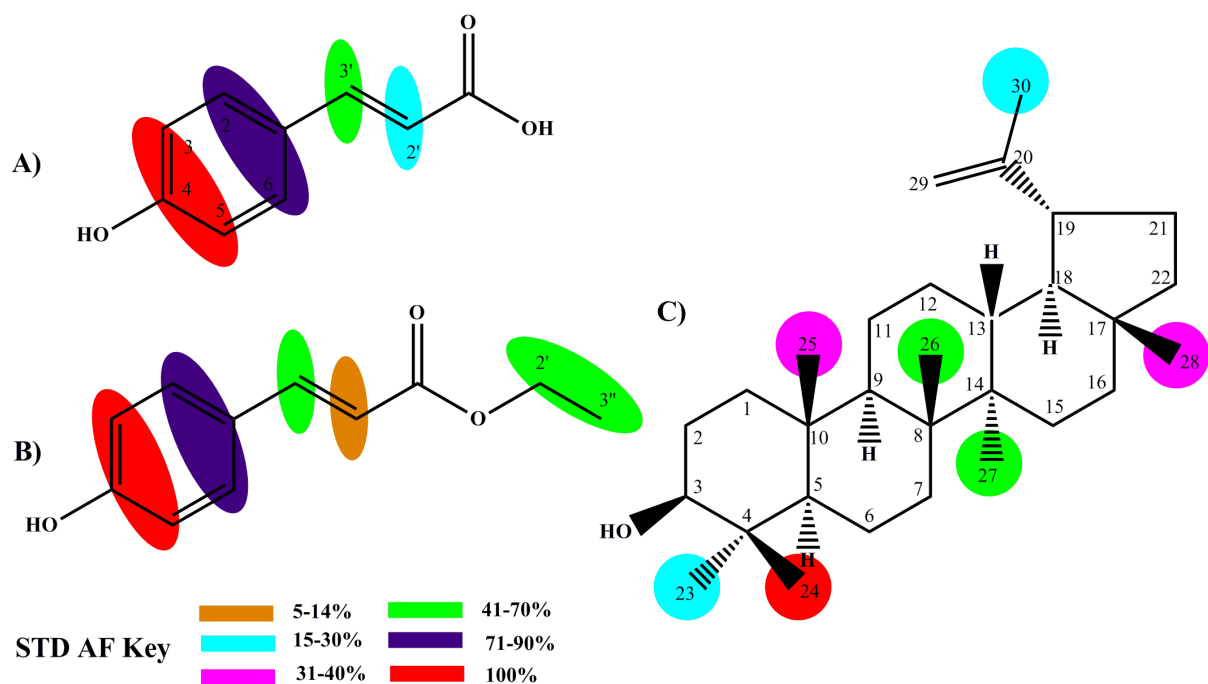


**Figure 55:** Structures of the recognized compounds (**1**, **2** and **3**) and their relative amplification factors (AF) with absolute numbering are shown. For more clarity in understanding the GEM results in the relative amplification factors (AF) were given different colors, where each color has a significance percentage AF as shown in the key.

Similarly, GEM calculation was performed from the water suspended portion (Figure 52C) of the ethyl acetate extract in order to observe which part of the molecule is showing more interaction. In this case, a 100 % effect was calculated from the hydrogens 3/5 of compounds **1** and **2**, respectively. Following this second large STD effect was calculated for the adjacent hydrogens (2/6) from the aromatic moiety. The extension coming off the parent cinnamic acid structure remained prominent with above 50 % AF. Nevertheless, the unsaturated hydrogens from both compounds could not provide a strong interaction with this GEM results. Based on these GEM results it would be not surprising to say that these compounds (**1** and **2**) were presenting interaction pattern where the only edges are involved. Indeed, the compound **2** could be a better inhibitor because it might provide greater interaction with the help of the



extension that is coming off long way, which can cover large surface area of the enzyme's cavity.

Further consolidation to our STD NMR results from the *Terminalia* extract, additional experiments 2D-NOESY with and without protein were also performed. NOESY experiments are well-established for obtaining the bound conformations of the ligands, within the ligand-receptor complex.<sup>94, 97</sup> In this experiment, the correlation time ( $\tau_c$ ) is a paramount parameter that decides whether a small compound is in contact with the larger one or not. Since small molecules possess short correlation time and a longer relaxation rate, therefore, they provide positive NOEs. On the other hand, in the bound state this shorter  $\tau_c$  changed to the longer one, resulting in a strong negative NOE.<sup>94, 97</sup> For this purpose, same sample of the ethyl acetate fraction with AChE addition was utilized to acquire the respective Tr-NOESY spectra that were utilized earlier for STD NMR. Conversely, for NOESY, new sample of the ethyl acetate fraction was prepared. Both experiments were performed with the almost similar condition and observed the NOEs growth carefully. NOE build-up effect generated faster in the Tr-NOESY experiment, as compared to the NOESY—a characteristic of the bound conformation.<sup>69</sup> The comparison of both spectra (NOESY and Tr-NOESY) clearly inferred the interaction as results of the change in correlation time of these interacting compounds (Figure 56). The hydrogens (2/6 and 3/5) of compounds **1** and **2**, those provided strong STD effect, became more intense in the Tr-NOESY experiment. Furthermore, in the Lupeol signal region, few peaks that were not present in the NOESY spectrum became clear in the Tr-NOESY spectrum. In conclusion of these results, we can say that the Tr-NOESY experiment mimic exactly the same results as we had obtained from the STD experiment. Thus, in the light of combined STD NMR and Tr-NOESY experiment these recognized compounds from the *Terminalia Chebula* RETZ were showing excellent interaction. Since all three compound

are previously known inhibitor of AChE hence might provide a best example of the inhibition and in controlling Alzheimer disease.

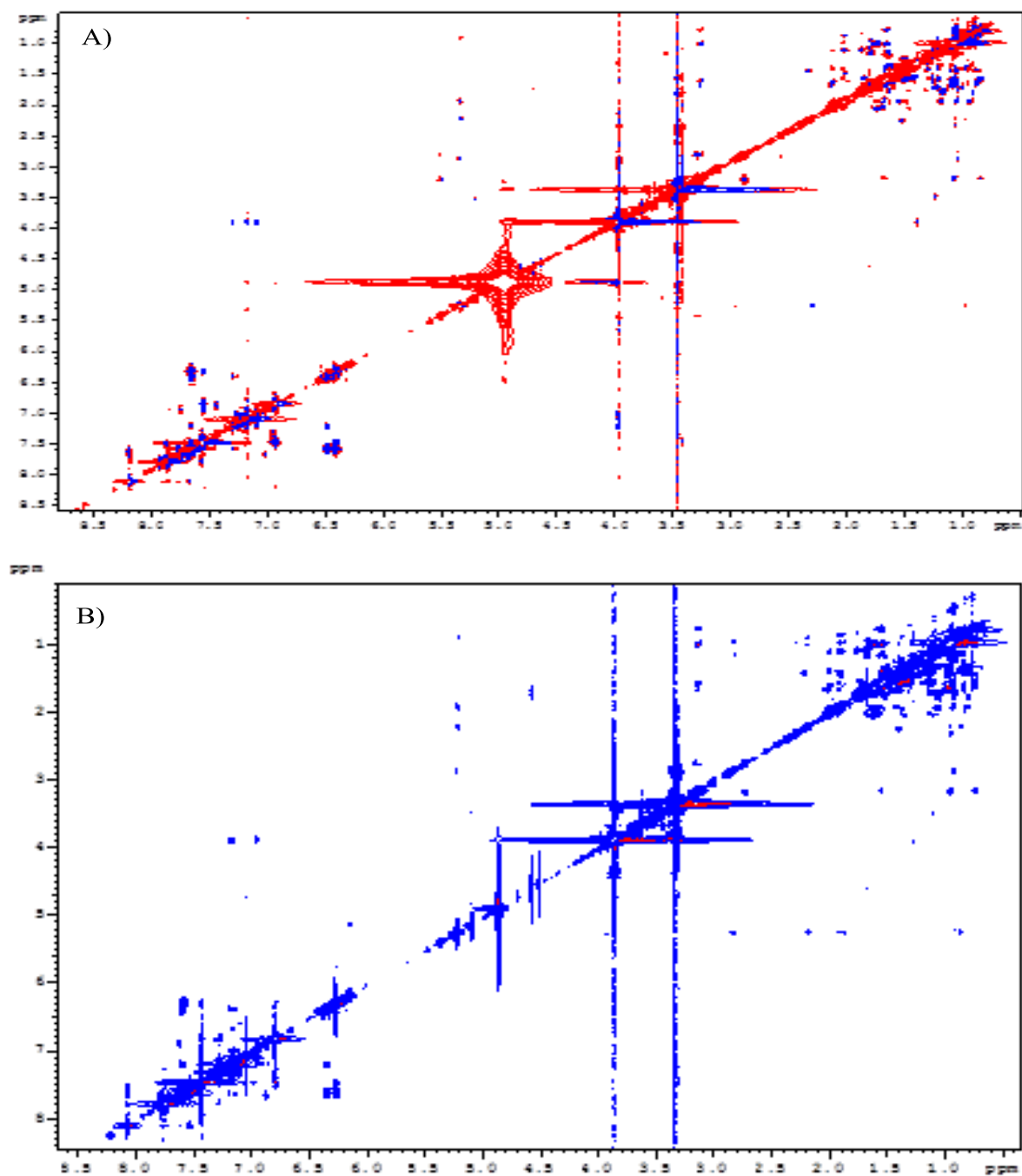


**Fig 56:** A side by side view of the 2D NOESY (A) and Tr-NOESY (B) spectrum were shown, where the NOESY spectrum is 5 times zoomed for clarity.

Finally, the diffusion edited NMR experiments were attempted to point out the existence of the observed interaction that could be seen from the STD NMR and Tr-NOESY data. The diffusion edited NMR is only applicable to the system with fast exchange, where the strength of the system to hold the ligand-receptor complex can also be measured. Since the self-diffusion depends on the physical parameters like size, shape and geometry of the molecule.<sup>133</sup> Therefore, it is well understood that the smaller molecules diffused more rapidly than larger ones. Furthermore, for a fast ligand-receptor exchange system, the diffusion coefficient of the small molecule will be equal to the weight average of the all bound and free states.<sup>128</sup>

To calculate the self-diffusion, we assumed that our system is in equilibrium, rapid, reversible, all binding sites with equal dissociation constant and equally independent. Since the diffusion coefficient of the macromolecule does not get affected when a small molecule binds to it, therefore, the diffusion coefficient of this protein is no longer an unknown quantity, hence, a single experiment is enough instead of various titrations.<sup>227</sup> Moreover, the potential of these diffusion edited experiments has been well evaluated to observe the ligand-receptor interaction.<sup>123</sup> In the view of the fact that a small molecule when binds with the macromolecule changes its diffusion coefficient values. Therefore, we have decided to calculate diffusion coefficient of these recognized compounds from extract by the addition of AChE and alone within this complex system.

A simple 1D bipolar diffusion edited spin echo pulse was employed to the system containing 2mg of the extract alone and with 50 $\mu$ M AChE. We supposed 1:1 ligands versus protein ratio in this system. Eight different 1D DOSY spectra were acquired by systematically incremented gradient strength to 5 %, 10 %, 20%, 35%, 45%, 60%, 80%, and 98%. Three peaks (one from each compound) were chosen because all were sharp rather than broaden, and having stability in

the chemical shift values. The attenuation of the selected peaks (7.42 ppm for **1**, 6.36 ppm for **2**, and 0.76 ppm for **3**) against increasing gradient strength were shown in figure 57.

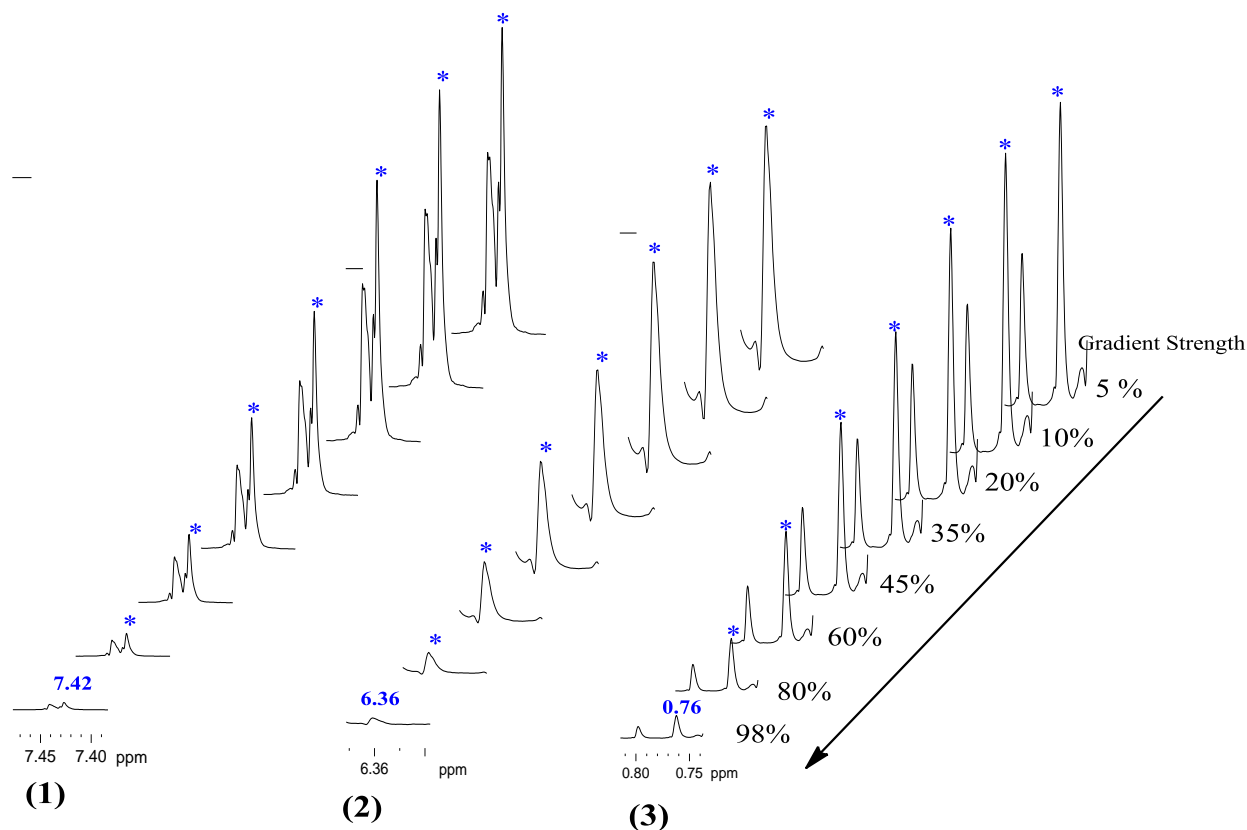
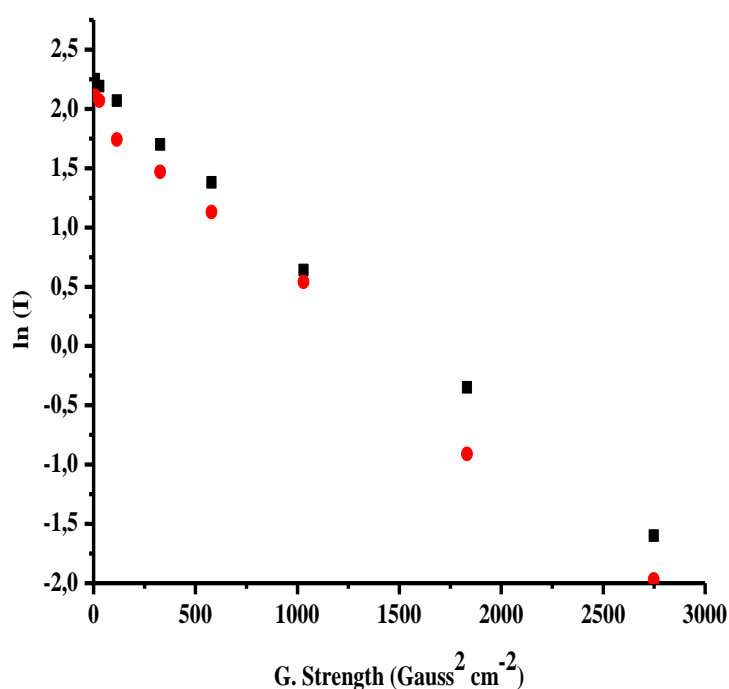


**Figure 57:** The intensity attenuations of the three selected peaks with asterick (7.42, 6.36 and 0.76 ppm) for compound **1**, **2**, and **3** were shown as function of increasing (top to bottom) strength of gradients. In 8 experiments the gradient field strengths from top to bottom were kept 2.67, 5.35, 10.7, 18.72, 2407, 32.1, 42.8, and 52.43 Gauss/cm respectively.

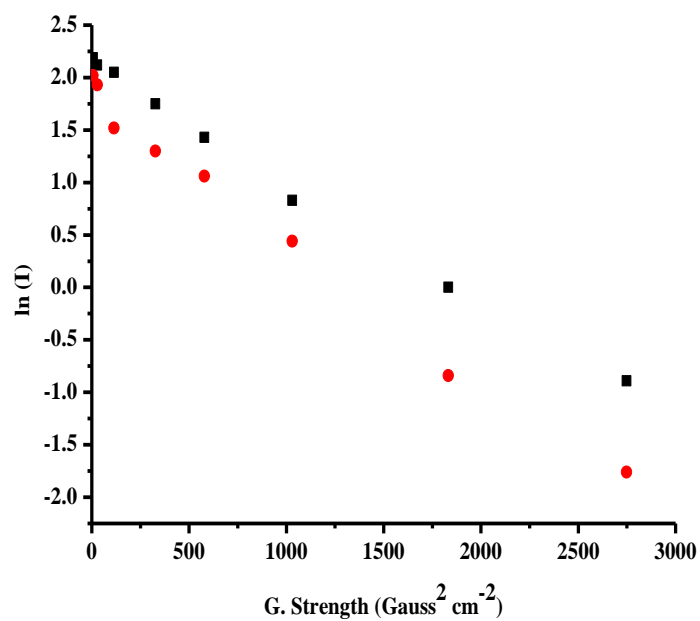
Figure 57 depicts the facts that the larger molecules show less change in the diffusion opposed to the smaller molecules; and by increasing the gradient strength the signal intensities either decrease or completely wipe out the spectrum—as suggested by Stejskal-Tanner in equation 23.<sup>228</sup>

$$\ln I = -\gamma^2 g^2 \delta^2 \left( \Delta - \frac{\delta}{3} \right) D \quad (23)$$

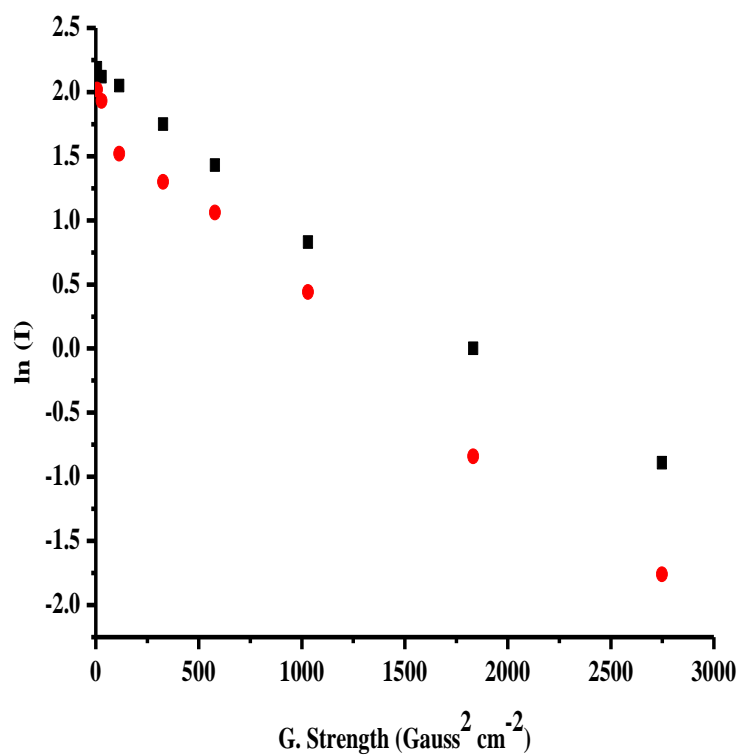
Where  $I$ ,  $\gamma$ ,  $g$ ,  $\delta$ ,  $\Delta$ , and  $D$  stand for the intensity of the signal, gyromagnetic ratio of the targeted nucleus, field strength in gauss/cm, duration of gradient pulse, gradient interval, and diffusion respectively. The calculation for the  $D$  is very simple; the slope of the linear plot of signal intensities versus other parameters in the equation 23 is the translational diffusion of that compound.<sup>224</sup> The selected signal intensities with and without AChE addition were plotted as a function of the field strength because all other parameters in the equation 1 were constant, a straight line for each single experiment was obtained. Therefore, single peak intensity against increasing  $g$  values with and without addition was shown in figure 58A-C to observe clear diffusional changes, and resulting calculated  $D$  values were depicted in Table 7.



A)



B)



C)

**Figure 58** A-C: Scattered plot for the signal intensity attenuations vs. square of gradients strength applied during the BPPLD 1D sequence; the slope of these lines provides the self-diffusion  $D$ .

Table 7 portrays the diffusion coefficient values of the three compounds (**1-3**) in presence and absence of the enzyme. The change in diffusion coefficient values of the each compound with and without AChE is significant of the binding between these small molecules and their host. Compound **3** (lupeol) showed larger change in the diffusion upon addition of the AChE with the significant change from  $1.86 \pm 0.04 \times 10^{-9} \text{ m}^2/\text{s}$  to  $0.172 \pm 0.01 \times 10^{-9} \text{ m}^2/\text{s}$ . Similarly, compound **2**, followed after the compound **3** with a change in diffusion coefficient from  $1.54 \pm 0.02 \times 10^{-9} \text{ m}^2/\text{s}$  to  $1.86 \pm 0.04 \times 10^{-9} \text{ m}^2/\text{s}$ . Nevertheless, compound **1** (4-hydroxy cinnamic acid) presented an anomalous behaviour, perhaps that might be because of the insufficient concentrations or some competitions with other binders in the extract or convection problems. The overall combine strategies from STD, Tr-NOESY and diffusion experiments provided a best example of the extract studies where, a typical binding behaviour of AChE—selectively binding with its inhibitors from a large library, could be seen.

**Table 7:** Diffusion coefficients values of the compounds as calculated from the linear fit of the series of 1D-DOSY spectra.

<b>Compounds</b>	<b>Diffusion (<math>10^{-9} \text{ m}^2/\text{s}</math>) in absence of AChE</b>	<b>Diffusion (<math>10^{-9} \text{ m}^2/\text{s}</math>) in presence of AChE</b>
<b>1</b>	$2.41 \pm 0.02$	$1.91 \pm 0.03$
<b>2</b>	$1.91 \pm 0.01$	$1.54 \pm 0.02$
<b>3</b>	$1.86 \pm 0.04$	$0.172 \pm 0.01$

## 6.4 Conclusions

Drug discovery is a long process that takes over a decade to get proper practise in daily life. Therefore, numerous new techniques with a number of various methods are helping to reduce this period. In this context, NMR seems to be an ideal choice because of its property to see the non-bonded interactions and non-invasive nature. On the other hand, ligand-ligand and ligand-receptor interactions are of prime importance, especially, this is particularly true in the case of body functions and the disease controlling mechanisms. Therefore, by targeting AChE, the data obtained would have an enormous impact on designing the new drugs for controlling Alzheimer's disease. In this viewpoint, performed study is a best example of the lead recognition and characterization from an enormous library of the compounds, towards a vital enzyme (AChE). Since *Terminalia Chebula* is well known for its massive biological activities, therefore, obtained results, perhaps will open a new window for the chemists and pharmaceuticals. The application of NMR methods to a medicinal plant extract can be proved fruitful to the pharmaceuticals in order to reduce the long drug discovery process. STD NMR and DOSY are the valuable tools for obtaining information about binding of small molecules to protein. Moreover, GEM results inferred the site implication that is responsible for the primary interaction. More importantly, the results of NMR screening might help in designing a more potent and selective inhibitors by taking the example of the cinnamic acid-influenced scaffolds in controlling Alzheimer's disease, in the light of the cholinergic speculation.





## 7. Salient Features of the Thesis

Alzheimer's disease is the one of the foremost alarming threat to the elder populations, especially, to the western countries, which takes lives of thousands of people per year. However, up-to-date there is no single treatment available that could provide an absolute control to this massacre. More importantly, before the autopsy report it is not possible to discriminate this disease from other types of dementia. Since from its first-time diagnosis, various methods are being utilized to come across this problem. Until now, according to molecular speculation, the one significant way is to inhibit the acetylcholinesterase activity, and in this way to regain of cholinergic response can be achieved. Therefore, in this context, here we have selected different types of the AChE inhibitors to observe the particular molecular recognition. To accomplish this objective, we have helped by different NMR methods. Since NMR is the significant tool for the ligand-receptor interaction studies because, it is non-destructive, non-invasive and physiological conditions are similar to the environment where a drug will be applied. The most routinely and robust methods like STD NMR, Tr-NOESY, and Diffusion-ordered spectroscopy has been employed during this these.

For the first application of NMR methods, a set of four coumarin derivatives AChE inhibitors have been utilized. The competition between the a current drug (Tacrine ) and these selected targets were made on dissociation constant values. STD titration driven results have shown that the compound 1 has a stronger affinity to AChE. Therefore, a similar competition based on substitutions on parent coumarin ring were performed inter-inhibitors. The superiority of interaction was seen in the compound 1 having two significant extensions responsible for interaction. These results were exactly mimics by the docking simulation and, inferred the explicit bindings. Moreover, docking simulation driven calculations have shown that the compounds with longer

extensions coming from the parent coumarin ring proved to be implicated in three simultaneous locus. Therefore, based on the combined NMR and docking results we have declared our compound 1 better than Tacrine, which can alternate to this.

Similarly, by using STD, Tr-NOESY and DOSY NMR a competition study has been performed with three inhibitors (Gallic acid, 4-umbelliferone, and Scopoletin) in chapter 5. In this analysis, interestingly, we found that none of the inhibitors compete for gallic acids site. However, on higher concentrations of inhibitors to AChE the change in chemical shifts of these small molecules were observed. We suggest these changes because of the saturation of the binding sites results in these shifts of peaks. Finally, the diffusion coefficient were calculated with and without AChE via DOSY, the change in diffusion values explicitly provided the binding evidence.

Lastly, the recognition protocol was applied to an ethyl acetate fraction of Terminalia Chebula extract. This plant is famous to possess a plethora of biological activity and is known as king of medicine. In a large number of compounds, only three were provided the evidence of binding by peak appearance in STD spectrum. As a result of combined NMR and Mass spectrometry unequivocal structural characterization, 4-hydroxycinnamic acid, Ethyl 4-hydroxycinnamate, and lupeol was confirmed to involved in bindings. Intriguingly, the STD driven results disclosed the binding behavior of AChE in only accepting its inhibitor.

In conclusion, as a step towards Alzheimer's control, a significant progress has been made towards the investigations of the binding of the different class of inhibitors towards AChE of *Electrophorus Electricus*. And, for the first time in the Federal University of Sao Carlos, Brazil, this determination of the

bound conformation of any inhibitors to AChE by means of NMR spectroscopy was successfully performed.



## 8. Bibliography

1. CUMMINGS, J. L., Alzheimer's Disease. *New England Journal of Medicine* **2004**, 351 (1), 56-67.
2. BURNS, A.; ILIFFE, S., *Alzheimer's disease*. **2009**; Vol. 338.
3. HOWES, M. J. R.; PERRY, N. S. L.; HOUGHTON, P. J.; HOWES, M. J. R.; PERRY, N. S. L.; HOUGHTON, P. J., Plants with traditional uses and activities, relevant to the management of Alzheimer's disease and other cognitive disorders. *Phytotherapy Research* **2003**, 17 (Scientific review), 1-18.
4. FRANCIS, P. T.; PALMER, A. M.; SNAPE, M.; WILCOCK, G. K., The cholinergic hypothesis of Alzheimer's disease: a review of progress. *Journal of Neurology, Neurosurgery & Psychiatry* **1999**, 66 (2), 137-147.
5. Alzheimer's disease facts and figures. *Alzheimer's & Dementia* **2008**, 4 (2), 110-133.
6. FERRI, C. P.; PRINCE, M.; BRAYNE, C.; BRODATY, H.; FRATIGLIONI, L.; GANGULI, M.; HALL, K.; HASEGAWA, K.; HENDRIE, H.; HUANG, Y.; JORM, A.; MATHERS, C.; MENEZES, P. R.; RIMMER, E.; SCAZUFCA, M., Global prevalence of dementia: a Delphi consensus study. *The Lancet* 366 (9503), 2112-2117.
7. SIFFERLIN, A., Alzheimer's Bigger Killer Than We Realize, Study Says. *The Time Magazine*, March 5, 2014.
8. BERRIOS, G. E., Alzheimer's disease: A conceptual history. *International Journal of Geriatric Psychiatry* **1990**, 5 (6), 355-365.
9. <http://www.brightfocus.org/alzheimers/about/understanding/brain-with-alzheimers.html>

- 10.**2010 Alzheimer's disease facts and figures. *Alzheimer's & Dementia: The Journal of the Alzheimer's Association* 6 (2), 158-194.
- 11.** TERRY, R. D.; MASLIAH, E.; SALMON, D. P.; BUTTERS, N.; DETERESA, R.; HILL, R.; HANSEN, L. A.; KATZMAN, R., Physical basis of cognitive alterations in alzheimer's disease: Synapse loss is the major correlate of cognitive impairment. *Annals of Neurology* **1991**, 30 (4), 572-580.
- 12.**YAFFE, K.; TOCCO, M.; PETERSEN, R. C.; SIGLER, C.; BURNS, L. C.; CORNELIUS, C.; KHACHATURIAN, A. S.; IRIZARRY, M. C.; CARRILLO, M. C., The epidemiology of Alzheimer's disease: Laying the foundation for drug design, conduct, and analysis of clinical trials. *Alzheimer's & Dementia: The Journal of the Alzheimer's Association* **2012**, 8 (3), 237-242.
- 13.** COURT, J. A.; PERRY, E. K., Dementia: the neurochemical basis of putative transmitter orientated therapy. *Pharmacol Ther* **1991**, 52 (3), 423-443.
- 14.**ODDO, S.; CACCAMO, A.; KITAZAWA, M.; TSENG, B. P.; LAFERLA, F. M., Amyloid deposition precedes tangle formation in a triple transgenic model of Alzheimer's disease. *Neurobiology of Aging* **2003**, 24 (8), 1063-1070.
- 15.**ODDO, S.; CACCAMO, A.; SHEPHERD, J. D.; MURPHY, M. P.; GOLDE, T. E.; KAYED, R.; METHERATE, R.; MATTSON, M. P.; AKBARI, Y.; LAFERLA, F. M., Triple-Transgenic Model of Alzheimer's Disease with Plaques and Tangles: Intracellular A $\beta$  and Synaptic Dysfunction. *Neuron* **2003**, 39 (3), 409-421.

16. MUDHER, A.; LOVESTONE, S., Alzheimer's disease – do tauists and baptists finally shake hands? *Trends in Neurosciences* **2002**, 25 (1), 22-26.
17. TERRY, R. D.; MASLIAH, E.; HANSEN, L. A., Structural basis of the cognitive alterations in Alzheimer disease. In *Alzheimer disease*, Terry, R. D.; Katzman, R.; Bick, K. L., Eds. Raven Press: New York, NY, US, 1994; pp 179-196.
18. SU, J. H.; CUMMINGS, B. J.; COTMAN, C. W., Plaque biogenesis in brain aging and Alzheimer's disease: I. Progressive changes in phosphorylation states of paired helical filaments and neurofilaments. *Brain Research* **1996**, 739 (1–2), 79-87.
19. BLENNOW, K.; ZETTERBERG, H.; MINTHON, L.; LANNFELT, L.; STRID, S.; ANNAS, P.; BASUN, H.; ANDREASEN, N., Longitudinal stability of CSF biomarkers in Alzheimer's disease. *Neuroscience Letters* **2007**, 419 (1), 18-22.
20. ALIM, M. A.; MA, Q.-L.; TAKEDA, K.; AIZAWA, T.; MATSUBARA, M.; NAKAMURA, V.; ASADA, A.; SAITO, T.; XKAJI, M.; YOSHII, M.; HISANAGA, S.; UÉDA, K., Demonstration of a role for a-synuclein as a functional microtubule-associated protein. *Journal of Alzheimer's Disease* **2004**, 6 (4), 435-442.
21. WEGGEN, S.; ERIKSEN, J. L.; DAS, P.; SAGI, S. A.; WANG, R.; PIETRZIK, C. U.; FINDLAY, K. A.; SMITH, T. E.; MURPHY, M. P.; BULTER, T.; KANG, D. E.; MARQUEZ-STERLING, N.; GOLDE, T. E.; KOO, E. H., A subset of NSAIDs lower amyloidogenic A[ $\beta$ ]42 independently of cyclooxygenase activity. *Nature* **2001**, 414 (6860), 212-216.



22. WYSS-CORAY, T.; MUCKE, L., Inflammation in Neurodegenerative Disease—A Double-Edged Sword. *Neuron* **2002**, *35* (3), 419-432.
23. SMITH, M. A.; CASADESUS, G.; JOSEPH, J. A.; PERRY, G., Amyloid- $\beta$  and  $\tau$  serve antioxidant functions in the aging and Alzheimer brain. *Free Radical Biology and Medicine* **2002**, *33* (9), 1194-1199.
24. TERRY, A. V.; BUCCAFUSCO, J. J., The Cholinergic Hypothesis of Age and Alzheimer's Disease-Related Cognitive Deficits: Recent Challenges and Their Implications for Novel Drug Development. *Journal of Pharmacology and Experimental Therapeutics* **2003**, *306* (3), 821-827.
25. BARTUS, R. T., On Neurodegenerative Diseases, Models, and Treatment Strategies: Lessons Learned and Lessons Forgotten a Generation Following the Cholinergic Hypothesis. *Experimental Neurology* **2000**, *163* (2), 495-529.
26. BUSH, A. I., Metal complexing agents as therapies for Alzheimer's disease. *Neurobiology of Aging* **2002**, *23* (6), 1031-1038.
27. TANIGUCHI, S.; SUZUKI, N.; MASUDA, M.; HISANAGA, S.-I.; IWATSUBO, T.; GOEDERT, M.; HASEGAWA, M., Inhibition of Heparin-induced Tau Filament Formation by Phenothiazines, Polyphenols, and Porphyrins. *Journal of Biological Chemistry* **2005**, *280* (9), 7614-7623.
28. AIROLDI, C.; CARDONA, F.; SIRONI, E.; COLOMBO, L.; SALMONA, M.; SILVA, A.; NICOTRA, F.; LA FERLA, B., cis-Glycofused benzopyran compounds as new amyloid-[small beta] peptide ligands. *Chemical Communications* **2011**, *47* (37), 10266-10268.
29. MESSER, W., Cholinergic agonists and the treatment of Alzheimer's disease. *Current Topics in Medicinal Chemistry* **2002**, *2*, 353-358.

- 30.KARAKAYA, T.; FUßER, F.; SCHRÖDER, J.; PANTEL, J., Pharmacological Treatment of Mild Cognitive Impairment as a Prodromal Syndrome of Alzheimer's Disease. *Current Neuropharmacology* **2013**, *11* (1), 102-108.
- 31.SHEN, Z. X., Brain cholinesterases: II. The molecular and cellular basis of Alzheimer's disease. *Medical Hypotheses* **2004**, *63* (2), 308-321.
- 32.IIJIMA, K.; LIU, H.-P.; CHIANG, A.-S.; HEARN, S. A.; KONSOLAKI, M.; ZHONG, Y., Dissecting the pathological effects of human A $\beta$ 40 and A $\beta$ 42 in Drosophila: A potential model for Alzheimer's disease. *Proceedings of the National Academy of Sciences of the United States of America* **2004**, *101* (17), 6623-6628.
- 33.GREGORY, G.; HALLIDAY, G., What is the dominant a $\beta$  species in human brain tissue? A review. *neurotox res* **2005**, *7* (1-2), 29-41.
- 34.WANG, P.; YANG, G.; MOSIER, D. R.; CHANG, P.; ZAIDI, T.; GONG, Y.-D.; ZHAO, N.-M.; DOMINGUEZ, B.; LEE, K.-F.; GAN, W.-B.; ZHENG, H., Defective Neuromuscular Synapses in Mice Lacking Amyloid Precursor Protein (APP) and APP-Like Protein 2. *The Journal of Neuroscience* **2005**, *25* (5), 1219-1225.
- 35.DONG, S.; DUAN, Y.; HU, Y.; ZHAO, Z., Advances in the pathogenesis of Alzheimer's disease: a re-evaluation of amyloid cascade hypothesis. *Transl Neurodegener* **2012**, *1* (1), 1-12.
- 36.FIALA, M.; CRIBBS, D. H.; ROSENTHAL, M.; BERNARD, G., Phagocytosis of Amyloid- $\beta$  and Inflammation: Two Faces of Innate Immunity in Alzheimer's Disease. *Journal of Alzheimer's Disease* **2007**, *11* (4), 457-463.

37. MEYER-LUEHMANN, M.; SPIRES-JONES, T. L.; PRADA, C.; GARCIA-ALLOZA, M.; DE CALIGNON, A.; ROZKALNE, A.; KOENIGSKNECHT-TALBOO, J.; HOLTZMAN, D. M.; BACSKAI, B. J.; HYMAN, B. T., Rapid appearance and local toxicity of amyloid- $\beta$  plaques in a mouse model of Alzheimer's disease. *Nature* **2008**, *451* (7179), 720-724.
38. MARTIN, L.; LATYPOVA, X.; WILSON, C. M.; MAGNAUDEIX, A.; PERRIN, M.-L.; YARDIN, C.; TERRO, F., Tau protein kinases: Involvement in Alzheimer's disease. *Ageing Research Reviews* **2013**, *12* (1), 289-309.
39. KOLAROVA, M.; GARCÍA-SIERRA, F.; BARTOS, A.; RICNY, J.; RIPOVA, D., Structure and Pathology of Tau Protein in Alzheimer Disease. *International Journal of Alzheimer's Disease* **2012**, *2012*, 13.
40. WILLIAMS, D. R., Tauopathies: classification and clinical update on neurodegenerative diseases associated with microtubule-associated protein tau. *Internal Medicine Journal* **2006**, *36* (10), 652-660.
41. NICOLET, Y.; LOCKRIDGE, O.; MASSON, P.; FONTECILLA-CAMPS, J. C.; NACHON, F., CRYSTAL Structure of Human Butyrylcholinesterase and of Its Complexes with Substrate and Products. *Journal of Biological Chemistry* **2003**, *278* (42), 41141-41147.
42. MOTEL, W. C.; COOP, A.; CUNNINGHAM, C. W., Cholinergic Modulation by Opioid Receptor Ligands: Potential Application to Alzheimer's Disease. *Mini reviews in medicinal chemistry* **2013**, *13* (3), 456-466.

- 43.** HOUGHTON, P. J.; REN, Y.; HOWES, M.-J., Acetylcholinesterase inhibitors from plants and fungi. *Natural Product Reports* **2006**, *23* (2), 181-199.
- 44.** DVIR, H.; SILMAN, I.; HAREL, M.; ROSENBERRY, T. L.; SUSSMAN, J. L., Acetylcholinesterase: From 3D structure to function. *Chemico-Biological Interactions* **2010**, *187* (1–3), 10-22.
- 45.** ZHANG, Y.; KUA, J.; MCCAMMON, J. A., Role of the Catalytic Triad and Oxyanion Hole in Acetylcholinesterase Catalysis: An ab initio QM/MM Study. *Journal of the American Chemical Society* **2002**, *124* (35), 10572-10577.
- 46.** OFEK, K.; SOREQ, H., Cholinergic involvement and manipulation approaches in multiple system disorders. *Chemico-Biological Interactions* **2013**, *203* (1), 113-119.
- 47.** ČOLOVIĆ, M. B.; KRSTIĆ, D. Z.; LAZAREVIĆ-PAŠTI, T. D.; BONDŽIĆ, A. M.; VASIĆ, V. M., Acetylcholinesterase Inhibitors: Pharmacology and Toxicology. *Current Neuropharmacology* **2013**, *11* (3), 315-335.
- 48.** ROSENBERRY, T. L.; MALLENDER, W. D.; THOMAS, P. J.; SZEGLETES, T., A steric blockade model for inhibition of acetylcholinesterase by peripheral site ligands and substrate. *Chemico-Biological Interactions* **1999**, *119–120* (0), 85-97.
- 49.** SZEGLETES, T.; MALLENDER, W. D.; ROSENBERRY, T. L., Nonequilibrium Analysis Alters the Mechanistic Interpretation of Inhibition of Acetylcholinesterase by Peripheral Site Ligands. *Biochemistry* **1998**, *37* (12), 4206-4216.

50. WLODEK, S. T.; CLARK, T. W.; SCOTT, L. R.; MCCAMMON, J. A., Molecular Dynamics of Acetylcholinesterase Dimer Complexed with Tacrine. *Journal of the American Chemical Society* **1997**, *119* (40), 9513-9522.
51. ZHOU, H.-X.; WLODEK, S. T.; MCCAMMON, J. A., Conformation gating as a mechanism for enzyme specificity. *Proceedings of the National Academy of Sciences* **1998**, *95* (16), 9280-9283.
52. TAI, K.; SHEN, T.; BÖRJESSON, U.; PHILIPPOPOULOS, M.; MCCAMMON, J. A., Analysis of a 10-ns Molecular Dynamics Simulation of Mouse Acetylcholinesterase. *Biophysical Journal* **2001**, *81* (2), 715-724.
53. SHEN, T. Y.; TAI, K.; MCCAMMON, J. A., Statistical analysis of the fractal gating motions of the enzyme acetylcholinesterase. *Physical Review E* **2001**, *63* (4), 041902.
54. QUINN, D. M., Acetylcholinesterase: enzyme structure, reaction dynamics, and virtual transition states. *Chemical Reviews* **1987**, *87* (5), 955-979.
55. TAYLOR, P.; RADIC, Z., The Cholinesterases: From Genes to Proteins. *Annual Review of Pharmacology and Toxicology* **1994**, *34* (1), 281-320.
56. BIRKS, J.; GRIMLEY EVANS, J.; IAKOVIDOU, V.; TSOLAKI, M.; HOLT, F.E. Rivastigmine for Alzheimer's disease. *Cochrane Dementia and Cognitive Improvement Group* **2009**, *2*, CD001191.
57. WATKINS, P. B.; ZIMMERMAN, H. J.; KNAPP, M. J.; GRACON, S. I.; LEWIS, K. W., Hepatotoxic effects of tacrine administration in patients with Alzheimer's disease. *JAMA* **1994**, *271* (13), 992-998.

- 58.**HYDE, C.; PETERS, J.; BOND, M.; ROGERS, G.; HOYLE, M.; ANDERSON, R.; JEFFREYS, M.; DAVIS, S.; THOKALA, P.; MOXHAM, T., Evolution of the evidence on the effectiveness and cost-effectiveness of acetylcholinesterase inhibitors and memantine for Alzheimer's disease: systematic review and economic model. *Age and Ageing* **2013**, *42* (1), 14-20.
- 59.**BOND, M.; ROGERS, G.; PETERS, J.; ANDERSON, R.; HOYLE, M., The effectiveness and cost-effectiveness of donepezil, galantamine, rivastigmine and memantine for the treatment of Alzheimer's disease (review of TA111): a systematic review and economic model. *Health Technology Assessment* **2012**, *16* (21), 469.
- 60.**SMULDERS, C. J. G. M.; BUETERS, T. J. H.; VAILATI, S.; VAN KLEEF, R. G. D. M.; VIJVERBERG, H. P. M., Block of Neuronal Nicotinic Acetylcholine Receptors by Organophosphate Insecticides. *Toxicological Sciences* **2004**, *82* (2), 545-554.
- 61.**SOGORB, M. A.; VILANOVA, E., Enzymes involved in the detoxification of organophosphorus, carbamate and pyrethroid insecticides through hydrolysis. *Toxicology Letters* **2002**, *128* (1-3), 215-228.
- 62.**HAYDEN, K. M.; NORTON, M. C.; DARCEY, D.; ØSTBYE, T.; ZANDI, P. P.; BREITNER, J. C. S.; WELSH-BOHMER, K. A.; For the Cache County Study, I., Occupational exposure to pesticides increases the risk of incident AD: The Cache County Study. *Neurology* **2010**, *74* (19), 1524-1530.
- 63.**COSTA, L. G., Current issues in organophosphate toxicology. *Clinica Chimica Acta* **2006**, *366* (1-2), 1-13.

64. MERCEY, G.; VERDELET, T.; RENOUE, J.; KLIACHYNA, M.; BAATI, R.; NACHON, F.; JEAN, L.; RENARD, P.-Y., Reactivators of Acetylcholinesterase Inhibited by Organophosphorus Nerve Agents. *Accounts of Chemical Research* **2012**, *45* (5), 756-766.
65. BLOCH, F.; HANSEN, W. W.; PACKARD, M., Nuclear Induction. *Physical Review* **1946**, *69* (3-4), 127-127.
66. PURCELL, E. M.; TORREY, H. C.; POUND, R. V., Resonance Absorption by Nuclear Magnetic Moments in a Solid. *Physical Review* **1946**, *69* (1-2), 37-38.
67. PELLECCIA, M.; SEM, D. S.; WUTHRICH, K., Nmr in drug discovery. *Nat Rev Drug Discov* **2002**, *1* (3), 211-219.
68. MEYER, B.; PETERS, T., NMR Spectroscopy Techniques for Screening and Identifying Ligand Binding to Protein Receptors. *Angewandte Chemie International Edition* **2003**, *42* (8), 864-890.
69. LUDWIG C., GUENTHER U.L. Ligand based NMR methods for drug discovery. *Frontiers in Bioscience* **2009**, *14*, 4565–4574.
70. BALCI, M., 2 - Resonance Phenomena. In *Basic <sup>1</sup>H- and <sup>13</sup>C-NMR Spectroscopy*, Balci, M., Ed. Elsevier Science: Amsterdam, **2005**; pp 9-24.
71. GHITTI, M.; MUSCO, G.; SPITALERI, A., NMR and Computational Methods in the Structural and Dynamic Characterization of Ligand-Receptor Interactions. In *Protein Conformational Dynamics*, Han, K.-l.; Zhang, X.; Yang, M.-j., Eds. Springer International Publishing: **2014**; Vol. 805, pp 271-304.
72. PELLECCIA, M.; BERTINI, I.; COWBURN, D.; DALVIT, C.; GIRALT, E.; JAHNKE, W.; JAMES, T. L.; HOMANS, S. W.;

- KESSLER, H.; LUCHINAT, C.; MEYER, B.; OSCHKINAT, H.; PENG, J.; SCHWALBE, H.; SIEGAL, G., Perspectives on NMR in drug discovery: a technique comes of age. *Nat Rev Drug Discov* **2008**, *7* (9), 738-745.
- 73.**VIEGAS, A.; MACEDO, A.; CABRITA, E., Ligand-Based Nuclear Magnetic Resonance Screening Techniques. In *Ligand-Macromolecular Interactions in Drug Discovery*, Roque, A. C. A., Ed. Humana Press: **2010**; Vol. 572, pp 81-100.
- 74.**WILLIAMSON, M. P., Using chemical shift perturbation to characterise ligand binding. *Progress in Nuclear Magnetic Resonance Spectroscopy* **2013**, *73* (0), 1-16.
- 75.**FERNÁNDEZ, C.; JAHNKE, W., New approaches for NMR screening in drug discovery. *Drug Discovery Today: Technologies* **2004**, *1* (3), 277-283.
- 76.**SHUKER, S. B.; HAJDUK, P. J.; MEADOWS, R. P.; FESIK, S. W., Discovering High-Affinity Ligands for Proteins: SAR by NMR. *Science* **1996**, *274* (5292), 1531-1534.
- 77.**BECATTINI, B.; CULMSEE, C.; LEONE, M.; ZHAI, D.; ZHANG, X.; CROWELL, K. J.; REGA, M. F.; LANDSHAMER, S.; REED, J. C.; PLESNILA, N.; PELLECCIA, M., Structure–activity relationships by interligand NOE-based design and synthesis of antiapoptotic compounds targeting Bid. *Proceedings of the National Academy of Sciences* **2006**, *103* (33), 12602-12606.
- 78.**BECATTINI, B.; PELLECCIA, M., SAR by ILOEs: An NMR-Based Approach to Reverse Chemical Genetics. *Chemistry – A European Journal* **2006**, *12* (10), 2658-2662.



- 79.**MEYER, B.; WEIMAR, T.; PETERS, T., Screening Mixtures for Biological Activity by NMR. *European Journal of Biochemistry* **1997**, *246* (3), 705-709.
- 80.**UNIONE, L.; GALANTE, S.; DIAZ, D.; CANADA, F. J.; JIMENEZ-BARBERO, J., NMR and molecular recognition. The application of ligand-based NMR methods to monitor molecular interactions. *MedChemComm* **2014**, *5* (9), 1280-1289.
- 81.**CALA, O.; GUILLIÈRE, F.; KRIMM, I., NMR-based analysis of protein–ligand interactions. *Analytical and Bioanalytical Chemistry* **2014**, *406* (4), 943-956.
- 82.**POST, C. B., Exchange-transferred NOE spectroscopy and bound ligand structure determination. *Current Opinion in Structural Biology* **2003**, *13* (5), 581-588.
- 83.**HENRICHSEN, D.; ERNST, B.; MAGNANI, J. L.; WANG, W.-T.; MEYER, B.; PETERS, T., Bioaffinity NMR Spectroscopy: Identification of an E-Selectin Antagonist in a Substance Mixture by Transfer NOE. *Angewandte Chemie International Edition* **1999**, *38* (1-2), 98-102.
- 84.**LI, D.; DEROSE, E.; LONDON, R., The inter-ligand Overhauser effect: A powerful new NMR approach for mapping structural relationships of macromolecular ligands. *J Biomol NMR* **1999**, *15* (1), 71-76.
- 85.**LI, D.; LONDON, R., Ligand discovery using the inter-ligand Overhauser effect: horse liver alcohol dehydrogenase. *Biotechnology Letters* **2002**, *24* (8), 623-629.
- 86.**REGA, M. F.; WU, B.; WEI, J.; ZHANG, Z.; CELLITTI, J. F.; PELLECCIA, M., SAR by Interligand Nuclear Overhauser Effects (ILOEs) Based Discovery of Acylsulfonamide Compounds Active against

Bcl-xL and Mcl-1. *Journal of Medicinal Chemistry* **2011**, *54* (17), 6000-6013.

- 87.** BECATTINI, B.; SARETH, S.; ZHAI, D.; CROWELL, K. J.; LEONE, M.; REED, J. C.; PELLECCIA, M., Targeting Apoptosis via Chemical Design: Inhibition of Bid-Induced Cell Death by Small Organic Molecules. *Chemistry & Biology* **2004**, *11* (8), 1107-1117.
- 88.** ORTS, J.; GRIESINGER, C.; CARLOMAGNO, T., The INPHARMA technique for pharmacophore mapping: A theoretical guide to the method. *Journal of Magnetic Resonance* **2009**, *200* (1), 64-73.
- 89.** XIA, Y.; ZHU, Q.; JUN, K.-Y.; WANG, J.; GAO, X., Clean STD-NMR spectrum for improved detection of ligand-protein interactions at low concentration of protein. *Magnetic Resonance in Chemistry* **2010**, *48* (12), 918-924.
- 90.** RADEMACHER, C.; GUIARD, J.; KITOV, P. I.; FIEGE, B.; DALTON, K. P.; PARRA, F.; BUNDLE, D. R.; PETERS, T., Targeting Norovirus Infection—Multivalent Entry Inhibitor Design Based on NMR Experiments. *Chemistry – A European Journal* **2011**, *17* (27), 7442-7453.
- 91.** BEGLEY, D. W.; ZHENG, S.; VARANI, G., Fragment-based discovery of novel thymidylate synthase leads by NMR screening and group epitope mapping. *Chemical Biology & Drug Design* **2010**, *76* (3), 218-233.
- 92.** Yan, J.; Kline, A. D.; Mo, H.; Shapiro, M. J.; Zartler, E. R., The effect of relaxation on the epitope mapping by saturation transfer difference NMR. *Journal of Magnetic Resonance* **2003**, *163* (2), 270-276.
- 93.** JOHNSON, M. A.; PINTO, B. M., Saturation Transfer Difference 1D-TOCSY Experiments to Map the Topography of Oligosaccharides Recognized by a Monoclonal Antibody Directed Against the Cell-Wall

Polysaccharide of Group A Streptococcus. *Journal of the American Chemical Society* **2002**, *124* (51), 15368-15374.

**94.**TANOLI, S. A. K.; TANOLI, N. U.; BONDANCIA, T. M.; USMANI, S.; KERSSEBAUM, R.; FERREIRA, A. G.; FERNANDES, J. B.; UL-HAQ, Z., Crude to leads: a triple-pronged direct NMR approach in coordination with docking simulation. *Analyst* **2013**, *138* (17), 5137-5145.

**95.**VOGTHERR, M.; PETERS, T., Application of NMR Based Binding Assays to Identify Key Hydroxy Groups for Intermolecular Recognition. *Journal of the American Chemical Society* **2000**, *122* (25), 6093-6099.

**96.**MAYER, M.; MEYER, B., Group Epitope Mapping by Saturation Transfer Difference NMR To Identify Segments of a Ligand in Direct Contact with a Protein Receptor. *Journal of the American Chemical Society* **2001**, *123* (25), 6108-6117.

**97.**TANOLI, S. A. K.; TANOLI, N. U.; BONDANCIA, T. M.; USMANI, S.; UL-HAQ, Z.; FERNANDES, J. B.; THOMASI, S. S.; FERREIRA, A. G., Human serum albumin-specific recognition of the natural herbal extract of *Stryphnodendron polyphyllum* through STD NMR, hyphenations and docking simulation studies. *RSC Advances* **2015**, *5* (30), 23431-23442.

**98.**RIBEIRO, J. P.; ANDRÉ, S.; CAÑADA, F. J.; GABIUS, H.-J.; BUTERA, A. P.; ALVES, R. J.; JIMÉNEZ-BARBERO, J., Lectin-Based Drug Design: Combined Strategy to Identify Lead Compounds using STD NMR Spectroscopy, Solid-Phase Assays and Cell Binding for a Plant Toxin Model. *ChemMedChem* **2010**, *5* (3), 415-419.

**99.**MARCELO, F.; DIAS, C.; MARTINS, A.; MADEIRA, P. J.; JORGE, T.; FLORÊNCIO, M. H.; CAÑADA, F. J.; CABRITA, E. J.; JIMÉNEZ-BARBERO, J.; RAUTER, A. P., Molecular Recognition of Rosmarinic

Acid from *Salvia sclareoides* Extracts by Acetylcholinesterase: A New Binding Site Detected by NMR Spectroscopy. *Chemistry – A European Journal* **2013**, *19* (21), 6641-6649

- 100.** TANOLI, S. K.; TANOLI, N.; USMANI, S.; ZAHEER UL, H.; FERREIRA, A., The exploration of interaction studies of smaller size, mostly ignored yet intrinsically inestimable molecules towards BSA; An example of STD and DOSY NMR. *Central European Journal of Chemistry* **2014**, *12* (3), 332-340.
- 101.** ANGULO, J.; ENRÍQUEZ-NAVAS, P. M.; NIETO, P. M., Ligand–Receptor Binding Affinities from Saturation Transfer Difference (STD) NMR Spectroscopy: The Binding Isotherm of STD Initial Growth Rates. *Chemistry – A European Journal* **2010**, *16* (26), 7803-7812.
- 102.** JAYALAKSHMI, V.; KRISHNA, N. R., Complete Relaxation and Conformational Exchange Matrix (CORCEMA) Analysis of Intermolecular Saturation Transfer Effects in Reversibly Forming Ligand–Receptor Complexes. *Journal of Magnetic Resonance* **2002**, *155* (1), 106-118.
- 103.** BHUNIA, A.; BHATTACHARJYA, S.; CHATTERJEE, S., Applications of saturation transfer difference NMR in biological systems. *Drug Discovery Today* **2012**, *17* (9–10), 505-513.
- 104.** WAGSTAFF, J. L.; TAYLOR, S. L.; HOWARD, M. J., Recent developments and applications of saturation transfer difference nuclear magnetic resonance (STD NMR) spectroscopy. *Molecular BioSystems* **2013**, *9* (4), 571-577.

- 105.** MAYER, M.; JAMES, T. L., NMR-Based Characterization of Phenothiazines as a RNA Binding Scaffold†. *Journal of the American Chemical Society* **2004**, *126* (13), 4453-4460.
- 106.** JAYALAKSHMI, V.; RAMA KRISHNA, N., CORCEMA refinement of the bound ligand conformation within the protein binding pocket in reversibly forming weak complexes using STD-NMR intensities. *Journal of Magnetic Resonance* **2004**, *168* (1), 36-45.
- 107.** JAYALAKSHMI, V.; BIET, T.; PETERS, T.; KRISHNA, N. R., Refinement of the Conformation of UDP-Galactose Bound to Galactosyltransferase Using the STD NMR Intensity-Restrained CORCEMA Optimization. *Journal of the American Chemical Society* **2004**, *126* (28), 8610-8611.
- 108.** ENRÍQUEZ-NAVAS, P. M.; MARRADI, M.; PADRO, D.; ANGULO, J.; PENADÉS, S., A Solution NMR Study of the Interactions of Oligomannosides and the Anti-HIV-1 2G12 Antibody Reveals Distinct Binding Modes for Branched Ligands\*. *Chemistry – A European Journal* **2011**, *17* (5), 1547-1560.
- 109.** ANGULO, J.; DÍAZ, I.; REINA, J. J.; TABARANI, G.; FIESCHI, F.; ROJO, J.; NIETO, P. M., Saturation Transfer Difference (STD) NMR Spectroscopy Characterization of Dual Binding Mode of a Mannose Disaccharide to DC-SIGN. *ChemBioChem* **2008**, *9* (14), 2225-2227.
- 110.** CLAASEN, B.; AXMANN, M.; MEINECKE, R.; MEYER, B., Direct Observation of Ligand Binding to Membrane Proteins in Living Cells by a Saturation Transfer Double Difference (STDD) NMR Spectroscopy Method Shows a Significantly Higher Affinity of Integrin  $\alpha$ IIB $\beta$ 3 in Native Platelets than in Liposomes. *Journal of the American Chemical Society* **2005**, *127* (3), 916-919.

111. PEREIRA, A.; PFEIFER, T. A.; GRIGLIATTI, T. A.; ANDERSEN, R. J., Functional Cell-Based Screening and Saturation Transfer Double-Difference NMR Have Identified Haplosamate A as a Cannabinoid Receptor Agonist. *ACS Chemical Biology* **2009**, *4* (2), 139-144.
112. DALVIT, C.; PEVARELLO, P.; TATÒ, M.; VERONESI, M.; VULPETTI, A.; SUNDSTRÖM, M., Identification of compounds with binding affinity to proteins via magnetization transfer from bulk water\*. *Journal of Biomolecular NMR* **2000**, *18* (1), 65-68.
113. DALVIT, C.; FOGLIATTO, G.; STEWART, A.; VERONESI, M.; STOCKMAN, B., WaterLOGSY as a method for primary NMR screening: Practical aspects and range of applicability. *Journal of Biomolecular NMR* **2001**, *21* (4), 349-359.
114. DALVIT, C.; COTTENS, S.; RAMAGE, P.; HOMMEL, U., Half-filter experiments for assignment, structure determination and hydration analysis of unlabelled ligands bound to <sup>13</sup>C/<sup>15</sup>N labelled proteins. *Journal of Biomolecular NMR* **1999**, *13* (1), 43-50.
115. GOSSERT, A.; HENRY, C.; BLOMMERS, M. J.; JAHNKE, W.; FERNÁNDEZ, C., Time efficient detection of protein–ligand interactions with the polarization optimized PO-WaterLOGSY NMR experiment. *J Biomol NMR* **2009**, *43* (4), 211-217.
116. HU, J.; ERIKSSON, P.-O.; KERN, G., Aroma WaterLOGSY: a fast and sensitive screening tool for drug discovery. *Magnetic Resonance in Chemistry* **2010**, *48* (12), 909-911.
117. DALVIT, C.; FASOLINI, M.; FLOCCO, M.; KNAPP, S.; PEVARELLO, P.; VERONESI, M., NMR-Based Screening with

Competition Water–Ligand Observed via Gradient Spectroscopy Experiments: Detection of High-Affinity Ligands. *Journal of Medicinal Chemistry* **2002**, *45* (12), 2610-2614.

- 118.** LUDWIG, C.; MICHIELS, P. J. A.; WU, X.; KAVANAGH, K. L.; PILKA, E.; JANSSON, A.; OPPERMANN, U.; GÜNTHER, U. L., SALMON: Solvent Accessibility, Ligand binding, and Mapping of ligand Orientation by NMR Spectroscopy. *Journal of Medicinal Chemistry* **2008**, *51* (1), 1-3.
- 119.** LUDWIG, C.; MICHIELS, P. J. A.; LODI, A.; RIDE, J.; BUNCE, C.; GÜNTHER, U. L., Evaluation of Solvent Accessibility Epitopes for Different Dehydrogenase Inhibitors. *ChemMedChem* **2008**, *3* (9), 1371-1376.
- 120.** HUO, R.; WEHRENS, R.; DUYNHOVEN, J. V.; BUYDENS, L. M. C., Assessment of techniques for DOSY NMR data processing. *Analytica Chimica Acta* **2003**, *490* (1–2), 231-251.
- 121.** MORRIS, K. F.; JOHNSON, C. S., Diffusion-ordered two-dimensional nuclear magnetic resonance spectroscopy. *Journal of the American Chemical Society* **1992**, *114* (8), 3139-3141.
- 122.** MORRIS, K. F.; JOHNSON, C. S., Resolution of discrete and continuous molecular size distributions by means of diffusion-ordered 2D NMR spectroscopy. *Journal of the American Chemical Society* **1993**, *115* (10), 4291-4299.
- 123.** LIN, M.; SHAPIRO, M. J.; WAREING, J. R., Diffusion-edited NMR-affinity NMR for direct observation of molecular interactions. *Journal of the American Chemical Society* **1997**, *119* (22), 5249-5250.

- 124.** PRICE, W. S., Pulsed-field gradient nuclear magnetic resonance as a tool for studying translational diffusion: Part II. Experimental aspects. *Concepts in Magnetic Resonance* **1998**, *10* (4), 197-237.
- 125.** PRICE, W. S., Pulsed-field gradient nuclear magnetic resonance as a tool for studying translational diffusion: Part 1. Basic theory. *Concepts in Magnetic Resonance* **1997**, *9* (5), 299-336.
- 126.** JAYAWICKRAMA, D. A.; LARIVE, C. K.; MCCORD, E. F.; ROE, D. C., Polymer additives mixture analysis using pulsed-field gradient NMR spectroscopy. *Magnetic Resonance in Chemistry* **1998**, *36* (10), 755-760.
- 127.** COLBOURNE, A. A.; MORRIS, G. A.; NILSSON; M., Local Covariance Order Diffusion-Ordered Spectroscopy: A Powerful Tool for Mixture Analysis. *Journal of the American Chemical Society* **2011**, *133* (20), 7640-7643.
- 128.** FIELDING, L.; NMR methods for the determination of protein-ligand dissociation constants. *Current Topic in Medicinal Chemistry* **2003**, *3*(1), 39-53.
- 129.** BOCIAN, W.; KAWĘCKI, R.; BEDNAREK, E.; SITKOWSKI, J.; WILLIAMSON, M. P.; HANSEN, P. E.; KOZERSKI, L., Binding of Topotecan to a Nicked DNA Oligomer in Solution. *Chemistry – A European Journal* **2008**, *14* (9), 2788-2794.
- 130.** YAN, J.; KLINE, A. D.; MO, H.; ZARTLER, E. R.; SHAPIRO, M. J., Epitope Mapping of Ligand–Receptor Interactions by Diffusion NMR. *Journal of the American Chemical Society* **2002**, *124* (34), 9984-9985.
- 131.** TREFI, S.; ROUTABOUL, C.; HAMIEH, S.; GILARD, V.; MALET-MARTINO, M.; MARTINO, R., Analysis of illegally



manufactured formulations of tadalafil (Cialis®) by <sup>1</sup>H NMR, 2D DOSY <sup>1</sup>H NMR and Raman spectroscopy. *Journal of Pharmaceutical and Biomedical Analysis* **2008**, *47* (1), 103-113.

- 132.** HODGE, P.; MONVISADE, P.; MORRIS, G. A.; PREECE, I., A novel NMR method for screening soluble compound libraries. *Chemical Communications* **2001**, (3), 239-240.
- 133.** DERRICK, T. S.; MCCORD, E. F.; LARIVE, C. K., Analysis of Protein/Ligand Interactions with NMR Diffusion Measurements: The Importance of Eliminating the Protein Background. *Journal of Magnetic Resonance* **2002**, *155* (2), 217-225.
- 134.** LEPRE, C. A.; MOORE, J. M.; PENG, J. W., Theory and Applications of NMR-Based Screening in Pharmaceutical Research. *Chemical Reviews* **2004**, *104* (8), 3641-3676.
- 135.** LI, D.; KERESZTES, I.; HOPSON, R.; WILLIARD, P. G., Characterization of Reactive Intermediates by Multinuclear Diffusion-Ordered NMR Spectroscopy (DOSY). *Accounts of Chemical Research* **2008**, *42* (2), 270-280.
- 136.** HAJDUK, P. J.; OLEJNICZAK, E. T.; FESIK, S. W., One-Dimensional Relaxation- and Diffusion-Edited NMR Methods for Screening Compounds That Bind to Macromolecules. *Journal of the American Chemical Society* **1997**, *119* (50), 12257-12261.
- 137.** CHEN, A.; SHAPIRO, M. J., NOE Pumping. 2. A High-Throughput Method To Determine Compounds with Binding Affinity to Macromolecules by NMR. *Journal of the American Chemical Society* **2000**, *122* (2), 414-415.

- 138.** DELFINI, M.; DI COCCO, M. E.; PICCIONI, F.; PORCELLI, F.; BORIONI, A.; RODOMONTE, A.; DEL GIUDICE, M. R., Tacrine derivatives–acetylcholinesterase interaction: 1 H NMR relaxation study. *Bioorganic chemistry* **2007**, *35* (3), 243-257.
- 139.** YIN, G.; LI, Y. M.; WEI, W.; JIANG, S. H.; ZHU, D. Y.; DU, W. H., Interactions of acetylcholinesterase with salvianolic acid B and rosmarinic acid from *Salvia miltiorhiza* water extract investigated by NMR relaxation rate. *Chinese Chemical Letters* **2008**, *19* (6), 747-751.
- 140.** SIEGAL, G.; AB, E.; SCHULTZ, J., Integration of fragment screening and library design. *Drug Discovery Today* **2007**, *12* (23–24), 1032-1039.
- 141.** JAHNKE, W.; RÜDISSER, S.; ZURINI, M., Spin label enhanced NMR screening. *Journal of the American Chemical Society* **2001**, *123* (13), 3149-3150.
- 142.** KUNTZ, I. D.; BLANEY, J. M.; OATLEY, S. J.; LANGRIDGE, R.; FERRIN, T. E., A geometric approach to macromolecule-ligand interactions. *Journal of molecular biology* **1982**, *161* (2), 269-288.
- 143.** WARREN, G. L.; ANDREWS, C. W.; CAPELLI, A.-M.; CLARKE, B.; LALONDE, J.; LAMBERT, M. H.; LINDVALL, M.; NEVINS, N.; SEMUS, S. F.; SENGER, S.; TEDESCO, G.; WALL, I. D.; WOOLVEN, J. M.; PEISHOFF, C. E.; Head, M. S., A Critical Assessment of Docking Programs and Scoring Functions. *Journal of Medicinal Chemistry* **2006**, *49* (20), 5912-5931.
- 144.** ROGNAN, D., Proteome-scale docking: myth and reality. *Drug Discovery Today: Technologies* **2013**, *10* (3), e403-e409.
- 145.** HALPERIN, I.; MA, B.; WOLFSON, H.; NUSSINOV, R., Principles of docking: An overview of search algorithms and a guide to

- scoring functions. *Proteins: Structure, Function, and Bioinformatics* **2002**, *47* (4), 409-443.
- 146.** HARTSHORN, M. J.; VERDONK, M. L.; CHESSARI, G.; BREWERTON, S. C.; MOOIJ, W. T. M.; MORTENSON, P. N.; MURRAY, C. W., Diverse, High-Quality Test Set for the Validation of Protein–Ligand Docking Performance. *Journal of Medicinal Chemistry* **2007**, *50* (4), 726-741.
- 147.** TAUFER, M.; CROWLEY, M.; PRICE, D. J.; CHIEN, A. A.; BROOKS, C. L., Study of a highly accurate and fast protein–ligand docking method based on molecular dynamics. *Concurrency and Computation: Practice and Experience* **2005**, *17* (14), 1627-1641.
- 148.** MENG, X.-Y.; ZHANG, H.-X.; MEZEI, M.; CUI, M., Molecular Docking: A powerful approach for structure-based drug discovery. *Current computer-aided drug design* **2011**, *7* (2), 146-157.
- 149.** KITCHEN, D. B.; DECORNEZ, H.; FURR, J. R.; BAJORATH, J., Docking and scoring in virtual screening for drug discovery: methods and applications. *Nature Reviews Drug Discovery* **2004**, *3* (11), 935-949.
- 150.** RAREY, M.; KRAMER, B.; LENGAUER, T.; KLEBE, G., A Fast Flexible Docking Method using an Incremental Construction Algorithm. *Journal of molecular biology* **1996**, *261* (3), 470-489.
- 151.** SCHLOSSER, J.; RAREY, M., Beyond the Virtual Screening Paradigm: Structure-Based Searching for New Lead Compounds. *Journal of Chemical Information and Modeling* **2009**, *49* (4), 800-809.
- 152.** PEARCE, B. C.; LANGLEY, D. R.; KANG, J.; HUANG, H.; KULKARNI, A., E-Novo: An Automated Workflow for Efficient Structure-Based Lead Optimization. *Journal of Chemical Information and Modeling* **2009**, *49* (7), 1797-1809.

- 153.** EWING, T. A.; Makino, S.; Skillman, A. G.; Kuntz, I., DOCK 4.0: Search strategies for automated molecular docking of flexible molecule databases. *J Comput Aided Mol Des* **2001**, *15* (5), 411-428.
- 154.** JONES, G.; WILLETT, P.; GLEN, R. C., Molecular recognition of receptor sites using a genetic algorithm with a description of desolvation. *Journal of Molecular Biology* **1995**, *245* (1), 43-53.
- 155.** STARK J.; POWERS R. Rapid Protein–Ligand Costructures Using Chemical Shift Perturbations. *Journal of the American Chemical Society* **2007**, *130* (2), 535-545.
- 156.** BAX, A., A spatially selective composite 90° radiofrequency pulse. *Journal of Magnetic Resonance (1969)* **1985**, *65* (1), 142-145.
- 157.** PARELLA, T.; Pulse Program Catalogue, NMRGuide4.0, Bruker BioSpin, 2004.
- 158.** CHOUDHARY, M. I.; NAWAZ, S. A.; ZAHEER UL, H.; AZIM, M. K.; GHAYUR, M. N.; LODHI, M. A.; JALIL, S.; KHALID, A.; AHMED, A.; RODE, B. M.; ATTA UR, R.; GILANI, A.-U.-H.; AHMAD, V. U., Juliflorine: A potent natural peripheral anionic-site-binding inhibitor of acetylcholinesterase with calcium-channel blocking potential, a leading candidate for Alzheimer’s disease therapy. *Biochemical and Biophysical Research Communications* **2005**, *332* (4), 1171-1179.
- 159.** SHEN, Y.; SHENG, R.; ZHANG, J.; HE, Q.; YANG, B.; HU, Y., 2-Phenoxy-indan-1-one derivatives as acetylcholinesterase inhibitors: A study on the importance of modifications at the side chain on the activity. *Bioorganic & Medicinal Chemistry* **2008**, *16* (16), 7646-7653.
- 160.** KIM, J. H.; CHOI, G. N.; KWAK, J. H.; JEONG, H. R.; JEONG, C.-H.; HEO, H. J., Neuronal cell protection and acetylcholinesterase

inhibitory effect of the phenolics in chestnut inner skin. *Food Science and Biotechnology* **2011**, 20 (2), 311-318.

- 161.** TABET, N., Acetylcholinesterase inhibitors for Alzheimer's disease: anti-inflammatories in acetylcholine clothing! *Age and Ageing* **2006**, 35 (4), 336-338.
- 162.** KIRBY, J.; GREEN, C.; LOVEMAN, E.; CLEGG, A.; PICOT, J.; TAKEDA, A.; PAYNE, E., A Systematic Review of the Clinical and Cost-Effectiveness of Memantine in Patients with Moderately Severe to Severe Alzheimer's Disease. *Drugs Aging* **2006**, 23 (3), 227-240.
- 163.** KIRBY, J.; GREEN, C.; LOVEMAN, E.; CLEGG, A.; PICOT, J.; TAKEDA, A.; PAYNE, E., A Systematic Review of the Clinical and Cost-Effectiveness of Memantine in Patients with Moderately Severe to Severe Alzheimer's Disease. *Drugs Aging* **2006**, 23 (3), 227-240.
- 164.** SILMAN, I.; MILLARD, C. B.; ORDENTLICH, A.; GREENBLATT, H. M.; HAREL, M.; BARAK, D.; SHAFFERMAN, A.; SUSSMAN, J. L., A preliminary comparison of structural models for catalytic intermediates of acetylcholinesterase. *Chemico-Biological Interactions* **1999**, 119, 43-52.
- 165.** SILMAN, I.; SUSSMAN, J. L., Acetylcholinesterase: 'classical' and 'non-classical' functions and pharmacology. *Current opinion in pharmacology* **2005**, 5 (3), 293-302.
- 166.** PERRY, E. K.; TOMLINSON, B. E.; BLESSED, G.; BERGMANN, K.; GIBSON, P. H.; PERRY, R. H., Correlation of cholinergic abnormalities with senile plaques and mental test scores in senile dementia. *BMJ* **1978**, 2 (6150), 1457-1459.

- 167.** BOLOGNESI, M. L.; ANDRISANO, V.; BARTOLINI, M.; BANZI, R.; MELCHIORRE, C., Propidium-based polyamine ligands as potent inhibitors of acetylcholinesterase and acetylcholinesterase-induced amyloid- $\beta$  aggregation. *Journal of Medicinal Chemistry* **2005**, *48* (1), 24-27.
- 168.** FRANCIS, P. T.; NORDBERG, A.; ARNOLD, S. E., A preclinical view of cholinesterase inhibitors in neuroprotection: do they provide more than symptomatic benefits in Alzheimer's disease? *Trends in pharmacological sciences* **2005**, *26* (2), 104-111.
- 169.** SCOTT, L. J.; GOA, K. L., Galantamine. *Drugs* **2000**, *60* (5), 1095-1122.
- 170.** QIZILBASH, N.; WHITEHEAD, A.; HIGGINS, J.; WILCOCK, G.; SCHNEIDER, L.; FARLOW, M.; COLLABORATION, D. T., Cholinesterase inhibition for Alzheimer disease: a meta-analysis of the tacrine trials. *JAMA* **1998**, *280* (20), 1777-1782.
- 171.** ENZ, A.; BODDEKE, H.; GRAY, J.; SPIEGEL, R., Pharmacologic and clinicopharmacologic properties of SDZ ENA 713, a centrally selective acetylcholinesterase inhibitor. *Annals of the New York Academy of Sciences* **1990**, *640*, 272-275.
- 172.** AHMED, M.; ROCHA, J. B. T.; CORRÊA, M.; MAZZANTI, C. M.; ZANIN, R. F.; MORSCH, A. L.; MORSCH, V. M.; SCHETINGER, M. R., Inhibition of two different cholinesterases by tacrine. *Chemico-Biological Interactions* **2006**, *162* (2), 165-171.
- 173.** HAMULAKOVA, S.; JANOVEC, L.; HRABINOVA, M.; KRISTIAN, P.; KUCA, K.; BANASOVA, M.; IMRICH, J., Synthesis, design and biological evaluation of novel highly potent tacrine congeners

for the treatment of Alzheimer's disease. *European journal of medicinal chemistry* **2012**, *55*, 23-31.

- 174.** WU, C.; YANG, J., Tacrine protection of acetylcholinesterase from inactivation by diisopropylfluorophosphate: a circular dichroism study. *Molecular pharmacology* **1989**, *35* (1), 85-92.
- 175.** ZHANG, Y.; HEI, T.; CAI, Y.; GAO, Q.; ZHANG, Q., Affinity binding-guided fluorescent nanobiosensor for acetylcholinesterase inhibitors via distance modulation between the fluorophore and metallic nanoparticle. *Analytical chemistry* **2012**, *84* (6), 2830-2836.
- 176.** VANZOLINI, K. L.; VIEIRA, L. C.; CORREA, A. G.; CARDOSO, C. L.; CASS, Q. B., Acetylcholinesterase immobilized capillary reactors–tandem mass spectrometry: An on-flow tool for ligand screening. *Journal of Medicinal Chemistry* **2013**, *56* (5), 2038-2044.
- 177.** DA SILVA, J. I.; DE MORAES, M. C.; VIEIRA, L. C. C.; CORRÊA, A. G.; CASS, Q. B.; CARDOSO, C. L., Acetylcholinesterase capillary enzyme reactor for screening and characterization of selective inhibitors. *Journal of pharmaceutical and biomedical analysis* **2013**, *73*, 44-52.
- 178.** MAYER, M.; MEYER, B., Characterization of ligand binding by saturation transfer difference NMR spectroscopy. *Angewandte Chemie International Edition* **1999**, *38* (12), 1784-1788.
- 179.** MEYER, B.; PETERS, T., NMR spectroscopy techniques for screening and identifying ligand binding to protein receptors. *Angewandte Chemie International Edition* **2003**, *42* (8), 864-890.
- 180.** BOURNE, Y.; GRASSI, J.; BOUGIS, P. E.; MARCHOT, P., Conformational flexibility of the acetylcholinesterase tetramer suggested

by X-ray crystallography. *Journal of Biological Chemistry* **1999**, 274 (43), 30370-30376.

- 181.** BON, S.; VIGNY, M.; MASSOULIÉ, J., Asymmetric and globular forms of acetylcholinesterase in mammals and birds. *Proceedings of the National Academy of Sciences* **1979**, 76 (6), 2546-2550.
- 182.** VIEGAS, A.; MANSO, J.; NOBREGA, F. L.; CABRITA, E. J., Saturation-transfer difference (STD) NMR: a simple and fast method for ligand screening and characterization of protein binding. *Journal of Chemical Education* **2011**, 88 (7), 990-994.
- 183.** MARI, S.; INVERNIZZI, C.; SPITALERI, A.; ALBERICI, L.; GHITTI, M.; BORDIGNON, C.; TRAVERSARI, C.; RIZZARDI, G. P.; MUSCO, G., 2D TR-NOESY Experiments Interrogate and Rank Ligand–Receptor Interactions in Living Human Cancer Cells. *Angewandte Chemie International Edition* **2010**, 49 (6), 1071-1074.
- 184.** KUNG, H. F.; LEE, C.-W.; ZHUANG, Z.-P.; KUNG, M.-P.; HOU, C.; PLÖSSL, K., Novel stilbenes as probes for amyloid plaques. *Journal of the American Chemical Society* **2001**, 123 (50), 12740-12741.
- 185.** WANG, B.; MAI, Y.-C.; LI, Y.; HOU, J.-Q.; HUANG, S.-L.; OU, T.-M.; TAN, J.-H.; AN, L.-K.; LI, D.; GU, L.-Q., Synthesis and evaluation of novel rutaecarpine derivatives and related alkaloids derivatives as selective acetylcholinesterase inhibitors. *European journal of medicinal chemistry* **2010**, 45 (4), 1415-1423.
- 186.** MUNOZ-MURIEDAS, J.; LOPEZ, J.; OROZCO, M.; LUQUE, F. J., Molecular modelling approaches to the design of acetylcholinesterase inhibitors: new challenges for the treatment of Alzheimer's disease. *Current pharmaceutical design* **2004**, 10 (25), 3131-3140.



- 187.** VAN BELLE, D.; DE MARIA, L.; IURCU, G.; WODAK, S. J., Pathways of ligand clearance in acetylcholinesterase by multiple copy sampling. *Journal of molecular biology* **2000**, 298 (4), 705-726.
- 188.** XU, Y.; COLLETIER, J. P.; JIANG, H.; SILMAN, I.; SUSSMAN, J. L.; WEIK, M., Induced-fit or preexisting equilibrium dynamics? Lessons from protein crystallography and MD simulations on acetylcholinesterase and implications for structure-based drug design. *Protein Science* **2008**, 17 (4), 601-605.
- 189.** KIM, W.-G.; CHO, K.-M.; LEE, C.-K.; YOO, I.-D., Terreulactone A, a novel meroterpenoid with anti-acetylcholinesterase activity from *Aspergillus terreus*. *Tetrahedron letters* **2002**, 43 (17), 3197-3198.
- 190.** SCHNEIDER, L. S., New therapeutic approaches to Alzheimer's disease. *The Journal of clinical psychiatry* **1995**, 57, 30-36.
- 191.** NEWMAN, D. J.; CRAGG, G. M., Natural Products as Sources of New Drugs over the Last 25 Years<sup>1</sup>. *Journal of natural products* **2007**, 70 (3), 461-477.
- 192.** OLIVEIRA, E.; ROMERO, M.; SILVA, M.; SILVA, B.; MEDEIROS, I., Intracellular calcium mobilization as a target for the spasmolytic action of scopoletin. *Planta medica* **2001**, 67 (7), 605-608.
- 193.** CARPINELLA, M. C.; FERRAYOLI, C. G.; PALACIOS, S. M., Antifungal synergistic effect of scopoletin, a hydroxycoumarin isolated from *Melia azedarach* L. fruits. *Journal of agricultural and food chemistry* **2005**, 53 (8), 2922-2927.
- 194.** PANDA, S.; KAR, A., Evaluation of the antithyroid, antioxidative and antihyperglycemic activity of scopoletin from *Aegle marmelos* leaves

in hyperthyroid rats. *PHYTOTHERAPY RESEARCH* **2006**, *20* (12), 1103-1105.

- 195.** MANUELE, M. G.; FERRARO, G.; ARCOS, M. L. B.; LÓPEZ, P.; CREMASCHI, G.; ANESINI, C., Comparative immunomodulatory effect of scopoletin on tumoral and normal lymphocytes. *Life sciences* **2006**, *79* (21), 2043-2048.
- 196.** ORHAN, I.; TOSUN, F.; SENER, B., Coumarin, anthroquinone and stilbene derivatives with anticholinesterase activity. *Zeitschrift für Naturforschung. C, A journal of biosciences* **2008**, *63* (11), 366.
- 197.** ROLLINGER, J. M.; HORNICK, A.; LANGER, T.; STUPPNER, H.; PRAST, H., Acetylcholinesterase inhibitory activity of scopolin and scopoletin discovered by virtual screening of natural products. *Journal of Medicinal Chemistry* **2004**, *47* (25), 6248-6254.
- 198.** TOFUKU, K.; YOKOUCHI, M.; MURAYAMA, T.; MINAMI, S.; KOMIYA, S., HAS3-related hyaluronan enhances biological activities necessary for metastasis of osteosarcoma cells. *International journal of oncology* **2006**, *29* (1), 175-183.
- 199.** KULKA, M., The potential of natural products as effective treatments for allergic inflammation: implications for allergic rhinitis. *Current topics in medicinal chemistry* **2009**, *9* (17), 1611-1624.
- 200.** PAL, C.; BINDU, S.; DEY, S.; ALAM, A.; GOYAL, M.; IQBAL, M. S.; MAITY, P.; ADHIKARI, S. S.; BANDYOPADHYAY, U., Gallic acid prevents nonsteroidal anti-inflammatory drug-induced gastropathy in rat by blocking oxidative stress and apoptosis. *Free Radical Biology and Medicine* **2010**, *49* (2), 258-267.

- 201.** KAWADA, M.; OHNO, Y.; RI, Y.; IKOMA, T.; YUUGETU, H.; ASAI, T.; WATANABE, M.; YASUDA, N.; AKAO, S.; TAKEMURA, G., Anti-tumor effect of gallic acid on LL-2 lung cancer cells transplanted in mice. *Anti-cancer drugs* **2001**, *12* (10), 847-852.
- 202.** LU, Y.; JIANG, F.; JIANG, H.; WU, K.; ZHENG, X.; CAI, Y.; KATAKOWSKI, M.; CHOPP, M.; To, S.-S. T., Gallic acid suppresses cell viability, proliferation, invasion and angiogenesis in human glioma cells. *European journal of pharmacology* **2010**, *641* (2), 102-107.
- 203.** BHATTACHARYA, A.; GHOSAL, S.; BHATTACHARYA, S. K., Antioxidant activity of tannoid principles of *Emblica officinalis* (amla) in chronic stress induced changes in rat brain. *Indian Journal of Experimental Biology* **2000**, *38* (9), 877-880.
- 204.** SCARTEZZINI, P.; ANTOGNONI, F.; RAGGI, M.; POLI, F.; SABBIONI, C., Vitamin C content and antioxidant activity of the fruit and of the Ayurvedic preparation of *Emblica officinalis* Gaertn. *Journal of Ethnopharmacology* **2006**, *104* (1), 113-118.
- 205.** FUKUMOTO, L.; MAZZA, G., Assessing antioxidant and prooxidant activities of phenolic compounds. *Journal of agricultural and food chemistry* **2000**, *48* (8), 3597-3604.
- 206.** XIMENES, V. F.; LOPES, M. G.; PETRONIO, M. S.; REGASINI, L. O.; SIQUEIRA SILVA, D. H.; DA FONSECA, L. M., Inhibitory effect of gallic acid and its esters on 2, 2'-azobis (2-amidinopropane) hydrochloride (AAPH)-induced hemolysis and depletion of intracellular glutathione in erythrocytes. *Journal of agricultural and food chemistry* **2010**, *58* (9), 5355-5362.

- 207.** Mukherjee, P. K.; Kumar, V.; Mal, M.; Houghton, P. J., Acetylcholinesterase inhibitors from plants. *Phytomedicine* **2007**, *14* (4), 289-300.
- 208.** COHEN, Y.; AVRAM, L.; FRISH, L., Diffusion NMR spectroscopy in supramolecular and combinatorial chemistry: an old parameter—new insights. *Angewandte Chemie International Edition* **2005**, *44* (4), 520-554.
- 209.** BAG, A.; BHATTACHARYYA, S. K.; CHATTOPADHYAY, R. R., The development of Terminalia chebula Retz.(Combretaceae) in clinical research. *Asian Pacific journal of tropical biomedicine* **2013**, *3* (3), 244-252.
- 210.** NAG, G.; DE, B., Acetylcholinesterase inhibitory activity of Terminalia chebula, Terminalia bellerica and Emblica officinalis and some phenolic compounds. *Int J Pharm Pharm Sci* **2011**, *13*, 121-4.
- 211.** CHENG, H.-Y.; LIN, T.-C.; YU, K.-H.; YANG, C.-M.; LIN, C.-C., Antioxidant and free radical scavenging activities of Terminalia chebula. *Biological and Pharmaceutical Bulletin* **2003**, *26* (9), 1331-1335.
- 212.** SALEEM, A.; HUSHEEM, M.; HÄRKÖNEN, P.; PIHLAJA, K., Inhibition of cancer cell growth by crude extract and the phenolics of Terminalia chebula retz. fruit. *Journal of Ethnopharmacology* **2002**, *81* (3), 327-336.
- 213.** MALEKZADEH, F.; EHSANIFAR, H.; SHAHAMAT, M.; LEVIN, M.; COLWELL, R. R., Antibacterial activity of black myrobalan (Terminalia chebula Retz) against Helicobacter pylori. *International Journal of Antimicrobial Agents* **2001**, *18* (1), 85-88.

- 214.** SUGUNA, L.; SINGH, S.; SIVAKUMAR, P.; SAMPATH, P.; CHANDRAKASAN, G., Influence of Terminalia chebula on dermal wound healing in rats. *Phytotherapy Research* **2002**, *16* (3), 227-231.
- 215.** JAGTAP, A. G.; KARKERA, S. G., Potential of the aqueous extract of Terminalia chebula as an anticaries agent. *Journal of Ethnopharmacology* **1999**, *68* (1–3), 299-306.
- 216.** TAMHANE M. D.; THORAT S. P.; REGE N. N.; DAHANUKAR S. A.; Effect of oral administration of Terminalia chebula on gastric emptying: an experimental study. *Journal of Postgraduate Medicine* **1997**, *43*(1), 12-13.
- 217.** SHIN, T. Y.; JEONG, H. J.; KIM, D. K.; KIM, S. H.; LEE, J. K.; KIM, D. K.; CHAE, B. S.; KIM, J. H.; KANG, H. W.; LEE, C. M.; LEE, K. C.; PARK, S. T.; LEE, E. J.; LIM, J. P.; KIM, H. M.; LEE, Y. M., Inhibitory action of water soluble fraction of Terminalia chebula on systemic and local anaphylaxis. *Journal of Ethnopharmacology* **2001**, *74* (2), 133-140.
- 218.** SABU, M. C.; KUTTAN, R., Anti-diabetic activity of medicinal plants and its relationship with their antioxidant property. *Journal of Ethnopharmacology* **2002**, *81* (2), 155-160.
- 219.** SHINDE S. L.; the antifungal activity of five terminalia species checked by paper disc method. *International Journal of Pharma Research and Development-Online* **2011**, *3*(2), 36-40.
- 220.** KIM, H.; CHO, J.; JEONG, E.; LIM, J.; LEE, S.; LEE, H., Growth-inhibiting activity of active component isolated from Terminalia chebula fruits against intestinal bacteria. *Journal of Food Protection*® **2006**, *69* (9), 2205-2209.

- 221.** KANNAN P, RAMADEVI S.R. AND WAHEETA HOPPER. Antibacterial activity of Terminalia chebula fruit extract, African Journal of Microbiology Research. **2009**, 3(4), 180-184.
- 222.** SOUARD, F.; MUÑOZ, E.; PEÑALVER, P.; BADÍA, C.; DEL VILLAR-GUERRA, R.; ASENSIO, J. L.; JIMÉNEZ-BARBERO, J.; VICENT, C., Sugar–Oligoamides: Bound-State Conformation and DNA Minor-Groove-Binding Description by TR-NOESY and Differential-Frequency Saturation-Transfer-Difference Experiments. *Chemistry – A European Journal* **2008**, 14 (8), 2435-2442.
- 223.** BARKER, G. R. I.; WARBURTON, E. C., Critical role of the cholinergic system for object-in-place associative recognition memory. *Learning & Memory* **2009**, 16 (1), 8-11.
- 224.** SRIVASTAVA, S.; SRIVASTAVA, S., New biologically active constituents from Terminalia chebula stem bark. *Indian journal of chemistry. Sect. B: Organic chemistry, including medical chemistry* **2004**, 43 (12), 2731-2733.
- 225.** KOSMULALAGE, K. S.; ZAHID, S.; UDENIGWE, C. C.; AKHTAR, S.; ATA, A.; SAMARASEKERA, R., Glutathione S-transferase, acetylcholinesterase inhibitory and antibacterial activities of chemical constituents of Barleria prionitis. *Zeitschrift Fur Naturforschung B* **2007**, 62 (4), 580.
- 226.** ZHELEVA-DIMITROVA, D. Z., Antioxidant and acetylcholinesterase inhibition properties of Amorpha fruticosa L. and Phytolacca americana L. *Pharmacognosy magazine* **2013**, 9 (34), 109.

- 227.** DAS, A.; WEI, Y.; PELCZER, I.; HECHT, M. H., Binding of small molecules to cavity forming mutants of a de novo designed protein. *Protein Science* **2011**, *20* (4), 702-711.
- 228.** Stejskal, E.; Tanner, J., Spin diffusion measurements: spin echoes in the presence of a time-dependent field gradient. *The journal of chemical physics* **1965**, *42* (1), 288-292.